PhD School in Physics
University of Turin

Universality and Factorization of Hadronic Scattering Processes in a TMD Approach

Andrea Simonelli

Supervisor: Prof. Mariaelena Boglione

External examiners: Prof. Alessandro Bacchetta
Prof. Leonard Gamberg

This dissertation is submitted for the
Doctor of Phylosophy Degree in *Physics*

September 2021

Universality and Factorization of hadronic scattering processes in a TMD approach

Andrea Simonelli

Abstract

Factorization theorems allow to separate out the universal, non-perturbative content of the hadronic cross section from its perturbative part, which can be computed in perturbative QCD, up to the desired order. In this thesis, I will frame the known TMD factorization theorems into a more general context, within which I derive a rigorous proof of factorization of the $e^+e^- \to hX$ cross section, sensitive to the transverse momentum of the detected hadron with respect to the thrust axis. I will show how this leads to three different kinematic regions, each associated to a different factorization theorem. In one of these regions, the factorization theorem has a new structure, which shares the features of both TMD and collinear factorization. In the corresponding cross section, the role of the rapidity cut-offs is investigated, as their physical meaning becomes increasingly evident.

Table of contents

Introduction

To understand how matter around us is made and how it keeps together, we rely on Quantum Chromo Dynamics (QCD), the theory of strong interactions where quarks and gluons are the elementary building blocks. Although its Lagrangian is well known, QCD is a very complex, self-interacting theory, which cannot be solved exactly. Quarks and gluons are the elementary fields of the theory, but there is no way to observe them directly. In fact, scattering experiments based on strong interactions result in jets of hadrons, which are bound states of the elementary quanta. The exact mechanism that governs how a quasi-free gas made up of quarks and gluons becomes a totally different state composed by hadronic matter is still not understood. Many models and theories have been proposed over the last 40 years, but none of them has yet been capable to catch all the features concerning confinement and hadronization.

Modern studies of high energy QCD processes are based on factorization theorems, that play a pivotal role in the study of strong interactions, as they allow to write the cross sections of hadronic processes in a form suitable for phenomenological analyses. Perturbative QCD alone is not sufficient to exploit the whole theory's predictive power since, even at lowest orders, several physical observables are affected by uncanceled infrared divergences. Through the factorization procedure, the divergent contributions are separated from the finite, computable parts and are collected into universal factors, as they can be extracted from a small set of experimental data and then used to predict any other observable that requires their contribution. Crucially, if universality is preserved, then the theory can be predictive. Therefore, research in this field is two-folded: in addition to the pure theoretical investigation, aimed to provide a solid proof of factorization of the processes that still lack of a proper factorization theorem, the phenomenological applications of the theory are fundamental in the extraction of universal non-perturbative factors.

If Q is some typical hard energy scale for a certain process (c.m. energy, momentum transfer, etc...), then, at the cost of an error suppressed by powers of m/Q, where m is a typical low energy (hadronic) mass scale (typically around ~ 1 GeV) , a factorization theorem recasts the cross section in terms of a convolution of contribution s which can be classified in terms of the following three categories:

Introduction

1. *Hard part.* It corresponds to the elementary subprocess and it provides the signature of the process, as it identifies the partonic scattering uniquely. It is fully computable in perturbation theory in terms of Feynman diagrams, up to the desired accuracy.

2. *Collinear parts.* These contributions are associated to the initial and/or final state hadrons of the process and contain the collinear divergences related to the massless particles emitted along the hadron direction. Each of them corresponds to a bunch of particles strongly boosted along this direction, which move almost collinearly, very fast. Due to their characteristic divergences, collinear parts cannot be fully computed in perturbation theory: their non-perturbative content has to be extracted from experimental data. Among all the particles in the collinear group, two of them deserve special attention: the *reference hadron* and the *reference parton*. If the collinear group refers to the initial state of the process, the reference hadron coincides with the initial hadron and the reference parton is the parton confined inside it that is struck in the hard scattering; if the collinear group refers to the final state, the reference hadron is the detected hadron and the reference parton is the fragmenting parton, i.e. the particle that initiates the hadronization process.

3. *Soft part.* It embeds the contribution due to the soft gluon radiation that connects the collinear parts and that flows through the detector. It contains soft divergences and carries non-perturbative information, therefore it cannot be computed in perturbation theory. And it cannot be directly extracted from data, either, as the energy of the soft radiation is so low that detectors are not sensitive to it. Since the collinear parts interact among each other *only* through soft gluons, their contribution can affect the cross section in a non-trivial way. Moreover, the soft part is *always* associated with the collinear terms and there is no way to extract them separately. This is sometimes referred to as "the soft factor problem".

As long as the physical observable are not sensitive to the transverse motion of the partons inside their parent hadron, the factorization procedure can be carried on rather simply, giving solid factorization theorems for a large set of processes. Since the information on the transverse motion of partons is neglected, such theorems are often labeled as "collinear". Many famous observables are known to obey to a collinear factorization theorem. Well known examples are for instance the cross section of Deep Inelastic Scattering (DIS) and e^+e^- annihilation [1–6]. In all these cases the contribution of the soft part is trivial. In particular, any time in addition to the collinear partons there are real emissions with large transverse momentum (compared to Q), the soft factor fully factorizes and its value reduces to unity. This is due to the fact that the soft gluons are kinematically overpowered and do not correlate the collinear parts anymore: in this way each collinear cluster of partons is totally independent from any other. As a consequence, only hard and collinear contributions appear explicitly in the final cross section. The great success of collinear factorization over the past forty years lays in its simplicity. In any collinear factorized cross section, it is always possible to associate each collinear part with a Parton Distribution Function (PDF) or a Fragmentation Function (FF), depending on whether the

associated reference hadron is in the initial or in the final state, respectively. Furthermore, the hard part is just the partonic version of the full process and then it is often referred as partonic cross section. As an example of a collinearly factorized process, one could consider the case of e^+e^- scattering where two spinless hadrons h_A and h_B are produced in the final state, in a configuration in which they are at wide angles but far from being back-to-back, in the center of mass frame (which, in this case, corresponds to the lab frame). The resulting cross section is given by (see for instance Eq. (12.84) in Ref. [7]):

$$\frac{d\sigma}{\left(\frac{d^3\vec{p}_A}{E_A}\right)\left(\frac{d^3\vec{p}_B}{E_B}\right)} = \sum_{j_A, j_B} \int \frac{d\hat{z}_A}{\hat{z}_A^2} \underbrace{d_{h_A/j_A}(\hat{z}_A)}_{\text{coll.}} \int \frac{d\hat{z}_B}{\hat{z}_B^2} \underbrace{d_{h_B/j_B}(\hat{z}_B)}_{\text{coll.}} \underbrace{\frac{d\hat{\sigma}_{j_A, j_B}}{\left(\frac{d^3\vec{k}_A}{\varepsilon_A}\right)\left(\frac{d^3\vec{k}_B}{\varepsilon_B}\right)}}_{\text{hard}}, \tag{1}$$

where $d\hat{\sigma}$ is the partonic cross section, while $d_{h_i/j_i}(\hat{z}_i)$, for $i = A, B$, are the FFs associated to the outgoing hadrons, with momenta $\vec{p}_A$ and $\vec{p}_B$, and to the fragmenting partons of flavor j_A and j_B, corresponding to the two collinear parts of the cross section of the process.

When the 3D-motion of partons is considered, finding a way to properly separate the various contributions a very tough task. On the other hand, Transverse Momentum Dependent (TMD) observables expose a much richer structure that may disclose some of the inner properties of hadronization and confinement. When the information on transverse motion survives in the final result, the corresponding factorization theorem is usually labeled as "TMD". In such cases, the soft factor does not reduce to unity, and soft gluons have a non-trivial impact on the cross section, as they correlate the collinear parts. This correlation originates from momentum conservation laws in the transverse direction. In fact, with no real emissions carrying large transverse momentum entering into the game, the low transverse momentum components of soft and collinear particles cannot be neglected anymore. As a consequence, it is not possible to associate a PDF or a FF to the collinear contributions: parton densities are now related to different and more general objects, known as Transverse Momentum Dependent parton functions, either TMD PDFs or TMD FFs depending on whether they refer to an initial or a final state hadron. As an example of a TMD factorized process, one can once again consider the production of two spinless hadrons from an e^+e- scattering where, this time, the two hadrons are almost back-to-back in the e^+e- center of mass frame. The full cross section is given by (see for instance Eq. (13.31) in Ref. [7]):

$$W^{\mu\nu}(Q, p_A, p_B) = \frac{8\pi^3 z_A z_B}{Q^2} \sum_f \underbrace{H^{\mu\nu}_{f,\bar{f}}(Q)}_{\text{hard}} \times$$

$$\times \int d^2\vec{k}_{A,hT}\, d^2\vec{k}_{B,hT}\, \underbrace{\mathbb{S}(\vec{q}_{hT} - \vec{k}_{A,hT} - \vec{k}_{B,hT})}_{\text{soft}}\, \underbrace{D_{h_A/f}(\vec{k}_{A,hT})D_{h_B/\bar{f}}(\vec{k}_{A,hT})}_{\text{coll.}},$$

$$\tag{2}$$

where $H^{\mu\nu}_{f,\bar{f}}(Q)$ is the hard part, $\mathbb{S}$ represents the soft factor and the functions $D_{h_i/f}$, for $i = A, B$, are the TMD FFs associated to the outgoing hadrons and to the fragmenting partons of flavor f and $\bar{f}$.

Notice that it is kinematics, and hence ultimately the hard part, that determines which fatorization scheme has to be used: if the two hadrons are back-to-back then TMD factorization, Eq. (2), must be applied, otherwise collinear factorization, Eq. (1), will be appropriate. Same process, two different factorization theorems. This is the most common situation. In fact, in general, one hadronic scattering process does not cover one single kinematic region: it rather extends over different kinematical ranges, all of them contributing to the final cross section. Therefore, each factorization theorem is associated to a certain kinematic configuration, which is determined by the values of the measured observables. For instance, in the case of e^+e^- into two hadrons, the observable that discriminates between collinear and TMD regime is the relative angle of h_A and h_B, which is related to the ratio of the transverse momentum q_T of the virtual boson produced in the leptonic scattering and the c.m. energy Q. When q_T/Q is large enough, the two hadrons are not back-to-back and collinear factorization of Eq. (1) holds. On the other hand, when $q_T << Q$, the process is in the TMD regime and the TMD factorization theorem of Eq. (2) should be used. This introduces a major issues in the phenomenological analyses. In fact, the factorization procedure does not provide the boundaries of the different kinematic configurations contributing to a process. For instance, there is no way to decide "how small" q_T/Q must be in order to apply the TMD formalism. However, since the ultimate aim is to predict a cross section valid over the whole q_T spectrum, it is extremely important that the two regimes can be matched in the intermediate region. This is still an open problem in SIDIS, which has a structure analogous to that of $e^+e^- \to h_A h_B$.

The problem of the matching is just one of the main issues related to TMD factorization. Another urgent question is whether it can be extended to other processes, beyond the known cases. Until the end of 2018, one of the processes that were still lacking of a solid factorization theorem was e^+e^- annihilation into a single hadron, sensitive to the transverse momentum of the detected hadron with respect to the axis of the jet of particles to which it belongs. At the beginning of 2019, the BELLE collaboration at KEK published the results of the measurements of this cross section [8], with the transverse momentum of the observed hadron measured with respect to the thrust axis. This is one of the measurements which go closer to being a direct observation of a partonic variable, the transverse momentum of the hadron with respect to its parent fragmenting parton, and they have indeed triggered a great interest of the high energy physics community, especially among the experts in the phenomenological study of TMD phenomena and factorization [9–18].

In this thesis, I propose the first proof of the factorization of such a QCD process, within a formalism inspired to the Collins-Soper-Sterman (CSS) factorization scheme. In particular, I show that, if the size of the transverse momentum of the detected hadron is neither too large to affect significantly the topology of the final state nor too small to be sensitive to the deflection due to soft radiation, then the cross section of $e^+e^- \to hX$ factorizes in a convolution between a partonic cross section, fully computable in perturbation theory, and a TMD Fragmentation Function. This is a new kind of structure, never encountered before in any known factorization theorem. It is a sort of hybrid of TMD and collinear factorization, and for this reason it will be dented as "collinear-TMD factorization

theorem". One of its most relevant features is related to the treatment of rapidity divergences. These arise as unregulated infinities into soft and collinear parts and they are due to the approximations introduced by the factorization procedure. Despite the various long-distance contributions are rapidity divergent, the full factorized cross-section is finite. Therefore, the rapidity divergences must cancel in the convolutions of the final result. There are many ways to regulate them. In Collins factorization formalism, they are regulated by tilting the Wilson lines associated to the soft contributions off the lightcone. This operation is totally analogous to the insertion of a sharp rapidity cut-off that prevents the integrations on rapitidities to diverge. Clearly, whatever regulator is used, one expects that the final cross section will not depend on it. However, for the collinear-TMD factorization theorem devised for $e^+e^- \to hX$ this does not happen. One could claim that this is a symptom of non-consistency of the corresponding factorization theorem (see for instance Ref. [17]). I do not interpret this as a failure of the factorization itself, but rather as a limit of the Collins factorization formalism in this particular process. In fact, even just from a simple kinematical study, it is clear that the rapidity cut-off is intimately related to the thrust, which in this case is measured. Hence, there must be a way to give it a physical meaning, beyond the role of a mere divergence regulator.

Like other hadronic processes, also $e^+e^- \to hX$ can occur in different kinematic regions. In particular, I show that in total there are three of them for a 2-jet final state, each one associated to a different factorization theorem. In particular, when the transverse momentum of the detected hadron is sensitive to the deflection caused by the soft radiation, the resulting factorization theorem has a structure very similar to a TMD factorized cross section. Instead, when the transverse momentum of the detected hadron is large enough to significantly affect the topology of the final state (and, ultimately, the measured value of thrust) the factorization theorem does not involve TMD FFs anymore. I will call these two kinematical ranges Region 1 and Region 3, respectively. The intermediate region discussed in the previous paragraph, called Region 2, is the widest in terms of phase space and also the most interesting from the point of view of the factorization theorems, as it embeds the properties of both TMD and collinear factorization schemes. This matches with the nomenclature introduced in Ref. [17].

The framework presented in this thesis not only includes the well-known TMD factorization theorems developed for e^+e^- annihilation into two back-to-back hadrons, SIDIS and Drell-Yan into a more general context, but it also extends the investigation of TMD physics beyond these benchmark processes, firstly by developing proper factorization theorems for $e^+e^- \to hX$. Furthermore, it could allow to study a much wider set of processes, also involving more than two TMD functions. For these reasons, this approach looks very promising and it may hopefully be one of the future keys to fundamental QCD issues.

Chapter 1

Universality in hadronic scattering processes

1.1 Introduction

The factorization procedure proposed by Collins, Soper and Sterman in the '80s [19–21] has become the benchmark for all the successive approaches designed to provide factorization theorems for hadronic processes. The most recent and complete form of such factorization procedure was devised by John Collins in its book "*Foundations of Perturbative QCD*" [7] and in the following I will refer to this scheme as the "Collins factorization formalism". A detailed illustration of this approach can be found in Appendix A. The Collins factorization formalism correctly reproduces the well-known collinear factorization theorems; in addition, and most importantly, it can successfully be applied to develop TMD factorization theorems for three observables: e^+e^- annihilation into two back-to-back hadrons, SIDIS and Drell-Yan. However, its extension to other observables sensitive to TMD physics is problematic[22, 7, 12, 23, 14].

In this chapter, I will investigate the causes of such difficulties, tracing them back to the property of universality of soft and collinear terms in the factorized cross sections. In particular, potentially dangerous universality-breaking effects arise from soft gluon emissions, encoded into the soft factor of the process. Usually, such contributions are re-absorbed into the TMDs definition, but I will show how this method fails when applied to hadronic processes different from those mentioned above, i.e. to processes which belong to a different "hadron-class", as I will explain in detail in Section 1.4.

This chapter follows closely the content of the paper "Universality-breaking effects in e^+e^- hadronic production processes" [12]. It is organized as follows. In the first part, Sections 1.2 and 1.3, I will briefly review the main features of the Collins factorization formalism, focusing on the soft and collinear contributions, associated to long-distance and non-perturbative effects. I will give the most general formal definitions of the soft factor and of the collinear factor, trying to highlight their physical intuitive interpretation, that is often slightly overlooked in related literature. In Section 1.4 I

will explore the properties of universality of soft and collinear parts. Hadronic processes are classified according to the general structure induced by the universal factors that contribute to their cross sections. The usual definition of TMDs is framed into this scheme in Section 1.4.1, while in Section 1.4.2 I will show how this definition must be necessarily modified for the development of a TMD factorization theorem for $e^+e^- \to hX$, where the soft gluons contribute to the final cross section in a different and non-trivial way.

1.2 Soft Factor

From the point of view of the soft gluons, each collinear group is simply a bunch of particles strongly boosted in a certain direction. The boost is so strong that the soft gluons are only sensitive to the color charge and to the direction of the collinear particles. As a consequence, the propagation of collinear particles is well approximated by a Wilson line in the direction of the corresponding collinear group, usually represented by double lines, see Appendix A. In the massless limit, the versor which identifies this direction is light-like. However, a light-like Wilson line brings unregulated rapidity divergences. In the Collins factorization formalism, these divergences are regulated by tilting each Wilson line associated to the soft factor from its reference direction w_i to the direction n_i. Such operation is analogous to the introduction of a rapidity cut-off y_i, in order to constrain the particles directed along the i-th direction to have a rapidity smaller than y_i. The final result for the cross section should not depend on these rapidity cut-offs, which then have to be removed in the final stage of the computation. Later on, I will show how this is not always the case, as there are special observables that, after being factorized, maintain a residual dependence on the rapidity regulator.

The transverse momentum space is the natural place for explicit perturbative computations, as Feynman diagrams are usually written in terms of momentum variables. Therefore, in principle, it would be the natural choice for introducing the definition of the ingredients concurring to the factorized cross section. However, these terms will have to be formally defined in the b_T space, i.e. the Fourier conjugate space of the transverse momentum. If $\vec{k}_{S,T}$ is the total transverse momentum of the real soft radiation flowing through the detector, then the soft factor of a generic process is defined as:

$$\mathbb{S}^{(0)}(k_{S,T}; \mu, y_i, j_k) = \int \frac{dk_S^+ \, dk_S^-}{(2\pi)^D} \quad \text{[diagram]} \quad , \qquad (1.1)$$


8

where D is the dimension of space time ($D = 4 - 2\varepsilon$ in dimensional regularization) and $\{y_i\}$ are Lorentz invariant combinations of the rapidity cut-offs ($i = 1, \ldots N$ where N is the number of collinear parts in the process). The dependence on the parton-types $j_1 \ldots j_N$ of the partons associated to the collinear parts is only on their color representation (fermions or gluons). In this regard, notice that the soft factor is a matrix in color space, that depends on the soft transverse momentum only through its modulus. In fact, since all the collinear information is replaced by spinless eikonal propagators, $\vec{k}_{S,T}$ is the only vector appearing in the soft factor. Therefore, $\mathbb{S}$ is always rotational invariant and depends only on the modulus $|\vec{k}_{S,T}| = k_{S,T}$. The label "NO S.I." reminds us not to consider the Wilson lines self energies. This implies that $N = 1$ is excluded, since it would correspond only to a Wilson line self energy-like contribution. Finally, this definition refers to a soft factor bare w.r.t. UV renormalization, as expressed by the label "(0)" . Even if $k_{S,T}$ must be small by power counting, the function in Eq. (1.1) can be analytically continued outside of the soft region, where the power counting weight does not apply anymore. As long as $k_{S,T}$ is an external variable, this anomalous behavior can hardly be seen. However, the proper definition of the soft factor is in the Fourier conjugate space of $k_{S,T}$, where the transverse momentum becomes an integration variable. Stretching $k_{S,T}$ to infinity, well outside of the soft region, will produce poles that can be interpreted as UV divergences.

The definition of Eq. (1.1) must be intended as an operative definition, useful to compute explicitly the soft factor at perturbative level. However, already at this stage, the main characteristic of the soft factor are perfectly evident. In fact, $\mathbb{S}$ is sensitive to the number $N \geq 2$ of collinear groups, each one associated to a reference hadron h. Therefore it is not totally blind to the rest of the process, but carries some residual information about the overall process. Clearly this property affects crucially the level of universality of soft factors. For this reason, in what follows I will always add a label "N-h" to the soft factor $\mathbb{S}$ in order to take into account this dependence.

The formal definition of the soft factor is given in terms of the impact parameter $\vec{b}_T$, the Fourier conjugate variable to $\vec{k}_{S,T}$. Here, the soft factor is expressed as the vacuum expectation value of a product of Wilson lines. In the following, the Fourier transformed quantities will be labeled by a tilde. We have:

$$\widetilde{\mathbb{S}}_{\text{N-h}}(b_T; \mu, y_i, j_k) = \int d^{D-2}\vec{k}_{S,T}\, e^{i\vec{k}_{S,T}\cdot\vec{b}_T}\, \mathbb{S}_{\text{N-h}}(\vec{k}_{S,T}, \mu, y_i, j_k) =$$

$$= Z_S(\mu, y_i, j_k)\langle 0|\prod_{i=1}^{N} W_{j_i}(\infty, -\vec{b}_T/2; n_i(y_i))^{\dagger}\prod_{k=1}^{N} W_{j_k}(\infty, \vec{b}_T/2; n_j(y_j))|0\rangle\,|_{\text{NO S.I.}}. \qquad (1.2)$$

The Wilson line $W_{j_i}(\infty, \vec{b}_T/2; n_i)$ goes from $\vec{b}_T/2$ towards infinity in the direction of n_i, which is off the light-cone thanks to the rapidity cut-off y_i, and has the color representation associated to the parton type j_i. The factor Z_S is the UV renormalization factor that cancels the poles generated when the $k_{S,T}$-integration region stretches outside of the soft region. Hence, differently from the definition given in Eq. (1.1), this time the soft factor is UV-renormalized.
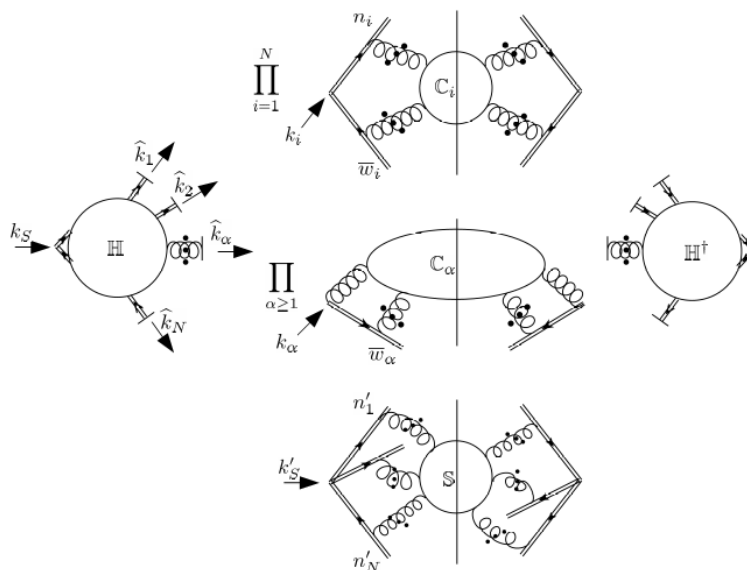
Fig. 1.1 Leading regions for the soft factor, $\mathbb{S}_{\text{N-h}}$, at small b_T.

The Fourier transform in Eq. (1.2) acts as an analytic continuation of the function $\mathbb{S}$ for any value of the soft transverse momentum. In fact, when the soft factor is Fourier transformed, the total soft transverse momentum $\vec{k}_{S,T}$ is integrated out and its dependence is replaced by $\vec{b}_T$. Roughly speaking, at fixed b_T all momenta with $k_{S,T} \leq \frac{1}{b_T}$ become accessible. This implies that when b_T is small $k_{S,T}$ can be very large, well beyond the original definition of the soft momentum region. As already pointed out, one of the consequences of such operation is the generation of UV divergences which will have to be canceled order by order by the UV counterterm Z_S. Then, at large $k_{S,T}$, i.e. at small b_T, there must be some hard factor that accounts for the UV behavior of the soft factor. Moreover, in this region the whole structure of the soft factor is modified and includes also the convolution of collinear and soft terms. All these parts can be disentangled by applying the factorization procedure to the soft factor itself, in the small-b_T regime, as pictorially represented in Fig. 1.1. The hard factor is associated to the external Wilson line vertices and contains hard subgraphs with highly virtual loops. There is a collinear subgraph corresponding to each Wilson line and all of them are connected by the soft subgraph. Furthermore, if the entering transverse momentum k_s is large enough, there can be more hard subgraphs $\mathbb{C}_\alpha$ with production of final-state jets of high transverse momentum. In this case collinear factorization holds and the soft factor (the lowest subgraph in Fig. 1.1) is unity. In each of these jet there is a fully inclusive sum/integral over final states, hence the sum-over-cuts argument presented in Ref. [7] allows us to consider them as being far off-shell and part of the hard factor, generating a "partonic cross section", i.e. a fully perturbative representation of the whole soft factor. Furthermore, there is no convolution between the hard part and the collinear factors $\mathbb{C}_i$, since the cut eikonal propagators that exit from the hard subgraphs do not carry momentum ($\widehat{k}_i \cdot w_i = 0$). In fact, the kinematic approximator associated to the hard factor suppresses all the weak components of collinear momenta, leaving to survive only those related to the reference direction of the collinear group. It also

removes all the rapidity cut-offs. This is represented by the "hat" on the momenta exiting the hard subgraph in Fig. 1.1. As a consequence, all the collinear parts are integrated 2-h soft factors and are unity as well. Therefore, the only remaining effective region is the hard factor with all the extra hard jets, giving the perturbative version of the original $\mathbb{S}_{\text{N-h}}$. This function can be computed by using web technologies (see for example Ref. [24–27]): it exponentiates, and the exponent is given by the sum of all the (multiparton) webs, i.e. closed sets of Feynman diagrams related by permutations on the external lines. Schematically:

$$
\mathbb{S}_{\text{N-h}}(b_T; \mu, y_i, j_k) \overset{\text{low } b_T}{\sim} \int d^{D-2}\vec{k}_{S,T}\, e^{i\vec{k}_{S,T}\cdot\vec{b}_T} \exp\left\{ \sum_{\text{W}\in\text{webs}} \sum_{\substack{\text{d, d'}\in \\ \text{graphs of W}}} \text{F}_\text{d}(k_{S,T}; \mu, y_i, j_k) R^{(\text{W})}_{\text{d, d'}} \text{c}_{\text{d'}} \right\},
$$
(1.3)

where $R^{(\text{W})}_{\text{d, d'}}$ is the mixing matrix that combines the kinematic and color factors, F and c respectively, of the diagrams belonging to the web W.

Eq. (1.3) provides a formula for the soft factor in the small-b_T region, but it cannot be trusted at large values of b_T. However, factorization gives no indication on where the perturbative region ends. Therefore, without any hint on the boundaries of the small-b_T regime, one has to separate it from the large-b_T region by hand. An easy method consists in modifying the functional dependence of $\widetilde{\mathbb{S}}_{\text{N-h}}$ with respect to $\vec{b}_T$ by introducing a function $\vec{b}_T^\star(\vec{b}_T)$ such that it coincides with $\vec{b}_T$ at small b_T, while at large b_T it is no larger than a certain $b_{\max}$. A possible choice, according to Ref. [19, 21, 7][1], is given by:

$$
\vec{b}_T^\star(b_T) = \frac{\vec{b}_T}{\sqrt{1 + b_T^2/b_{\max}^2}}
$$
(1.4)

Then, by dividing and multiplying $\widetilde{\mathbb{S}}_{\text{N-h}}$ by its small-b_T behavior, we can obtain an expression which holds valid at any value of b_T:

$$
\widetilde{\mathbb{S}}_{\text{N-h}}(b_T; \mu, y_i, j_k) = \widetilde{\mathbb{S}}_{\text{N-h}}(b_T^\star; \mu, y_i, j_k) \times \frac{\widetilde{\mathbb{S}}_{\text{N-h}}(b_T; \mu, y_i, j_k)}{\widetilde{\mathbb{S}}_{\text{N-h}}(b_T^\star; \mu, y_i, j_k)} =
$$

$$
= \int d^{D-2}\vec{k}_{S,T}\, e^{i\vec{k}_{S,T}\cdot\vec{b}_T^\star} \exp\left\{ \sum_{\text{W}\in\text{webs}} \sum_{\substack{\text{d, d'}\in \\ \text{graphs of W}}} \text{F}_\text{d}(k_{S,T}; \mu, y_i, j_k) R^{(\text{W})}_{\text{d, d'}} \text{c}_{\text{d'}} \right\} \times M_S(b_T; \mu, y_i, j_k),
$$
(1.5)

where $M_S(b_T; \mu, \{y_i\}_{i=1...N}, \{j_i\}_{i=1...N})$ is the fully non-perturbative function that models the N-h soft factor at large b_T, while the whole perturbative content is gathered in the webs.

---

[1]Different prescriptions can be found in the literature, see for example Ref. [28]

In the t'Hooft limit[2], the soft factor is strongly simplified. Regarding the perturbative part, the only surviving diagrams are planar and the exponentiation becomes trivial. Furthermore, We can also make some guess on the non-perturbative part which is, in principle, a fully arbitrary function, since there is no way to extract it independently from experiments. In this limit the non-perturbative contribution of $\widetilde{\mathbb{S}}_{\text{N-h}}$ only regards the incoherent emission of free glueballs, of every possible kind [3]. The function that models this kind of emission is a Poisson distribution, similarly to what happens for photons in QED. In this regard, lattice QCD could play an important role for investigating the properties of the long-distance behavior of N-h soft factors.

1.2.1 2-h Soft Factor

When the process involves two collinear parts, the soft factor connecting them is $\widetilde{\mathbb{S}}_{\text{2-h}}$. In this configuration, there is always a reference frame where the two directions for the collinear parts can be identified to the plus and the minus directions. Following the Collins factorization formalism, the Wilson lines are tilted with respect to these light-like directions by introducing two rapidity cut-offs y_1 and y_2. The original plus and minus directions are restored if the cut-offs are removed, i.e. by taking the limits $y_1 \to +\infty$ and $y_2 \to -\infty$. In total, there are four Wilson lines, two on each side of the final state cut. The only relevant case for applications involves Wilson lines that replace fermionic collinear partons. Hence, in the following I will drop the dependence on the parton types for simplicity. Furthermore, the 2-h soft factor is color singlet, proportional to the identity matrix in color space, i.e. $(\widetilde{\mathbb{S}}_{\text{2-h}})^i{}_j \propto \delta^i_j$. Then, $\widetilde{\mathbb{S}}_{\text{2-h}}$ is defined as the coefficient in front of the delta function. By using the definition in Eq. (1.2) I have:

$$
\begin{aligned}
\widetilde{\mathbb{S}}_{\text{2-h}}(b_T; \mu, y_1 - y_2) = &\, Z_S(\mu, y_1 - y_2) \times \\
&\times \frac{\text{Tr}_C}{N_C} \langle 0 | W(-\vec{b}_T/2, \infty; n_1(y_1))^\dagger W(\vec{b}_T/2, \infty; n_1(y_1)) \times \\
&\times W(\vec{b}_T/2, \infty; n_2(y_2))^\dagger W(-\vec{b}_T/2, \infty; n_2(y_2)) | 0 \rangle |_{\text{NO S.I.}},
\end{aligned}
\tag{1.6}
$$

where N_C is the number of colors available for quarks and antiquarks (3 in QCD). The Eq. (1.6) describes a loop for the full path outlined by the Wilson lines. It starts (e.g.) from $-\vec{b}_T/2$ and goes to $\vec{b}_T/2$, passing through ∞, along the almost plus direction n_1. Then it comes back, again passing through ∞, along the almost minus direction n_2. Notice that the only Lorentz invariant combination for a function depending on two rapidities (e.g. y_1 and y_2) is their difference (e.g. $y_1 - y_2$). It is possible to write the evolution equation for $\mathbb{S}_{\text{2-h}}$ in the b_T-space with respect to both rapidity cut-offs, y_1 and y_2, using a single rapidity-independent kernel $\widetilde{K}(b_T; \mu)$, often referred to as "Collins-Soper

---

[2]$N_C \to \infty$ and $\alpha_S N_C$ is fixed.

[3]In order to preserve unitarity the sum must run over *all* the possible final states.

kernel" or "soft kernel" defined as [7]:

$$\lim_{y_2 \to -\infty} \frac{\partial \log \widetilde{\mathbb{S}}_{\text{2-h}}(b_T; \mu, y_1 - y_2)}{\partial y_1} = \frac{1}{2} \widetilde{K}(b_T; \mu), \tag{1.7a}$$

$$\lim_{y_1 \to +\infty} \frac{\partial \log \widetilde{\mathbb{S}}_{\text{2-h}}(b_T; \mu, y_1 - y_2)}{\partial y_2} = -\frac{1}{2} \widetilde{K}(b_T; \mu). \tag{1.7b}$$

It has an anomalous dimension γ_K:

$$\frac{d \widetilde{K}(b_T; \mu)}{d \log \mu} = -\gamma_K(\alpha_S(\mu)), \tag{1.8}$$

where γ_K depends on μ through the strong coupling α_S and is independent of b_T. Then, $\widetilde{K}$ can be written as:

$$\widetilde{K}(b_T; \mu) = \widetilde{K}(b_T; \mu_0) - \int_{\mu_0}^{\mu} \frac{d\mu'}{\mu'} \gamma_K(\alpha_s(\mu')). \tag{1.9}$$

For large values of $(y_1 - y_2)$, the solution to the evolution equations Eqs. (1.7) is given by:

$$\widetilde{\mathbb{S}}_{\text{2-h}}(b_T; \mu, y_1 - y_2) = \widetilde{\mathbb{S}}_{\text{2-h}}(b_T; \mu_0, 0) \exp \left\{ \frac{y_1 - y_2}{2} \widetilde{K}(b_T; \mu) \right\} + \mathcal{O}\left(e^{-(y_1 - y_2)}\right), \tag{1.10}$$

where the reference values of the RG scale and of the rapidities are chosen to be μ_0 and $y_{1,0} = y_{2,0}$, respectively. In the solution of the evolution equation, two functions appear: the fixed scale soft factor $\widetilde{\mathbb{S}}_{\text{2-h}}(b_T; \mu_0, 0)$ and the soft kernel $\widetilde{K}(b_T; \mu)$. Both of them can be separated in terms of their perturbative and non-perturbative contents by using the $b^\star$ prescription, similarly to what was done in Eq. (1.5):

$$\widetilde{\mathbb{S}}_{\text{2-h}}(b_T; \mu_0, 0) = \widetilde{\mathbb{S}}_{\text{2-h}}(b_T^\star; \mu_0, 0) M_S(b_T); \tag{1.11}$$

$$\widetilde{K}(b_T; \mu) = \widetilde{K}(b_T^\star; \mu) - g_K(b_T). \tag{1.12}$$

Here, we are introducing the **soft model** M_S, which parametrizes the non-perturbative behavior of the 2-h soft factor that does not exponentiate. This is a *new* non-perturbative function that will have to be treated phenomenologically and that will play a pivotal role in the scheme presented in this thesis. On the other hand, the function g_K is a well-known object, representing the non-perturbative behavior of the Collins-Soper kernel. In fact, it will also appear in the study of collinear parts, as I will show in

the next section. Finally, consistency between Eqs. (1.5) and (1.10) requires that:

$$\lim_{\substack{y_1 \to +\infty \\ y_2 \to -\infty}} \int d^{D-2}\vec{k}_{S,T}\, e^{i\vec{k}_{S,T} \cdot \vec{b}_T^\star} \exp\left\{\sum_{W \in \text{webs}} \sum_{\substack{d,d' \in \\ \text{graphs of W}}} F_d(k_{S,T}; \mu, y_i, j_k)\, R_{d,d'}^{(W)}\, c_{d'}\right\} = \frac{y_1 - y_2}{2}\widetilde{K}(b_T^\star; \mu);$$

(1.13a)

$$\lim_{\substack{y_1 \to +\infty \\ y_2 \to -\infty}} M_S(b_T; \mu, y_1 - y_2) = M_S(b_T)\, e^{-\frac{y_1 - y_2}{2} g_K(b_T)};$$

(1.13b)

$$\widetilde{\mathbb{S}}_{2\text{-h}}(b_T^\star; \mu_0, 0) = 1.$$

(1.13c)

Notice that the non-perturbative function $M_S(b_T; \mu, y_1 - y_2)$ loses its dependence on μ in the large rapidity limit, as g_K does not depend on the RG scale. The two non-perturbative functions M_S and g_K should not contribute at small b_T by definition, hence they have to be constrained so that $g_K(b_T) \to 0$ and $M_S(b_T) \to 1$ when $b_T \to 0$. Furthermore, since the Fourier transform of $\widetilde{\mathbb{S}}_{2\text{-h}}$ has to be well behaved, the contribution of g_K and M_S should produce a proper suppression at large b_T. Notice that the factor in front of g_K, being proportional to the difference of the rapidity cut-offs, is always large and negative in the large rapidity cut-off limit. In conclusion, merging the results obtained in Eqs. (1.9) – (1.13) and neglecting corrections that vanish in the large rapidity limit, the 2-h soft factor in b_T space can be written as:

$$\widetilde{\mathbb{S}}_{2\text{-h}}(b_T; \mu, y_1 - y_2) = e^{-\frac{y_1 - y_2}{2}\left[\int_{\mu_0}^{\mu} \frac{d\mu'}{\mu'} \gamma_K(\alpha_S(\mu')) - \widetilde{K}(b_T^\star; \mu_0)\right]} M_S(b_T)\, e^{-\frac{y_1 - y_2}{2} g_K(b_T)}.$$

(1.14)

This result shows that the soft factor itself can be factorized in a purely perturbative part, calculable within pQCD, and a part which is genuinely non perturbative and, inevitably, will have to be committed to a phenomenological model, in this case embedded in the functions $M_S(b_T)$ and $g_K(b_T)$.

Although the definition of Eq. (1.6) implies that $\widetilde{\mathbb{S}}_{2\text{-h}} = 1$ at $b_T = 0$, a direct fixed order perturbative computation of $\widetilde{K}$ does not reproduce the correct behavior in this region. In this regard, since the soft factor is unity at $b_T = 0$, then $\widetilde{K}$ goes to zero at small b_T, but an explicit calculation gives instead a larger and larger value as b_T decreases, forcing $\widetilde{\mathbb{S}}_{2\text{-h}}$ to vanish in $b_T = 0$. This kind of problems arise because the integrated soft factor can be defined through perturbative QCD only as a bare quantity. A solution can be found by applying some regularization procedure, for instance one can modify the $b^\star$ prescription of Eq. (1.4) allowing for the introduction of a new parameter $b_{\text{MIN}} \neq 0$ that provides a minimum value for b_T (see Appendix A).

1.3 Collinear Parts and TMDs

Let's now consider a generic collinear part. All the collinear particles are boosted very strongly in the collinear group direction, that can be identified with the plus direction without loss of generality.

To them, everything outside of the collinear group is moving very fast in the opposite direction, so fast that the only surviving information is the color charge and the direction. In other words, as seen from the collinear factor, the rest of the process is well approximated by a light-like Wilson line flowing in the direction opposite to that of the collinear group, i.e. directed along the minus direction. Assuming for simplicity that the reference parton is a quark, if $\vec{k}_T$ is the total transverse momentum of the collinear group, then the collinear factor is defined as:

$$
\mathbb{C}_{j,h}^{(0)}(\xi, \vec{k}_T; \mu, y_P, -\infty) = \frac{\mathrm{Tr}_C}{N_C} \int \frac{dk^-}{(2\pi)^D}
$$

$$
\tag{1.15}
$$

where the color average Tr_C/N_C is due to the fact that collinear factors are color singlets and, analogously to the 2-h soft factor, they are defined as the coefficient in front of the delta in color space. The Wilson lines are directed along the minus direction and are considered without self energy contributions. Furthermore, similarly to the soft factor (see discussion below Eq. (1.1)), the definition in Eq. (1.15) refers to bare quantities, as expressed by the label "(0)". Therefore, it should be considered as an operative definition, useful to perform explicit perturbative computations. The variable ξ is the light-cone fraction of the momentum k of the reference parton, quark of flavor j, with respect to the momentum P of the reference hadron h, μ is the renormalization scale at which $\mathbb{C}$ is evaluated and y_P is the (very large) rapidity of the reference hadron. The definition of ξ in the initial and final state is given by:

$$
\xi = \begin{cases} x = \frac{k^+}{P^+} & \text{initial state hadron;} \\[2mm] z = \frac{P^+}{k^+} & \text{final state hadron,} \end{cases}
\tag{1.16}
$$

Notice that in the collinear factors we have indicated the full vectorial dependence on $\vec{k}_T$. Differently from the soft case, here the transverse momentum is not the only available vector: there is also at least one more vector, the momentum of the reference hadron, allowing for interesting interplay effects between, e.g. the spin of the parton and the hadron momentum, that constitute the core of all the rich phenomenology related to spin physics. The other important difference with soft factors regards the relation of collinear parts with the rest of the process. As opposed to the soft factor, the collinear factor $\mathbb{C}$ defined in Eq. (1.15) is *totally* blind to the rest of the process. It only depends on its intrinsic variables, as the collinear momentum fraction and the total transverse momentum. This property

generates different degrees of universality between soft and collinear contributions and it will be central in defining a criterion to classify general hadronic processes.

In the Fourier conjugate space, collinear parts are formally defined in terms of QCD operators. We have:

$$
\widetilde{\mathbb{C}}_{j,h}(\xi, \vec{b}_T; \mu, y_P, -\infty) = \int d^{D-2}\vec{k}_T \, e^{i\vec{k}_T \cdot \vec{b}_T} \, \mathbb{C}_{j,h}(\xi, \vec{k}_T; \mu, y_P, -\infty) =
$$

$$
= Z_C(\mu, y_P, -\infty) Z_2\left(\alpha_S(\mu)\right) \frac{\text{Tr}_C}{N_C} \int \frac{dx^-}{2\pi} \, e^{ik^+ x^-} \times
$$

$$
\times \begin{cases}
\langle P(h)|\overline{\psi}^{(0)}(-x/2)\, W_j(-x/2, x/2; \overline{w})\, \psi^{(0)}(x/2)|P(h)\rangle\,|_{\text{NO S.I.}} & \text{initial state,} \\[2ex]
\dfrac{1}{\xi} \times \displaystyle\sum_X \langle P(h), X; \text{out}|\overline{\psi}^{(0)}(-x/2)\, W_j(-x/2, \infty; \overline{w})^{\dagger}|0\rangle \times \\[1ex]
\quad \times \langle 0|W_j(x/2, \infty; \overline{w})\, \psi^{(0)}(x/2)|P(h), X; \text{out}\rangle\,|_{\text{NO S.I.}} & \text{final state,}
\end{cases}
\tag{1.17}
$$

where $x = (0, x^-, \vec{b}_T)$ and $\overline{w}$ is the light-like minus direction of the Wilson line. Since the Wilson lines are defined with bare gluon fields, the (anti)quark fields in the previous definitions are bare too. The wave-function renormalization counterterm Z_2 restores the renormalized fermion fields. The factor Z_C is the UV-counterterm that, order by order, cancels the poles generated by the stretching of the integration outside the collinear momentum region defined through power counting. Its role is totally analogous to the UV-counterterm introduced for soft factors in Eq. (1.2).

Differently from the soft case, here there is another type of *unregulated* divergences due to the light-like direction of the Wilson line. In fact, this implies that the collinear group defined by $\mathbb{C}$, strongly boosted along the plus direction, includes also particles with a low, or even a very large negative rapidity. This contradiction reflects in the computation by inducing the presence of unregulated infinities, known as rapidity divergences. In the Collins factorization formalism, this problem is solved by subtracting out these unphysical contributions from the collinear factor. The subtraction term coincides with the overlapping of the collinear momentum region with the soft momentum region and hence it describes particles which are soft-collinear: being collinear, they see the rest of the process flowing fast along the opposite (minus) direction, but being soft, they feel the collinear group as if it were strongly boosted along the plus direction. Therefore, such subtraction term is a 2-h soft factor (see Eq. (1.6)), with a light-like Wilson line pointing in the minus direction and a Wilson line slightly tilted off the plus direction. This tilting introduces a rapidity cut-off y_1 that regulates all the rapidity divergences associated with the definition of Eq. (1.17). Therefore, in one shot, the subtraction mechanism regulates the rapidity divergences of collinear factors and also cancels the double counting of the soft-collinear contributions. As a result, the *subtracted* collinear factors will give a correct description of truly collinear particles, i.e. quanta with low transverse momentum and large positive rapidity. In fact, after subtraction, the particles in $\mathbb{C}$ can only have a rapidity y such that $y_1 < y < y_P \sim +\infty$. Hence if y_1 is chosen to be sufficiently large, only strongly

boosted particles in the plus direction contribute to $\mathbb{C}$, according to the naive physical intuition. The final definition of the subtracted collinear factor is:

$$\widetilde{\mathbb{C}}_{j,h}^{\text{sub}}(\xi, \vec{b}_T; \mu, y_P - y_1) = Z_C^{\text{sub}}(\mu, y_P - y_1) Z_2\left(\alpha_S(\mu)\right) \lim_{y_{u_2} \to -\infty} \frac{\widetilde{\mathbb{C}}_{j,H}^{(0)}(\xi, \vec{b}_T; \mu, y_P - y_{u_2})}{\widetilde{\mathbb{S}}_{2\text{-h}}^{(0)}(b_T; \mu, y_1 - y_{u_2})}. \quad (1.18)$$

where the label "(0)" means that the corresponding factors are bare functions of bare fields.

Having given the general definition of collinear factors, TMDs can be obtained quite straightforwardly. In fact, as $\mathbb{C}$ is an operator acting onto the space of Dirac spinors, it belongs to the Clifford algebra built from the Dirac matrices $\{\gamma^\mu\}$. Neglecting all the dependences on partonic and hadronic variables, the expansion on the basis of this algebra gives:

$$\mathbb{C}^{\text{sub}} = \mathscr{S}\,\mathbb{I} + \mathscr{V}^\mu\,\gamma_\mu + \mathscr{A}^\mu\,\gamma^5\,\gamma_\mu + i\,\mathscr{P}\,\gamma^5 + i\,\mathscr{T}^{\mu\nu}\,\sigma_{\mu\nu}\gamma^5. \quad (1.19)$$

The TMDs are related to the coefficients $\mathscr{S}, \mathscr{V}, \dots, \mathscr{T}^{\mu\nu}$ of the expansion. Such coefficients can be further expanded in terms of all the Lorentz tensors contributing to the leading twist approximation (see e.g. Ref. [29]). This allows to isolate all the dependence on the vector part of $\vec{b}_T$ leaving a set of scalar functions depending only on the modulus b_T. These scalar functions are the TMDs. For example, the coefficient of γ^+ defines the unpolarized TMDs and the Sivers function:

$$\mathscr{V}^+ = \frac{\text{Tr}_D}{4}\left(\gamma^+ \mathbb{C}^{\text{sub}}\right) = \begin{cases} f_1 - \frac{1}{M}|\vec{S}_T \times \vec{k}_T|f_{1T}^\perp & \text{initial state}, \\ D_1 - \frac{1}{M}|\vec{S}_T \times \vec{k}_{h,T}|D_{1T}^\perp & \text{final state}. \end{cases} \quad (1.20)$$

The definition in Eq. (1.18) naturally extends to TMDs:

$$\widetilde{C}_{j,H}^{\text{sub}}(\xi, b_T; \mu, y_P - y_1) = \frac{\text{Tr}_D}{4}\left(\Gamma \widetilde{\mathbb{C}}_{j,H}^{\text{sub}}(\xi, \vec{b}_T; \mu, y_P - y_{u_2})\right)^{\substack{\text{leading} \\ \text{twist coeff.}}} =$$

$$= (Z_{\text{TMD}})(\mu, y_P - y_1) Z_2\left(\alpha_S(\mu)\right) \lim_{y_{u_2} \to -\infty} \frac{\frac{\text{Tr}_D}{4}\left(\Gamma \widetilde{\mathbb{C}}_{j,H}^{(0)}(\xi, \vec{b}_T; \mu, y_P - y_{u_2})\right)^{\substack{\text{leading} \\ \text{twist coeff.}}}}{\widetilde{\mathbb{S}}_{2\text{-h}}^{(0)}(b_T; \mu, y_1 - y_{u_2})} =$$

$$= (Z_{\text{TMD}})(\mu, y_P - y_1) Z_2\left(\alpha_S(\mu)\right) \lim_{y_{u_2} \to -\infty} \frac{\widetilde{C}_{j,H}(\xi, b_T; \mu, y_P - y_1))}{\widetilde{\mathbb{S}}_{2\text{-h}}^{(0)}(b_T; \mu, y_1 - y_{u_2})} \quad (1.21)$$

where Γ is the proper Dirac matrix combination to extract the desidered TMD and Z_{TMD} is its own UV counterterm. The label "leading twist coeff." means that the TMDs are obtained, after the projection onto the Clifford Algebra, as the coefficients of the expansion at leading twist. The operator definition of TMD as given in Eq. (1.21), which follows directly from the TMD factorization will be referred to as the **factorization definition**. Notice that within this definition, the TMD describes purely collinear particles, as all the soft-collinear contributions have been subtracted out.

In this section, the TMDs have been presented as totally process-independent objects. However, the expansion of Eq. (1.19) also includes terms which do not obey to time-reversal invariance, even at leading twist. TMDs associated to such terms change sign under time reversal transformations, hence are called T-odd TMDs. They are particularly relevant in processes involving initial state hadronic interactions, as Drell-Yan and proton-proton collisions. In fact, the property of being T-odd crucially follows from the action of the time reversal operator on the direction of the Wilson lines appearing into the TMD definition. In particular, future pointing Wilson lines, associated to final state interactions, are mapped into (sign reversed) past pointing Wilson lines, associated to initial state interactions [30]. An important consequence is that T-odd TMD PDFs, when extracted from SIDIS, have the opposite sign with respect to the same TMDs extracted from Drell-Yan [31–35]. Such effects concern controlled and calculable violation of universality, as the TMDs in different reactions can be related to each other [7].

1.3.1 Evolution Equations for TMDs

In the factorization definition[4] of TMDs, Eq. (1.21), a 2-h soft factor appears as a consequence of the subtraction mechanism. Therefore, the results of Section 1.2.1 can be used to write the evolution equation (Collins-Soper evolution) for $\widetilde{C}$ with respect to the rapidity cut-off y_1. On the other hand, the evolution with respect to the scale μ (i.e. the Renormalization Group evolution) is ruled by the anomalous dimension γ_C. The equations are given by:

$$\frac{\partial \log \widetilde{C}_{j,h}(\xi, b_T; \mu, \zeta)}{\partial \log \sqrt{\zeta}} = \frac{1}{2} \widetilde{K}(b_T; \mu), \tag{1.22a}$$

$$\frac{\partial \log \widetilde{C}_{j,h}(\xi, b_T; \mu, \zeta)}{\partial \log \mu} = \gamma_C \left(\alpha_S(\mu), \frac{\zeta}{\mu^2} \right), \tag{1.22b}$$

which, for later convenience, have been re-written in terms of a new variable, ζ, defined as follows:

$$\begin{cases} \zeta = (M_h x)^2 \, e^{2(y_P - y_1)} & \text{initial state hadron;} \\ \zeta = \left(\frac{M_h}{z} \right)^2 e^{2(y_P - y_1)} & \text{final state hadron,} \end{cases} \tag{1.23}$$

where M_h is the mass of the reference hadron, while x and z are the light-cone fractions of the momentum of the reference parton with respect to the hadron. Thanks to the definitions in Eq. (1.16), in both initial and final states the following relation holds: $\zeta = 2(k^+)^2 e^{-2y_1}$. Together with the RG evolution of $\widetilde{K}$ given in Eq. (1.8), the CS evolution of γ_C follows from Eqs. (1.22):

$$\frac{\partial \gamma_C \left(\alpha_S(\mu), \zeta/\mu^2 \right)}{\partial \log \sqrt{\zeta}} = -\frac{1}{2} \gamma_K(\alpha_S(\mu)), \tag{1.24}$$

---

[4]In the following, I will drop the superscript "sub" since, from now on, I will always refer to subtracted quantities.

which gives:

$$\gamma_C\left(\alpha_S(\mu), \zeta/\mu^2\right) = \gamma_C\left(\alpha_S(\mu), 1\right) - \frac{1}{4}\gamma_K(\alpha_S(\mu))\log\frac{\zeta}{\mu^2}. \tag{1.25}$$

Finally, it is a standard result that the solution of TMDs evolution equations reads [7, 36, 37]

$$\widetilde{C}_{j,h}(\xi, b_T; \mu, \zeta) = \underbrace{\left(\widetilde{\mathscr{C}}_j^k(b_T^\star; \mu_0, \zeta_0) \otimes c_{k,h}(\mu_0)\right)(\xi)}_{\text{TMD at reference scales}} \times$$

$$\times \underbrace{\exp\left\{\frac{1}{4}\widetilde{K}(b_T^\star; \mu_0)\log\frac{\zeta}{\zeta_0} + \int_{\mu_0}^{\mu}\frac{d\mu'}{\mu'}\left[\gamma_C(\alpha_S(\mu'), 1) - \frac{1}{4}\gamma_K(\alpha_S(\mu'))\log\frac{\zeta}{\mu'^2}\right]\right\}}_{\text{Perturbative Sudakov Factor}} \times$$

$$\times \underbrace{(M_C)_{j,h}(\xi, b_T)\exp\left\{-\frac{1}{4}g_K(b_T)\log\frac{\zeta}{\zeta_0}\right\}}_{\text{Non-Perturbative content}} \tag{1.26}$$

where the standard choices for the reference values of the scales are[5]:

$$\mu_0 = \mu_b = \frac{2e^{-\gamma_E}}{b_T^\star}; \tag{1.27a}$$

$$\zeta_0 = \mu_b^2; \tag{1.27b}$$

$$\begin{cases} \overline{\zeta}_0 = (M_h x)^2 & \text{initial state;} \\ \overline{\zeta}_0 = \left(\frac{M_h}{z}\right)^2 & \text{final state.} \end{cases} \tag{1.27c}$$

In the solution of the evolution equation the $b_T^\star$ prescription, Eq. (1.4), has been used in order to separate the perturbative from the non-perturbative content, in complete analogy to what was done for the soft factor in Section 1.2.1. In particular, in Eq. (1.26), the non-perturbative behavior of the TMD is described by two functions. The first is g_K, the *same* function that appears in Eq. (1.14), describing the long-distance behavior of the Collins-Soper kernel. The second is the **TMD model** function $(M_C)_{j,h}(\xi, b_T)$, that embeds the genuine non-perturbative behavior of the TMD. It is the collinear counterpart of the soft model but, in contrast, M_C does not depend only on b_T, but also on the collinear momentum fraction ξ, the flavor of the reference parton and the type of reference hadron associated to the collinear part. By definition, the model should not influence the TMD at small b_T. Furthermore, since the Fourier transform of the TMD has to be well behaved, the model should be sufficiently suppressed at large b_T[6]. These properties restrict the behaviour of the non-perturbative

---

[5]Notice that the reference value of ζ is different in the perturbative and in the non-perturbative parts. This follows from the application of the evolution equation to $\widetilde{C}(\xi, \vec{b}_T; \mu_0, \zeta_0)/\widetilde{C}(\xi, \vec{b}_T^\star; \mu_0, \zeta_0)$, which gives $M_C(b_T)\exp(-1/4 g_K(b_T)\log\zeta_0/\overline{\zeta}_0)$.

[6]Although the function g_K gives a suppression factor in Eq. (1.26), it is modulated by (minus) the logarithm of ζ and consequently it may create problems when the rapidity cut-off becomes too low.

function M_C at small and large b_T as follows

$$\lim_{b_T \to 0} M_C(\dots, b_T) = 1; \qquad\qquad \lim_{b_T \to \infty} M_C(\dots, b_T) = 0. \qquad (1.28)$$

The small-b_T perturbative behavior is obtained with a procedure analogous to that used for soft factors. Also in this case, the Fourier transform acts as an analytic continuation of the TMD (and in general of the collinear factors) outside the collinear momentum region defined by power counting. Then, in the small-b_T region, the TMDs can be further factorized in order to expose their hard, soft and collinear contributions. Once again, this gives a collinear factorization theorem that leads to a convolution of a finite (calculable in perturbative QCD) hard coefficient $\mathscr{C}$ with the TMD *integrated* over $\vec{k}_T$, which are the usual PDFs and FFs. The structure is the Operator Product Expansion (OPE) in the r.h.s of the first line in Eq. (1.26):

$$\widetilde{C}_{j,h}(\xi, b_T; \mu, \zeta) \overset{\text{low } b_T}{\sim}$$

$$\sim \left(\widetilde{\mathscr{C}}_j^{\,k}(b_T; \mu, \zeta) \otimes c_{k,h}(\mu) \right)(\xi) = \begin{cases} \left(\widetilde{\mathscr{C}}_{j}^{\ k}(b_T; \mu, \zeta) \otimes f_{k/h}(\mu) \right)(x) & \text{initial state,} \\[2ex] z^{-2+2\varepsilon} \left(d_{h/k}(\mu) \otimes \widetilde{\mathscr{C}}^k_{\ j}(b_T; \mu, \zeta) \right)(z) & \text{final state.} \end{cases}$$

$$(1.29)$$

where $\widetilde{\mathscr{C}}_j^{\,k}$ are the Wilson Coefficients of the OPE, which are matrices in the flavor space. A sum over flavor k is implicit. In the second line of Eq. (1.29) I distinguish the Wilson Coefficients of the initial state from those corresponding to the final state according to the position of their upper and lower flavor indices. For more details on the convolutions see Appendix A. The integrated TMDs are indicated by lowercase letters; in particular $c_{k,h}$ denotes a generic integrated TMD, while f and d label usual PDFs and usual FFs, respectively.

Finally, a comment on integrated TMDs. Their definition suggests that they must coincide with the Fourier transformed TMDs in $b_T = 0$. However, perturbative QCD fails to give the right result in $b_T = 0$ because of the new UV divergences introduced by the integral over the whole range of k_T. The most evident signal of this problem is that $\widetilde{C}$ goes to zero as $b_T \to 0$ and the usual collinear PDFs and FFs are not recovered. This problem is completely analogous to that encountered in Section 1.2.1 and it can be solved in a similar way, by defining a regularization procedure for the definition of the integrated TMDs (see Appendix A).

1.4   *N*-h Universality and Process Classification

The soft and collinear factors presented in the previous Sections play a leading role in the study of non-perturbative QCD. In fact, they encode the long-distance phenomena at the heart of the

hadronization and confinement and hence they offer a unique perspective to investigate the inner properties of strong interactions, through the phenomenological analysis of hadronic processes. The universality of the non-perturbative part of the factorized cross section is then a necessary requirement to have a predictive theory. In fact, if the non-perturbative quantities had to be extracted again for each individual process, the phenomenological analysis of a hadronic cross sections would be reduced to a mere fit of experimental data.

However, soft and collinear factors have a different level of universality. If being universal is the property of being *totally* process-independent, then only collinear parts (and by extension TMDs) can satisfy this requirement[7]. In fact, the factorization definition, introduced in Eq. (1.21), implies that TMDs are completely blind to the global features of the process, like kinematics, as they depend only on their internal variables, i.e. the collinear momentum fraction ξ and the transverse momentum $\vec{k}_T$ of the reference hadron with respect to the reference parton. On the other hand, as pointed out in Section 1.2, soft factors are not completely process-independent. In fact, they depend on the number N of the collinear factors involved in the factorized cross section, each related to its reference parton of type j and to its reference hadron h. Therefore, they are not insensitive to the kinematics of the process in which they appear, because they depend both on the number of the Wilson lines replacing the collinear parts and also on their color representation, which is fixed by the parton type j and differs from quark and gluons. However, at fixed N and for reference partons of the same kind, soft factors are actually the same, modulo crossing symmetry. Clearly, this is a lower level of universality compared to collinear factors.

Since N is the number of reference hadrons participating to the hadronic process, in the following I will define this property as N-h universality. Hence, schematically:

$$\begin{matrix} \text{process dependent} \\ \text{(hard parts)} \end{matrix} < \begin{matrix} \textit{N}\text{-h universal} \\ \text{(soft factors)} \end{matrix} < \begin{matrix} \text{universal} \\ \text{(TMDs)} \end{matrix} \qquad (1.30)$$

where the symbol "$<$" means "less universal than" and TMDs are intended to be defined through the factorization definition of Eq. (1.21). Eq. (1.30) introduces a hierarchy based on universality. The lowest level is occupied by quantities, like the hard part, that are completely process dependent but fully computable in perturbation theory. At the top of the hierarchy there are quantities, like collinear factors and TMDs, that are absolutely process independent: they carry non-perturbative information but their universality properties guarantee that they can be extracted from one particular process and then used in any other. In the middle there are quantities which are only N-h universal, like soft factors. As they carry non-perturbative information, they cannot be computed perturbatively. They too have to be extracted from experimental data, but they can only be used for the processes involving the same number of collinear groups. As a consequence, N-h universality can be exploited to introduce a general way to classify hadronic processes. Formally, a process belongs to the **N-h class** if it globally involves N collinear parts, which can appear in the initial and/or in the final state, in all possible

---

[7]Here, I am not considering the violation of universality associated with T-odd TMDs, discussed at the end of Section 1.3.

combinations and for all the allowed kind of reference partons. This is a very simple criterion, as it does not take into account anything but the numbers of hadrons appearing in the signature of the hadronic process. Then, for instance, $e^- p \to \pi X$ and $p \bar{p} \to \mu^- \mu^+$ belong to the 2-h class, while $p p \to \pi X$ belongs to the 3-h class. Furthermore, kinematics is not considered for this classification. Therefore, the processes are classified *independently* of the factorization scheme (collinear or TMD) required to get the corresponding factorization theorems. For example, $e^+ e^- \to h_1 h_2$ belongs to the 2-h class when the two hadrons are almost back-to-back, where TMD factorization holds, but also when the two hadrons are far from the back-to-back configuration, where instead collinear factorization works.

Different N-h class means different soft factors, as $\mathbb{S}_{\text{N-h}}$ is N-h universal (modulo crossing symmetry and the possible color representations of its Wilson lines). However, belonging to different N-h classes does not affect the the universality of the TMDs, as long as they are defined through Eq. (1.21). This is a crucial issue. In fact, the definition commonly used for TMDs differs from the factorization definition introduced in the previous section, as it combines purely collinear facors with $\widetilde{\mathbb{S}}_{\text{2-h}}$ factors. This is mainly due to historical reasons, since originally TMDs were defined within the 2-h class, in order to make the related TMD factorization theorems suitable for phenomenological analyses of SIDIS and $e^+ e^- \to h_1 h_2 X$ processes.

1.4.1 The 2-h Class

Until 2019, when the BELLE Collaboration provided the first measurement of the $e^+ e^- \to h X$ cross section, differential in the transverse momentum of the detected hadron with respect to the thrust axis [8], only three processes were almost exclusively used to study TMD physics:

- $e^+ e^-$ annihilation into two almost back-to-back hadrons;

- Semi-Inclusive DIS (SIDIS) for small values of transverse momentum of the detected hadron,

- Drell-Yan scattering, for small values of transverse momentum of the lepton pair

These three processes involve in total two collinear parts, distributed in all the possible combinations among initial and/or final state. Therefore, the triplet $\{l\bar{l} \to h_1 h_2; \, l h_1 \to l h_2; \, h_1 h_2 \to l\bar{l}\}$ forms the 2-h class and all these three processes share the same[8] soft factor $\widetilde{\mathbb{S}}_{\text{2-h}}$. This result can be proved formally, see for instance Ref. [7]. Their TMD factorization theorems can be schematically written as:

$$\frac{d\sigma_{\text{2-h}}}{d\xi_1 \, d\xi_2 \, d\vec{q}_T} = \text{H}_{\text{process}} \int d^2\vec{b}_T \, e^{-i\vec{q}_T \cdot \vec{b}_T} \, \widetilde{C}_2(\xi_2, b_T, y_{h_2} - y_2) \widetilde{\mathbb{S}}_{\text{2-h}}(b_T, y_1 - y_2) \widetilde{C}_1(\xi_1, b_T, , y_{h_1} - y_1)$$

(1.31)

---

[8]Notice that in this case charge conservation allows only two fermions as reference partons.

where ξ_i for $i = 1, 2$ is the light-cone momentum fraction of hadron h_i with respect to the associated reference parton, while $\vec{q}_T$ is the transverse momentum of the virtual boson that mediates the interaction. In $e^+ e^- \to h_1 h_2$ it is related to the relative angle between the two hadrons, in SIDIS it is proportional to the transverse momentum of the detected hadron and in Drell-Yan scattering it is the transverse momentum of the lepton pair. Then the TMD factorization theorems presented in Eq. (1.31) are valid when q_T is small compared to the hard energy scale Q that characterizes the process (c.m. energy in $e^+ e^-$ annihilation and Drell-Yan scattering, total momentum transfer in SIDIS). In Eq. (1.31), H_{process} is the process-dependent hard factor. The soft gluon contributions are encoded into the soft factor $\widetilde{\mathbb{S}}_{2\text{-h}}$, defined formally in Eq. (1.6) and written explicitly as solution of the evolution equations in Eq. (1.14). The two TMDs $\widetilde{C}_1$ and $\widetilde{C}_2$ are associated to the two hadrons h_1 and h_2 and describe pure collinear particles, as they are defined through the factorization definition of Eq. (1.21), which leads to the form presented in Eq. (1.26). By using the given definitions for the soft factor and the TMDs, the cross section of Eq. (1.31) does not depend on the rapidity cut-offs y_1 and y_2. In total, there is a minimum of four non-perturbative functions that need to be extracted from experimental data:

- $g_K(b_T)$ defined in Eq. (1.12), that describes the long-distance (large b_T) behavior of the Collins-Soper kernel;

- The soft model $M_S(b_T)$ introduced in Eq. (1.11), that encodes the long-distance behavior of the non-exponentiating part of $\widetilde{\mathbb{S}}_{2\text{-h}}$;

- The two TMD models $M_i(\xi_i, b_T)$, that play the same role of the soft model in the TMDs. In principle, besides the dependence on b_T, they can depend also on the light-cone momentum fraction ξ_i, on the flavor of the reference parton and on the type of reference hadron, see Eq. (1.26)

Clearly, the phenomenological extraction of three unknown multivariate functions is a very difficult task, even combining all the available data on the three reference hadron processes. In particular, M_S is really problematic. It is not associated directly to the observed hadrons and it is always entangled with the TMD models. This is due to the intrinsic correlation between the two collinear parts induced by the soft factor in Eq. (1.31). In conclusion, to make the formula in Eq. (1.31) suitable for phenomenology, we should try and reduce the number of non-perturbative unknown functions.

Remaining within the 2-h class, a brilliant way to solve this problem is to absorb the contribution of the soft factor into the TMDs. Let's consider the combination of soft and collinear contributions in Eq. (1.31); by writing explicitly the factorization definition of the TMDs we have:

$$\widetilde{C}_2(\xi_2, b_T, y_{h_2} - y_2)\,\widetilde{\mathbb{S}}_{2\text{-h}}(b_T, y_1 - y_2)\,\widetilde{C}_1(\xi_1, b_T, y_{h_1} - y_1) =$$

$$= \lim_{\substack{y_{u_1} \to +\infty \\ y_{u_2} \to -\infty}} \frac{\widetilde{C}_2^{\text{uns.}}(\xi_2, b_T, y_{u_1} - y_{h_2})}{\widetilde{\mathbb{S}}_{2\text{-h}}(b_T, y_{u_1} - y_2)}\,\widetilde{\mathbb{S}}_{2\text{-h}}(b_T, y_1 - y_2)\,\frac{\widetilde{C}_1^{\text{uns.}}(\xi_1, b_T, y_{h_1} - y_{u_2})}{\widetilde{\mathbb{S}}_{2\text{-h}}(b_T, y_1 - y_{u_2})} \tag{1.32}$$

All three soft factors in the previous equations have the *same* functional form, but they are functions of different combinations of rapidities. Therefore, they can be re-organized by re-defining the TMDs as (see for instance [7, 37]):

$$\widetilde{C}_1^{\text{sqrt}}(\xi_1, \vec{b}_T; \mu, y_{h_1} - y_n) =$$

$$= \lim_{\substack{y_{u_1} \to +\infty \\ y_{u_2} \to -\infty}} \widetilde{C}_+^{\text{uns.}}(\xi_1, \vec{b}_T; \mu, y_{h_1} - y_{u_2}) \sqrt{\frac{\widetilde{\mathbb{S}}_{\text{2-h}}(b_T; \mu, y_{u_1} - y_n)}{\widetilde{\mathbb{S}}_{\text{2-h}}(b_T; \mu, y_{u_1} - y_{u_2}) \widetilde{\mathbb{S}}_{\text{2-h}}(b_T; \mu, y_n - y_{u_2})}}, \qquad (1.33a)$$

$$\widetilde{C}_2^{\text{sqrt}}(\xi_2, \vec{b}_T; \mu, y_n - y_{h_2}) =$$

$$= \lim_{\substack{y_{u_1} \to +\infty \\ y_{u_2} \to -\infty}} \widetilde{C}_2^{\text{uns.}}(\xi_2, \vec{b}_T; \mu, y_{u_1} - y_{h_2}) \sqrt{\frac{\widetilde{\mathbb{S}}_{\text{2-h}}(b_T; \mu, y_n - y_{u_2})}{\widetilde{\mathbb{S}}_{\text{2-h}}(b_T; \mu, y_{u_1} - y_{u_2}) \widetilde{\mathbb{S}}_{\text{2-h}}(b_T; \mu, y_{u_1} - y_n)}}. \qquad (1.33b)$$

This TMD definition is often referred to as the **square root definition**. There are many advantages to it. First of all, a single rapidity cut-off y_n is sufficient to regularize all rapidity divergences. Furthermore the Collins-Soper evolution equations are unified and symmetrized. The product of Eqs. (1.33a) and (1.33b) reproduces the same combination of Eq. (1.32). As a consequence, the 2-h cross sections assume a "Parton-Model"-like structure, where all soft gluons are reabsorbed into the TMD definition, very convenient for phenomenological applications:

$$\frac{d\sigma_{\text{2-h}}}{d\xi_1 d\xi_2 d\vec{q}_T} = H_{\text{process}} \int d^2\vec{b}_T \, e^{-i\vec{q}_T \cdot \vec{b}_T} \, \widetilde{C}_2(\xi_2, b_T, y_{h_2} - y_2) \widetilde{\mathbb{S}}_{\text{2-h}}(b_T, y_1 - y_2) \widetilde{C}_1(\xi_1, b_T, , y_{h_1} - y_1) =$$

$$= H_{\text{process}} \int d^2\vec{b}_T \, e^{-i\vec{q}_T \cdot \vec{b}_T} \, \widetilde{C}_2^{\text{sqrt}}(\xi_2, b_T, y_{h_2} - y_n) \widetilde{C}_1^{\text{sqrt}}(\xi_1, b_T, , y_{h_1} - y_n). \qquad (1.34)$$

This re-definition of collinear factors actually decreases by one the number of non-perturbative unknown functions to be extracted from experimental data. In particular, the soft model M_S is absorbed by the TMD models M_i. This result can be obtained by comparing directly the factorization definition of Eq. (1.21) with the square root definition of Eq. (1.33a) (the comparison with Eq. (1.33b) is totally analogous). Since the unsubtracted TMDs are the same in the two definitions [7], the comparison proceeds straighforwardly by exploiting the expression given for the 2-h soft factor in Eq. (1.14). We have:

$$\frac{\widetilde{C}^{\text{sqrt}}(\xi, \vec{b}_T; \mu, y_P - y_n)}{\widetilde{C}(\xi, \vec{b}_T; \mu, y_P - y_1)} =$$

$$= \lim_{\substack{y_{u_1} \to +\infty \\ y_{u_2} \to -\infty}} \sqrt{\frac{\widetilde{\mathbb{S}}_{\text{2-h}}(b_T; \mu, y_{u_1} - y_n)}{\widetilde{\mathbb{S}}_{\text{2-h}}(b_T; \mu, y_{u_1} - y_{u_2}) \widetilde{\mathbb{S}}_{\text{2-h}}(b_T; \mu, y_n - y_{u_2})}} \widetilde{\mathbb{S}}_{\text{2-h}}(b_T; \mu, y_1 - y_{u_2}) =$$

$$= \sqrt{M_S(b_T)} \times e^{\frac{(y_1 - y_n)}{2} \widetilde{K}(b_T^\star; \mu)} e^{-\frac{(y_1 - y_n)}{2} g_K(b_T)}, \qquad (1.35)$$

This is an exact result, since all the neglected errors of order $\mathcal{O}\left(e^{-y_1}, e^{-y_n}\right)$ As a consequence, the two definitions are related as:

$$\widetilde{C}^{\,\mathrm{sqrt}}(\xi, \vec{b}_T; \mu, y_P - y_1) = \sqrt{M_S(b_T)} \times \widetilde{C}(\xi, \vec{b}_T; \mu, y_P - y_1). \tag{1.36}$$

Therefore, the TMDs defined with the square root definition are obtained from the TMDs defined with the factorization definition simply multiplying them by a square root of the soft model M_S. This is a very important result, as it shows that the choice of TMD definition only affects the long-distance behavior of the TMDS (at large b_T) while having no impact on the perturbative part. Consequently, in momentum space, C^{sqrt} will differ from C mainly in the small k_T region. In other words, the absorption of the soft gluons contributions into the collinear parts can be interpreted as a *deformation* of the TMD models, which in the two definitions are related as[9]:

$$M_C^{\mathrm{sqrt}}(\xi, b_T) = M_C(\xi, b_T) \times \sqrt{M_S(b_T)}, \tag{1.37}$$

where the dependence of M_C on the flavor of the reference parton and on the kind of reference hadron has been omitted for simplicity. Then, the fact that the product of $\widetilde{C}_1^{\,\mathrm{sqrt}}$ and $\widetilde{C}_2^{\,\mathrm{sqrt}}$ gives exactly the same combination of Eq. (1.32) follows straightforwardly, since:

$$M_2(\xi_2, b_T) M_S(b_T) M_1(\xi_1, b_T) \equiv M_2^{\mathrm{sqrt}}(\xi_2, b_T) M_2^{\mathrm{sqrt}}(\xi_1, b_T). \tag{1.38}$$

In conclusion, the square root definition offers an ideal framework to perform the phenomenological study of the 2-h class of processes since, as a result of the manipulations that lead to Eq. (1.38), it succeeds in reducing the number of unknown non-perturbative functions appearing in the cross section.However, the square root definition makes it impossible to disentangle the non-perturbative soft effects due to M_S which, instead, remains explicit when using the factorization definition for the TMD. Distributing the 2-h soft factor to the two TMDs as in Eq. (1.34) lowers their level of universality, as it contaminates the truly universal collinear parts with an object like $\widetilde{\mathbb{S}}_{2\text{-h}}$ which is universal only inside the 2-h class. On the other hand, abandoning the square root definition of the TMDs in favor of the factorization definition, will force us to face the soft factor problem and take a new (and potentially very hard) challenge: reformulating the way we do phenomenology, in terms of newly defined fundamental objects, where the soft factors are modeled explicitly rather than absorbed in the definition of the TMDs.

---

[9]This relation holds only in one direction: if TMDs are re-defined through the square root definition, then their non-perturbative models are related to their counterparts in the factorization definition through Eq. (1.37). However, there are cases in which M_C is multiplied by $\sqrt{M_S}$ but the definition of Eqs. (1.33) is not recovered.

1.4.2 The 1-h Class

Processes that involve only one reference hadron are DIS and $l^+l^- \to hX$, where one single hadron appears either in the initial state or in the final state. Any TMD observable derived from them necessarily requires the measurement of one additional quantity, to specifies the direction with respect to which the transverse momentum is considered. In the 2-h class this is not necessary, as the direction of one of the hadrons provides a natural reference. The direction of the relevant parton is indeed the most natural choice to investigate the 3D structure of hadrons and, for annihilation events, this direction coincides with the axis of the jet in which the hadron is detected. In such case, the determination of the thrust axis is a valuable experimental estimate of the fragmenting parton direction (see Appendix B). In the Collins factorization formalism this additional variable is not taken into account, since the reference parton can be directed along *any* direction as long as it does not deviate too much from that of the reference hadron. The implementation this kind of information into the formalism presented in Sections 1.2 and 1.3 will be investigated in the next Chapters.

Furthermore, the two above mentioned processes of the 1-h class have another common feature. Both in DIS and in $e^+e^- \to hX$ there is *always* at least one collinear factor which is not associated to any observed hadron. This peculiar situation appears anytime real emissions, carrying a large transverse momentum, are produced in the hard scattering. Then, each of these highly transverse partons generate an independent jet of particles in the final state. If no hadrons are detected in these jets, then the associated collinear factors do not have any reference hadron. At any order in perturbation theory, there is no final state escaping the cut and the whole collinear subgraph is completely crossed by it. As a consequence, the collinear divergences associated to the collinear factor can be consistently avoided by deforming all the integration contours in the UV momentum region. The neat effect is that such collinear contributions become fully perturbative objects, as well as the hard factor. For a rigorous proof see Ref. [7]. Therefore, in the following, I will refer to these highly transverse jets as "hard jets". The processes belonging to the 1-h class are, intrinsically, much more inclusive than those belonging to the 2-h class. Therefore, they always present (at least one) perturbative collinear factor, even when kinematics forbids the production of hard jets, i.e. for small values of momentum transfer in DIS or for a 2-jet final state topology in annihilation processes. This is pictorially represented in Fig. 1.2.

On the other hand, the role of soft gluons in the 1-h class is not so obvious. In general, when TMD effects are not considered, if there is at least one hard jet, then the whole soft factor of the process becomes trivial. This is a fundamental issue in deriving collinear factorization theorems and can easily be understood in terms of momentum conservation. In fact, the soft transverse momentum is inevitably overpowered by the large transverse momentum of the parton that generates the hard jet, and hence it can be neglected. As a consequence, the soft factor is integrated and becomes unity. This follows straightforwardly from the operator definition of Eq. (1.2) and it is shown explicitly for
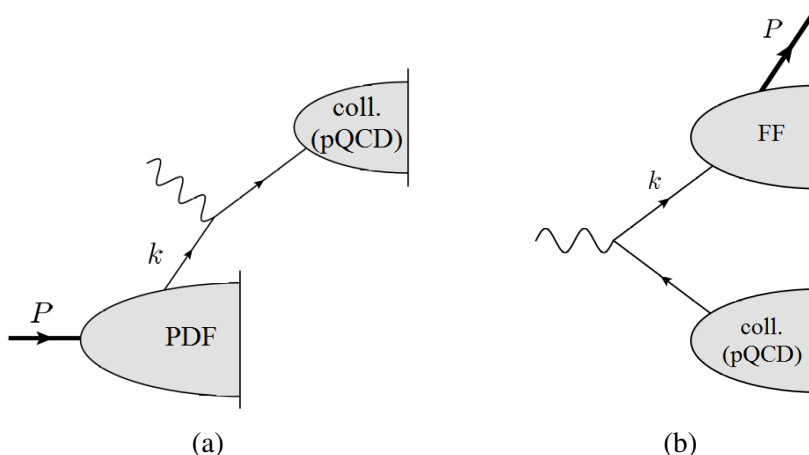
Fig. 1.2 Pictorial representation of hadronic tensors in DIS (a) and in $l^+l^- \to hX$ (b). In both cases, a parton generated in the hard scattering is associated to a collinear factor completely crossed by the final state cut and hence computable in perturbation theory. The soft gluon emissions are not shown.

$\widetilde{\mathbb{S}}_{\text{2-h}}$ in Appendix A. For a rigorous proof see Ref. [7]. When the soft factor is trivial, it is common to gather all the perturbative collinear factors associated with the hard jets together with the hard subgraph, in order to join all the perturbative contributions into a single object, which plays the role of a partonic cross section. However, when TMD effects are taken into account, there are kinematics configurations that forbid the production of hard jets but nevertheless still allow for the presence of a perturbative collinear factor. In this cases, the soft transverse momentum is unavoidably connected to the transverse momentum of the collinear parton associated with the jet, and hence it can be somehow accessed experimentally. This issues will be addressed in the next Chapter, where I will consider the case of $e^+e^- \to hX$, in the case where the thrust axis is determined.

1.5   Conclusions

Following the Collins factorization formalism, soft factors and TMDs are defined as in Section 1.2 and 1.3, respectively. They both are fundamental objects in developing factorization theorems, as they encode the non-perturbative behavior of QCD. They are universal, but in a different manner: while TMDs are truly universal objects and once extracted they can be used in any cross section that requires their contribution, soft factors have a minor degree of universality. They can be considered universal in the same sense of TMDs only for processes with the same number N of collinear parts. Such property has been defined "N-h universality" in Section 1.4 and hadronic processes have been classified in N-h classes according to it. The 2-h class is a particularly relevant case, since the classic TMD factorization theorems for e^+e^- annihilation into two hadrons, SIDIS and Drell-Yan have been determined within it. For this reason, the commonly used definition for the TMDs is not the factorization definition presented in Eq. (1.21), but rather the square root definition of Eqs. (1.33), in

which the soft factor $\widetilde{\mathbb{S}}_{\text{2-h}}$ appearing in the 2-h cross sections is absorbed into the TMDs themselves. Such re-definition of collinear factors is *optimal* for the 2-h class, as it beautifully simplifies the 2-h cross section making it suitable for phenomenological applications as shown in Section 1.4.1. As long as we restrict to 2-h processes, the square root definition constrains the phenomenological analyses enough to allow for the extraction of the non-perturbative functions appearing in the cross sections, at the cost of a total loss of information about the long-distance behavior of the soft factor, since the soft model M_S is completely absorbed into the TMDs and does not play an active role in the factorization theorems anymore.

In the next Chapters, I will consider $e^+e^- \to hX$, which is a 1-h process. Therefore, it must present a soft factor different from $\widetilde{\mathbb{S}}_{\text{2-h}}$. The square root definition of TMDs cannot be extended to this process straightforwardly, as we have at most to compensate for the differences of the soft gluons contribution. The methodology proposed in this thesis aims to follow a different approach. Instead of using the TMDs defined with the usual square root definition, I will adopt the factorization definition as fundamental. In this way, TMDs keep their universality and can be used also outside the 2-h class. Also, soft factors are promoted from mysterious black boxes to active characters in phenomenological analyses. In fact, in this framework their non-perturbative content must be extracted from experimental data as well as that of the TMDs. In particular, combining the data of $e^+e^- \to hX$ with the data of 2-class processes, it would be possible to access directly to M_S. In other words, in this framework phenomenological analyses are constrained not by decreasing the number of non-perturbative unknown functions, but instead by increasing the number of processes that can be exploited. In this regards, Eqs. (1.36) and (1.37) are particularly important from the phenomenological point of view, as they relate the TMDs obtained from data analyses based on the square root definition to the TMDs extracted using the factorization definition. The simple relation between the two definitions allows to profit of the past experience and to benefit of all the results obtained in previous analyses, while extending the scheme to all those processes which could not be considered before, because they belong to a different hadron class. Special experimental efforts will be required in order to gather a large number of high quality data corresponding to several different processes, which will then be analyzed simultaneously in a completely consistent framework. The latest analyses of the BELLE Collaboration and the current plans towards the realization of a new Electron Ion Collider (EIC) are indeed moving towards this direction [8, 38–40].

28

Chapter 2

$e^+e^- \to hX$ as a 1-h class process

2.1 Introduction

Recently, the BELLE collaboration has measured $e^+e^- \to hX$ cross section, as a function of P_T, the transverse momentum of the detected hadron with respect to the thrust axis [8] at a c.m. energy of about 10 GeV. This can be considered a break-through measurement in the investigation of the 3D structure of hadrons, as it offers a direct glance to the transverse motion of the fragmenting partons. Here the role of partons transverse momenta can be explored through a slightly different perspective with respect to the usual TMD processes that, during the last twenty years, have become the benchmark of TMD studies:, $e^+e^- \to h_1 h_2$, SIDIS and Drell-Yan scattering. These data [8], rich of information and characterized by very high statistics, might allow to perform phenomenological analyses of an unprecedented quality. On the other hand, the theory community has been facing several difficulties in developing suitable TMD factorization theorems for this process, which hides a series of pitfalls that other TMD processes do not present.

The Collins factorization formalism, as presented in Ref. [7], cannot be directly applied to $e^+e^- \to hX$. According to the classification introduced in Section 1.4, having only one hadron detected in the final state, the process considered by BELLE falls into the 1-h class. Therefore, the contribution of the soft gluons is described by a soft factor *different* from that appearing into the 2-h cross sections. As a consequence, the cross section of $e^+e^- \to hX$ cannot be casted in a form that allows to define the TMDs in the conventional way, i.e. by including part of the soft radiation generated in the process inside the TMDs themselves through the square root definition, Eq. (1.33). This is a serious impediment which endangers the possibility to exploit the valuable information encoded in the BELLE experimental data in phenomenological studies. On the other hand, the factorization definition introduced in Eq. (1.21) preserves the universality properties of the TMDs by leaving out any process-dependent soft content. One intriguing consequence of adopting this definition is that soft factors must now play an active role in phenomenological analyses, as their non-perturbative content has to be extracted from experimental data as well as the TMDs.

Event-shape variables are extremely important tools for studying hadronic processes, as they are safe from soft and collinear divergences and have reduced experimental uncertainties. In particular, one of the most used event-shape variables is thrust, defined in Eq. (B.13). Its value T describes the topology of the final state of the process, ranging from $T = 0.5$ for a perfectly spherical symmetric distribution to $T = 1$. for an exactly pencil-like event. In the intermediate configurations, the particles in the final state group gather and generate the jets: thrust keeps track of the number of jets, which decreases as T increases. In particular, the number of jets corresponds to the total number of collinear factors in the final state, whether they are associated to a reference hadron or not. Therefore, the classification of hadron processes is not affected by the value of T. In other words, $e^+e^- \to hX$ belongs to the 1-h class regardless of its final state topology.

The measurement of thrust is crucial to get a TMD observable from e^+e^- annihilation into a single hadron. In fact, the thrust axis provides a valid estimate of the axis of the jet in which the hadron is detected, which coincides with the direction of the fragmenting parton (see Appendix B for further details). Hence, according to the discussion in Section 1.4.2, the determination of the thrust is that further information that specifies the direction with respect to which the transverse momentum of the detected hadron has to be considered. On the other hand, the value of T also introduces a further correlation among the momenta generating the soft and the collinear subgraphs, in addition to the usual correlation induced by momentum conservation.

The aim of this thesis, and in particular of the following Chapters, is to provide a consistent framework in which solid TMD factorization theorems can be developed for the $e^+e^- \to hX$ scattering process, on the basis of the definitions presented in Chapter 1. The factorized cross section will be differential in three variables:

- The fractional energy z_h of the detected hadron, defined in Eq. (B.7);

- The thrust T, defined in Eq. (B.13);

- The transverse momentum P_T of the detected hadron with respect to the thrust axis, assumed to be the direction of the jet to which h belongs, the same direction of the fragmenting parton.

A very detailed description of the $e^+e^- \to HX$ kinematics, with special focus on the configuration of the BELLE experiment, is presented in Appendix B.

2.2 General structure of the cross section

Regardless of the final state topology, the general structure of the cross section of $e^+e^- \to hX$ is given by the Lorentz contraction of a leptonic tensor $L_{\mu\nu}$, corresponding to the initial state configuration, together with the hadronic tensor $W_h^{\mu\nu}$, which describes the strong-interaction contribution to the

process. Labeling P the momentum of the detected hadron, we have:

$$\frac{d\sigma}{\left(d^3\vec{P}/2E_P\right)_{\text{LAB}} d^2\vec{P}_T\, dT} = \frac{4\alpha^2}{Q^6} L_{\mu\nu} W_h^{\mu\nu}. \tag{2.1}$$

where the Lorentz invariant phase space measure of P is intended to be expressed in the LAB-frame:

$$\left(\frac{d^3\vec{P}}{2E_P}\right)_{\text{LAB}} = \frac{Q^2}{8} z_h\, dz_h\, d\cos\theta\, d\phi \left[1 + \mathcal{O}\left(\frac{M_h^2}{Q^2}\right)\right], \tag{2.2}$$

where θ is the angle of the detected hadron relative to the electron, while ϕ is its angle with respect to the X-axis in the LAB-frame. The cross section measured by BELLE is insensitive to the value of θ, as well as the azimuthal angle[1] ϕ, hence in the final result they will be integrated out. Therefore:

$$\frac{d\sigma}{dz_h\, d^2\vec{P}_T\, dT} = z_h \frac{\alpha^2}{2Q^4} \int_0^{2\pi} d\phi \int_{-1}^1 d\cos\theta\, L_{\mu\nu} W_h^{\mu\nu}(z_h, T, \vec{P}_T). \tag{2.3}$$

These angular integrations can be easily carried out after giving the explicit definitions of the leptonic and the hadronic tensor.

The leptonic tensor is defined as the lowest order of the electromagnetic vertex $e^+e^- \to \gamma^\star$ with unpolarized leptons, and it is given by:

$$L^{\mu\nu} = l_1^\mu l_2^\nu + l_2^\mu l_1^\nu - g^{\mu\nu} l_1 \cdot l_2, \tag{2.4}$$

where, as in Appendix B, l_1 and l_2 are the momenta of the electron and the positron, respectively.

The hadronic tensor $W_h^{\mu\nu}$ depends on the momentum P of the outgoing hadron and on the momentum q of the boson connecting the initial with the final state. Furthermore, it encodes the whole dependence on the thrust T, as it describes the final state contribution to the process. Its formal definition is:

$$
\begin{aligned}
W_h^{\mu\nu}(P, q, T) &= \\
&= 4\pi^3 \sum_X \delta(p_X + P - q)\, \delta(T - T_{\text{def.}}(p_X, P)) \langle 0| j^\mu(0)|P, X, \text{out}\rangle \langle P, X, \text{out}|j^\nu(0)|0\rangle = \\
&= \frac{1}{4\pi} \sum_X \int d^4z\, e^{iq\cdot z} \delta(T - T_{\text{def.}}(p_X, P)) \langle 0| j^\mu(z/2)|P, X, \text{out}\rangle \langle P, X, \text{out}|j^\nu(-z/2)|0\rangle, \tag{2.5}
\end{aligned}
$$

where j^μ are the electromagnetic currents for the hadronic fields and $T_{\text{def.}}$ corresponds to the definition of thrust given in Eq. (B.13). The final state is represented as $|P, X, \text{out}\rangle$ and corresponds to the topology associated with the thrust value and to the measured transverse momentum of the hadron

---

[1]This is significant only if the X-axis in the LAB-frame can be defined unambiguously, as in the case of polarized leptons.

with respect to the thrust axis. The factor $1/(4\pi)$ in the last line coincides with the normalization used in Ref. [7]. The definition of Eq. (2.5) is hardly usable for explicit computational purposes. For this reason, it is useful to decompose the hadronic tensor in terms of Lorentz-invariant structure functions:

$$W_h^{\mu\nu} = \left(-g^{\mu\nu} + \frac{q^\mu q^\nu}{q^2}\right) F_{1,h} + \frac{\left(P^\mu - q^\mu \frac{P\cdot q}{q^2}\right)\left(P^\nu - q^\nu \frac{P\cdot q}{q^2}\right)}{P\cdot q} F_{2,h}. \tag{2.6}$$

Then, the projections of $W_h^{\mu\nu}$ onto its relevant Lorentz tensors are:

$$-g_{\mu\nu} W_h^{\mu\nu} = 3F_{1,h} + \frac{z_h}{2} F_{2,h} + \mathcal{O}\left(\frac{M^2}{Q^2}\right); \tag{2.7a}$$

$$\frac{P_\mu P_\nu}{Q^2} W_h^{\mu\nu} = \left(\frac{z_h}{2}\right)^2 \left[F_{1,h} + \frac{z_h}{2} F_{2,h}\right] + \mathcal{O}\left(\frac{M^2}{Q^2}\right), \tag{2.7b}$$

and they are much easier to be computed explicitly in perturbation theory.

Given the Lorentz structures of the leptonic tensor, Eq. (2.4), and of the hadronic tensor, Eq. (2.6), it is quite easy the derivation the following decomposition into transverse (T) and longitudinal (L) contributions of the full differential cross section:

$$2\pi \frac{d\sigma}{dz_h\, d\cos\theta\, d\phi\, d^2\vec{P}_T\, dT} = \frac{3}{8}\left(1 + \cos^2\theta\right) \frac{d\sigma_T}{dz_h\, d^2\vec{P}_T\, dT} + \frac{3}{4}\sin^2\theta \frac{d\sigma_L}{dz_h\, d^2\vec{P}_T\, dT}. \tag{2.8}$$

By using this expression, the integrations over ϕ and θ of Eq. (2.3) are straightforward. The result is:

$$\frac{d\sigma}{dz_h\, d^2\vec{P}_T\, dT} = \frac{d\sigma_T}{dz_h\, d^2\vec{P}_T\, dT} + \frac{d\sigma_L}{dz_h\, d^2\vec{P}_T\, dT}. \tag{2.9}$$

Moreover, by exploiting the Eqs. (2.7), the transverse and the longitudinal components of the cross section can be related to the structure functions of the hadronic tensor:

$$\frac{1}{\sigma_B} \frac{d\sigma_T}{dz_h\, d^2\vec{P}_T\, dT} = z_h F_{1,h}(z_h, \vec{P}_T, T); \tag{2.10a}$$

$$\frac{1}{\sigma_B} \frac{d\sigma_L}{dz_h\, d^2\vec{P}_T\, dT} = \frac{z_h}{2}\left(F_{1,h}(z_h, \vec{P}_T, T) + \frac{z_h}{2} F_{2,h}(z_h, \vec{P}_T, T)\right), \tag{2.10b}$$

where σ_B is the Born cross section:

$$\sigma_B = \frac{4\pi\alpha^2}{3Q^2}. \tag{2.11}$$

An interesting case occurs when the projection of the hadronic tensor with respect to $P_\mu P_\nu$, Eq. (2.7b), is zero (or can be neglected). In this case, the two structure functions are not independent
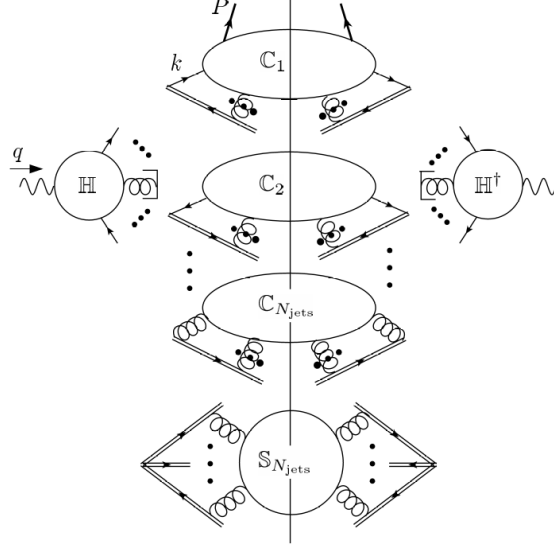
Fig. 2.1 Leading momentum regions for the hadronic tensor $W_h^{\mu\nu}$. The hard subgraphs, one on each side of the final state cut, are labeled by $\mathbb{H}$. The soft subgraph, labeled by $\mathbb{S}_{N_{\text{jets}}}$, represent the contribution of the soft gluons. It has as many Wilson lines as the number of jets in the final state. The collinear subgraphs are labeled by $\mathbb{C}_i$, for $i = 1, \dots N_{\text{jets}}$. Only $\mathbb{C}_1$ contains non-perturbative contributions.

anymore and in fact $F_{2,h} = -\frac{2}{z_h} F_{1,h}$. As a consequence, the hadronic tensor can be written as:

$$W_{h;(T)}^{\mu\nu} = H_T^{\mu\nu} F_{1,h}, \tag{2.12}$$

where I defined the transverse tensor:

$$H_T^{\mu\nu} = \left[-g^{\mu\nu} + \frac{P^\mu q^\nu + P^\nu q^\mu}{P \cdot q} - q^2 \frac{P^\mu P^\nu}{(P \cdot q)^2} \right]. \tag{2.13}$$

Furthermore, the longitudinal cross section vanishes. Hence, in this case the detection of a hadron perpendicular to the beam axis is suppressed.

2.3 Leading momentum regions in $e^+e^- \to hX$

The topology of the final state is determined by the value of thrust T: the closer T to 1, the lower the number N_{jets} of observed jets. The minimum $N_{\text{jets}} = 2$ corresponds to a 2-jet configuration while the limit $N_{\text{jets}} \to \infty$ is associated with an homogeneous spherical distribution of particles. In e^+e^- annihilation, the 2-jet case is the most probable configuration, as any further jet is associated to an extra power of α_S at partonic level. However, in this section we will not fix N_{jets}, in order to work in the most general case.

The general structure of the hadronic tensor $W_h^{\mu\nu}$ in terms of its hard, soft and collinear contributions is represented in Fig. 2.1, where each blob corresponds to a leading momentum region. The delta on thrust in Eq. (2.5) introduces a correlation among the total collinear and soft momenta flowing into the corresponding subgraph. As a consequence, each blob in Fig. 2.1 acquires a dependence on T. The hard subgraph $\mathbb{H}$ represents the production of N_{jets} partons dressed with all the required far off-shell virtual corrections. Its dependence on T is trivial, as in $\mathbb{H}$ the thrust is fixed to the value that it would acquire for an exact N_{jets}-configuration, i.e. $T = 1$ for $N_{\text{jets}} = 2$, $T \sim 2/3$ for $N_{\text{jets}} = 3$ and so on. Each parton exiting from the hard subgraph generates a collinear factor which results in a jet of particles. Therefore, in total there are N_{jets} collinear factors, all equipped with the proper subtraction of the soft-collinear overlapping terms as in Eq. (1.21). Furthermore, there is a soft subgraph $\mathbb{S}_{N_{\text{jets}}}$ that correlates the collinear contributions. It has as many Wilson lines as N_{jets}^2. The thrust dependence encoded into soft and collinear contribution gives the deviation from the exact value associated with the hard scattering that reproduces the observed topology of the final state. For instance, in the 2-jet case T is close, but not exactly equal, to 1, and this value is obtained only after considering the proper contributions of soft and collinear emissions. The pictorial representation of Fig. 2.1 corresponds to the following equation:

$$
W_h^{\mu\nu}(z_h, \vec{P}_T, T) = \sum_{N_{\text{jets}} \geq 2} \sum_{j_1} \int \frac{d^D k_1}{(2\pi)^D} \sum_{j_2} \int \frac{d^D k_2}{(2\pi)^D} \prod_{\alpha=3}^{N_{\text{jets}}} \int \frac{d^D k_\alpha}{(2\pi)^D} \mathbb{C}_\alpha(k_\alpha)_{j_\alpha}
$$

$$
\times \text{Tr}_D \left\{ P_1 \mathbb{C}_1(k_1, P)_{j_1} \overline{P}_1 \mathbb{H}^\mu_{j_1, \dots j_{N_{\text{jets}}}}(\widehat{k}_1, \dots \widehat{k}_{N_{\text{jets}}}) P_2 \mathbb{C}_2(k_2)_{j_2} \overline{P}_2 (\mathbb{H}^\dagger)^\nu_{j_1 \dots j_{N_{\text{jets}}}}(\widehat{k}_1, \dots \widehat{k}_{N_{\text{jets}}}) \right\}
$$

$$
\times \int \frac{d^D k_S}{(2\pi)^D} \mathbb{S}_{N_{\text{jets}}; j_1 \dots j_{N_{\text{jets}}}}(k_S) \, \delta\left(q - k_1 - k_2 - \sum_\alpha k_\alpha - k_S\right)
$$

$$
\times \delta\left(\vec{P}_T \left[1 + \mathcal{O}\left(\frac{P_T^2}{Q^2}\right)\right] + \frac{P^+}{k_1^+} \vec{k}_T(\vec{k}_{1,T}, \vec{k}_{S,T})\right) \delta\left(T - T_{\text{def.}}(k_1, k_2, \dots, k_{N_{\text{jets}}}, k_S)\right), \quad (2.14)
$$

All quantities in the above equation are computed in the h-frame, where the detected hadron has no transverse momentum and it is directed along the plus direction. However, the hadronic tensor depends on P_T, which is the transverse momentum of the detected hadron *in the parton frame*, where it is the fragmenting parton that has zero transverse component. In the last line of the previous equation, the first delta function sets the relation between the measured transverse momentum $\vec{P}_T$ of the detected hadron and the transverse momentum $\vec{k}_T$ of the fragmenting parton, according to Eq. (B.11). Both of them are considered with respect to the thrust axis, although in different frames. Notice that $\vec{k}_T$ does not necessarily coincide with the total transverse momentum $\vec{k}_{1,T}$ entering into the collinear factor $\mathbb{C}_1$ associated to the detected hadron. In fact, it can also depend on the total soft transverse momentum $\vec{k}_{S,T}$, when the direction of the thrust axis is modified by soft recoiling.

Following the Collins factorization formalism, in the hard contributions $\mathbb{H}$ (and its h.c.), the parton momenta are approximated and only their leading components are considered. This is the meaning of

---

[2]Notice that $\mathbb{S}_{N_{\text{jets}}}$ is a matrix in color space. All its color indices are contracted with the hard subgraphs and the whole hadronic tensor is colorless, as required.

the "$\wedge$" hats on them. In practice, the momentum $\widehat{k}_\alpha$ is k_α projected onto the reference direction w_α of its corresponding collinear part:

$$\widehat{k}_\alpha = w_\alpha \frac{k_\alpha \cdot \overline{w}_\alpha}{w_\alpha \cdot \overline{w}_\alpha}, \tag{2.15}$$

where $\overline{w}_\alpha$ is the direction opposite to w_α. More details can be found in Appendix A. Since the reference frame of the fragmenting parton corresponds (by definition) with the hadron frame, the reference direction of $\mathbb{C}_1$ is the plus direction $w_1 = (1, 0, \vec{0}_T)$ and hence the approximated momentum of the fragmenting quark is simply $\widehat{k}_1 = k_1^+ w_1$. Kinematics impose constraints on the possible values that k_1^+ can assume, since $P^+ < k_1^+ < P^+/z_h$ (see Appendix B.).

In addition to the thrust dependence, each collinear factor $\mathbb{C}_j$ is a function of the total entering momentum k_j and on the type j of the corresponding parton (either a gluon or a quark/antiquark of flavor $j/\bar{j}$), and, being color singlets, they are averaged over the color of the initiating parton. Among them, $\mathbb{C}_1$ and $\mathbb{C}_2$ are associated to the fermionic legs of the quark and the antiquark. Charge conjugation sets $j_2 = \bar{j}_1$. Furthermore, they appear associated to the fermionic projectors, P_i and $\overline{P}_i$ for $i = 1, 2$, which connect them to the hard parts. See Appendix A for more details on the factorization procedure. Since the hard part and the collinear parts are computed in the same frame, the expressions for these projectors are simply:

$$P_i = \frac{\slashed{w}_i \slashed{\overline{w}}_i}{2} \quad \text{and} \quad \overline{P}_i = \frac{\slashed{\overline{w}}_i \slashed{w}_i}{2}, \tag{2.16}$$

where the direction $\overline{w}_i$ indicates the direction opposite to w_i. The projectors defined above will be fundamental in extracting the leading twist FFs of the quark and the anti-quark in the cross section. All the other collinear parts, $\mathbb{C}_\alpha$, are generated by gluons. In this case, the role of the fermionic projectors of Eq. (2.16) is played by a gluon density matrix $\rho_{j'j}$ that encodes the information about the gluon polarization.

Among all collinear factors, only $\mathbb{C}_1$ is really relevant for studying the non-perturbative effects of hadronization. In fact, all the $\mathbb{C}_{i \neq 1}$ are completely crossed by the final state cut apart from $\mathbb{C}_1$, as the detected hadron h is not included in the sum over final states. As discussed in Section 1.4.2, collinear factors not associated to any reference hadron are suppressed in the collinear region they are supposed to describe, since order by order in perturbation theory the integrations contours can be deformed away from the collinear singularity. Consequently, they are effectively full perturbative contributions, in the same sense of the hard factors. They only contribute to the thrust distribution, without affecting the dependence on P_T and z_h of the final cross section. For instance, in the 2-jet case, $\mathbb{C}_2$ is the only one among these perturbative collinear factors. Later on, we will see how its contribution is reduced to the usual jet thrust function defined in Eq. (D.12).

Since $\mathbb{C}_1$ is the only relevant non-perturbative contribution to the cross section, all the information about the hadronization process in encoded into it. Therefore, one would expect to find a straightforward relation between $\mathbb{C}_1$ and the TMD FF which describes how the detected hadron h originates from the fragmentation of a parton of type j_1. However, according to the definitions given

in Section 1.3, TMDs depend only on the intrinsic variables of the collinear group to which they are associated, i.e. the collinear momentum fraction and the relative transverse momentum between reference hadron and reference parton. Any further dependence on the global properties of the process undermines their universality properties. For instance, an eventual dependence on thrust would link the TMDs to the topology of the final state, reducing their applicability to a few, specific kinematic configurations. Therefore, to get a factorization theorem involving a proper TMD FF, we will remove any T-dependent term from $\mathbb{C}_1$ (or any k_1 dependence in the condition that fixed the thrust). This is our first hypothesis on the hadronic tensor:

H.1 The fragmentation process is insensitive to the topology of the final state, or, equivalently, the radiation collinear to the detected hadron does not affect the experimentally measured value of thrust. As a consequence, $\mathbb{C}_1$ does not depend on T.

Later on in this Chapter, this hypothesis will be reconsidered and slightly softened. Finally, in Chapter 3, it will be abandoned and I will show how in the 2-jet configuration there is a kinematic region where the dependence on thrust must be kept inside $\mathbb{C}_1$. This of course does not lead to a TMD FF in the final cross section. For the moment being, we will just assume that this first hypothesis holds as specified in **H.1**.

Much less trivial is the role of soft gluons in Eq. (2.14). They are described by the soft factor $\mathbb{S}_{N_{\text{jets}}}$, which is defined exactly as in Eq. (1.2) but modified to allow for the dependence on thrust, constrained to the value that T assumes in the soft momentum region. The full computation of the soft factor $\mathbb{S}_{N_{\text{jets}}}$ according to its most general definition, Eq. (1.2), will be presented in Chapter 3, for the relevant case of a 2-jet final state topology. For the moment being, I will show how it is possible to deal with $\mathbb{S}_{N_{\text{jets}}}$ by exploiting momentum conservation and some further considerations in order to avoid its explicit, general calculation.

First of all, let's consider the case in which the number of observed jets is greater than two, i.e. $N_{\text{jets}} > 2$. In this case, each perturbative collinear factor must be associated to a hard jet, i.e. generated by a parton with a large transverse momentum (of order Q). This is necessary to have at least three distinct and independent jets of particles in the final state. However, all these hard jets are *evenly distributed* in 3D-space. In fact, given that $k_{1,T}$ and $k_{S,T}$ are much lower than Q, momentum conservation implies that the sum of all transverse momenta of the hard jets is small too, as $\vec{k}_{1,T} + \vec{k}_{S,T} + \sum_{\alpha}^{N_{\text{jets}}} \vec{k}_{\alpha,T} = 0$. Despite this, $\mathbb{C}_\alpha$ is still a perturbative object and this holds because, order by order, it is possible to deform the momenta circulating in $\mathbb{C}_\alpha$ away from the collinear singularity into the UV region. In this sense, we are allowed to consider $\vec{k}_{\alpha,T}$ as a large transverse momentum. Therefore, it is possible to make the sum $\sum_{\alpha}^{N_{\text{jets}}} \vec{k}_{\alpha,T}$ as large as we wish, by applying a suitable deformation to the related integration contours. The problem is that this operation breaks the momentum conservation. It can be considered valid *only if* also the soft transverse momentum can be deformed and considered large, in order to compensate the change induced by the vectors $\vec{k}_{\alpha,T}$. Then, in the momentum conservation $\vec{k}_{1,T}$ is overpowered by the UV-sized momenta and hence the

corresponding delta can be written as:

$$\delta \left(\vec{k}_{1,T} + \sum_{\alpha=2}^{N_{\text{jets}}} \vec{k}_{\alpha,T} + \vec{k}_{S,T} \right) \sim \delta \left(\sum_{\alpha=2}^{N_{\text{jets}}} \vec{k}_{\alpha,T}^{\text{UV}} + \vec{k}_{S,T}^{\text{UV}} \right), \quad \text{for } N_{\text{jets}} > 2. \tag{2.17}$$

where the label "UV" reminds us to consider $\vec{k}_{\alpha,T}$ and $\vec{k}_{S,T}$ in the UV momentum region. Then, if the deformation of $\vec{k}_{S,T}$ is allowed, the soft factor has to be considered a fully perturbative object, on the same footage of the factors $\mathbb{C}_\alpha$. Consequently, the contribution of soft gluons, although non-trivial, turns out to be totally computable in perturbation theory. We can follow the same strategy of collinear factorization and gather all the perturbative contributions (hard subgraphs, the factors $\mathbb{C}_\alpha$, $\mathbb{S}_{N_{\text{jets}}}$) in a single thrust-dependent function playing the role of the partonic cross section. The structure of the final cross section will be the same of that obtained in a collinear factorization scheme but, due to the dependence on the transverse momentum of the detected hadron, the interpretation will be TMD.

If the deformation of the soft transverse momentum is not allowed, the final factorization theorem will look different. This happens when the soft transverse momentum has to be considered as an external variable, with its size fixed so that it belongs to the power counting region, i.e. $k_{S,T} \ll Q$. In this case, it cannot be deformed anymore. This is the configuration in which the soft gluon emissions are able to generate a sensitive deflection of the detected hadron, affecting the measured value of the observed P_T. In fact, in this case, the transverse momentum of the detected hadron is strongly correlated with the soft transverse momentum, which is then constrained by experimental measurement. In the following, we will assume that this is not the case, by requiring our second hypothesis:

H.2 The soft gluon emissions do not affect the size of the measured P_T. As a consequence, the soft factor is a fully perturbative thrust-dependent function.

In Chapter 3 I will drop **H.2** in order to develop a TMD factorization theorem suitable for the kinematic configuration sensitive to soft gluons emissions, in the case of a 2-jet final state. This case is indeed emblematic and represents the benchmark for this kind of calculations. In this configuration there are no hard jets, as the antiquark is emitted backward with respect to the fragmenting quark; hence, it must carry a low transverse momentum to satisfy momentum conservation. Nevertheless, its transverse momentum $\vec{k}_{2T}$ can be deformed into the UV region. As in the general case, the soft transverse momentum needs to be deformed too, in order to preserve momentum conservation. Therefore, the analogue of Eq. (2.17) can be written as:

$$\delta \left(\vec{k}_{1,T} + \vec{k}_{2,T} + \vec{k}_{S,T} \right) \sim \delta \left(\vec{k}_{2,T}^{\text{UV}} + \vec{k}_{S,T}^{\text{UV}} \right), \tag{2.18}$$

Later on, I will show that, if **H.2** holds true, the contribution of soft gluons in the 2-jet case is indeed described by the usual soft thrust function, defined in Eq. (D.6).

Another consequence of the validity of **H.2** is that any information about $\vec{k}_{S,T}$ inside the delta that relates the measured P_T to the transverse momentum of the fragmenting parton can be neglected. In other words, in the last line of Eq. (2.14) we can set $\vec{k}_T \equiv \vec{k}_{1,T}$.

As a consequence of the application of the kinematic requirements **H.1** and **H.2**, the residual dependence of the cross section on the weak components of k_1, k_1^- and k_{1T}, is relegated to $\mathbb{C}_1$, which is connected to the rest of the process only through a convolution on k_1^+.

2.4   Collinear-TMD factorization theorem

Following the discussion in the previous Section, if the two hypothesis **H.1** and **H.2** hold, then the structure of the factorized cross section is analogous to that obtained from a classic collinear factorization theorem, where all the fully perturbative contributions are gathered in the so-called partonic cross section. This represents the full process at parton level and is completely computable by using perturbation theory techniques. Besides the hard subgraphs, the partonic cross section includes also all the perturbative collinear factors associated to the production of hard jets and the soft factor, all thrust-dependent functions predicted, order by order, solely by pQCD. Differently from the usual collinear factorization theorems, however, the final cross section is sensitive to TMD effects, encoded into the collinear subgraph associated to the detected hadron. This contribution is therefore related to a TMD FF.

Then, the final structure results in some sort of hybrid version of collinear and TMD factorization, from now on indicated as **collinear-TMD**. The hadronic tensor can hence be written as:

$$W_h^{\mu\nu}(z_h, \vec{P}_T, T) = \sum_{j_1} \int_{P^+}^{P^+/z_h} dk_1^+ \, \delta \left(\vec{P}_T \left[1 + \mathcal{O}\left(\frac{P_T^2}{Q^2} \right) \right] + \frac{P^+}{k_1^+} \vec{k}_{1,T} \right)$$

$$\times \int \frac{dk_1^- \, d^{D-2}\vec{k}_{1,T}}{(2\pi)^D} \, \mathrm{Tr}_D \left\{ \mathrm{P}_1 \mathbb{C}_1(k_1, P)_{j_1, H} \overline{\mathrm{P}}_1 \mathcal{H}_{j_1}^{\mu\nu}(Q, k_1^+, T) \right\}. \tag{2.19}$$

In the above equation, all the contributions that can be totally predicted by perturbative QCD have been collected in the factor $\mathcal{H}^{\mu\nu}$. Notice that, while the collinear part $\mathbb{C}_1$ depends on all the components of k_1, this fully perturbative term depends only on its leading component, $k_1^+ \equiv \widehat{k}_1$. Then, $\mathbb{C}_1$ and $\mathcal{H}^{\mu\nu}$ are not completely disentangled, because a convolution over k_1^+ will survive. In the following the index "1" related to the fragmenting parton will be dropped, as it has become redundant.

Let's focus first on the contribution given by the collinear factor. Applying the fermionic projectors and parity conservation, the only surviving contribution in the case of $e^+e^- \to hX$ is the coefficient of γ^- in the expansion of Eq. (1.20):

$$\mathrm{P}\mathbb{C}(k, P)_{j,h}\overline{\mathrm{P}} = \gamma^- \, \frac{\mathrm{Tr}_D}{4} \left\{ \gamma^+ \mathbb{C}(k, P)_{j,h} \right\}. \tag{2.20}$$

The Dirac trace of $\gamma^+\mathbb{C}(k,P)_{j,h}$ defines two TMD FFs (as in Eq. (1.20)):

$$\frac{1}{\widehat{z}}\int\frac{dk^-}{(2\pi)^D}\frac{\mathrm{Tr}_D}{4}\left\{\gamma^+\mathbb{C}(k,P)_{j,h}\right\}=$$
$$=D_{1,h/j}(\widehat{z},|-\widehat{z}\,\vec{k}_T|)-\frac{1}{M_h}|\vec{S}_T\times\vec{k}_T|D_{1T,h/j}^{\perp}(\widehat{z},|-\widehat{z}\,\vec{k}_T|),\tag{2.21}$$

where the components of the fragmenting parton momentum k are evaluated in the hadron-frame (see Appendix B). M_h and $\vec{S}_T$ are the mass and the transverse spin of the detected hadron, while $\widehat{z}=P^+/k^+$ is the collinear momentum fraction of the hadron h with respect to the fragmenting parton. It is the partonic version of z_h. The function $D_{1,h/j}$ is the unpolarized TMD FF, while $D_{1T,h/j}$ is the Sivers-like TMD FF. In the following, the sum of their contributions in the second line of Eq. (2.21) will be collectively indicated $D_{j,h}(\widehat{z},-\widehat{z}\,\vec{k}_T)$.

Notice that the TMDs in Eq. (2.21) are defined according to the factorization definition of Eq. (1.21). Therefore, as there is no non-perturbative soft contribution, the rearrangement of soft factors commonly applied to a 2-h class cross sections cannot take place. As a consequence, the final cross section will not contain any TMD defined through the square root definition of Eq. (1.33).

Eq. (2.20) implies that the Dirac trace in Eq. (2.19) acts on the matrix γ^- from Eq. (2.20) and on the fully perturbative factor $\mathscr{H}^{\mu\nu}$. This leads to the definition of the partonic tensor $\widehat{W}_j^{\mu\nu}$, which is the partonic counterpart of the hadronic tensor $W_h^{\mu\nu}$:

$$\widehat{W}_j^{\mu\nu}(\widehat{k},q,T)=\mathrm{Tr}_D\left\{k^+\gamma^-\mathscr{H}_j^{\mu\nu}(Q,k^+,T)\right\},\tag{2.22}$$

where $\widehat{k}=k^+w_1$ (see below Eq. (2.15)) and hence $k^+\gamma^-=\widehat{k}=\sum_{\mathrm{spin}}u(\widehat{k})\bar{u}(\widehat{k})$. Eq. (2.22) is the algebraic expression corresponding to the pictorial representation given in Fig. 2.2. The role of the detected hadron is now played by the fragmenting parton, that has momentum $\widehat{k}$ directed along the plus direction. Analogously to the structure of the hadronic tensor presented in Fig. 2.2, the partonic tensor is composed by hard, soft and collinear contributions. All this terms are fully perturbative thrust-dependent functions. The hard subgraphs, labeled by V and $V^\star$ in Fig. 2.2, are associated to the dressing with virtual emissions of the hard vertex. The soft gluon emissions are described by the perturbative soft factor $S_{N_{\mathrm{jets}}}$. Also, there are as many perturbative collinear factors, labeled by J_i, as the number of detected jets. Notice that, when $N_{\mathrm{jets}}=2$, there is only the contribution J_B associated to the backward radiation. Moreover, since $\widehat{W}_j^{\mu\nu}$ is meant to represent the whole process at parton level, there is also a contribution associated to the radiation collinear to the fragmenting parton. Such term in the final cross section overlaps the collinear momentum region covered by the TMD FF and hence it must be equipped with a proper *subtraction procedure*, which will be described in the next subsection. For the moment being, the partonic tensor (and, by extension, the partonic cross section) is intended to be already subtracted.
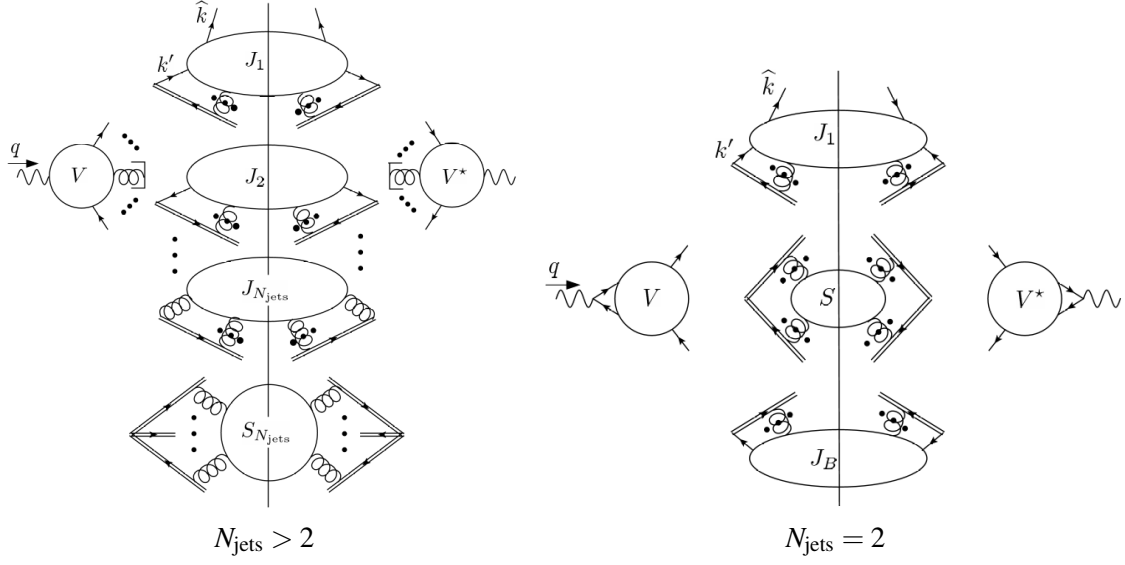
$N_{\text{jets}} > 2$ $N_{\text{jets}} = 2$

Fig. 2.2 Leading regions for the partonic tensor $\widehat{W}_j^{\mu\nu}$ in the case of a multi-jet configuration (left panel) and for a 2-jet configuration (right panel). All the blobs are associated to thrust-dependent functions. The blobs labeled by V (and its complex conjugate) are associated to the virtual dressing of the hard vertex, while those labeled by J_i are related to the radiation along the i-th direction. In the 2-jet case the label "B" stand for "backward radiation". The soft gluon emissions are described by the perturbative thrust-dependent function $S_{N_{\text{jets}}}$. Being the partonic representation of the whole process, there is also a blob, labeled by J_1, describing the radiation collinear to the fragmenting parton of momentum $\widehat{k}$. Such contribution in the final cross section overlaps the collinear momentum region covered by the TMD FF and hence it must be equipped with a proper subtraction procedure.

By inserting Eq. (2.20) and Eq. (2.22) into the expression of the hadronic tensor given in Eq. (2.19), we obtain:

$$
\begin{aligned}
W_h^{\mu\nu}(z_h, \vec{P}_T, T) &= \\
&= \sum_j \int_{z_h}^1 \frac{d\widehat{z}}{\widehat{z}} \, \widehat{W}_j^{\mu\nu}(z_h/\widehat{z}, Q, T) \int d^{D-2}\vec{k}_T \left(\widehat{z} D_{j,h}(\widehat{z}, -\widehat{z}\vec{k}_T), \right) \delta\left(\vec{P}_T \left[1 + \mathscr{O}\left(\frac{P_T^2}{Q^2}\right)\right] + \widehat{z}\vec{k}_T \right) = \\
&= \sum_j \int_{z_h}^1 \frac{d\widehat{z}}{\widehat{z}^2} \, \widehat{W}_j^{\mu\nu}(z_h/\widehat{z}, Q, T) D_{j,h}(\widehat{z}, \vec{P}_T) \left[1 + \mathscr{O}(\frac{P_T^2}{Q^2})\right].
\end{aligned}
\tag{2.23}
$$

where in the last step we used the delta function and set the space-time dimension[3] to $D = 4$.

From the last expression given for the hadronic tensor, it is quite easy to recover the final factorized cross section. The partonic analogue of Eq. (2.1) defines the partonic cross section:

$$
\frac{d\widehat{\sigma}_j}{d^3\vec{k}/2E_{\widehat{k}}\, dT} = \frac{2\alpha^2}{Q^6} L_{\mu\nu} \widehat{W}_j^{\mu\nu}.
\tag{2.24}
$$

---

[3] The final result is UV finite.

It represents the partonic process $e^+e^- \to jX$, where j identifies the type of the fragmenting parton, of momentum $\widehat{k}$. The Lorentz invariant phase space in the l.h.s of Eq. (2.24) can be written as:

$$\frac{d^3\vec{\widehat{k}}}{2E_{\widehat{k}}} = \frac{1}{2}d|\vec{\widehat{k}}|\,|\vec{\widehat{k}}|\,d\cos\theta\,d\phi = \frac{Q^2}{8}\frac{z_h}{\widehat{z}}d\left(\frac{z_h}{\widehat{z}}\right)d\cos\theta\,d\phi, \qquad (2.25)$$

with θ and ϕ being the same angles appearing in Eq. (2.2), as the momentum of the fragmenting parton is approximated in such a way to be directed in the same direction of the detected hadron. In conclusion, the final result for the factorized cross section is:

$$\frac{d\sigma}{dz_h\,d^2\vec{P}_T\,dT} = \sum_j \int_{z_h}^1 \frac{d\widehat{z}}{\widehat{z}}\frac{d\widehat{\sigma}_j}{d(z_h/\widehat{z})\,dT}\,D_{j,h}(\widehat{z},\vec{P}_T)\left[1 + \mathscr{O}(\frac{P_T^2}{Q^2},\frac{M_h^2}{Q^2})\right]. \qquad (2.26)$$

This is the announced collinear-TMD factorization theorem. It has the same structure of the classic collinear factorized cross sections; however, instead of being a convolution between a partonic cross section and a FF, Eq. (2.26) it contains the convolution of a partonic cross section with a TMD FF. Schematically:

Collinear factorization	Collinear-TMD factorization
$\widehat{\sigma}_j \otimes \underbrace{d_{h/j}}_{\text{FF}}$	$\widehat{\sigma}_j \otimes \underbrace{D_{h/j}}_{\text{TMD FF}}$

As in usual collinear factorization theorems, the partonic cross section must be equipped with a proper subtraction mechanism in order to cancel the double counting due to the overlapping with the collinear momentum region. This issue will be addressed in Section 2.4.1.

Moreover, as already stressed, the TMDs in Eq. (2.26) are defined through the factorization definition of Eq. (1.21) instead of the commonly used square root definition of Eq. (1.33). This is a general feature of collinear-TMD factorization theorems. In fact, since the soft gluon contribution is totally perturbative, there are no other non-perturbative terms a part from those encoded into the TMDs. In practice, the TMD model extracted from $e^+e^- \to hX$ is different from that extracted from $e^+e^- \to h_1h_2$, since the latter contains part of the information associated with the soft gluon emissions that correlate the two collinear parts related to the two hadrons, i.e. a square root of the soft model M_S, as explicitly shown in Eq. (1.37). This is particularly relevant when performing a phenomenological analysis that combines data of single- and double hadro-production, or, more generally, when comparing the TMDs extracted from a collinear-TMD factorization theorem as that in Eq. (2.26) with the TMDs historically defined in the 2-h class. In these regards see, for example, two different approaches adopted in Refs. [9, 18].

The factorization theorem presented in Eq. (2.26) contains the full vectorial dependence on the transverse momentum $\vec{P}_T$ of the detected hadron. However, the azimuthal angle in the XY-plane of the parton frame cannot be determined experimentally and hence the only dependence on $\vec{P}_T$ is on its modulus. In fact, the only angular dependence in the TMD contribution $D_{j,h}$ may originate from

the Sivers-like contribution $|\vec{S}_T \times \vec{P}_T|$ (see Eq. (2.21)). On the other hand, as explained in Ref. [38], the transverse spin of the hadron is orthogonal to its transverse momentum with respect to the axis of the jet, identified with the thrust axis. Hence $|\vec{S}_T \times \vec{P}_T| = \pm S_T P_T$ for any choice of the X-axis in the parton frame. Therefore, the integration over the azimuthal angle associated to $\vec{P}_T$ is trivial and results just in a 2π factor on the r.h.s of Eq. (2.26). Consequently, the factorization theorem can also be written as:

$$\frac{d\sigma}{dz_h \, dP_T^2 \, dT} = \pi \sum_j \int_{z_h}^1 \frac{d\widehat{z}}{\widehat{z}} \frac{d\widehat{\sigma}_j}{d(z_h/\widehat{z}) \, dT} \, D_{j,h}(\widehat{z}, P_T) \left[1 + \mathscr{O}(\frac{P_T^2}{Q^2}, \frac{M_h^2}{Q^2})\right]. \tag{2.27}$$

where:

$$D_{j,h}(\widehat{z}, P_T) = D_{1,h/j}(\widehat{z}, P_T) \mp \frac{\widehat{z}}{M_h} S_T P_T D_{1T,h/j}^\perp(\widehat{z}, P_T). \tag{2.28}$$

Finally, according to Section 1.3, since TMDs are properly defined in the Fourier conjugate space, it is more convenient to write the cross section using their b_T-space counterparts, given by:

$$D_{j,h}(\widehat{z}, P_T) \left[1 + \mathscr{O}(\frac{P_T^2}{Q^2})\right] = \int \frac{d^2\vec{b}_T}{(2\pi)^2} \, e^{i\frac{\vec{P}_T}{\widehat{z}} \cdot \vec{b}_T} \, \widetilde{D}_{j,h}(\widehat{z}, b_T), \tag{2.29}$$

where the factor $1/\widehat{z}$ in the Fourier factor is due to the change of variables from $\vec{k}_T$ (h-frame) to $\vec{P}_T$ (p-frame), as $\vec{b}_T$ has been defined as the variable conjugate to $\vec{k}_T$. Finally, the factorization theorem can also be written as:

$$\frac{d\sigma}{dz \, dP_T^2 \, dT} = \pi \sum_j \int_{z_h}^1 \frac{d\widehat{z}}{\widehat{z}} \frac{d\widehat{\sigma}_j}{d(z_h/\widehat{z}) \, dT} \int \frac{d^2\vec{b}_T}{(2\pi)^2} \, e^{i\frac{\vec{P}_T}{\widehat{z}} \cdot \vec{b}_T} \, \widetilde{D}_{j,h}(\widehat{z}, b_T) \left[1 + \mathscr{O}(\frac{M_h^2}{Q^2})\right]. \tag{2.30}$$

From Eq. (2.29) and also comparing the last version of the factorization theorem with Eqs. (2.26) and (2.27), it appears as if the Fourier transform had absorbed the corrections to the final result of order $\mathscr{O}\left(P_T^2/Q^2\right)$. As stressed in the first chapter, the Fourier transform acts as an analytic continuation extending the TMD also beyond the original momentum region. This is an important effect to keep in mind when performing any phenomenological application based on formulae like Eq. (2.30). In fact, the TMD is originally modeled in the b_T-space and afterward tested on data, in the transverse momentum space. Therefore, the cross section showed in Eq. (2.30), even if formally well defined for any value of P_T, can only be trusted where $P_T \ll Q$ or, more precisely, where $P_T \ll P^+ = z_h Q/\sqrt{2}$, which is the actual condition that allows to consider the outgoing hadron as a collinear particle, according to the power counting rules.

2.4.1 Subtraction Mechanism and Rapidity cut-offs

The collinear-TMD factorization theorems devised above show a rather simple structure, and phenomenological analyses based on them surely benefits from it. However, there are two issues that in the previous sections have not be considered. The first is the need for a subtraction procedure of the partonic cross section. As already stressed, having arranged the terms in the final result as in Eq. (2.26) leads to an overlapping between the momentum regions covered by the TMD FF and the partonic cross section. Secondly, in all the formulas provided above, the TMDs have been presented as depending only on transverse momentum and collinear momentum fraction. However, from Section 1.3, we known that TMDs are also equipped with a rapidity cut-off y_1 (alternatively written as ζ as in Eq. (1.23)). This is required in the subtraction mechanism of the overlapping between soft and collinear momentum regions, as y_1 acts as a lower bound for the rapidity of the particles described by the TMD, which are supposed to be collinear, hence very fast moving along their reference direction. On the other hand, physical observables should not depend on the regularization procedure used to weight the divergences encountered in their computations. Rapidity divergences are not an exception. However, clearly, the factorization theorems presented in Section 2.4 do not satisfy this requirement. In fact, the TMD FFs have a very specific dependence on ζ, given by their Collins-Soper evolution equation presented in Eq. (1.22). The partonic cross section surely cannot evolve in the opposite way, as it does not depend on b_T.

This is one of the issues, possibly the most important, related to collinear-TMD factorization theorems. Later on in this Chapter and more deeply in the next, I will show how a dependence on the rapidity cut-off survives in the factorized cross section presented in this section, despite the cancellation of *all* the UV and rapidity divergences. This fact has been recently interpreted as an inconsistency of the factorization theorem [17]. However, in this thesis I will follow a different approach, mostly because a clear signal of the failure of the factorization procedure would be the presence of uncancelled divergences in the final cross section, which here is not that case. The only possibility to give a consistent interpretation of a factorization theorem in the form of Eq. (2.26) is to reconsider the role of the rapidity cut-offs. In particular, I will take their explicit presence in the final result as an indication to promote them from mere computational tools to quantities with a deeper physical meaning. From now on, this will be a leitmotiv throughout this thesis, and it will be investigated more and more deeply, as the factorization procedure presented here becomes more accurate.

The unsubtracted partonic tensor $\widehat{W}_j^{\mu\nu;\text{uns.}}$ has been defined in Eq. (2.22). It represents the process $\gamma^\star \to jX$, where j identifies the type of the fragmenting parton, either the flavor of a (anti)quark or a gluon. Its leading regions are represented in Fig. 2.2. However, the definition of Eq. (2.22) is not particularly useful for direct computation. It is actually much easier to derive the partonic analogue of the hadronic tensor $W_h^{\mu\nu}$ from its factorization theorem in Eq. (2.23). This can be obtained by making the following replacements:

- The fragmenting parton plays the role of the detected hadron, hence $h \mapsto j$. Moreover $z_h \mapsto z = k^+/q^+ = z_h/\widehat{z}$ and also $\vec{P}_T \mapsto \vec{k}_T$.

- The radiation collinear to j is generated by a parton of momentum k'. Then the collinear momentum fraction becomes $\widehat{z} \mapsto \rho = k^+/k'^+$.

- The transverse momentum $\vec{k}'_T$ is the total transverse momentum entering the collinear factor, therefore, according to the definitions given in Section 1.3, it must be equal to the transverse momentum of the fragmenting parton (provided that the soft recoiling of the thrust axis is not considered). Hence for the delta function we have the replacement $\delta\left(\vec{P}_T + \widehat{z}\,\vec{k}_T\right) \mapsto \delta\left(\vec{k}'_T - \vec{k}_T\right)$.

Applying these replacements to Eq. (2.23) gives:

$$W_j^{\mu\nu;\text{uns.}}(z, \vec{k}_T, T) = \sum_i \int_z^1 \frac{d\rho}{\rho} \, \widehat{W}_i^{\mu\nu}(z/\rho, Q, T) \left(\rho \, D_{i,j}(\rho, -\rho \vec{k}_T),\right), \qquad (2.31)$$

which is the partonic version of Eq. (2.23) and gives the unsubtracted partonic tensor in transverse momentum space. The collinear-TMD structure of the factorization theorem derived for the hadronic tensor is inherited by its partonic counterpart. In Eq. (2.31) all the quantities are totally computable in perturbation theory. In particular, the function $D_{i,j}$ is the j-from-i TMD FF contribution in momentum space, defined as the partonic version of Eq. (1.15). The Eq. (2.31) encodes the subtraction procedure, as the subtracted partonic tensor is identified with the coefficient $\widehat{W}_i^{\mu\nu}$ in the convolution with the TMDs.

Despite its simplicity, Eq. (2.31) presents some delicate issues that must be considered carefully. First of all, the subtracted partonic tensor must be a finite quantity, which means that it must not show any poles in ε when dimensional regularization is applied. On the other hand, TMD FFs are collinearly divergent. Therefore, such collinear divergence should be passed on also to by the unsubtracted partonic tensor on the l.h.s. of Eq. (2.31). Moreover, as their hadronic counterparts, the functions $D_{i,j}$ are properly defined in the Fourier conjugate space to $\vec{k}_T$. Hence, the expression of Eq. (2.31) should be given in b_T space, in order to deliver a suitable procedure for the determination of the coefficients $\widehat{W}_i^{\mu\nu}$. This operation is less trivial than it looks. The Fourier transform of $D_{i,j}$ gives the *bare* TMD FF contribution, which must be renormalized with the proper UV-counterterm $Z_{\text{TMD};i,j}$. Therefore, since the l.h.s. of Eq. (2.31) is UV-finite, the subtracted partonic tensor $\widehat{W}_i^{\mu\nu}$ has to be considered a bare quantiti too, which needs a renormalization factor that exactly compensate that of the TMDs, i.e.

$Z_{\text{TMD};i,j}^{-1}$. In practice, in the b_T space we have:

$$
\underbrace{\widetilde{\widehat{W}}_j^{\mu\nu;\text{uns.}}(\varepsilon; z, \vec{b}_T, T)}_{\text{coll. divergent}} = \sum_i \int_z^1 \frac{d\rho}{\rho} \underbrace{\widehat{W}_i^{\mu\nu,(0)}(\varepsilon; z/\rho, T)}_{\text{UV divergent}} \underbrace{\rho \, \widetilde{D}_{i,j}^{(0)}(\varepsilon; \rho, \vec{b}_T)}_{\text{UV divergent and coll. divergent}} =
$$

$$
= \sum_{i,k,l} \int_z^1 \frac{d\rho}{\rho} \left[\widehat{W}_k^{\mu\nu}(z/\rho, T) Z_{\text{TMD};i,k}^{-1}(\varepsilon) \right] \left[Z_{\text{TMD};i,l}(\varepsilon) \, \rho \, \widetilde{D}_{l,j}(\varepsilon; \rho, \vec{b}_T) \right]
$$

$$
= \sum_k \int_z^1 \frac{d\rho}{\rho} \widehat{W}_k^{\mu\nu}(z/\rho, T) \underbrace{\rho \, \widetilde{D}_{k,j}(\varepsilon; \rho, \vec{b}_T)}_{\text{coll. divergent}}, \tag{2.32}
$$

where we used $\sum_i Z_{\text{TMD};i,k}^{-1} Z_{\text{TMD};i,l} = \delta_{k,l}$. The previous equation gives the operative definition to compute the subtracted partonic tensor at any order in perturbation theory. In fact, at order α_S^n we have:

$$
\widehat{W}_j^{\mu\nu;[n]}(z, T) = \widetilde{\widehat{W}}_j^{\mu\nu;\text{uns.};[n]}(\varepsilon; z, \vec{b}_T, T) - \sum_k \sum_{m=1}^n \int_z^1 \frac{d\rho}{\rho} \widehat{W}_k^{\mu\nu;[n]}(z/\rho, T) \left(\rho \, \widetilde{D}_{k,j}^{[m]}(\varepsilon; \rho, \vec{b}_T) \right), \tag{2.33}
$$

The explicit NLO expression for the gluon-from-quark and quark-from-quark unpolarized TMD FFs are collected in Appendix A.3.

Eq. (2.32) embeds the procedure commonly applied to RG-renormalize the partonic cross sections in collinear factorization, highlighting once again the hybrid nature of collinear-TMD factorization theorems. As a consequence, the subtracted partonic tensor has an anomalous dimension equal and opposite to the anomalous dimension of the TMD FFs, which depends only on the type j of the fragmenting parton:

$$
\frac{\partial}{\partial \log \mu} \log \left(\widehat{W}_j^{\mu\nu}(z/\rho, T) \right) = -\gamma_D^{(j)}. \tag{2.34}
$$

This property will be explicitly verified in the 2-jet case later on in this chapter. Therefore, the final factorized cross section is RG-invariant:

$$
\frac{\partial}{\partial \log \mu} \left(\frac{d\sigma}{dz_h \, d^2\vec{P}_T \, dT} \right) = 0. \tag{2.35}
$$

The role played by the rapidity cut-offs is much less obvious and the derivation of some kind of CS-evolution for the final cross section can be hardly guessed just by inspection of Eq. (2.31). For this reason, let's consider again the leading region structure of the unsubtracted partonic cross section depicted in Fig. 2.2. Each blob, except V and $V^\star$ associated to the pure virtual hard vertex, is equipped with proper rapidity cut-offs. The soft contribution $S_{N_{\text{jets}}}$ depends on all of them, because its Wilson lines are tilted off the corresponding reference directions. On the other hand, each perturbative

collinear factor J_i depends only on the associated rapidity cut-off y_i, because of the subtraction of the soft-collinear terms as in Eq. (1.21). All these rapidity cut-offs, except y_1 which is associated to the radiation collinear to the fragmenting parton, are combined in such a way that $\widehat{W}_j^{\mu\nu;\text{uns.}}$ does not depend on them. This is the consequence of not integrating over $\vec{k}_T'$ in the J_1 blob. Then, y_1 appears in two different places: the soft function and the collinear factor, J_1. On the other hand, also the TMD FFs depend on y_1. In the subtractions, the cancellation between the dependence on y_1 in $\widehat{W}_j^{\mu\nu;\text{uns.}}$ and in $\widetilde{D}_{i,j}$ is not exact; hence, the subtracted partonic tensor is left with a remaining dependence on the rapidity cut-off. In fact, the subtraction removes the overlapping between the "hard"[4] and the collinear momentum region, but does not affect the soft momenta. Therefore, the dependence of $S_{N_{\text{jets}}}$ on y_1 is uncanceled.

Differently from the dependence on the RG-scale, the dependence on the rapidity cut-off of the subtracted partonic tensor cannot compensate that of the TMDs. In fact, the CS-evolution presented in Eq. (1.22) is ruled by the soft kernel $\widetilde{K}$ which depends on b_T. Hence, the CS-evolution of $\widehat{W}_j^{\mu\nu}$ is inevitably different, as the subtracted partonic tensor does not depend on the transverse momentum. As a consequence, the final factorized cross section is not CS-invariant:

$$\frac{\partial}{\partial \log \sqrt{\zeta}} \left(\frac{d\sigma}{dz_h \, d^2\vec{P}_T \, dT} \right) \neq 0. \tag{2.36}$$

Therefore, in the factorized cross section all the rapidity divergences have been canceled, but an unexpected dependence on the regulator is left in the final result. As discussed at the beginning of this section, this will not be interpreted as a failure of the factorization procedure, but instead as an opportunity to investigate the inner physical nature of the rapidity cut-offs. An observable sensitive both to TMD effects and to thrust offers a beautiful chance to proceed along this path. In fact, there must be an intrinsic relation between the rapidity cut-off used in the Collins factorization formalism and the (experimentally accessible) thrust, T. There is a simple kinematic argument that naively shows this relation. In fact, if y_P is the rapidity of the detected hadron, then, neglecting all mass corrections, its minimum value is associated to the value of T. In fact, there is a kinematic constraint on P_T/z_h, which cannot be larger than $\sqrt{1-T}\,Q$, see Ref. [17]. This follows directly from the definition of thrust in Eq. (B.13). Therefore, in the parton frame:

$$y_P = \frac{1}{2} \log \frac{P^+}{P^-} = \log \frac{z_h Q}{\sqrt{P_T^2 + M_h^2}} \geq -\frac{1}{2} \log (1 - T) + \mathcal{O}\left(\frac{M_h^2}{P_T^2} \right), \tag{2.37}$$

Then, thrust acts as a rapidity cut-off, since y_P can be considered a good estimate for the rapidity of all the particles belonging to the same collinear group of the detected hadron. This role of thrust will be confirmed later in explicit computations. However, within the Collins formalism, it is not possible to set the precise relation between y_1 and T. In this regard, Eq. (2.37) should be considered just as a naive argument based only on kinematics, without claiming to be formally well founded. In any

---

[4]Here "hard" means the momentum region covered by the fully perturbative partonic tensor.

case, since the rapidity cut-off and the thrust are intimately related, the hypotesis **H.1** can be slightly softened: the collinear factor associated to the TMD FFs can depend on the topology of the final state, but only through the rapidity cut-off.

In any case, if y_1 can somehow be associated to a measured quantity, it cannot simply be a mere computational tool: instead it should be promoted to an actual physical observable. Notice that this is a *new* feature. In the past, different methods to regulate rapidity divergences have been developed, and one of the most elegant is the Rapidity Renormalization Group (RRG), used mainly in SCET-based approaches to factorization, see Refs. [41, 42]. In this approach, rapidity divergences are regularized applying a procedure totally analogous to that used for UV divergences, i.e. by introducing an auxiliary scale ν, that is the counterpart of μ, and taking the derivative with respect to $\log \nu$, which plays the role of the CS-evolution. The collinear and TMD factorization theorems obtained with RRG match exactly those derived within the Collins formalism. [43, 44]. Therefore, collinear-TMD factorization must produce a cross section which is not RRG-invariant. Such issue is never encountered with the scale μ, as *any* physical observable is RG-invariant. This holds because μ actually is an auxiliary scale and there is no way to relate it to an observable. experimental measure. Therefore the nature of the scale ν must be deeply different from its RG counterpart. By extension, wherever the regularization procedure is used to treat rapidity divergences, the regulator must acquire a real physical meaning and collinear-TMD factorized observables, like the cross section presented in Eq. (2.27), may be the necessary tools to investigate this important feature.

In the following two sections I will investigate the physical meaning of the rapidity cut-off by using two different methods, suitable for the LO and NLO of the collinear-TMD cross section presented in Eqs. (2.30), for a 2-jet topology of the final state.

2.5 The role of rapidity cut-offs in the lowest order cross sections

In this section, I will present a first attempt to assign more physical significance to the rapidity cut-off. The procedure illustrated here should be viewed as a phenomenological tool that makes the TMDs invariant with respect to the choice of the rapidity cut-off, useful for a LO analysis of the cross section presented in Eq. (2.26). Notice that the transformation presented in this section has nothing to do with the Rapidity Renormalization Group (RRG) mentioned in the previous Sections, used mainly in SCET-based approaches to factorization (see for instance Refs. [41, 42]).

The roughest approximation of the collinear-TMD factorized cross section presented in Eq. (2.26) is obtained by computing the partonic cross section at LO. The result can be found in Eq. (C.7). We will consider the case of a spinless detected hadron for simplicity. As a consequence, the Sivers-like contribution in Eq. (2.21) vanish, and only unpolarized TMD FFs appear in the cross section. Their LL

approximation is given in Eq. (A.59). Therefore the cross section of Eq. (2.30) for spinless hadrons, at LO and LL accuracy is given by:

$$
\left(\frac{d\sigma}{dz\, dP_T^2\, dT}\right)^{\text{LO, LL}} = \frac{4\pi^2\alpha^2}{3z_h^2 Q^2}\, N_C\, \delta(1-T) \int \frac{d^2\vec{b}_T}{(2\pi)^2}\, e^{i\frac{\vec{P}_T}{z_h}\cdot\vec{b}_T} \left(\sum_f e_f^2 d_f(z_h,\mu_b)\right)
$$

$$
\times \exp\left\{\log\left(\frac{Q}{\mu_b}\right) g_1(x) + \frac{1}{4}\log\left(\frac{\zeta}{Q^2}\right) g_2^K(x)\right\}
$$

$$
\times M_{D_{1,f/h}}(z_h, b_T)\, \exp\left\{-\frac{1}{4} g_K(b_T)\log\left(z_h^2\frac{\zeta}{M_h^2}\right)\right\} \left[1 + \mathcal{O}(\frac{M_h^2}{Q^2})\right], \tag{2.38}
$$

where we used the factorization theorem as expressed in Eq. (2.30). The main feature of Eq. (2.38) is that the whole dependence on the rapidity cut-off is contained in the TMD FF. As expected, the final factorized cross section is RG-invariant (trivially in this case) but not CS-invariant. Also, since the LO-LL approximation reduces the whole T-dependence in the final result to a delta function, the kinematics argument of Eq. (2.37) that relates ζ to thrust cannot be used. Therefore, in this case, the rapidity cut-off is a totally arbitrary number, unrelated to any experimentally measured quantity.

At this stage, any attempt to give a physical meaning to the cross section of Eq. (2.38) may seem useless. In fact, such formula is hardly useful for phenomenological analyses, as it applies only to strictly pencil-like configurations, where $T = 1$. Such events are unrealistic in real experiments and the pencil-like configuration can only be considered as an ideal limit for a 2-jet topology. Nevertheless, looking for a solution to this problem gives some interesting insights on the role of the rapidity cut-offs in the Collins factorization formalism and provides a first attempt to assign them a deeper physical meaning.

The cross section in Eq. (2.38) is not CS-invariant because TMDs are not invariant with respect to the choice of the rapidity cut-off. This is not much of a problem, as TMDs are not physical observables and they depend on μ as well as y_1. Hence they can be considered at a fixed, and finite, value of y_1. However, they can be made rapidity cut-off invariant with respect to a new "symmetry" that mixes their perturbative and non-perturbative content, based on a transformation related to a shift of the rapidity cut-off.

The transformation rule for a shift in the rapidity cut-off follows from the behavior of TMDs under the action of the CS-derivative and can easily be obtained from the solution of the evolution equations in Eq. (1.26). Setting y_1 to $\widehat{y}_1 = y_1 - \theta$, where θ is some real number, and neglecting the dependence on all variables except ζ, the TMD in b_T-space transforms as:

$$
\widetilde{C}(\zeta) \mapsto \widetilde{C}(\widehat{\zeta}) = \widetilde{C}(\zeta)\exp\left[\frac{1}{2}\theta\,\widetilde{K}\right], \tag{2.39}
$$

Therefore, the full effect of this transformation is a *dilation factor* which depends on the soft kernel $\widetilde{K}(b_T, \mu)$ and the shift parameter θ. The transformed TMD describes a different physical configuration, as the rapidities of the collinear particles have been shrinked to a narrower range. In particular, as
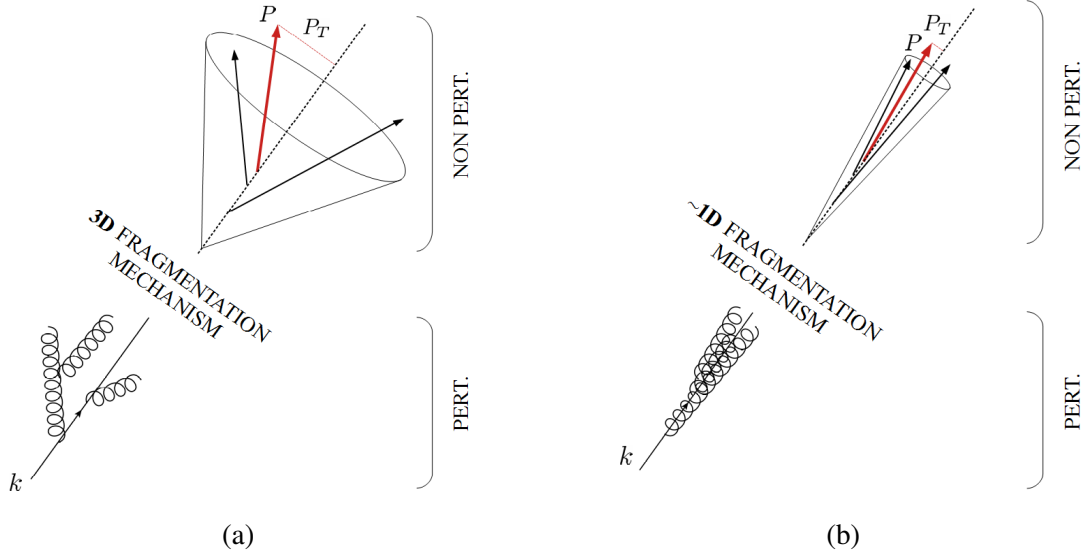
(a)   (b)

Fig. 2.3 Pictorial representation of a TMD Fragmentation Function, in which the separation between perturbative and non-perturbative regime is explicitly shown, corresponding to two different values of the rapidity cut-off. In panel (a) the rapidity cut-off of the TMD FF is set to a generic value y_1. In panel (b) the rapidity cut off has been shifted to $\widehat{y}_1 > y_1$. The two TMDs represent different physical configurations, as the range spanned by the rapidities of the particles belonging to those TMDs are different. The more y_1 increases, the more the fragmentation mechanism approaches a 1-dimensional configuration.

$\widehat{y}_1$ approaches $+\infty$, as required by the Collins factorization formalism, the particles belonging to the collinear group become more and more tightly aligned along their reference direction. In this sense, in the limit of infinite rapidity cut-off, the collinear particle motion is basically 1-dimensional and the 3D picture of the hadron structure may result altered. This is represented pictorially in Fig. 2.3. Since the non-perturbative information about the 3D structure of the hadrons is encoded into the TMD model M_C, the transformation required to compensate the effect of the shift of the rapidity cut-off of Eq. (2.39) can only be associated to M_C. It cannot involve the other non-perturbative function appearing in Eq. (1.26), g_K, as it also appears in the 2-h soft factor and hence its modification would reflect also on the soft gluons contributions. The resulting transformed TMD will describe the same physical configuration of the initial TMD, because the alteration due to the tightened range of rapidity will be totally reabsorbed by the transformed model. Then, for any $\theta < 0$ such transformation is defined as:

$$y_1 \mapsto \mathscr{D}_\theta(y_1) = y_1 - \theta, ; \tag{2.40a}$$

$$M_C \mapsto \mathscr{D}_\theta(M_C) = M_C \exp\left[-\frac{1}{2}\theta\widetilde{K}\right]. \tag{2.40b}$$

The transformed model, Eq. (2.40b), has the same properties of Eq. (1.28). In fact, since the soft kernel $\widetilde{K}$ goes to zero at small b_T, then the dilation factor is 1 for $b_T \sim 0$. Furthermore, since $\widetilde{K}$ is

basically negative, at large b_T the dilation factor give an additional suppression beside those due to the properties of g_K and M_C. Therefore, the transformation defined in Eq. (2.40b) is well defined only for $\theta < 0$, otherwise the behavior of the transformed model at large distances would be compromised. On the other hand, a very large and positive θ would lead to a rapidity cut-off far from the limit $y_1 \to +\infty$. Eqs. (2.40) define a new transformation. Due to the dilation factor in front of the model, such transformation will be referred to as a **rapidity dilation** (RD) and indicated by $\mathscr{D}_\theta$. From the definitions given above one can directly see that TMDs are invariant under rapidity dilations, or RD-invariant:

$$\widetilde{C}(\zeta, M_C) \mapsto \mathscr{D}_\theta \left(\widetilde{C}(\zeta, M_C) \right) = \widetilde{C} \left(\zeta e^{2\theta}, \mathscr{D}_\theta M_C \right) = \widetilde{C}(\zeta, M_C), \quad \text{for any } \theta < 0. \tag{2.41}$$

Notice that being RD-invariant is different from being CS-invariant. In fact, rapidity dilations act not only on the rapidity cut-off, but also on the non-perturbative TMD model, balancing the perturbative and non-perturbative information in order to keep their combination invariant. Rapidity dilations allow to consider the rapidity cut-off larger and larger, while keeping the naive physical picture associated to the TMD to be the same. This is shown in Fig. 2.3, where panel (a) and panel and (b) represent TMDs described by $C(\zeta, M_D)$ and $C(\mathscr{D}_\theta \zeta, M_D)$, respectively, with $\mathscr{D}_\theta \zeta < \zeta$. Interestingly, this interpretation is totally equivalent to considering the two TMDs evaluated within the same range of rapidity but associated to two different non-perturbative models, i.e. interpreting the TMD depicted in panel (a) as described by $C(\mathscr{D}_\theta \zeta, \mathscr{D}_\theta M_D)$ and the TMD in panel (b) as described by $C(\zeta, \mathscr{D}_\theta M_D)$. Roughly speaking, the model associated with a certain choice describes how collinear particles with rapidity in the range[5] $y_1 \le y < \infty$ behave in the non-perturbative regime. Notice that this picture is closely reminiscent of the kinematics argument presented in Eq. (2.37), even if here it is not considered at all. In fact, the higher the rapidity cut-off, the closer the hadronization process to a pencil-like configuration.

Rapidity dilations have to be interpreted as a phenomenological tool. Two groups can independently extract the same TMD from the same set of data for different values of the rapidity cut-off, for instance by using a cross section like Eq. (2.38). Then, rapidity dilations set the relation between the two TMD models derived from the two extractions. A detailed illustrtion of this mechanism can be found in Ref. [12].

Not all quantities encountered in Chapter 1 are RD-invariant. In particular, rapidity dilations have been defined in Eq. (2.40) to make invariant the TMDs as defined in Section 1.3, i.e. with the reference direction coinciding with the plus direction. However, rapidity dilations do not commute with the Z-axis reflection and TMDs associated to the minus direction are not RD-invariant. This is an important issue, as the behaviour under z-axis reflection, which simply exchanges the plus and minus directions, is particularly relevant for processes belonging to the 2-h class (see Sec. 1.4.1), where two TMDs associated to opposite directions appear. If R_Z is the Lorentz transformation that reverses the

---

[5]In the real world, quite different from the massless limit, the upper bound is y_P, the large and positive rapidity of the reference hadron.

Z-axis, then the rapidity of the reference hadron swaps its sign under the action of R_Z. On the other hand, the rapidity cut-off does not represent the rapidity of any real particle, but rather a mere number that sets the minimum value that the rapidity of collinear particles can assume. Hence it is trivially invariant under the action of R_z. However, the particles belonging to the collinear group associated to the TMD in the minus direction should have a very large negative rapidity, consistent with the limit $y_1 \to +\infty$. Therefore, a proper rapidity cut-off would be $y_2 = -y_1$, as if y_1 had changed its sign. Finally, the action of R_Z gives:

$$\begin{cases} y_P & \mapsto R_Z\,(y_P) = -y_P; \\ y_1 & \mapsto R_Z\,(y_1) = y_1 \stackrel{def}{=} -y_2. \end{cases} \tag{2.42}$$

As a consequence, the variable ζ for a TMD in the minus direction is obtained by simply replacing $\zeta_+ \propto \exp\,(y_P - y_1)$ with $\zeta_- \propto \exp\,(y_2 - y_P)$ and the full TMD transforms as:

$$\widetilde{C}_+(\zeta_+) \mapsto R_Z\left(\widetilde{C}_+(\zeta_+)\right) = \widetilde{C}_-(\zeta_-), \tag{2.43}$$

where only the dependence on the rapidity cut-off has been made explicit.

As anticipated, the reflection with respect the Z-axis and rapidity dilations do not commute. In fact, if the rapidity cut-off y_1 of $\widetilde{C}_+$ is shifted, then the rapidity cut-off y_2 of $\widetilde{C}_-$ is shifted as well, but with the sign reversed. This can easily be seen by a direct computation, with the help of Eqs. (2.40a) and (2.42):

$$\mathscr{D}_\theta\,(y_2) = \mathscr{D}_\theta\,(-y_1) = -y_1 + \theta = y_2 + \theta. \tag{2.44}$$

Therefore, according to Eq. (2.40b), the TMD model of $\widetilde{C}_-$ transforms as:

$$\mathscr{D}_\theta\,(M_{C_-}) = M_{C_-} \exp\left[\frac{1}{2}\theta\,\widetilde{K}\right]. \tag{2.45}$$

However, in the $\widetilde{C}_-$ the rapidity cut-off appears with the opposite sign with respect to $\widetilde{C}_+$. Hence, there is no more compensation between the rapidity shift and the transformed model, and the TMDs defined along the minus direction are not invariant under rapidity dilations. In other words, R_Z and $\mathscr{D}_\theta$ do not commute:

$$R_Z\,\mathscr{D}_\theta\,\widetilde{C}_+(\zeta_+) = R_Z\,\widetilde{C}_+(\zeta_+) = \widetilde{C}_-(\zeta_-); \tag{2.46a}$$

$$\mathscr{D}_\theta\,R_Z\,\widetilde{C}_+(\zeta_+) = \mathscr{D}_\theta\,\widetilde{C}_-(\zeta_-) = \widetilde{C}_-(\zeta_-)\exp\left[\theta\,\widetilde{K}\right]. \tag{2.46b}$$

Another relevant object which is not invariant under rapidity dilations is the 2-h soft factor (see Eq. (1.14)). A rapidity dilation acts on $\widetilde{\mathbb{S}}_{2\text{-h}}$ only by shifting the two rapidity cut-offs y_1 and y_2, as the soft model M_S is not affected by the transformation defined in Eq. (2.40). Since $\mathscr{D}_\theta\,(y_1 - y_2) =$

$y_1 - y_2 - 2\theta$, the RD-transformation of the 2-h soft factor is given by:

$$\mathscr{D}_\theta \widetilde{\mathbb{S}}_{\text{2-h}} = \widetilde{\mathbb{S}}_{\text{2-h}} \exp\left[-\theta \, \widetilde{K}\right]. \tag{2.47}$$

As a consequence of Eqs. (2.41), (2.46b) and (2.47), the relevant structure appearing in the 2-h cross sections, Eq. (1.31), is RD-invariant:

$$\mathscr{D}_\theta \left(\widetilde{C}_-(\zeta_-)\widetilde{\mathbb{S}}_{\text{2-h}}(y_1 - y_2)\widetilde{C}_+(\zeta_+)\right) = \left(\widetilde{C}_-(\zeta_-)\exp\left[\theta \, \widetilde{K}\right]\right)\left(\widetilde{\mathbb{S}}_{\text{2-h}}\exp\left[-\theta \, \widetilde{K}\right]\right)\widetilde{C}_+(\zeta_+) \equiv$$
$$\equiv \widetilde{C}_-(\zeta_-)\widetilde{\mathbb{S}}_{\text{2-h}}(y_1 - y_2)\widetilde{C}_+(\zeta_+). \tag{2.48}$$

In particular, notice that $\widetilde{C}_+$ is RD-invariant but not CS-invariant, $\widetilde{C}_-$ and $\widetilde{\mathbb{S}}_{\text{2-h}}$ are nor RD-invariant neither CS-invariant, the 2-h cross sections are both RD-invariant and CS-invariant.

2.6   The role of the rapidity cut-off beyond lowest order

The relation between the rapidity cut-off and thrust can hardly be appreciated in a trivial LO-LL approximation of the factorized cross section, Eq. (2.38), The rapidity dilations presented in Section 2.5 can give some hint about the physical interpretation of the rapidity cut-off in the Collins factorization formalism, but do not relate ζ with T explicitly. Furthermore, they are not sufficient to explain the cross section dependence on the rapidity cut-off beyond the lowest order. In fact in this case, as explained in Section 2.4.1, also the (subtracted) partonic tensor depends on ζ but, differently from the TMDs, it does not include any non-perturbative contribution that can reabsorb such dependence. In terms of Section 2.5, it is nor RD-invariant, neither CS-invariant.

In this section, I will show how the relation between ζ and T can be made explicit by introducing a **topology cut-off** that forces the partonic cross section to describe the proper final state configuration. This is a further variable, not included into the original Collins factorization formalism. Without this extra ingredient, it is not possible to recover a precise relation between the rapidity cut-off and thrust. In particular, I will follow the approach presented in Ref. [13], which is a modified version of the formal derivation of the factorization presented in this Chapter.

The starting point is the collinear-TMD factorization theorem of Eq. (2.26), but the partonic tensor is computed in a non-conventional way. The idea takes inspiration from the available phase space for three particles, which corresponds to a real gluon emission at NLO. Neglecting all the masses and by labeling the three particles momenta as k_i, the squared amplitude and the phase space will depend on all the possible combination of their scalar products, which can be expressed in terms of the following variables:

$$y_1 = \frac{2}{Q^2} k_2 \cdot k_3; \quad y_2 = \frac{2}{Q^2} k_3 \cdot k_1; \quad y_3 = \frac{2}{Q^2} k_1 \cdot k_2, \tag{2.49}$$
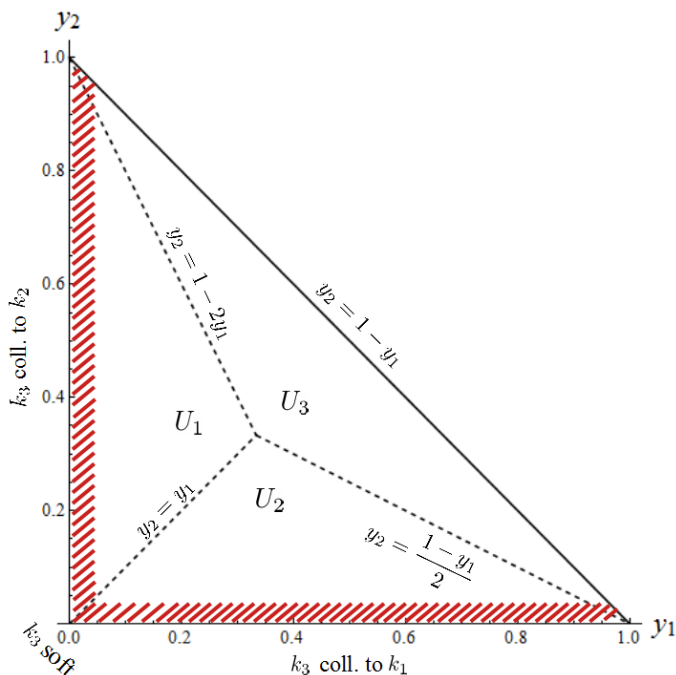
Fig. 2.4 The phase space available for the three final state massless particles of momenta k_1, k_2 and k_3. It cannot extend beyond the edge given by $y_2 = 1 - y_1$ (or $y_3 = 0$), due to momentum conservation. The dashed red bands represent the quasi 2-jet configurations, where y_1 and/or y_2 are zero. The sub-regions U_i correspond to a value of thrust given by $\tau = y_i$.

subject to the constraint $\sum_i y_i = 1$, due to the momentum conservation $q = k_1 + k_2 + k_3$.

Therefore, when $y_1 \to 0$ or $y_2 \to 0$, the momentum k_3 is collinear to k_2 or to k_1, respectively. Instead, when both $y_1 \to 0$ and $y_2 \to 0$, the momentum k_3 is soft. These are the configurations corresponding to a 2-jet topology. A standard result regards the value of the thrust, which corresponds to the minimum among the y_i:

$$\tau = \min \{y_1, y_2, y_3\}, \tag{2.50}$$

where, as commonly set for a 2-jet topology, we have defined the variable $\tau = 1 - T$. Then the 2-jet limit corresponds to $\tau = 0$. Eq. (2.50) allows to divide the available phase space in three regions, as shown in Fig. 2.4. One of the three particles plays the role of the fragmenting parton, therefore it does not cross the final state cut. Assuming that k_1 is not included in the sum over final states, the integration over the phase space involves only k_2 and k_3, and it reduces to a single integration over y_2 after applying the momentum conservation delta. Furthermore, it must be equipped with the condition that fixes thrust, according to Eq. (2.50). With only this limited information, the integration is insensitive to TMD effects. Instead of keeping track of the total transverse momentum associated to the radiation collinear to the fragmenting parton, the TMD dependence can be inserted "by hand" introducing a topology cut-off $\tau_{\text{MAX}}^\perp$ sensitive to TMD effects. Such cut-off forces the phase space

integration to be constrained inside the region denoted by the red bands in Fig. 2.4, by restricting the values that τ can assume to be at most $\tau_{\text{MAX}}^\perp$. Then, the limit $\tau_{\text{MAX}}^\perp \to 0$ corresponds to the 2-jet limit. In order to satisfy **H.2**, the topology cut-off should not act on soft radiation. Finally, the phase space integration is given by:

$$
\Pi_S\left(\tau, \tau_{\text{MAX}}^\perp\right) =
$$

$$
= \int \frac{d^{3-2\varepsilon}\vec{k}_2}{(2\pi)^{3-2\varepsilon}\,2|\vec{k}_2|} \frac{d^{3-2\varepsilon}\vec{k}_3}{(2\pi)^{3-2\varepsilon}\,2|\vec{k}_3|} (2\pi)^{4-2\varepsilon}\,\delta(q - k_1 + k_2 + k_3)\,\theta\left(\tau_{\text{MAX}}^\perp - \tau\right)\sum_i \delta\left(\tau - y_i\right) =
$$

$$
= (4\pi)\frac{1}{2}\frac{1}{(4\pi)^2} S_\varepsilon\, Q^{-2\varepsilon}\,\theta\left(\tau_{\text{MAX}}^\perp - \tau\right)(1-z)^{-\varepsilon}\times
$$

$$
\left\{ \underbrace{\theta\left(z - \frac{2}{3}\right)\int_{\frac{1-z}{z}}^{2-\frac{1}{z}} d\alpha\,\alpha^{-1-\varepsilon}(1-\alpha)^{1-\varepsilon}\,\delta(\tau - (1-z))}_{U_1} + \right.
$$

$$
+ \underbrace{\left[\theta\left(\frac{2}{3} - z\right)\int_0^{\frac{1}{2}} + \theta\left(z - \frac{2}{3}\right)\int_0^{\frac{1-z}{z}}\right] d\alpha\,\delta\left(\alpha - \frac{\tau}{z}\right)}_{U_2} +
$$

$$
\left. + \underbrace{\left[\theta\left(\frac{2}{3} - z\right)\int_{\frac{1}{2}}^{1} + \theta\left(z - \frac{2}{3}\right)\int_{2-\frac{1}{z}}^{1}\right] d\alpha\,\delta\left(\alpha - (1 - \frac{\tau}{z})\right)}_{U_3} \right\}\alpha^{-1-\varepsilon}(1-\alpha)^{1-\varepsilon},
\tag{2.51}
$$

where the following change of variable has been applied:

$$
y_1 = 1 - z, \quad y_2 = \alpha z, \quad y_3 = z(1-\alpha).
\tag{2.52}
$$

The expression in Eq. (2.51) will be our "TMD-inspired" procedure to compute the NLO thrust-dependent phase space integral. Then, we have to compute the square amplitudes corresponding to the various allowed kinematics configurations to obtain the final expression for the unsubtracted partonic tensor within this modified scheme. Notice that, with the procedure introduced above, the factorization of $\widetilde{W}^{\mu\nu;\text{uns.}}$ into its leading regions, as shown in Fig. 2.2(b), is achieved by letting the topology cut-off tend to zero, instead of exploiting the action of the Collins kinematics approximators (see Appendix A). This leads to an important difference with respect to the Collins factorization formalism presented in Chapter 1: without the prescriptions offered by the canonical factorization procedure, there is no trace of rapidity cut-offs. Their role is in fact played by the topology cut-off, which takes the place of ζ. Therefore, this modified version of the formalism shed light on the relation between the rapidity cut-off and the experimentally measured thrust, T.

In the following, I will briefly review the results of Ref. [13] by showing how the final factorized cross section is derived in this approach.
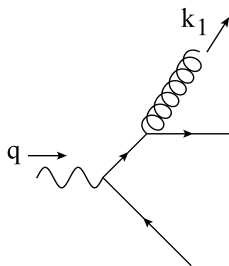
Fig. 2.5 The only 1-loop Feynman graph contributing to $\widehat{W}_g^{\mu\nu}$, when the gluon is emitted by the quark. The emission from the antiquark line is analogous.

2.6.1 Fragmenting Gluon in the Modified Formalism

In a 2-jet topology, the detected hadron is never a product of the fragmentation of a gluon. In fact, of the two jets observed in the final state, one is initiated by the quark, the other by the antiquark. Therefore, any explicit computation must show a suppression corresponding to this channel. In this section, I will show how such suppression is naturally obtained in the modified formalism presented in the previous discussion. Furthremore, being much simpler than the case of a fragmenting fermion, the fragmentation of a gluon serves as an ideal framework to introduce the main features associated to the computation of the final state tensor.

At 1-loop, the only Feynman diagram to be considered is represented in Fig. 2.5, where we assume that the gluon is emitted from the quark line. The emission from the antiquark is totally analogous. Even without performing an explicit computation, it is quite easy to deduce the reasons of the suppression for this kinematics configuration in the 2-jet case. In fact, after emitting the gluon, the fermion cannot deviate drastically from its original direction, otherwise it would generate a third jet. Hence it can only proceed almost collinearly to the gluon. In principle, a 2-jet configuration may be achieved also if the fermion becomes soft or if it is reflected backwards after the emission of the gluon, but such configurations are suppressed by power counting. As a consequence, the only relevant kinematical configuration in the 2-jet limit is given by the fermion being collinear to the emitted fragmenting gluon. However, this is exactly the same configuration that has to be subtracted out in the final result, in order to avoid double counting due to the overlapping with the collinear momentum region.

The squared amplitude is given by:

$$M_g^{\mu\nu;[1]}(\varepsilon; \mu, \{y_i\}) = \left(\text{} \right)^{\mu\nu} , \qquad (2.53)$$

55

where, according to standard conventions (see for instance Ref. [7]) the polarization vector $e(k_1, \lambda)$ of the on-shell fragmenting gluon is defined to have zero plus and minus components[6]. The projections of $M_g^{\mu\nu;[1]}$ onto the relevant Lorentz structures are:

$$-g_{\mu\nu} M_g^{\mu\nu;[1]}(\varepsilon; \mu, \{y_i\}) = H_0 g^2 \mu^{2\varepsilon} 4 C_F \left[1 + 2 \frac{y_1}{(1-y_1)^2} - \varepsilon \right] \frac{y_3}{y_2}; \tag{2.54a}$$

$$\frac{k_{1,\mu} k_{1,\nu}}{Q^2} M_g^{\mu\nu;[1]}(\varepsilon; \mu, \{y_i\}) = H_0 g^2 \mu^{2\varepsilon} 2 C_F \frac{1}{1-\varepsilon} \left[1 + 2 \frac{y_1}{(1-y_1)^2} y_3 - \varepsilon \right] y_3, \tag{2.54b}$$

where H_0 has been defined in Eq. (C.8b). Notice that Eq. (2.54b) is regular in both $y_1 = 0$ and $y_2 = 0$, consequently it is suppressed in the 2-jet limit. The unsubtracted partonic tensor is obtained by integrating the Eqs. (2.54) over the phase space of Eq. (2.51), in the limit where the topology cut-off $\tau_{\text{MAX}}^\perp$ vanishes. The only contribution that survives comes from the integration over the region denoted by U_2 for the projection onto the metric tensor of Eq. (2.54a). In fact, U_2 corresponds to the kinematic configuration where the emitting fermion is collinear to the fragmenting gluon and, as expected, it is the only one not to be suppressed in the 2-jet limit. The result is:

$$\frac{\alpha_S}{4\pi} \left(-g_{\mu\nu} \widehat{W}_g^{\mu\nu,[1]} \right) \overset{\tau_{\text{MAX}}^\perp \to 0}{\sim} H_0 \frac{\alpha_S}{4\pi} J_{g/q}^{[1]}(\varepsilon; \tau, z) \, \theta \left(\tau_{\text{MAX}}^\perp - \tau \right), \quad \text{Re } \varepsilon < 0, \tag{2.55}$$

where $J_{g/q}^{[1]}$ is the 1-loop gluon-from-quark fragmenting jet function, defined in Eq. (D.18). The details of the calculation can be found in Ref. [13]. Now, we have to write the TMD dependence on the topology cut-off explicitly. The fragmenting jet functions result from an integration over the transverse momentum $\vec{k}_T$ entering into the subgraph associated to the radiation collinear to the outgoing parton, in this case the fragmenting gluon. Such transverse momentum is related to thrust through Eq. (D.17), which asserts that τ is proportional to k_T/Q. Therefore, the power counting region where $k_T \ll Q$ corresponds to the 2-jet configuration. Despite this, the integration covers the whole spectrum of k_T. Hence, we can set the topology cut-off in such a way to force the transverse momentum to stay inside the power counting region, by setting an upper limit, for instance equal to the power counting energy scale $\lambda << Q$, used to indicate the size of the collinear momenta. This results in replacing the combination of the gluon-from-quark fragmenting jet function with the topological cut-off by the Fourier transform of the gluon-from-quark generalized fragmentation jet function [45], which will be discussed in more detail in Chapter 3, with the further constraint $k_T \le \lambda$ on the size of the transverse momentum. In practice:

$$\int d^{2-2\varepsilon} \vec{k}_T \, \theta \left(\tau_{\text{MAX}}^\perp - \tau \right) \longmapsto \int d^{2-2\varepsilon} \vec{k}_T \, e^{i\vec{k}_T \cdot \vec{b}_T} \, \theta \left(\lambda^2 - k_T^2 \right). \tag{2.56}$$

---

[6]In general, the only requirement on $e(k_1, \lambda)$ is $k_1 \cdot e(k_1, \lambda) = 0$ and $e(k_1, \lambda) \cdot e(k_1, \lambda)^\star = 1$.
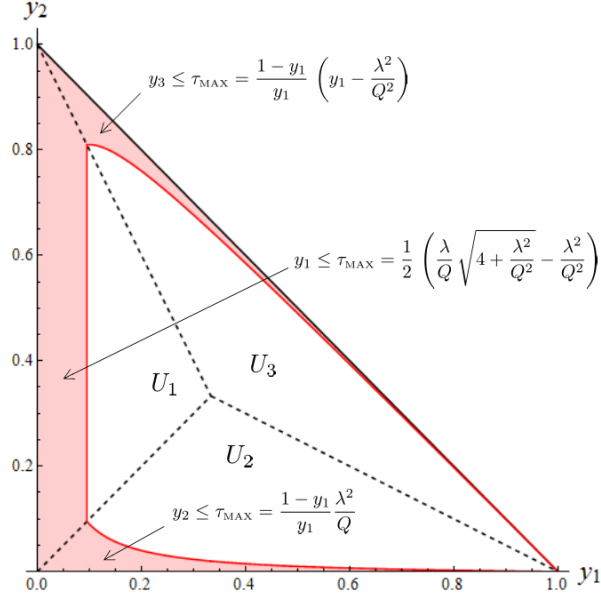
Fig. 2.6 Action of the cut-off $\tau_{\text{MAX}}(\lambda)$ on the phase space for the three final state particles, according to Eq. (2.59). In this case $\lambda = 0.1\,Q$. Notice that the red region shrinks as $\lambda/Q \to 0$.

The neat effect is that the limit $\tau_{\text{MAX}}^{\perp} \to 0$ is replaced by the limit $\lambda \to 0$. Therefore, in this formalism, the unsubtracted partonic tensor is still the partonic counterpart of the whole process, but with the transverse momentum of the fragmenting parton constrained inside the power counting region.

The application of Eq. (2.56) into Eq. (2.55) is equivalent to making the following substitution:

$$J_{g/q}^{[1]}\left(\varepsilon;\tau,z\right)\,\theta\left(\tau_{\text{MAX}}^{\perp}-\tau\right)\longmapsto J_{g/q,\,\text{mod.}}^{[1]}\left(\varepsilon;\tau,z,\lambda\right)=J_{g/q}^{[1]}\left(\varepsilon;\tau,z\right)\theta\left(\frac{\lambda^2}{Q^2}-\frac{1-z}{z}\tau\right),\quad\text{for }\lambda\to 0.$$

(2.57)

This expressions defines the *modified* gluon-from-quark fragmenting jet function at 1-loop. Notice that the whole b_T-dependence is washed away in the limit $\lambda \to 0$. The ε-expansion of the previous expression is not straightforward, because of the interplay between the thrust distributions associated with $J_{g/q}^{[1]}$ and the Heaviside theta containing the cut-off. The result is:

$$\frac{\alpha_S}{4\pi}J_{g/q,\,\text{mod.}}^{[1]}\left(\varepsilon;\tau,z,\lambda\right)=$$
$$=\frac{\alpha_S}{4\pi}2\,C_F\,S_\varepsilon\,\theta(1-z)\frac{1+(1-z)^2-\varepsilon z^2}{z^2}\left(-\frac{1}{\varepsilon}-\log\frac{\mu^2}{\lambda^2}\right)\delta(\tau)+\mathcal{O}\left(\frac{\lambda^2}{Q^2}\right)+\mathcal{O}\left(\varepsilon\right),\quad\text{Re }\varepsilon<0.$$

(2.58)

Comparing Eq. (2.58) to the analogous term in Eq. (2.55), the relation between the topology cut-off

$\tau_{\text{MAX}}^\perp$ and the IR power counting scale can expressed explicitly:

$$\frac{\lambda^2}{Q^2} - \frac{1-z}{z}\tau > 0 \Rightarrow \begin{cases} 0 \le z \le \frac{1}{1+\lambda^2/Q^2} \text{ and } 0 \le \tau \le \frac{z}{1-z}\frac{\lambda^2}{Q^2} \equiv \tau_{\text{MAX}}^\perp(\lambda) \\ \\ \frac{1}{1+\lambda^2/Q^2} \le z \le 1 \text{ and } 0 \le \tau \le 1 \end{cases} \tag{2.59}$$

Notice that this choice sets $\tau_{\text{MAX}}^\perp = 1$ only in a thin slice of the phase space, where z is very close to 1. This fact will be crucial in the fragmenting fermion case, as $z \to 1$ is the effect of a soft approximation which should not effect the action of the topology cut-off according to **H.2**. Furthermore, $\tau_{\text{MAX}}^\perp \to 0$ consistently implies $\lambda^2/Q^2 \to 0$ as expected. Finally, the unsubtracted partonic tensor computed in the modified formalism is:

$$\widehat{W}_{g,\text{mod.}}^{\mu\nu,[1],\text{uns.}}(\varepsilon; z, \tau; \lambda) = H_T^{\mu\nu} \widehat{F}_{1,g,\text{mod.}}^{[1],\text{uns.}}(\varepsilon; z, \tau; \lambda), \quad \text{Re}\,\varepsilon < 0, \tag{2.60}$$

where:

$$\widehat{F}_{1,g,\text{mod.}}^{[1],\text{uns.}}(\varepsilon; z, \tau; \lambda^2/Q^2 \to 0) = \frac{H_0}{2} J_{g/q,\text{mod.}}^{[1]}(\varepsilon; \tau, z, \lambda) \quad \text{Re}\,\varepsilon < 0. \tag{2.61}$$

and the transverse tensor $H_T^{\mu\nu}$ has been defined in Eq. (2.13).

The subtraction mechanism in this modified formalism is totally analogous to the procedure described in Section 2.4.1. The only difference is in the Fourier transform: instead of covering the whole range in k_T, it stops at $k_T = \lambda$ according to Eq. (2.56). Assuming a spinless detected hadron, for simplicity, the modified version of the subtraction term is given by the modified version of the Fourier transform of the gluon-from-quark unpolarized TMD FF $D_{g/q}$, which has been computed at 1-loop in transverse momentum space in Eq. (A.39). Againg, all the b_T-dependence is suppressed by powers of λ^2/Q^2. We have:

$$\frac{\alpha_S}{4\pi} \widetilde{D}_{g/q;\text{mod.}}^{[1]}(\varepsilon; z, \lambda) = \int d^{2-2\varepsilon}\vec{k}_T \, e^{i\vec{k}_T \cdot \vec{b}_T} D_{g/q}^{[1]}(\varepsilon; z, k_T) \theta\left(\lambda^2 - k_T^2\right) =$$

$$= \frac{\alpha_S}{4\pi} 2 C_F S_\varepsilon \frac{1+(1-z)^2 - \varepsilon z^2}{z^3}\left(-\frac{1}{\varepsilon} - \log\frac{\mu^2}{\lambda^2}\right) + \mathscr{O}\left(\frac{\lambda^2}{Q^2}\right) + \mathscr{O}(\varepsilon), \quad \text{Re}\,\varepsilon < 0. \tag{2.62}$$

Therefore, the modified version of the 1-loop subtracted partonic tensor descends directly from Eq. (2.33) and it is given by:

$$\widehat{W}_{g,\text{mod.}}^{\mu\nu;[1]}(z,\tau,\lambda) = \widehat{W}_{g,\text{mod.}}^{\mu\nu,[1],\text{uns.}}(\varepsilon; z, \tau; \lambda) - \sum_k \int_z^1 \frac{d\rho}{\rho} \widehat{W}_k^{\mu\nu;[0]}(z/\rho, \tau)\left(\rho \widetilde{D}_{g/k;\text{mod.}}^{[1]}(\varepsilon; \rho, \lambda)\right) =$$

$$= H_T^{\mu\nu} \frac{H_0}{2}\left[J_{g/q,\text{mod.}}^{[1]}(\varepsilon; \tau, z, \lambda) - \delta(\tau) z \widetilde{D}_{g/q;\text{mod.}}^{[1]}(\varepsilon; z, \lambda)\right] \equiv$$

$$\equiv H_T^{\mu\nu} \widehat{F}_{1,g,\text{mod.}}^{[1]}(z, \tau; \lambda) = \mathscr{O}\left(\frac{\lambda^2}{Q^2}\right), \tag{2.63}$$
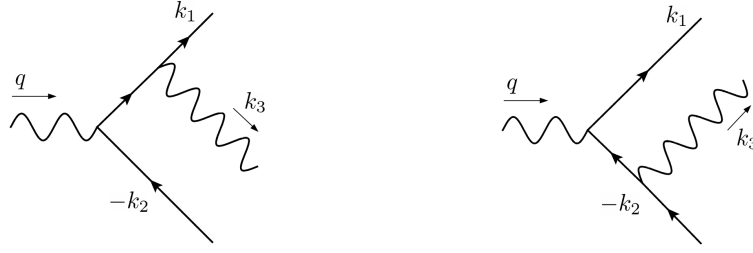
Fig. 2.7 The 1-loop Feynman graphs contributing to $\widehat{W}_f^{\mu\nu}$.

where we used the expression of Eq. (C.6) for the partonic tensor at LO. Notice that $\widehat{W}_k^{\mu\nu;[0]}$ is not affected by the modified formalism as its final state configuration is pure 2-jet. Eq. (2.63) implies a partonic cross section suppressed by $\mathcal{O}\left(\frac{\lambda^2}{Q^2}\right)$ as well:

$$\frac{d\widehat{\sigma}_{g,\,\text{mod.}}^{[1]}}{dz\,dT} = \sigma_B \, z \widehat{F}_{1,\,g,\,\text{mod.}}^{[1]}(z,\,\tau;\lambda) = \mathcal{O}\left(\frac{\lambda^2}{Q^2}\right). \tag{2.64}$$

As expected, the fragmenting gluon configuration is suppressed for a 2-jet topology. Most importantly, in this modified formalism such suppression is given by the limit $\lambda \to 0$ which is ultimately related to the limit $\tau_{\text{MAX}}^{\perp} \to 0$ by Eq. (2.59). Therefore, this is the explicit realization of the expected topological suppression.

2.6.2   Fragmenting Fermion in the Modified Formalism

In this case, the detected hadron is produced by the fragmentation of a fermion of flavor f, assumed to be a quark for simplicity. The case of a fragmenting antiquark is totally analogous. This is the first non-trivial contribution to the thrust-dependence of the final cross section. Furthermore, the modified formalism applied to this kinematic configuration leads to an explicit relation between the topology cut-off and the rapidity cut-off, which turns into a relation with an experimentally accessible quantity, i.e. thrust.

The contribution of the virtual gluon emission (the hard vertex V is represented in Fig. 2.2b) is associated to a pure pencil-like final state; hence it is not relevant for the action of the topology cut-off. The 1-loop result can be found in Appendix C. Therefore, in the following I will focus on the real gluon emission contribution, associated to the two Feynman graphs represented in Fig. 2.7. The 2-jet configuration are obtained when the gluon is collinear to the antiquark (backward radiation), when it is soft and when it is emitted collinearly to the fragmenting quark. The squared amplitudes are given

by:

$$M^{\mu\nu;[1]}_{f,\text{real}}(\varepsilon; \mu, \{y_i\}) =$$

$$(2.65)$$

which leads to the following projections onto the relevant Lorentz structures:

$$- g_{\mu\nu} M^{\mu\nu,[1]}_{f,\text{real}}(\varepsilon; \mu, \{y_i\}) = H_{0,f}\, g^2\, 8 C_F\, \mu^{2\varepsilon} \left[\left(\frac{y_3}{y_1 y_2} - \varepsilon \right) + \frac{(1-\varepsilon)}{2} \left(\frac{y_1}{y_2} + \frac{y_2}{y_1} \right) \right]; \qquad (2.66a)$$

$$\frac{k_{1,\mu} k_{1,\nu}}{Q^2} M^{\mu\nu,[1]}_{f,\text{real}}(\varepsilon; \mu, \{y_i\}) = H_{0,f}\, g^2\, 2 C_F\, \mu^{2\varepsilon}\, y_3. \qquad (2.66b)$$

where $H_{0,f}$ is defined in Eq. (C.8b). Analogously to the procedure adopted in the previous section, the unsubtracted partonic tensor in the modified formalism is obtained by integrating Eqs (2.66) over the phase space given in Eq. (2.51), in the limit $\tau^{\perp}_{\text{MAX}} \to 0$. Then, thanks to the identification between the topology cut-off and the IR power counting scale λ presented in Eq. (2.59), the result is intended as the limit $\lambda \to 0$.

The integration of (2.66b) is suppressed in the topology limit because it is non-singular for vanishing y_1 and/or y_2. The result of the integration of Eq. (2.66a) is:

$$- g_{\mu\nu} \widehat{W}^{\mu\nu,[1],\text{uns.}}_{f,\text{real,mod.}}(\varepsilon; z, \tau; \lambda) =$$
$$= H_{0,f} \left[\delta(1-z) \left(S^{[1]}(\varepsilon; \tau) + J^{[1]}_B(\varepsilon; \tau) \right) + J^{[1]}_{q/q,\text{mod}}(\varepsilon; \tau, z, \lambda) \right], \quad \text{Re}\, \varepsilon < 0, \qquad (2.67)$$

where we have used $\tau^{\perp}_{\text{MAX}}(\lambda)\, \delta(1-z) = 1$, which ensures **H.2** is valid. The details of the computation can be found in Ref. [13]. The expression in Eq. (2.67) encodes all the expected contribution associated to a 2-jet topology. The functions J_B and S are, respectively, the (backward) jet thrust function and the soft function commonly found in thrust-dependent cross sections in the 2-jet limit. They are defined in Eqs. (D.12) and (D.6) [46–48]. In the modified formalism, such contributions are totally insensitive to the action of the topology cut-off. On the other hand, the modified quark-from-quark fragmenting jet function $J_{q/q,\text{mod}}$ is associated to the configuration where the gluon is emitted collinearly to the fragmenting quark. Hence, it inevitably overlaps with the same momentum region of the TMD FFs in the final cross section. Its 1-loop expression is given by:

$$J^{[1]}_{q/q,\text{mod}}(\varepsilon; \tau, z, \lambda) = J_{q/q}(\varepsilon; \tau, z)\, \theta \left(\frac{\lambda^2}{Q^2} - \frac{1-z}{z} \tau \right), \qquad (2.68)$$

The ε-expansion of the previous expression is totally not straightforward, as in addition to the thrust distributions, in this case there are also terms proportional to z-distributions and the interplay between such contributions and the cut-off condition makes the computation highly non-trivial. The result is[7]:

$$
\frac{\alpha_S}{4\pi} J_{q/q,\mathrm{mod}}^{[1]}(\varepsilon;\tau,z,\lambda) = \frac{1}{z}\frac{\alpha_S}{4\pi} Z_{q/q,\mathrm{coll}}^{[1]}(\varepsilon;z)\delta(\tau)+
$$
$$
+\frac{\alpha_S}{4\pi} 2C_F S_\varepsilon\,\delta(1-z)\left\{\delta(\tau)\left[\frac{2}{\varepsilon^2}+\frac{1}{\varepsilon}\left(\frac{3}{2}+2\log\left(\frac{\mu^2}{Q^2}\right)\right)\right]-\frac{2}{\varepsilon}\left(\frac{1}{\tau}\right)_+\right\}+
$$
$$
+\frac{\alpha_S}{4\pi} 2C_F S_\varepsilon\left\{\delta(\tau)\left[-\delta(1-z)\log\left(\frac{\lambda^2}{\mu^2}\right)\left(\log\left(\frac{\lambda^2}{\mu^2}\right)-2\log\left(\frac{\mu^2}{Q^2}\right)\right)+\frac{1-z}{z}\left(1+\log\left(\frac{\lambda^2}{\mu^2}\right)\right)+\right.\right.
$$
$$
\left.\left.+2\left(\frac{1}{1-z}\right)_+\log\left(\frac{\lambda^2}{\mu^2}\right)\right]-2\delta(1-z)\left(\frac{1}{\tau}\right)_+\log\left(\frac{\mu^2}{Q^2}\right)+2\delta(1-z)\left(\frac{\log\tau}{\tau}\right)_+\right\},\quad \mathrm{Re}\,\varepsilon<0.
$$
$$
\tag{2.69}
$$

where $Z_{q/q,\mathrm{coll}}$ is the UV counterterm of quark-from-quark FFs, defined in Eq. (A.54). Notice that it encodes the collinear divergence of the quark-from-quark TMD FF and hence it will vanish in the subtraction. Finally, including also the contribution from the virtual gluon emission of Eq. (C.15), the unsubtracted partonic tensor for the fragmenting fermion in the modified formalism is given by:

$$
\widehat{W}_{f,\mathrm{mod}.}^{\mu\nu,[1],\mathrm{uns}.}(\varepsilon;z,\tau;\lambda) = H_T^{\mu\nu}\,\widehat{F}_{1,f,\mathrm{mod}}^{[1],\mathrm{uns}.}(\varepsilon;z,\tau;\lambda)
\tag{2.70}
$$

where:

$$
\widehat{F}_{1,f,\mathrm{mod}}^{[1],\mathrm{uns}.}(\varepsilon;z,\tau;\lambda) = \frac{H_{0,f}}{2}\left[\delta(1-z)\left(\delta(\tau)V^{[1]}(\varepsilon)+S^{[1]}(\varepsilon;\tau)+J_B^{[1]}(\varepsilon;\tau)\right)+J_{q/q,\mathrm{mod}}^{[1]}(\varepsilon;\tau,z,\lambda)\right]
\tag{2.71}
$$

Following the same argument used for the fragmenting gluon case, the subtraction term is the modified Fourier transform of the quark-from-quark TMD FF defined in Eq. (A.54). Analogously to its canonical counterpart, the result gives the *bare* quantity; however, the UV counterterm needed for the renormalization is exactly the same as that given in Eq. (A.50). Finally, we have:

$$
\frac{\alpha_S}{4\pi}\widetilde{D}_{q/q;\mathrm{mod}.}^{[1],(0)}(\varepsilon;z,\zeta,\lambda) = \int d^{2-2\varepsilon}\vec{k}_T\, e^{i\vec{k}_T\cdot\vec{b}_T} D_{q/q}^{[1]}(\varepsilon;z,k_T,\zeta)\theta\left(\lambda^2-k_T^2\right) =
$$
$$
= \frac{1}{z^2}\frac{\alpha_S}{4\pi} Z_{q/q,\mathrm{coll}}^{[1]}(\varepsilon;z)-\frac{\alpha_S}{4\pi} Z_{q/q,\mathrm{TMD}}^{[1]}(\varepsilon)\delta(1-z)+
$$
$$
+\frac{\alpha_S}{4\pi} 2C_F S_\varepsilon\left\{\frac{1}{2}\delta(1-z)\left[\log^2\left(\frac{\lambda^2}{\mu^2}\right)+2\log\left(\frac{\lambda^2}{\mu^2}\right)\log\left(\frac{\zeta}{\lambda^2}\right)\right]+\right.
$$
$$
\left.+\frac{1}{z^2}-\frac{1}{z}+\left(\frac{1}{z^2}+\frac{1}{z}+\frac{2}{(1-z)_+}\right)\log\left(\frac{\lambda^2}{\mu^2}\right)\right\},\quad \mathrm{Re}\,\varepsilon<0.
\tag{2.72}
$$

---

[7]In Ref. [13] not all the non-leading divergences in $\log\left(\lambda^2/Q^2\right)$ have been considered. This produces a missing cancellation among the z-dependent terms which results in a non-trivial dependence on z in the final result.

Clearly, the renormalized version of the previous equation is obtained by adding the UV counterterm $Z^{[1]}_{q/q, \mathrm{TMD}}$. Moreover, if the subtraction is performed with the bare quantity, also the partonic tensor will need a renormalization and its UV counterterm will be exactly *opposite* to the UV counterterm of the modified TMD. This is in agreement with the procedure adopted to renormalize the partonic tensor in the canonical formalism, as presented in Eq. (2.32).

In conclusion, the renormalized partonic tensor for the case of a fragmenting quark is obtained as:

$$
\begin{aligned}
\widehat{W}^{\mu\nu,[1]}_{f,\mathrm{mod.}}&(z,\tau;\zeta,\lambda) = \\
&= \widehat{W}^{\mu\nu,[1],\mathrm{uns.}}_{f,\mathrm{mod.}}(\varepsilon;z,\tau;\lambda) - \sum_k \int_z^1 \frac{d\rho}{\rho}\, \widehat{W}^{\mu\nu;[0]}_k(z/\rho,\tau)\left(\rho\,\widetilde{D}^{[1]}_{q/q;\mathrm{mod.}}(\varepsilon;\rho,\zeta,\lambda)\right) = \\
&= H^{\mu\nu}_T\, \frac{H_{0,f}}{2}\left[\delta(1-z)\left(\delta(\tau)V^{[1]}(\varepsilon) + S^{[1]}(\varepsilon;\tau) + J^{[1]}_B(\varepsilon;\tau)\right) + \right. \\
&\left. + J^{[1]}_{q/q,\mathrm{mod}}(\varepsilon;\tau,z,\lambda) - \delta(\tau)z\widetilde{D}^{[1]}_{q/q;\mathrm{mod.}}(\varepsilon;\rho,\zeta,\lambda)\right] \equiv H^{\mu\nu}_T\, \widehat{F}^{[1]}_{1,f,\mathrm{mod}}(z,\tau;\lambda),
\end{aligned}
\tag{2.73}
$$

where:

$$
\begin{aligned}
\widehat{F}^{[1]}_{1,f,\mathrm{mod}}&(z,\tau;\zeta,\lambda) = \\
&= H_{0,f}C_F\,\delta(1-z)\left[\delta(\tau)\left(-\frac{9}{2} + \frac{2\pi^2}{3} - \log\left(\frac{\zeta}{\mu^2}\right)\log\left(\frac{\lambda^2}{\mu^2}\right) - \frac{1}{2}\log^2\left(\frac{\lambda^2}{\mu^2}\right) - \right.\right. \\
&\left.\left. - \frac{3}{2}\log\left(\frac{\mu^2}{Q^2}\right) - 2\log\left(\frac{\lambda^2}{\mu^2}\right)\log\left(\frac{\mu^2}{Q^2}\right) - \log^2\left(\frac{\mu^2}{Q^2}\right)\right) - \frac{3}{2}\left(\frac{1}{\tau}\right)_+ - 4\left(\frac{\log\tau}{\tau}\right)_+\right].
\end{aligned}
\tag{2.74}
$$

Then, the final result for the NLO partonic cross section follows straightforwardly:

$$
\frac{d\widehat{\sigma}^{[1]}_{f,\mathrm{mod.}}}{dzdT} = \sigma_B\, z\,\widehat{F}^{[1]}_{1,f,\mathrm{mod}}(z,\tau;\zeta,\lambda).
\tag{2.75}
$$

Notice that the z-dependence is trivial: in the final cross section the behavior in z is entirely described by the TMD FFs. Furthermore, this final result is a finite quantity, as all the divergences have been canceled. There is still track of the regulators: μ for the UV divergences and ζ for the rapidity divergences. The latter, in particular, originates from the subtraction term, as the matrix elements contributing to the modified TMD are the same of the canonical Collins formalism. The action of the RG easily takes care of the dependence on μ which can be set to Q as usual. However, as expected, the final cross section is not CS-invariant and the modified partonic cross section as well as the TMD FFs depend on ζ. Differently to the canonical formulation of the factorization theorem, in this case there is also the topology cut-off λ playing its role in the game. It has a double function: on one side it forces the modified partonic cross section to describe the 2-jet region, on the other side it constrains the total transverse momentum of the radiation collinear to the detected hadron to be in the power counting region. This last feature is crucial, as, for on-shell particles, a constraint on transverse

momentum automatically leads to a constraint on rapidity (and vice-versa). Then, the transverse momentum of the emitted gluon (see Fig. 2.7) is constrained by $k_T \leq (1-z)\sqrt{\zeta} \leq \sqrt{\zeta}$ and also by $k_T \leq \lambda$. This means that the topology cut-off plays the same role of the canonical rapidity cut-off and hence they can be set to be the same, $\zeta = \lambda$.

The double nature of the topology cut-off makes it more flexible than ζ. Its direct relation to the topology of the process can be made more explicit by exploiting the kinematic argument of Eq. (2.37). In fact, on one side $k_T \leq P_T/z_h \leq \sqrt{\tau}Q$, on the other $k_T \leq \lambda$ and the natural choice for the topology cut-off is $\lambda = \sqrt{\tau}Q$. Therefore, the limit $\lambda \to 0$ literally corresponds to the 2-jet limit. Summarizing:

$$\zeta = \lambda = \sqrt{\tau}Q \longrightarrow y_1 = -\frac{1}{2}\log\tau, \tag{2.76}$$

in total agreement with the kinematics argument. Also, Eq. (2.76) matches with the naive picture of Fig. 2.3. In fact, the canonical limit on the rapidity cut-off $y_1 \to \infty$ in this modified formalism corresponds to the 2-jet limit $\tau \to 0$ and the rapidity cut-off is linked *directly* to the experimentally measured value of thrust. The more y_1 approaches infinity, the narrower the jet in which the hadron is detected, approaching the pencil-like configuration.

The practical implementation of the relation in Eq. (2.76) into a fixed order computation is hardly viable. The NLO expression of the modified partonic cross section shows that all the dependence on λ (and ζ) is embedded in the logarithms in the coefficient of $\delta(\tau)$. Therefore, a straightforward substitution $\lambda^2 = \tau Q^2$ into Eq. (2.74) cannot be implemented, as it would lead to ill-defined terms as $\delta(\tau)\log(\tau)$. This is the same kind of trouble that would appear if $y_1 = +\infty$ is set straightforwardly in the final factorization theorem of Eq. (2.26). Ultimately, this problems opens the question of the implementation of a proper thrust resummation[8] for a cross section as that in Eq. (2.74). A simple short-cut consists in staying away from the dangerous region near $\tau = 0$ and writing the fixed order cross section neglecting all contributions associated to a pencil-like configuration. This can be easily obtained by removing the whole $\delta(\tau)$ term and the "plus" signs from the thrust distributions in Eq. (2.74). Then, the final result has a very simple expression:

$$\frac{d\widehat{\sigma}_{f,\,\text{mod.}}^{[1]}}{dz\,dT} = -\sigma_B\,e_f^2\,C_F\,N_C\,\delta(1-z)\frac{3+8\log\tau}{\tau}. \tag{2.77}$$

As long as the phenomenological analyses do not include data associated to very large values of T, this formula for the partonic cross section is expected to apply. Even if this result has been found within a modified version of the canonical factorization formalism, I will show in Chapter 3 that the same partonic cross section can be derived without introducing a topology cut-off.

---

[8]In Ref. [13] a resummed expression is obtained by considering λ and τ independent untill the very end of the computation and using the relation $\lambda = \sqrt{\tau}Q$ only in the final result, written as the solution of a proper evolution equation with respect to the topology cut-off. This produces an exponentially suppressed term in the partonic cross section, unfortunately not powerful enough to describe the behavior around $T \sim 1$.

By using the NLO partonic cross section of Eq. (2.77) and the NLL unpolarized TMD FF presented in Eq. (A.60), we can write the collinear-TMD factorized cross section of Eq. (2.30) at NLO-NLL accuracy for a 2-jet final state configuration:

$$
\frac{d\sigma}{dz\,dP_T^2\,dT} \overset{\text{NLO, NLL}}{=} -\frac{4\pi^2\alpha^2}{3z_h^2 Q^2} C_F N_C \frac{3+8\log(1-T)}{1-T} \int \frac{d^2\vec{b}_T}{(2\pi)^2} e^{i\frac{\vec{P}_T}{z_h}\cdot\vec{b}_T} \sum_f e_f^2 \Big(d_{h/f}(z_h,\mu_b) +
$$

$$
+ \frac{\alpha_S(\mu_b)}{4\pi} \int_{z_h}^1 \frac{d\rho}{\rho} \left\{ d_{h/f}(z_h/\rho,\mu_b) \left[\rho^2 \mathscr{C}_{q/q}^{[1]}(\rho) \right] + d_{h/g}(z_h/\rho,\mu_b) \left[\rho^2 \mathscr{C}_{g/q}^{[1]}(\rho) \right] \right\} \Big) \times
$$

$$
\times \exp\left\{ \log\left(\frac{Q}{\mu_b}\right) g_1(x) + g_2(x) \frac{1}{4}\log(1-T) \left(g_2^K(x) + \frac{1}{\log\left(\frac{Q}{\mu_b}\right)} g_3^K(x) \right) \right\} \times
$$

$$
\times M_{D_{1,f/h}}(z_h,b_T) \exp\left\{ -\frac{1}{4} g_K(b_T) \log\left(z_h^2(1-T)\frac{Q^2}{M_h^2} \right) \right\} \left[1 + \mathscr{O}\left(\frac{M_h^2}{Q^2}\right) \right], \tag{2.78}
$$

where we have set $\mu = Q$ thanks to RG-invariance and $\zeta = (1-T)Q^2$ from the relation of Eq. (2.76).

2.7 Conclusions

The factorization of the $e^+e^- \to hX$ cross section, sensitive to the transverse momentum P_T of the detected hadron with respect to the thrust axis, represents a really hard challenge from the theoretical point of view. According to the classification of Section 1.4, this process belongs to the 1-h class. This fact has important consequences that make its factorization properties deeply different from those of the TMD processes belonging to the 2-h class. If the radiation collinear to the jet in which the hadron is detected does not affect the experimental measurement of thrust (**H.1**) and if the soft radiation does not affect the experimental measurement of P_T (**H.2**), then the factorization theorem (see Eq. (2.26)) assumes a *hybrid* form between the usual collinear factorization and TMD factorization. It has the same structure of a collinear factorized cross section but here the fully perturbative partonic cross section is convoluted with a TMD FF, rather than a FF, which must be extracted from experimental data. For this reason, such hybrid factorization theorem has been called "collinear-TMD".

There are two remarkable features associated with this hybrid collinear-TMD factorized cross section. The first is that the TMD FFs appearing in the final result *are not* defined in the usual way, through the square root definition, Eq. (1.33), devised for 2-h class TMD cross sections. This definition cannot be applied to 1-h processes, as there is no other non-perturbative contribution besides that of the TMD itself. Instead, the TMDs appearing in Eq. (2.26) are defined according to the factorization definition presented in Eq. (1.21). They describe only particles collinear to the detected hadron, without including any information about the soft radiation of the process. In fact, all the soft contributions are embedded perturbatively inside the partonic cross section. This must be taken into account when performing any phenomenological study. The TMD FFs extracted in this way will

differ by a square root of the soft model M_S from those obtained by fitting SIDIS and $e^+e^- \to h_1 h_2$ data.

The other issue involves the role of the rapidity cut-offs in collinear-TMD factorization theorems. In fact, both the TMD and the partonic cross section show a dependence on the rapidity cut-off ζ appearing into the TMDs definition. However, the final cross section cannot be CS-invariant, mainly because the CS-evolution of the TMDs is b_T-dependent while the partonic cross section depends only on the collinear momentum fraction and on thrust. For the lowest order computation, the rapidity dilations presented Section 2.5 offer a viable solution, at least to the phenomenological level. However, their action is not useful when higher ordercorrections are taken into account. In this Chapter and throughout this thesis, I will not interpret the dependence on the rapidity cut-off of the final result as an inconsistency of the factorization procedure. In fact, there is a intimate connection between ζ and the topology of the final state, which ultimately relates the rapidity cut-off to the thrust. This connection does not appears explicitly within the Collins factorization formalism. However, if an additional topology cut-off is inserted into the factorization procedure, then this somehow takes the place of ζ and has the added benefit of being directly related to thrust. This approach has been shown in Section 2.6 to NLO, for a 2-jet final state configuration. In this modified formalism, the rapidity cut-off is finally set to τQ^2 and hence the 2-jet limit $\tau \to 0$ corresponds explicitly to the canonical limit $y_1 \to \infty$ of the Collins formalism. This solution cannot be implemented straightforwardly into the fixed order partonic cross section, as it would expose the rapidity divergences in $T = 1$. However, it offers the possibility to shed light on the real physical meaning of the rapidity cut-off. It cannot be considered as a mere computational tool introduced solely to regulate the rapidity divergences. More appropriately, it should be assigned a specific physical meaning, given its relation to the measured value of thrust.

The collinear-TMD factorization theorem presented in this chapter offers a unique perspective on this issue. In fact, the conventional TMD factorization theorems provide CS-invariant cross sections, where the whole dependence on the rapidity cut-off is completely washed out in the interplay between TMDs and the contribution of the soft gluons. Instead, collinear-TMD factorized cross sections make such dependence explicit, providing a concrete tool to investigate the physical meaning behind the regulators of rapidity divergences.

Chapter 3

Kinematics regions in a 2-jet topology

3.1 Introduction

The collinear-TMD factorization theorem devised for $e^+e^- \to hX$ in the previous Chapter has been obtained within the Collins factorization formalism, by making use of very general properties associated to the interplay between the hard, soft and collinear contributions to the cross section, and also with the help of some additional assumptions on the role of soft and collinear radiation in the actual experimental measurement. In particular, we have required that the transverse motion of the particles radiated collinearly to the detected hadron does not modify the final state topology of the event (**H.1**), and also that the transverse momenta of the soft gluons do not deflect the trajectory of the detected hadron (**H.2**). This kind of "top-down" approach is very powerful, as it allows us to avoid the traps and threats that a "bottom-up" approach, entirely based on perturbation theory, could present. On the other hand, the steps of the factorization proof are much clearer within a "bottom-up" approach, where the various contributions can be readily disentangled and made more explicit transparent, order by order in pQCD. The downside of this methodology is that perturbative computations may be remarkably difficult, especially when the formalism has to be adapted to include one additional observable variable, in this case thrust. Of course, under the same assumptions. both schemes should ultimately return the same result.

The purpose of this Chapter is to show an alternative road to factorization, through a "bottom-up" approach. I will present the explicit calculation of the leading contributions to the partonic version of the whole process, which corresponds to the partonic tensor introduced in the previous Chapter, at NLO in the perturbative QCD expansion and for the relevant case of a 2-jet configuration. The results will then be generalized to all orders. I will show how, following this alternative procedure, all the results of Chapter 2 can be recovered. Moreover, I will also consider the cases in which the additional approximations **H.1** and **H.2** are removed. This will lead to three different factorization theorems, each corresponding to a different kinematic region. In this regard, the results of Chapter 2

will be associated to Region 2, where both the kinematic requirements hold true. These results are crucial for phenomenological analyses, as they provide a criterion for data selection which ensures that the appropriate factorization theorem is applied to the right data subset. I will also provide an algorithm based on the 1-loop computation that allows to identify each kinematical region by comparing properly defined ratios involving measured quantities, like z_h, P_T and T.

3.2 Conventions and nomenclature

As extensively discussed in Section 2.3, the leading momentum regions for $e^+e^- \to hX$ involve hard, soft and collinear contributions, and each term can be expanded in series of α_S and approached within perturbative QCD. Such decomposition can be performed explicitly, order by order, by applying the kinematics approximators defined in Ref. [7] and reviewed in Appendix A. I will follow the conventions introduced in Appendix D, where a label "∘" is used to specify when an approximator has to be applied without its rapidity cut-off. This is a relevant issue only for soft and soft-collinear approximators, as the unsubtracted collinear parts are already defined without rapidity cut-offs. Moreover, I will denote the two hemispheres defined by the thrust axis as S_A and S_B, where the first is the hemisphere in which hadron h is detected. In the case of soft radiation, the particles can be emitted either in S_A or in S_B with the same probability. Therefore, the soft approximators are equipped with a further label "+" or "−" as an indication of the hemisphere in which the particle is emitted. Finally, following the nomenclature introduced in Appendix A, the various subgraphs singled out by the action of the approximators will be labeled as "A", "B", "S" or "H", depending, respectively, on whether the particles circulating inside them are collinar to the fragmenting parton, collinear to the backward direction, soft or hard (far off-shell).

Not all the contributions singled out by the factorization procedure are relevant for the study of TMD effects. Since each of them returns a picture of the whole process in a specific momentum region, they all depend somehow on the transverse momentum of the fragmenting parton $\vec{k}_T$. Sometimes such dependence is trivial, as for the case of the backward emitted radiation. In other cases, the relevance for the TMD physics depends on whether the considered term contributes significantly to the transverse deflection from the thrust axis of the detected hadron. Leaving aside the reasons that allow to consider a certain contribution relevant or not for studying TMD effects, if a term is "TMD-relevant" then it must be considered in the Fourier conjugate space of $\vec{k}_T$, as this is the natural framework in which TMDs and soft factors are defined (see Sections 1.2 and 1.3). On the other hand, if a term is "TMD-irrelevant" then it must be integrated over the whole spectrum of transverse momentum, which is equivalent to washing out the information on $\vec{k}_T$. In this section, I will refer to TMD-relevant (Fourier transformed) quantities as "factors" and, if not specified differently, I will indicate them with capital Greek letters. Instead, I will refer to TMD-irrelevant ($\vec{k}_T$ integrated) quantities as "functions" and, if not already defined differently, I will indicate them with capital italics

Latin letters. The following scheme summarizes the notation:

$$\text{TMD-relevant} \longleftrightarrow \int d^{2-2\varepsilon}\vec{k}_T \, e^{i\vec{k}_T \cdot \vec{b}_T} \longleftrightarrow \underset{\text{(capital Greek letters)}}{\text{factor}}$$

$$\text{TMD-irrelevant} \longleftrightarrow \int d^{2-2\varepsilon}\vec{k}_T \longleftrightarrow \underset{\text{(capital italics Latin letters)}}{\text{function}}$$

Notice that the contributions of the momentum region corresponding to particles moving collinearly to the fragmenting parton are *always* TMD-relevant, as they embody the core and essence of the TMD effects. On the other hand, contributions associated to backward radiation are *always* TMD-irrelevant, trivially because, being emitted into the hemisphere opposite to the detected hadron, they cannot affect its transverse motion. Therefore, being TMD-relevant or not is crucial only for soft (and soft-collinear) momentum regions, as soft radiation emitted in the hemisphere S_A may (or may not) contribute to the transverse momentum of the detected hadron. Clearly, this is strictly connected to the validity of the assumption **H.2**. Finally, since this Chapter is devoted to the computation of the partonic version of the whole process, I will drop the label "uns." from the partonic tensor, meaning that it contains also the information encoded into the (partonic version of) the TMD FFs, which ultimately causes an overlap in the final factorized cross section. On the other hand, in all those cases in which I refer to a subtracted quantity, I will add an explicit label "sub."

3.3 A benchmark study: the fragmenting gluon case

The "bottom-up" approach to the factorization procedure discussed in this chapter involves the solution of some very tough integrals, due to the non-trivial interplay between thrust and transverse momentum dependence. The solution of such integrals require non-standard techniques, even just for a NLO approximation. Therefore, it is convenient to show the procedure and some of this advanced mathematical tools in the simple case of a fragmenting gluon, in analogy to what was done within the modified formalism framework in Section 2.6.1. This will serve as a benchmark study for the treatment of the more relevant case of a fragmenting fermion, which actively contributes to the final result. Clearly, we have to recover the expected result also in this "bottom-up" approach. For a 2-jet final state, one jet is generated by a quark, the other by its corresponding antiquark, while the chance of a jet being produced by a gluon is strongly suppressed.

For the case of a fragmenting gluon, there is only one Feynman diagram to be considered, shown in Fig. 2.5. The corresponding squared amplitude has been presented in Eqs. (2.53), (2.54). The expression of the phase space is similar to Eq. (2.51), however, instead of introducing an artificial TMD-sensitive topology cut-off as in Section 2.6, we explicitly keep track of the total transverse momentum of the radiation collinear to the fragmenting parton. This is realized by the partonic version of the condition that sets the relation between the transverse momentum $\vec{P}_T$ of the detected hadron and the transverse momentum $\vec{k}_T$ of the fragmenting parton. As discussed in Section 2.4.1,

this condition just sets $\vec{k}_T$ equal to the total transverse momentum $\vec{k}'_T$ entering into the A-subgraph. Therefore, with respect to Eq. (2.51), we have to implement the following replacement:

$$\theta\left(\tau_{\text{MAX}}^{\perp} - \tau\right) \longmapsto \delta\left(\vec{k}_T - \vec{k}'_T\right) \tag{3.2}$$

Since the definition of the A-subgraph depends on the action of the kinematics approximator, the expression of $\vec{k}'_T$ can be different for each leading momentum region. In fact, the action of T_R modifies *any* element involved into the calculation of the partonic tensor, not only the squared amplitudes. Also the momentum conservation delta and the condition that fixes the thrust must be modified consistently. Apart from these differences in the procedure of the computation, all the considerations of Section 2.6.1 hold. In particular, the power counting suppresses both the configurations in which the emitting fermion reflects backward (action of T_B) and when it turns soft (action of T_S), regardless of the hemisphere in which it is directed. Therefore, the only leading momentum region is realized by the fermion being collinear to the fragmenting gluon, obtained through the action of T_A. Therefore we have:

$$\widehat{W}_g^{\mu\nu,\,[1]}\left(\varepsilon; z, \tau, k_T\right) = T_A\left[\widehat{W}_g^{\mu\nu,\,[1]}\left(\varepsilon; z, \tau, k_T\right)\right] + \begin{array}{c}\text{power suppressed}\\\text{corrections}\end{array}, \tag{3.3}$$

where the T_A approximator gives:

$$T_A\left[\widehat{W}_g^{\mu\nu,\,[1]}\left(\varepsilon; z, \tau, k_T\right)\right] = \sum_f \int \frac{dk^+}{k^+} {}^\star\widehat{W}_f^{\mu\nu,\,[0]}(k^+, Q)\,\Gamma_{g/q}^{[1]}\left(\varepsilon; k^+/k'^+, k_T, \tau\right) =$$

$$= \sum_f \int \frac{d\rho}{\rho} {}^\star\widehat{W}_f^{\mu\nu,\,[0]}(z/\rho, Q)\,\Gamma_{g/q}^{[1]}\left(\varepsilon; \rho, k_T, \tau\right), \tag{3.4}$$

where, as discussed in Section 2.4.1, the collinear momentum fractions are defined as $z = k^+/q^+$ and $\rho = k^+/k'^+$. Moreover, ${}^\star W_f^{\mu\nu,\,[0]}$ is the partonic tensor at LO, computed in Eq. (C.6), but considered without its (trivial) dependence on thrust, as the whole τ-content is included into the function $\Gamma_{g/q}$. This is the 1-loop gluon-from-quark generalized fragmentation jet function (GFJF)[1], defined as:

$$\Gamma_{g/q}^{[1]}\left(\varepsilon; z, k_T, \tau\right) = \int \frac{dk^-}{(2\pi)^{4-2\varepsilon}} \frac{\text{Tr}_C}{N_C} \frac{\text{Tr}_D}{4} \left(\gamma^+ \begin{array}{c} \includegraphics \end{array} \right) \delta\left(\tau - \frac{z}{1-z}\frac{k_T^2}{Q^2}\right) =$$

$$= \frac{\alpha_S}{4\pi} 2 C_F S_\varepsilon \frac{\Gamma(1-\varepsilon)}{\pi^{1-\varepsilon}} \frac{\mu^{2\varepsilon}}{k_T^2} \theta(1-z)\frac{1 + (1-z)^2 - \varepsilon z^2}{z^2}\delta\left(\tau - \frac{z}{1-z}\frac{k_T^2}{Q^2}\right). \tag{3.5}$$

---

[1]In the literature [45, 17], the GFJFs are usually indicated by $\mathscr{G}$. In this thesis I will be consistent with the nomenclature introduced in Section 3.3. Furthermore, in analogy to TMD FFs the GFJFs are usually defined with a normalization factor of $1/z$, which here is not considered.

Notice that this definition coincides with the transverse momentum space expression of the unsubtracted collinear parts, presented in Eq. (1.15), properly projected onto the relevant term of the Clifford algebra basis and at leading twist (see Eq. (1.20), appropriately modified to be suitable for gluons). Differently from the objects defined in Chapter 1, in Eq. (3.5) there is, in addition, the explicit thrust-dependence. Without the condition that fixes the thrust, Eq. (3.5) would be extactly the definition of the gluon-from-quark TMD FF in momentum space (a part from a normalization factor $1/z$), as can be verified by comparing this expression with Eq. (A.39). However, in transverse momentum space is (paradoxically) difficult to capture the size of the overlapping between the collinear momentum region covered by the partonic tensor and the TMD FFs. In the following, I will investigate this issue in the Fourier conjugate space of $\vec{k}_T$, where TMDs are properly defined. In fact, according to discussion in Section 3.2, the action of T_A gives always a TMD-relevant term.

The delta function in Eq. (3.5) fixes the relation between τ and k_T. In particular, as already noticed in Section 2.6, the 2-jet limit $\tau \to 0$ corresponds to the power counting region $k_T \ll Q$. This bond breaks down when we Fourier transform $\Gamma_{g/q}$, since this operation inevitably stretches the transverse momentum beyond the power counting region. As a consequence, the result of the F.T. will also include contributions that are *outside* the 2-jet region. Naively, we may expect that in b_T-space the 2-jet limit corresponds to the large-b_T region. In the following, this will be verified explicitly. The Fourier transform gives:

$$
\widetilde{\Gamma}_{g/q}^{[1]}\left(\varepsilon; z, b_T, \tau\right) =
$$
$$
= \frac{\alpha_S}{4\pi} 2 C_F S_\varepsilon \left(\frac{\mu}{Q}\right)^{2\varepsilon} \frac{1 + (1-z)^2 - \varepsilon z^2}{z^2} \left(\frac{1-z}{z}\right)^{-\varepsilon} \theta(1-z)\, \tau^{-1-\varepsilon}\ {}_0F_1 \left(1-\varepsilon; -\tau \frac{1-z}{z} \frac{b^2}{4}\right).
$$
(3.6)

where $b = b_T Q$ and the hypergeometric function can also be written as:

$$
{}_0F_1 \left(1-\varepsilon; -\tau \frac{1-z}{z} \frac{b^2}{4}\right) = \Gamma(1-\varepsilon) \left(\frac{b}{2}\sqrt{\tau \frac{1-z}{z}}\right)^{\varepsilon} J_{-\varepsilon} \left(b\sqrt{\tau \frac{1-z}{z}}\right)
$$
(3.7)

Now, we may be tempted to expand the hypergeometric function in powers of τ in Eq. (3.6) and assume the lowest order in τ provides a good description of the 2-jet region. However, this also implies that $b << 1$, which naively does not correspond to the power counting region of small k_T. This confirms that in the Fourier conjugate space, the 2-jet limit is much less trivial than in the transverse momentum space. In fact, a proper treatment of this issue involves dealing with the ε-expansion of Eq. (3.6) in terms of τ-distributions. In order to accomplish this, we will make use of a rather simple trick, that can always be exploited in presence of functions of some variable x that varies in the range $[0, 1]$, divergent at most as simple poles when x approaches 0. In fact, if $f(x)$ is a function that behaves
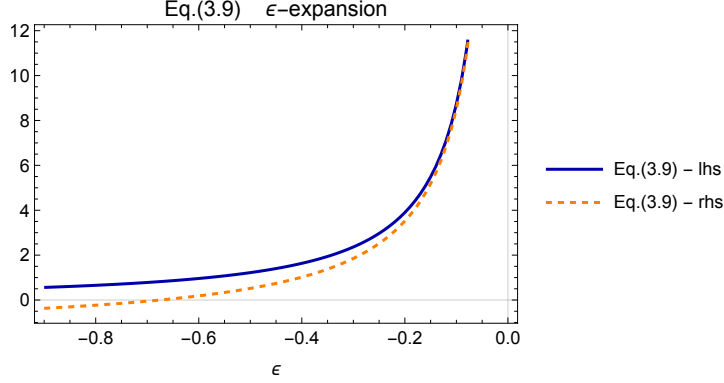
Fig. 3.1 The term $\tau^{-1-\varepsilon}{}_0F_1\left(1-\varepsilon; -\tau\frac{1-z}{z}\frac{b^2}{4}\right)$ in Eq. (3.6), (solid, blue line) is compared with its small ε-expansion (orange, dashed line) given by Eq. (3.8). These lines are obtained by integrating the r.h.s and l.h.s of Eq. (3.9) with a test function chosen as $T(\tau) = e^{-\tau}$.

at most as $\sim 1/x$ when $x \to 0$, then we can recast it as:

$$f(x) = \delta(x) \int_0^1 d\alpha f(\alpha) + (f(x))_+ \tag{3.8}$$

With this technique, we can reorganize the dependence on τ in Eq. (3.6) and disentangle it from the dependence on b when $\tau = 0$. After this operation we can then safely perform the ε-expansion.

$$\tau^{-1-\varepsilon}{}_0F_1\left(1-\varepsilon; -\tau\frac{1-z}{z}\frac{b^2}{4}\right) =$$

$$= -\frac{1}{\varepsilon}{}_1F_2(-\varepsilon; 1-\varepsilon, 1-\varepsilon; -\frac{1-z}{z}\frac{b^2}{4})\delta(\tau) + \left(\tau^{-1-\varepsilon}{}_0F_1\left(1-\varepsilon; -\tau\frac{1-z}{z}\frac{b^2}{4}\right)\right)_+ =$$

$$= \delta(\tau)\left(-\frac{1}{\varepsilon} - \frac{1-z}{z}\frac{b^2}{4}{}_2F_3\left(1,1;2,2,2;-\frac{1-z}{z}\frac{b^2}{4}\right)\right) + \left(\frac{J_0\left(b\sqrt{\tau\frac{1-z}{z}}\right)}{\tau}\right)_+ + \mathcal{O}(\varepsilon) \tag{3.9}$$

where $\mathrm{Re}(\varepsilon) < 0$ is required for convergence. We have pushed the expansion up to $\mathcal{O}(\varepsilon^0)$ since the remaining ε-dependent terms in Eq. (3.6) do not present any pole in ε.

Now we are ready to consider the large-b_T limit, in order to bring the result back to the 2-jet approximation. Let's define for simplicity $a = \frac{b^2}{4}\frac{1-z}{z}$. Then, since z in the collinear region cannot be too close to 1 (large values of z, $z \to 1$, can only be reached in the soft approximation), the limit $a \to \infty$ will correspond to the asymptotic behavior for large values of b. Finding the asymptotic behavior of the term multiplying the $\delta(\tau)$ in the last line of Eq. (3.9) is quite easy. In fact we have:

$$a\,{}_2F_3\left(1,1;2,2,2;-a\right) =$$

$$= \log\left(a\,e^{2\gamma_E}\right) + \frac{1}{a^{3/4}}\frac{1}{\sqrt{\pi}}\cos\left(2\sqrt{a} + \frac{\pi}{4}\right) + \mathcal{O}\left(\frac{1}{a^{5/4}} \times \begin{array}{c}\text{oscillating}\\\text{function}\end{array}\right). \tag{3.10}$$

On the other hand, a proper estimation of the asymptotic behavior of the plus distribution in Eq. (3.9) is much less trivial. Clearly, the Bessel function J_0 behaves as $\sim a^{-1/2}$ for large-a. However, such a rough estimation compromises the τ dependence, which becomes $\sim \tau^{-5/4}$, not integrable anymore for *any* test function $T(\tau)$. Such an operation should therefore be performed more carefully. With the help of a test function $T(\tau)$, the following asymptotic series can be obtained by integrating N times by parts:

$$\int_0^1 d\tau\, T(\tau) \left(\frac{J_0\left(2\sqrt{a\tau}\right)}{\tau} \right)_+ = S_N(\sqrt{a}) + R_N(\sqrt{a}). \tag{3.11}$$

where we have introduced:

$$S_N(\sqrt{a}) = \sum_{j=0}^{N-1} (-1)^j \frac{J_{j+1}(2\sqrt{a})}{a^{(j+1)/2}} \frac{d^j}{d\tau^j} \left(\frac{T(\tau) - T(0)}{\tau} \right) \Bigg|_{\tau=1} ; \tag{3.12}$$

$$R_N(\sqrt{a}) = (-1)^N a^{-N/2} \int_0^1 d\tau \frac{d^N}{d\tau^N} \left(\frac{T(\tau) - T(0)}{\tau} \right) \tau^{N/2} J_N(2\sqrt{a\tau}). \tag{3.13}$$

The series $S_{N\to\infty}$ diverges for any value of a, however its partial sums (for finite N) can be used to compute the integral of Eq. (3.11) to any desired accuracy. In fact, R_N is of order $a^{-(N+1)/2-1/4}$ and can be made small at will. Furthermore, the derivative of the test function in Eq. (3.12) can be rewritten as:

$$\frac{d^j}{d\tau^j} \left(\frac{T(\tau) - T(0)}{\tau} \right) = \frac{(-1)^j j!}{\tau^j} \left(\frac{T(\tau) - T(0)}{\tau} + \sum_{k=1}^j \frac{(-1)^k}{k!} \frac{T^{[j]}(\tau)}{\tau^{1-k}} \right). \tag{3.14}$$

Hence, we can recast S_N in the following form:

$$S_N(\sqrt{a}) = \sum_{j=0}^{N-1} j! \frac{J_{j+1}(2\sqrt{a})}{a^{(j+1)/2}} \left[-T(0) + \sum_{k=0}^j \frac{(-1)^k}{k!} \frac{T^{[j]}(1)}{\tau^{1-k}} \right], \tag{3.15}$$

which at level of distribution becomes:

$$\left(\frac{J_0\left(2\sqrt{a\tau}\right)}{\tau} \right)_+ = \sum_{j=0}^{N-1} j! \frac{J_{j+1}(2\sqrt{a})}{a^{(j+1)/2}} \left[-\delta(\tau) + \sum_{k=0}^j \frac{1}{k!} \delta^{[k]}(1-\tau) \right] + \mathcal{O}\left(a^{-\frac{(3+2N)}{4}} \right), \tag{3.16}$$

where $\delta^{[k]}(1-\tau)$ is the k-th distributional derivative of $\delta(1-\tau)$, which, setting $\tau = 1$, produces (boundary) terms that are not contributing to the 2-jet limit and hence that will be thrown away. Notice that the integration of each side of Eq. (3.16) gives zero as required. Now, we have a correct asymptotic expansion of the plus distribution appearing in the last line of Eq. (3.9). In the 2-jet
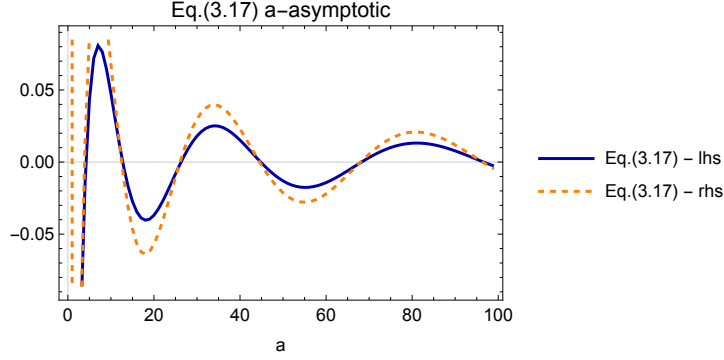
Fig. 3.2 The distribution $\left(\frac{J_0\left(2\sqrt{a\tau}\right)}{\tau}\right)_+$ in Eq. (3.16), (solid, blue line) is compared with its large b-expansion (orange, dashed line) as obtained in Eq. (3.17). These lines are obtained by integrating with a test function chosen as $T(\tau)=e^{-\tau}$.

approximation, its crudest estimation is given by:

$$
\begin{aligned}
\left(\frac{J_0\left(2\sqrt{a\tau}\right)}{\tau}\right)_+ &= -\delta(\tau)\frac{J_1(2\sqrt{a})}{\sqrt{a}} + \mathcal{O}\left(\frac{1}{a} \times \frac{\text{Bessel}}{\text{function}}\right) \\
&= \delta(\tau)\frac{1}{a^{3/4}}\frac{1}{\sqrt{\pi}}\cos\left(2\sqrt{a}+\frac{\pi}{4}\right) + \mathcal{O}\left(\frac{1}{a^{5/4}} \times \frac{\text{oscillating}}{\text{function}}\right)
\end{aligned}
\tag{3.17}
$$

Notice that this result cancels exactly the first correction to the logarithm in Eq. (3.10). This does not happen by chance; it can be verified at any order $\mathcal{O}\left(a^{-k/4}\right)$, for $k=3,\dots,2N$, for any N. Finally, the ε-expansion in the 2-jet limit for the l.h.s. of Eq. (3.9) is given by:

$$
\begin{aligned}
\tau^{-1-\varepsilon}{}_0F_1\left(1-\varepsilon;-\tau\frac{1-z}{z}\frac{b^2}{4}\right) &\overset{2-\text{jet}}{=} \delta(\tau)\left(-\frac{1}{\varepsilon}-2\log\left(\frac{b}{c_1}\right)-\log\left(\frac{1-z}{z}\right)\right) + \\
&+ \mathcal{O}(\varepsilon) + \mathcal{O}\left(b^{-\frac{3+2N}{2}}\right), \quad \forall N=0,1,\dots
\end{aligned}
\tag{3.18}
$$

where $c_1=2e^{-\gamma_E}$. Inserting this result in Eq. (3.6), we can write the large-b asymptotic behavior of $\widetilde{\Gamma}_{g/q}$ (in the following expressed with the label "ASY"), which has to be considered as its 2-jet approximation. We have:

$$
\widetilde{\Gamma}_{g/q}^{[1],\text{ASY}}(\varepsilon;z,b_T,\tau) = \delta(\tau)z\widetilde{D}_{g/q}^{[1]}(\varepsilon;z,b_T) + \mathcal{O}\left(b^{-\frac{3+2N}{2}}\right), \quad \forall N=0,1,\dots.
\tag{3.19}
$$

where $\widetilde{D}_{g/q}[1]$ the 1-loop gluon-from-quark TMD FF in b_T-space as defined in Eq. (A.42). Notice how the whole dependence on the thrust has been washed away in the 2-jet approximation. Finally:

$$
\widetilde{\widehat{W}}_g^{\mu\nu,[1]}(\varepsilon;z,\tau,b_T) = \sum_f\int\frac{d\rho}{\rho}\sum_f\int\frac{d\rho}{\rho}\widehat{W}_f^{\mu\nu,[0]}(z/\rho,Q,\tau)\left(\rho\,\widetilde{D}_{g/q}^{[1]}(\varepsilon;z,b_T)\right) + \frac{\text{power suppressed}}{\text{corrections}}.
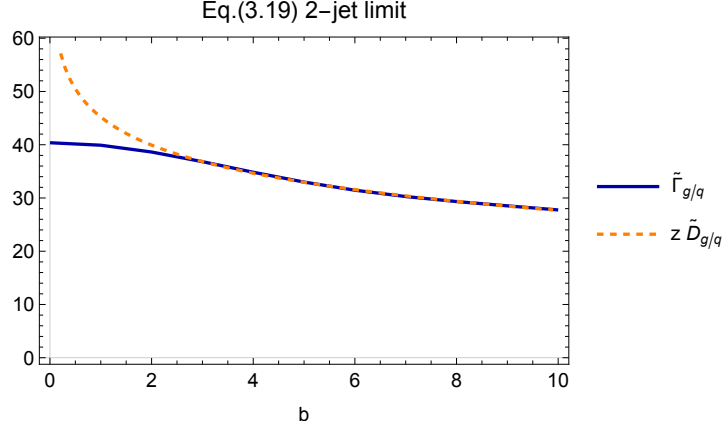\tag{3.20}
$$

Fig. 3.3 The gluon-from-quark GFJF in Eq. (3.6), (solid, blue line) is compared to its 2-jet limit (orange, dashed line) in the l.h.s. of Eq. (3.19). The plotted lines are obtained by integrating with a test function chosen as $T(\tau) = e^{-\tau}$.

Notice that the $\delta(\tau)$ in Eq. (3.19) recreates the LO partonic tensor as defined in Eq. (C.6). The power suppresed terms involve both the errors associated to the factorization procedure of Eq. (3.3), and also the errors associated to the 2-jet limit of Eq. (3.19).

Eq. (3.20) is a crucial result. In the 2-jet limit, the 1-loop contribution of the fragmenting gluon turns out to be simply the gluon-from-quark TMD FF, plus a remnant which is power suppressed. Therefore, in b_T-space, the overlapping with the contribution of the TMD FFs is self-evident. In fact, the subtraction mechanism described in Section 2.4.1 simply returns the power suppressed terms of Eq. (3.19). This means that the subtracted partonic tensor, which describes the "core" of the process, is power suppressed in the 2-jet limit, recovering the same result obtained withing the modified formalism of Section 2.6.1.

Most importantly, the result of Eq. (3.19) could have been obtained much more easily by neglecting the condition on thrust from the very beginning, already in the transverse momentum space, Eq. (3.5). This approximation is indeed the realization of assumption **H.1**. In fact, neglecting the relation between collinear transverse momentum and thrust corresponds to the kinematic configuration in which the detected hadron does not modifyvthe topology of the final statevand, ultimately, the measured value of T. This circumstance happens any time the detected hadron does not have a transverse momentum large enough to cause a significant spread of the jet to which it belongs to. The jet could well be wide, but not due to the direction of the detected hadron.

When the detected hadron causes the jet spreading, then the whole final state is inevitably far from the ideal pencil-like configuration, making the value of the thrust to decrease, as shown pictorially in Fig. 3.4. If this is the case, then the relation between k_T and τ in Eq. (3.5) cannot be neglected anymore. Moreover, the large-b_T limit is not a faithful representation of this kinematics configuration, as the thrust cannot reach the ideal limit $\tau = 0$ because of the size of k_T, large enough to forbid a pencil-like final state. In this case, the final result in b_T-space is given by the Fourier transform of the
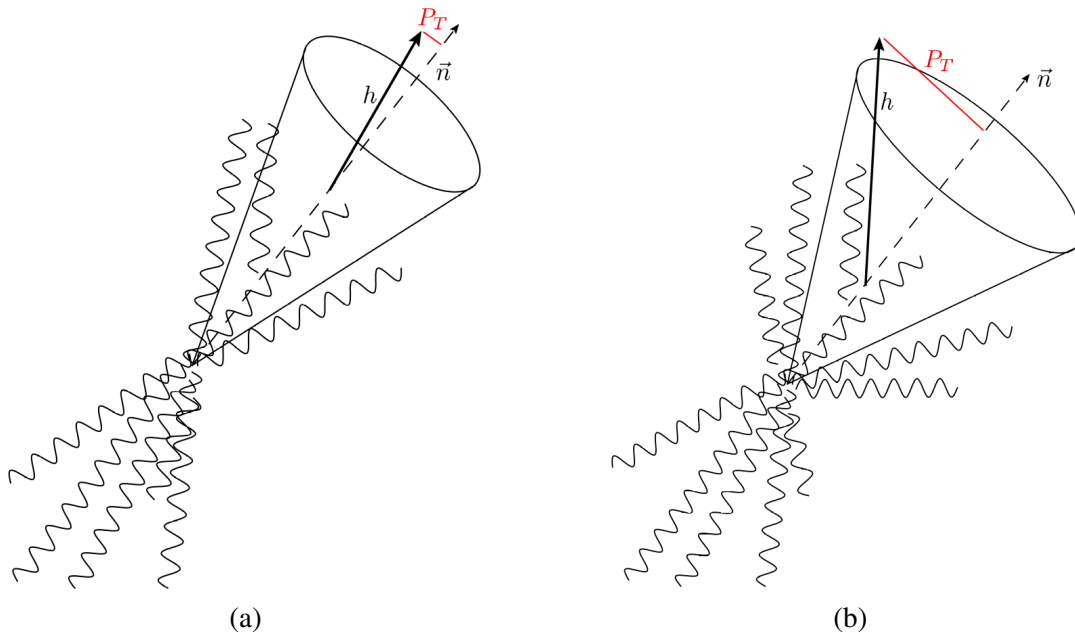
Fig. 3.4 Pictorial representation of 2-jet configurations in which the assumption **H.1** holds true (a) and in which instead it is not valid (b). In the case (a) the detected hadron is rather close to the thrust axis $\vec{n}$ and hence it does not affect the topology of the final state. In the case (b) the detected hadron causes a significant spread of the jet which affects the final state configuration, and ultimately the measured value of T.

gluon-from-quark GFJF of Eq. (3.6). Despite the differences with the case that lead to Eq. (3.19), the conclusions are the same, since the subtraction mechanism has to be modified in order to be adapted to this different kinematics configuration. In fact, the procedure discussed in Section 2.4.1 was devised assuming that **H.1** holds true. However, the modification is straightforward, as it is enough to replace the TMD FFs with the GFJFs in the subtraction term of Eqs. (2.32) and (2.33), and hence also in the factorization theorem in Eq. (2.26). In this case the final cross section is a convolution between a fully perturbative partonic cross section and a generalized fragmentation jet function. I will consider this different factorization theorem more in detail later on in this Chapter. For the moment being, it is sufficient to notice that when this different subtraction procedure is applied to Eq. (3.6), the result is trivially zero.

Therefore, also when **H.1** is not satisfied, the detected hadron is not generated by the fragmentation of a gluon in the 2-jet case.

3.4 Backward Radiation

In a 2-jet topology, the detected hadron is generated by the fragmentation of a fermion, which will be assumed to be a quark of flavor f. The fragmentation of an antiquark is totally analogous. In

this section I will consider the contribution of the radiation emitted in the direction opposite to the fragmenting quark, which will be denoted as backward radiation. At 1-loop order, we have to consider the two Feynman diagrams of Fig. 2.7, which lead to the squared amplitudes presented in Eqs. (2.65) and (2.66). If the gluon is emitted in the S_B-hemisphere, then there are two leading momentum regions. The first is associated to the configuration in which the gluon is collinear to the antiquark and is obtained through the action of the approximator T_B. The other regards the emission of a soft gluon, and it is given by applying the approximator T_S^-. These two momentum regions overlap, hence we have to remove the double counting of the same contributions. The overlapping region is associated to a gluon which can be considered soft-collinear: it has a very small energy but also a large (and, in this case, negative) rapidity. Such contribution is obtained by the combination of approximators $T_B T_S \equiv T_S T_B$. Notice that the label "$-$" is redundant in such combination, as the action of T_B already encodes the information about the selection of the hemisphere.

All these approximators act on the squared matrix elements as well as on the integration of the phase space, as defined in the previous Section. In particular, in a backward approximation, there is no transverse momentum flowing into the A-subgraph, and hence $\vec{k}'_T = 0$. This confirms that all the contributions associated to the backward radiation are TMD-irrelevant.

In conclusion, the 1-loop contribution of the backward radiation to the partonic tensor can be written as:

$$\widehat{W}_{f,\text{backward}}^{\mu\nu,[1]}(\varepsilon; z, \tau, k_T) = \left(T_S^- - T_S T_B + T_B \right) \left[\widehat{W}_f^{\mu\nu,[1]}(\varepsilon; z, \tau, k_T) \right] + \begin{matrix} \text{power suppressed} \\ \text{corrections} \end{matrix}. \qquad (3.21)$$

In the following, the three contributions involved in the previous expression will be considered separately.

Soft approximation

The action of T_S^- leads to the following approximation:

$$T_S^- \left[\widehat{W}_f^{\mu\nu,[1]}(\varepsilon; z, \tau, k_T) \right] = \int \frac{d\rho}{\rho} \star \widehat{W}_f^{\mu\nu,[0]}(z/\rho, Q)\, \delta(1-\rho)\mathcal{S}_-^{[1]}(\varepsilon; \tau)\, \delta\left(\vec{k}_T\right), \qquad (3.22)$$

where I used the same conventions adopted in the previous section. In the previous expression, I have introduced the **generalized soft thrust function** $\mathcal{S}$. Its definition is obtained by integrating (instead of Fourier transforming) the 2-h soft factor, defined as in Eq. (1.1), with the further explicit dependence on thrust, implemented as for the usual soft thrust function, defined as in Eq. (D.6). In practice, it is defined modifying the usual soft thrust function by introducing the rapidity divergence regulator. In the case of the Collins factorization formalism, this is achieved by tilting the two Wilson lines off the light-cone, see Appendix A. Therefore, besides the dependence on thrust, $\mathcal{S}$ depends also on the rapidity cut-offs.

The label "$-$" associated to the generalized soft thrust function in Eq. (3.22) reminds that only the contribution associated to the hemisphere S_B has to be taken into account. This is realized by imposing

that the rapidity of the backward radiations cannot be positive. At 1-loop order, it is sufficient to set $l^- > l^+$, where l is the momentum of the radiated soft gluon. Therefore, we have:

$$\mathcal{S}_-^{[1]}(\varepsilon; \tau, y_1, y_2) =$$

$$= \int \frac{d^D l}{(2\pi)^D} \theta\left(l^- - l^+\right) \delta\left(\tau - \frac{l^+}{q^+}\right) \left(\text{} + h.c. \right) =$$

$$= \frac{\alpha_S}{4\pi} 4 C_F S_\varepsilon \left(\frac{\mu}{Q}\right)^{2\varepsilon} \tau^{-1-2\varepsilon} \int_{-\infty}^0 dy \, e^{2\varepsilon y} \frac{1 + e^{-2(y_1-y_2)}}{\left(1 - e^{-2(y_1-y)}\right)\left(1 - e^{2(y_2-y)}\right)} + h.c., \tag{3.23}$$

where in the last step we made a change of variables in order to expose the range of the rapidity of the gluon $y = \frac{1}{2}\log\left(\frac{l^+}{l^-}\right)$, which is negative as required for backward radiation. The integration gives:

$$\int_{-\infty}^0 dy \, e^{2\varepsilon y} \frac{1 + e^{-2(y_1-y_2)}}{\left(1 - e^{-2(y_1-y)}\right)\left(1 - e^{2(y_2-y)}\right)} = \frac{1}{2} \frac{1 + e^{-2(y_1-y_2)}}{1 - e^{-2(y_1-y_2)}} \frac{1}{1 - 2\varepsilon}$$

$$\times \left\{ -e^{-y_2} \left[{}_2F_1\left(1, 1+2\varepsilon; 2+2\varepsilon; e^{-y_2}\right) - {}_2F_1\left(1, 1+2\varepsilon; 2+2\varepsilon; -e^{-y_2}\right) \right] + \right.$$

$$\left. + e^{-y_1} \left[{}_2F_1\left(1, 1+2\varepsilon; 2+2\varepsilon; e^{-y_1}\right) - {}_2F_1\left(1, 1+2\varepsilon; 2+2\varepsilon; -e^{-y_1}\right) \right] \right\} =$$

$$= \frac{1}{2}\left(\frac{1}{\varepsilon} + \left(-e^{2y_2}\right)^\varepsilon \Gamma(-\varepsilon)\Gamma(1+\varepsilon) + \mathcal{O}\left(e^{-2y_1}, e^{2y_2}, e^{-2(y_1-y_2)}\right) \right). \tag{3.24}$$

Inserting this result in Eq. (3.23) and neglecting the errors due to the vanishing rapidity cut-offs, we obtain:

$$\mathcal{S}_-^{[1]}(\varepsilon; \tau, y_2) = \frac{\alpha_S}{4\pi} 2 C_F S_\varepsilon \left(\frac{\mu}{Q}\right)^{2\varepsilon} \tau^{-1-2\varepsilon} \left(\frac{1}{\varepsilon} + \left(-e^{2y_2}\right)^\varepsilon \Gamma(-\varepsilon)\Gamma(1+\varepsilon) + h.c. \right). \tag{3.25}$$

Notice that whole dependence on the rapidity cut-off y_1 is suppressed in the final result. Therefore, I dropped it from the l.h.s of the previous equation. This is a general feature: only the dependence on the rapidity cut-off relevant for the considered hemisphere survives. In fact, the analogous contribution of the hemisphere S_A to the generalized soft thrust function is obtained from Eq. (3.25) by replacing[2] y_2 with $-y_1$:

$$\mathcal{S}_+(\varepsilon; \tau, y_1) = \mathcal{S}_-(\varepsilon; \tau, -y_1) \tag{3.26}$$

---

[2]Notice that this is the same replacement derived in Section 2.5 in studying the behavior of the TMDs under a Z-axis reflection.

There is a straightforward factorization theorem that relates the contributions of the two hemispheres to the total generalized soft thrust function:

$$\mathcal{S}\left(\varepsilon; \tau, y_1 - y_2\right) = \mathcal{S}_+\left(\varepsilon; \tau, y_1\right)\mathcal{S}_-\left(\varepsilon; \tau, y_2\right). \tag{3.27}$$

Finally, it is interesting to point out that the result of Eq. (3.25) can be equivalently written as:

$$\mathcal{S}_-^{[1]}\left(\varepsilon; \tau, y_2\right) = S_-^{[1]}\left(\varepsilon; \tau\right) + \frac{\alpha_S}{4\pi}2C_F S_\varepsilon \left(\frac{\mu}{Q}\right)^{2\varepsilon} \tau^{-1-2\varepsilon}\Gamma(-\varepsilon)\Gamma(1+\varepsilon)\left(\left(-e^{2y_2}\right)^\varepsilon + h.c.\right), \tag{3.28}$$

where $S_- \equiv \frac{1}{2}S$ is the backward radiation contribution to the usual 1-loop soft thrust function. If we had removed the rapidity cut-offs from the very beginning in the definition of the generalized soft thrust function, Eq. (3.23), this would have been the whole final result. However, retaining y_1 and y_2 in the calculation leads to an extra term depending on the leading cut-off of the hemisphere, in this case y_2. Such extra term will have to cancel out when we will subtract the overlapping with the collinear contribution.

Soft-collinear approximation (overlapping)

The action of $T_S T_B$ produces the following approximation:

$$T_S T_B \left[\widehat{W}_f^{\mu\nu,[1]}\left(\varepsilon; z, \tau, k_T\right)\right] = \int \frac{d\rho}{\rho} \star \widehat{W}_f^{\mu\nu,[0]}(z/\rho, Q)\,\delta(1-\rho)\mathcal{Y}_-^{[1]}\left(\varepsilon; \tau\right)\delta\left(\vec{k}_T\right). \tag{3.29}$$

In this expression I have introduced the **soft-collinear thrust functions** $\mathcal{Y}_\pm$. In particular, the contribution associated to the hemisphere S_B is involved in Eq. (3.29). Differently from $\mathcal{S}$, this functions does not have a counterpart among the usual thrust functions reviewed in Appendix D. It is defined as the subtraction term of the TMDs[3], Eq. (1.18), integrated (instead of Fourier transformed) over $\vec{k}_T$, and modified to include the explicit dependence on the thrust, whose value is soft-approximated as in Eq. (D.5). In practice, $\mathcal{Y}_\pm$ are defined similarly to $\mathcal{S}$, but tilting only the Wilson line pointing in the reference direction indicated by the collinear approximator. Therefore, the soft-collinear thrust functions acquire a dependence on the rapidity cut-off associated to the tilted Wilson line. At 1-loop

---

[3]The TMDs are intended defined in the factorization definition, Eq. (1.21).

order and for the backward radiation contribution we have:

$$\mathcal{Y}^{[1]}_-(\varepsilon; \tau, y_2) =$$

$$= \int \frac{d^D l}{(2\pi)^D} \delta\left(\tau - \frac{l^+}{q^+}\right) \left(+ h.c. \right) =$$

$$= \frac{\alpha_S}{4\pi} 4 C_F S_\varepsilon \left(\frac{\mu}{Q}\right)^{2\varepsilon} \tau^{-1-2\varepsilon} \int_{-\infty}^{+\infty} dy \, e^{2\varepsilon y} \frac{1}{\left(1 - e^{2(y_2 - y)}\right)} + h.c. \tag{3.30}$$

Notice that the action of T_B makes the Heaviside theta that selects the (-)-hemisphere redundant, as $T_B \theta(l^- - l^+) = \theta(l^-)$. However this condition is already encoded into the requirement that the emitted gluon is on-shell at the final state cut. As a consequence, differently from Eq. (3.23), the integration on the rapidity of the gluon is unbounded from below. The integral in Eq. (3.30) has the following solution:

$$\int_{-\infty}^{+\infty} dy \, e^{2\varepsilon y} \frac{1}{\left(1 - e^{2(y_2 - y)}\right)} = \frac{1}{2} \left(e^{2y_2}\right)^\varepsilon \left[B_{e^{2y_2}}(-\varepsilon, 0) - B_{e^{-2y_2}}(1 + \varepsilon, 0)\right] =$$

$$= \frac{1}{2} \left(-e^{2y_2}\right)^\varepsilon \Gamma(-\varepsilon)\Gamma(1 - \varepsilon) + \mathcal{O}\left(e^{2y_2}\right), \tag{3.31}$$

where B is the incomplete Beta function. Inserting this result into Eq. (3.30) we obtain:

$$\mathcal{Y}^{[1]}_-(\varepsilon; \tau, y_2) = \frac{\alpha_S}{4\pi} 2 C_F S_\varepsilon \left(\frac{\mu}{Q}\right)^{2\varepsilon} \tau^{-1-2\varepsilon} \Gamma(-\varepsilon)\Gamma(1 + \varepsilon) \left(\left(-e^{2y_2}\right)^\varepsilon + h.c.\right). \tag{3.32}$$

As for the soft case, the analogous contribution in the opposite hemisphere, resulting from the action of $T_S T_A$ can be easily obtained from Eq. (3.32) by replacing y_2 by $-y_1$:

$$\mathcal{Y}_+(\varepsilon; \tau, y_1) = \mathcal{Y}_-(\varepsilon; \tau, -y_1) \tag{3.33}$$

Notice that if we had removed the rapidity cut-off from the very beginning, already in the definition of $\mathcal{Y}$ in Eq. (3.30), then the integration over the rapidity of the emitted gluon would have been scaleless and hence vanishing in full dimensional regularization. This is the reason for which the soft-collinear thrust functions do not have a counterpart among the thrust-dependent functions usually encountered in the factorization of $e^+ e^-$ annihilation processes.

In this case, the fact that r.h.s of Eq. (3.32) is non vanishing is crucial for the success of the subtraction mechanism. In fact, the result found for $\mathcal{Y}_-$ is exactly equal to the extra term, rapidity

cut-off dependent, obtained in the calculation of S_-, Eq. (3.28). Therefore:

$$S_-^{[1]}(\varepsilon;\tau,y_2) - \mathcal{Y}_-^{[1]}(\varepsilon;\tau,y_2) = S_-^{[1]}(\varepsilon;\tau).\tag{3.34}$$

In other words, the *subtracted* soft contribution associated to the backward emission, obtained through the action of $\left(T_S^- - T_S T_B\right)$, is totally independent of the rapidity cut-off y_2. Therefore, we can derive the following factorization theorems, which generalize Eq. (3.34), as well as the analogous equation holding for the S_A-hemisphere, to all orders:

$$S_+(\varepsilon;\tau) = \frac{S_+(\varepsilon;\tau,y_1)}{\mathcal{Y}_+(\varepsilon;\tau,y_1)};\tag{3.35a}$$

$$S_-(\varepsilon;\tau) = \frac{S_-(\varepsilon;\tau,y_2)}{\mathcal{Y}_-(\varepsilon;\tau,y_2)}.\tag{3.35b}$$

In conclusion, this factorization theorems, together with Eq. (3.27), lead to:

$$S(\varepsilon;\tau) = \frac{S_+(\varepsilon;\tau,y_1)}{\mathcal{Y}_+(\varepsilon;\tau,y_1)}\frac{S_-(\varepsilon;\tau,y_2)}{\mathcal{Y}_-(\varepsilon;\tau,y_2)}.\tag{3.36}$$

which encodes the relations between the usual soft thrust function and the soft and soft-collinear thrust functions defined in this Section.

Collinear approximation

Finally, the effect of the action of the T_B approximator gives:

$$T_B\left[\widehat{W}_f^{\mu\nu,[1]}(\varepsilon;z,\tau,k_T)\right] = \int\frac{d\rho}{\rho}\star\widehat{W}_f^{\mu\nu,[0]}(z/\rho,Q)\,\delta(1-\rho)J^{[1]}(\varepsilon;\tau)\,\delta\left(\vec{k}_T\right).\tag{3.37}$$

where J is the usual jet thrust function at 1 loop[4], defined in Eq. D.12. In this case, we do not have any rapidity cut-off, since in (unsubtracted) collinear parts the Wilson lines are defined along the light-cone.

Final result for backward radiation

Combining the results above and inserting them into Eq. (3.21), we can write the final expression for the contribution of the backward radiation to the partonic tensor. In transverse momentum space

---

[4]In principle, in the pure Collins factorization formalism, masses cannot be neglected in the collinear contributions. However, since in this case we are dealing with rather low scales ($Q \sim 10$ GeV for the BELLE experiment) that prevent the presence of heavy quarks, we will put all masses to zero

we have:

$$\widehat{W}^{\mu\nu,[1]}_{f,\text{backward}}(\varepsilon; z, \tau, k_T) =$$
$$= \int \frac{d\rho}{\rho} \star \widehat{W}^{\mu\nu,[0]}_f(z/\rho, Q)\, \delta(1-\rho) \left[S^{[1]}_-(\varepsilon; \tau) + J^{[1]}(\varepsilon; \tau) \right] \delta\left(\vec{k}_T\right) + \begin{smallmatrix}\text{power suppressed}\\\text{corrections}\end{smallmatrix}, \quad (3.38)$$

where I used Eq. (3.34) to combine soft and soft-collinear contributions. The power suppressed terms contains both the errors due to the approximations introduced by the factorization procedure and also the terms neglected in the limit of large rapidity cut-off. Since the dependence on $\vec{k}_T$ is trivial, in b_T-space we have simply:

$$\widetilde{\widehat{W}}^{\mu\nu,[1]}_{f,\text{backward}}(\varepsilon; z, \tau, b_T) =$$
$$= \int \frac{d\rho}{\rho} \star \widehat{W}^{\mu\nu,[0]}_f(z/\rho, Q)\, \delta(1-\rho) \left[S^{[1]}_-(\varepsilon; \tau) + J^{[1]}(\varepsilon; \tau) \right] + \begin{smallmatrix}\text{power suppressed}\\\text{corrections}\end{smallmatrix}. \quad (3.39)$$

3.5 Region 1: TMD factorization

The contributions associated to the radiation emitted in the same hemisphere of the detected hadron are of course the most interesting. They encode the whole information on the TMD effects, hence they are the keystone for exploring the rich kinematic structure underlying the process we are investigating. The leading momentum regions are the counterpart of those considered in the previous section, properly modified in order to describe the emission in the S_A hemisphere. Therefore, when the emitted gluon is soft, the partonic tensor is well approximated by the action of T_S^+, while, when it is collinear to the fragmenting quark, the approximation obtained through T_A is faithful. Moreover, there is the overlapping region between these two configurations, where the gluon is soft-collinear. In this case, it has a very low energy but also a large (and positive) rapidity and the corresponding contribution is well approximated by the action of $T_S T_A \equiv T_A T_S$ approximator. Therefore, the 1-loop contribution to the partonic tensor of the radiation emitted into the S_A-hemisphere (forward) can be written as:

$$\widehat{W}^{\mu\nu,[1]}_{f,\text{forward}}(\varepsilon; z, \tau, k_T) = \left(T_S^+ - T_S T_A + T_A \right) \left[\widehat{W}^{\mu\nu,[1]}_f(\varepsilon; z, \tau, k_T) \right] + \begin{smallmatrix}\text{power suppressed}\\\text{corrections}\end{smallmatrix}. \quad (3.40)$$

The most important difference with respect to the cases discussed in Section 3.4 is in the role that each of these contributions plays in the generation of significant TMD effects. In other words, following the nomenclature introduced in Section 3.2, not all these three kinematics configurations may be TMD relevant. Indeed, when the gluon is radiated collinearly to the fragmenting quark, it contributes actively to the deflection of the detected hadron with respect to the thrust axis. Therefore, as pointed out in Section 3.2, the action of T_A produces a TMD-relevant term. For soft and soft-
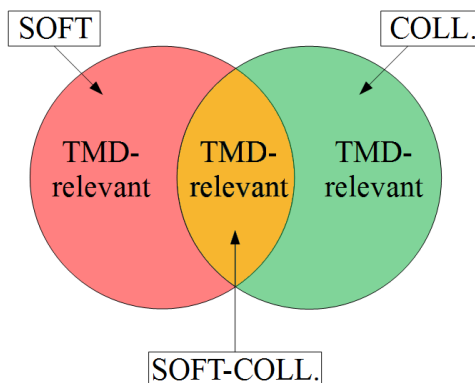
Fig. 3.5 Pictorial representation of leading momentum regions associated to the radiation in the S_A hemisphere in Region 1, where the assumption **H.2** is false. If soft gluons are TMD-relevant, this automatically extends to soft-collinear gluons, as collinear radiation is always TMD-relevant.

collinear gluons this is not as straightforward, first of all because, according to power counting, their transverse momentum has a much smaller size than that of the collinear emission (see Appendix A).

In particular, we have founded the factorization theorem devised in Chapter 2 on the assumption **H.2** that the soft radiation did not affect the measured value of P_T. The purpose of this section is to derive a factorization theorem *without* this requirement, i.e. by considering the soft gluon contribution as a TMD-relevant quantity. Notice that, if the soft contributions are TMD-relevant, automatically also the overlapping soft-collinear momentum region must be considered TMD-relevant, as shown pictorially in Fig. 3.5. In this case, the size of the transverse momentum of the detected hadron has to be very small in order to be sensitive to soft radiation, which posses a very low transverse momentum according to power counting rules. In other words, a sizeably large P_T is the signal that soft gluons are not contributing to TMD effects. As a consequence, the kinematic configuration discussed at the end of Section 3.3, where the assumption **H.1** is false, is automatically excluded as it requires larger values of P_T. Schematically, this can be expressed as:

$$\mathbf{H.2} \text{ false} \longrightarrow \mathbf{H.1} \text{ true.} \tag{3.41}$$

Of course, the previous argument can be reversed, leading to:

$$\mathbf{H.1} \text{ false} \longrightarrow \mathbf{H.2} \text{ true.} \tag{3.42}$$

Summarizing, these hypotheses cannot be false at the same time.

The kinematic region corresponding to these initial hypothesis (**H.2** false, **H.1** true) will be indicated as **Region 1**, following the same nomenclature introduced in Ref. [17]. Clearly, the final factorization theorem derived for this region will be different from that presented in Eq. (2.26). In fact, its structure will be much more similar to the standard TMD factorization theorems obtained for 2-h class cross sections presented in Section 1.4.1.
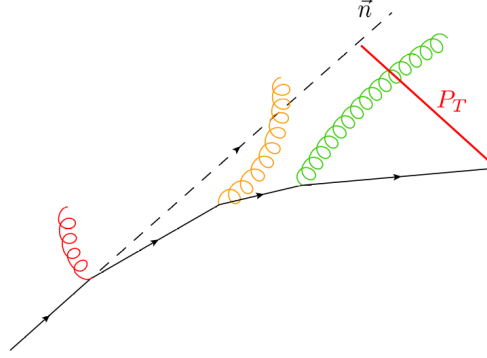
Fig. 3.6 Pictorial representation of the effect of a TMD-relevant soft radiation. The final P_T, measured with respect to the thrust axis $\vec{n}$, is the result of several deflections due to emission/absorption of radiation. When the soft gluons (red) are TMD-relevant, they deflect the detected hadron affecting its transverse momentum. This effect must be added to the analogous contributions of soft-collinear gluons (orange) and collinear gluons (green).

Soft approximation

If the soft radiation is TMD-relevant, the action of T_S^+ gives a non-trivial dependence on $\vec{k}_T$:

$$T_S^+ \left[\widehat{W}_f^{\mu\nu,[1]}(\varepsilon; z, \tau, k_T) \right] = \int \frac{d\rho}{\rho} \star \widehat{W}_f^{\mu\nu,[0]}(z/\rho, Q)\, \delta(1-\rho)\Sigma_+^{[1]}(\varepsilon; \tau, k_T), \qquad (3.43)$$

where I have introduced the **soft thrust factor** Σ. It is defined exactly as $\widetilde{\mathbb{S}}_{\text{2-h}}$, presented in Section 1.2.1, but with an explicit dependence on thrust implemented as in the usual soft thrust function, through Eqs. (D.5). Therefore, Σ depends not only on the total soft transverse momentum and on the rapidity cut-offs associated to the tilted Wilson lines, but also on τ. In Eq. (3.43) only the contribution of the soft thrust factor to the S_A hemisphere is involved. At 1-loop order it is defined in momentum space as:

$$\Sigma_+^{[1]}(\varepsilon; \tau, k_T, y_1, y_2) =$$

$$= \int \frac{dl^+ dl^-}{(2\pi)^D} \theta\left(l^+ - l^-\right) \delta\left(\tau - \frac{l^-}{q^-}\right) \left(\text{diagram} + h.c. \right) =$$

$$= \frac{\alpha_S}{4\pi} 2 C_F S_\varepsilon \frac{\Gamma(1-\varepsilon)}{\pi^{1-\varepsilon}} \mu^{2\varepsilon} \frac{1}{k_T^2} \int_0^{+\infty} dy \frac{1 + e^{-2(y_1 - y_2)}}{\left(1 - e^{-2(y_1 - y)}\right)\left(1 - e^{2(y_2 - y)}\right)} \delta\left(\tau - \frac{k_T}{Q} e^{-y}\right) + h.c.$$

$$(3.44)$$

Notice how the Heaviside theta enforces the gluon to be emitted in the (+)-hemisphere. Moreover, in analogy to the generalized soft thrust function S_+ defined in Section 3.4, we should expect that only

the rapidity cut-off relevant for the considered hemisphere (in this case y_1) will contribute explicitly to the final result.

The Fourier transform of the Eq. (3.44) can be written in the following form:

$$\widetilde{\Sigma}_+^{[1]} (\varepsilon; \tau, b_T, y_1, y_2) = \int d^{2-2\varepsilon} \vec{k}_T \, e^{i\vec{k}_T \cdot \vec{b}_T} \, \Sigma_+^{[1]} (\varepsilon; \tau, k_T, y_1, y_2) =$$

$$= \frac{\alpha_S}{4\pi} 2 C_F S_\varepsilon \left(\frac{\mu}{Q} \right)^{2\varepsilon} \Gamma(1-\varepsilon) \frac{1+e^{-2(y_1-y_2)}}{1-e^{-2(y_1-y_2)}} \left(\frac{b}{c1} \right)^\varepsilon e^{-\gamma_E \varepsilon} \tau^{-1-\varepsilon} \times$$

$$\times \left(I_\varepsilon \left(\tau b, e^{-2y_1} \right) - I_\varepsilon \left(\tau b, e^{-2y_2} \right) \right) + h.c., \tag{3.45}$$

where $b = b_T Q$ and where we have defined the integral:

$$I_\varepsilon (a, r) = \int_0^1 dx \frac{x^{\varepsilon/2}}{x-r} J_{-\varepsilon} \left(\frac{a}{\sqrt{x}} \right) \tag{3.46}$$

The solution to this integral requires advanced mathematical tools and non-standard techniques. Because of its importance, the procedure adopted for its solution is shown, step-by-step, in Appendix E. Therefore, from Eqs. E.15 and (E.17), the integral appearing in Eq. (3.45) admit the following solutions:

$$I_\varepsilon(\tau b, r_1) = \left(\frac{\tau b}{2} \right)^{-\varepsilon} \frac{1}{\varepsilon \Gamma(1-\varepsilon)} {}_1F_2 \left(-\varepsilon; 1-\varepsilon, 1-\varepsilon; -\frac{\tau^2 b^2}{4} \right) +$$

$$+ \left(\frac{\tau b}{2} \right)^\varepsilon \Gamma(-\varepsilon) - 2 \left(-r_1 \right)^{\varepsilon/2} K_{-\varepsilon} \left(\frac{\tau b}{\sqrt{-r_1}} \right) + \mathcal{O}(r_1); \tag{3.47a}$$

$$I_\varepsilon \left(\tau b, \frac{1}{r_2} \right) = \mathcal{O}(r_2), \tag{3.47b}$$

where I set $r_1 = e^{-2y_1}$ and $r_2 = e^{2y_2}$. As expected, the dependence on y_2 vanishes in the limit $y_2 \to -\infty$ and the final result depends only on y_1.

Inserting the Eqs. (3.47) into Eq. (3.45), we obtain the expression for the Fourier transform soft thrust factor at 1-loop order:

$$\widetilde{\Sigma}_+^{[1]} (\varepsilon; \tau, b_T, y_1) =$$

$$= \frac{\alpha_S}{4\pi} 2 C_F S_\varepsilon \left(\frac{\mu}{Q} \right)^{2\varepsilon} \left\{ \frac{\tau^{-1-2\varepsilon}}{\varepsilon} {}_1F_2 \left(-\varepsilon; 1-\varepsilon, 1-\varepsilon; -\frac{\tau^2 b^2}{4} \right) + \right.$$

$$+ \frac{1}{\tau} \left(\frac{b}{c1} \right)^{2\varepsilon} e^{-2\gamma_E \varepsilon} \Gamma(1-\varepsilon) \Gamma(-\varepsilon) - 2\tau^{-1-\varepsilon} \left(-e^{-2y_1} \right)^{\varepsilon/2} K_{-\varepsilon} \left(\frac{\tau b}{\sqrt{-r_1}} \right) +$$

$$\left. + \mathcal{O} \left(e^{-2y_1}, e^{2y_2}, e^{-2(y_1-y_2)} \right) \right\} + h.c., \tag{3.48}$$
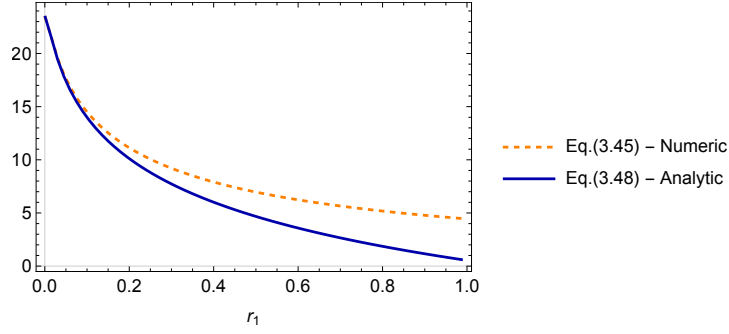
Fig. 3.7 The analytical behaviour of $\widetilde{\Sigma}_+^{[1]}(\varepsilon; \tau, b_T, y_1)$, (solid, blue line), is compared to its numerical counterpart (orange, dashed line). These lines are obtained by integrating with a test function chosen as $T(\tau) = e^{-\tau}$.

where $c_1 = 2e^{-\gamma_E}$. The analogous contribution in the opposite hemisphere $\widetilde{\Sigma}_-$ can be easily obtained from Eq. (3.48) bt replacing y_1 with $-y_2$. This is a general property:

$$\widetilde{\Sigma}_-(\varepsilon; \tau, b_T, y_2) = \widetilde{\Sigma}_+(\varepsilon; \tau, b_T, -y_2). \tag{3.49}$$

Furthermore, a generalization of the factorization theorem in Eq. (3.27) holds for unintegrated quantities:

$$\widetilde{\Sigma}(\varepsilon; \tau, b_T, y_1 - y_2) = \widetilde{\Sigma}_+(\varepsilon; \tau, b_T, y_1)\widetilde{\Sigma}_-(\varepsilon; \tau, b_T, y_2). \tag{3.50}$$

In Eq. (3.48), only the first term presents the expected "soft" behavior for the thrust $\tau^{-1-2\varepsilon}$, i.e. the same dependence shown by the usual soft thrust function at 1-loop order, Eq. (D.6). This will not be of concern, as the extra terms will be canceled after the subtraction of the overlapping soft-collinear contribution, similarly to what was done for the case of the backward radiation. For this reason, in the following I will focus on the "pure soft" term, i.e. contribution in the first line of Eq. (3.48):

$$\widetilde{\Sigma}_{+;\,\mathrm{pure\,soft}}^{[1]}(\varepsilon; \tau, b_T) = \frac{\alpha_S}{4\pi} 4C_F S_\varepsilon \left(\frac{\mu}{Q}\right)^{2\varepsilon} \frac{\tau^{-1-2\varepsilon}}{\varepsilon} \, {}_1F_2\left(-\varepsilon; 1-\varepsilon, 1-\varepsilon; -\frac{\tau^2 b^2}{4}\right), \tag{3.51}$$

where we also added its complex conjugate counterpart. Notice that without the hypergeometric function ${}_1F_2$, the soft thrust factor would be equal to the usual soft thrust function S_+, restricted to the S_A hemisphere.

Following the same argument used for the benchmark case of the fragmenting gluon, since in momentum space τ is proportional to the soft transverse momentum k_T, then the 2-jet limit where $\tau \to 0$ corresponds to the power counting region where $k_T \ll Q$. Therefore, after the Fourier transform, the region of interest is at large-b_T. Applying the trick of Eq. (3.8) we can write:
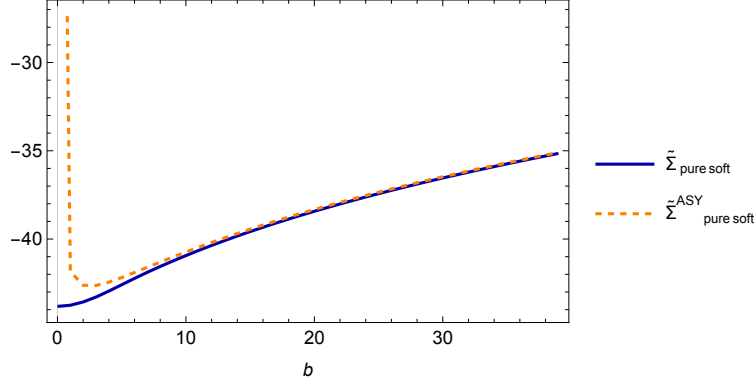
Fig. 3.8 The "pure soft" thrust factor (solid, blue line), Eq. (3.51), is compared to its asymptotic large-b behaviour (dashed, orange line), Eq. (3.53). These lines are obtained by integrating with a test function chosen as $T(\tau) = e^{-\tau}$.

$$\frac{\tau^{-1-2\varepsilon}}{\varepsilon} \, {}_1F_2\left(-\varepsilon; 1-\varepsilon, 1-\varepsilon; -\frac{\tau^2 b^2}{4}\right) = \delta(\tau)\left[-\frac{1}{2\varepsilon^2} \, {}_2F_3\left(-\varepsilon, -\varepsilon; 1-\varepsilon, 1-\varepsilon, 1-\varepsilon; -\frac{b^2}{4}\right)\right] +$$

$$+ \left(\frac{\tau^{-1-2\varepsilon}}{\varepsilon} \, {}_1F_2\left(-\varepsilon; 1-\varepsilon, 1-\varepsilon; -\frac{\tau^2 b^2}{4}\right)\right)_+ =$$

$$= \delta(\tau)\left[-\frac{1}{2\varepsilon^2} + \frac{b^2}{8} \, {}_3F_4\left(1,1,1; 2,2,2,2; -\frac{b^2}{4}\right)\right] +$$

$$+ \frac{1}{\varepsilon}\left(\frac{1}{\tau}\right)_+ - 2\left(\frac{\log\tau}{\tau}\right)_+ + \left(\tau\frac{b^2}{4} \, {}_2F_3\left(1,1; 2,2,2; -\frac{\tau^2 b^2}{4}\right)\right)_+ + \mathcal{O}(\varepsilon) =$$

$$= \delta(\tau)\left[-\frac{1}{2\varepsilon^2} + \log^2\left(\frac{b}{c_1}\right)\right] + \frac{1}{\varepsilon}\left(\frac{1}{\tau}\right)_+ + 2\log\left(\frac{b}{c_1}\right)\left(\frac{1}{\tau}\right)_+ + \begin{array}{c}\text{terms suppressed} \\ \text{in the limit } b\to\infty\end{array} + \mathcal{O}(\varepsilon)$$

$$(3.52)$$

where in the second step we ε-expanded and in the last one we extracted the asymptotic behavior at large-b. Finally:

$$\widetilde{\Sigma}^{[1],\,\text{ASY}}_{+;\,\text{pure soft}}(\varepsilon; \tau, b_T) = \frac{\alpha_S}{4\pi} 4 C_F S_\varepsilon \left\{ -\frac{1}{2\varepsilon^2}\delta(\tau) + -\frac{1}{\varepsilon}\left[\delta(\tau)\log\left(\frac{\mu}{Q}\right) - \left(\frac{1}{\tau}\right)_+\right] + \right.$$

$$\left. + \log\left(\frac{b_T \mu}{c_1}\right)\left[2\left(\frac{1}{\tau}\right)_+ + \delta(\tau)\left(\log\left(\frac{b_T \mu}{c_1}\right) - 2\log\left(\frac{\mu}{Q}\right)\right)\right]\right\}. \qquad (3.53)$$

Soft-collinear approximation (overlapping)

As discussed at the beginning of this section, if the soft approximation gives a TMD-relevant contribution the same must hold also for the soft-collinear momentum region. The result of the action of $T_S T_A$ gives:

$$T_S T_A\left[\widehat{W}^{\mu\nu,[1]}_f(\varepsilon; z, \tau, k_T)\right] = \int \frac{d\rho}{\rho} {}_\star \widehat{W}^{\mu\nu,[0]}_f(z/\rho, Q)\,\delta(1-\rho)\Upsilon^{[1]}_+(\varepsilon; \tau, k_T), \qquad (3.54)$$

where I have introduced the **soft-collinear thrust factor** $\Upsilon_\pm$, whose S_A-hemisphere contribution is involved into Eq. (3.43). This object is defined in the same way of the subtraction term of the TMDs, Eq. (1.21), but with in addition the dependence on thrust implemented as in Eq. (D.5). Therefore, $\Upsilon_\pm$ depends on the total soft-collinear transverse momentum, on the rapidity cut-off associated to the tilted Wilson line of its definition and also on the thrust. At 1-loop order, the forward hemisphere contribution is then defined as:

$$\Upsilon_+^{[1]}(\varepsilon; \tau, k_T, y_1) =$$

$$= \int \frac{dl^+ dl^-}{(2\pi)^D} \delta\left(\tau - \frac{l^-}{q^-}\right) \left(\vphantom{\int} \qquad\qquad + h.c. \right) =$$

$$= \frac{\alpha_S}{4\pi} 2 C_F S_\varepsilon \frac{\Gamma(1-\varepsilon)}{\pi^{1-\varepsilon}} \mu^{2\varepsilon} \frac{1}{k_T^2} \int_{-\infty}^{+\infty} dy \frac{1}{1-e^{-2(y_1-y)}} \delta\left(\tau - \frac{k_T}{Q}e^{-y}\right) + h.c. \tag{3.55}$$

Notice that, analogously to the case of backward radiation, in soft-collinear contributions the range of the rapidity of the radiated particles is unconstrained. In fact, differently from Eq. (3.44), the rapidity of the emitted gluon in Eq. (3.55) is unbounded from below. Its Fourier transform leads to:

$$\widetilde{\Upsilon}_+^{[1]}(\varepsilon; \tau, b_T\, y_1) = \int d^{2-2\varepsilon}\vec{k}_T\, e^{i\vec{k}_T \cdot \vec{b}_T}\, \Upsilon_+^{[1]}\left(\varepsilon; \tau, \vec{k}_T\, y_1\right) =$$

$$= \frac{\alpha_S}{4\pi} 2 C_F S_\varepsilon \left(\frac{\mu}{Q}\right)^{2\varepsilon} \Gamma(1-\varepsilon) \left(\frac{b}{c_1}\right)^\varepsilon e^{-\varepsilon\gamma_E} \tau^{-1-\varepsilon} \int_0^\infty \frac{x^{\varepsilon/2}}{x - e^{-2y_1}} J_{-\varepsilon}\left(\frac{\tau b}{\sqrt{x}}\right) + h.c. \tag{3.56}$$

The solution of the integral can be obtained through the same procedure used to solve the integration in Eq. (3.46). The result can be found in Eq. (E.18) and it is given by:

$$\int_0^\infty \frac{x^{\varepsilon/2}}{x - r_1} J_{-\varepsilon}\left(\frac{\tau b}{\sqrt{x}}\right) = -2(-r_1)^{\varepsilon/2} K_{-\varepsilon}\left(\frac{\tau b}{\sqrt{-r_1}}\right) + \left(\frac{\tau b}{2}\right)^\varepsilon \Gamma(-\varepsilon), \tag{3.57}$$

where $r_1 = e^{-2y_1}$. This is an exact result, as there are no terms suppressed in the limit $r_1 \to 0$. Inserting this result in Eq. (3.56) we obtain:

$$\widetilde{\Upsilon}_+^{[1]}(\varepsilon; \tau, b_T, y_1) = \frac{\alpha_S}{4\pi} 2 C_F S_\varepsilon \left(\frac{\mu}{Q}\right)^{2\varepsilon} \left\{ \frac{1}{\tau} \left(\frac{b}{c1}\right)^{2\varepsilon} e^{-2\gamma_E \varepsilon} \Gamma(1-\varepsilon)\Gamma(-\varepsilon) - \right.$$

$$\left. - 2\tau^{-1-\varepsilon}\Gamma(1-\varepsilon)\left(-e^{-2y_1}\right)^{\varepsilon/2} K_{-\varepsilon}\left(\frac{\tau b}{\sqrt{-e^{-2y_1}}}\right) \right\} + h.c. \tag{3.58}$$

As anticipated above, the extra terms associated to an unexpected thrust dependence in Eq. (3.48) are exactly canceled after subtraction of the soft-collinear found above. Therefore, only the "pure soft"

term remains after elimination of the double counting:

$$\widetilde{\Sigma}_+^{[1]}(\varepsilon;\tau,b_T,y_1) - \widetilde{\Upsilon}_+^{[1]}(\varepsilon;\tau,b_T,y_1) = \widetilde{\Sigma}_{+;\text{pure soft}}^{[1]}(\varepsilon;\tau,b_T,y_1). \tag{3.59}$$

which is the analogous of Eq. (3.34). Such result, together with its counterpart in the opposite hemisphere, can be generalized to all orders leading to the following factorization theorems:

$$\widetilde{\Sigma}_{+;\text{pure soft}}(\varepsilon;\tau,b_T) = \frac{\widetilde{\Sigma}_+(\varepsilon;\tau,b_T,y_1)}{\widetilde{\Upsilon}_+(\varepsilon;\tau,b_T,y_1)}; \tag{3.60a}$$

$$\widetilde{\Sigma}_{-;\text{pure soft}}(\varepsilon;\tau,b_T) = \frac{\widetilde{\Sigma}_-(\varepsilon;\tau,b_T,y_2)}{\widetilde{\Upsilon}_-(\varepsilon;\tau,b_T,y_2)}. \tag{3.60b}$$

Together with Eq. (3.50), these factorization theorems lead to:

$$\widetilde{\Sigma}_{\text{pure soft}}(\varepsilon;\tau,b_T) = \frac{\widetilde{\Sigma}_+(\varepsilon;\tau,b_T,y_1)}{\widetilde{\Upsilon}_+(\varepsilon;\tau,b_T,y_1)}\frac{\widetilde{\Sigma}_-(\varepsilon;\tau,b_T,y_2)}{\widetilde{\Upsilon}_-(\varepsilon;\tau,b_T,y_2)}. \tag{3.61}$$

which is the counterpart of Eq. (3.36) for unintegrated quantities.

Finally, following the same procedure adopted so far, we have to study the large-b_T behavior of the soft collinear factor, as this is a faithful description of the 2-jet limit, provided that **H.2** is false. The large-b asymptotic of $\widetilde{\Upsilon}_+^{[1]}$ can be obtained, once again, exploiting the trick of Eq. (3.8). Notice that the two contributions in Eq. (3.58) are separately divergent as $\tau \to 0$, but their sum is integrable. We have:

$$\frac{1}{\tau}\left(\frac{b}{c1}\right)^{2\varepsilon} e^{-2\gamma_E\,\varepsilon}\,\Gamma(1-\varepsilon)\Gamma(-\varepsilon) - 2\tau^{-1-\varepsilon}\Gamma(1-\varepsilon)\,(-r_1)^{\varepsilon/2}\,K_{-\varepsilon}\left(\frac{\tau b}{\sqrt{-r_1}}\right) =$$

$$= \delta(\tau)\frac{1}{2}\Bigg\{ (-r_1)^\varepsilon\,\Gamma(1-\varepsilon)\Gamma(1+\varepsilon)\Gamma(-\varepsilon)\left[\frac{\Gamma(-\varepsilon)}{\Gamma(1-\varepsilon)^2}\,{}_1F_2\left(-\varepsilon;1-\varepsilon,1-\varepsilon;-\frac{b^2}{4r_1}\right) + \right.$$

$$+ \left(\frac{b}{c1}\right)^{2\varepsilon} e^{-2\varepsilon\gamma_E}\,(-r_1)^{-\varepsilon}\,G_{1,3}^{2,0}\left(\frac{b^2}{4r_1}\,\bigg|\,\begin{matrix}1\\0,0,-\varepsilon\end{matrix}\right)\Bigg] -$$

$$- \left(\frac{b}{c1}\right)^{2\varepsilon} e^{-2\varepsilon\gamma_E}\Gamma(1-\varepsilon)\Gamma(-\varepsilon)\left(H_{-\varepsilon} - 2\log\left(\frac{b}{c_1}\right) + \log r_1\right)\Bigg\} +$$

$$+ \left(\frac{1}{\tau}\left(\frac{b}{c1}\right)^{2\varepsilon} e^{-2\gamma_E\,\varepsilon}\,\Gamma(1-\varepsilon)\Gamma(-\varepsilon) - 2\tau^{-1-\varepsilon}\Gamma(1-\varepsilon)\,(-r_1)^{\varepsilon/2}\,K_{-\varepsilon}\left(\frac{\tau b}{\sqrt{-r_1}}\right)\right)_+ =$$

$$= \frac{1}{2\varepsilon^2}\delta(\tau) + \frac{1}{\varepsilon}\left[-\left(\frac{1}{\tau}\right)_+ + \frac{1}{2}\log(-r_1)\delta(\tau)\right] - 2\log\left(\frac{b}{c_1}\right)\left(\frac{1}{\tau}\right)_+ -$$

$$- \delta(\tau)\left[\log^2\left(\frac{b}{c_1}\right) - \log\left(\frac{b}{c_1}\right)\log(-r_1)\right] + \begin{matrix}\text{terms suppressed}\\ \text{in the limit } b\to\infty\end{matrix} + \mathcal{O}(\varepsilon) \tag{3.62}$$

Therefore, the contribution of soft-collinear gluons in a 2-jet configuration is obtained by inserting this result into Eq. (3.58). We have:

$$\widetilde{\Upsilon}_{+}^{[1],\text{ASY}}\left(\varepsilon;\tau,b_T,y_1\right) =$$

$$= \frac{\alpha_S}{4\pi}2C_F S_\varepsilon \left\{ \frac{1}{\varepsilon^2}\delta(\tau) + \frac{1}{\varepsilon}\left[-2\left(\frac{1}{\tau}\right)_+ + \delta(\tau)\log\left(e^{-2y_1}\right) + 2\delta(\tau)\log\left(\frac{\mu}{Q}\right)\right] + \right.$$

$$\left. + 2\log\left(\frac{b_T\mu}{c_1}\right)\left[-2\left(\frac{1}{\tau}\right)_+ + \delta(\tau)\left(\log\left(e^{-2y_1}\right) - \log\left(\frac{b_T\mu}{c_1}\right) + 2\log\left(\frac{\mu}{Q}\right)\right)\right]\right\}. \quad (3.63)$$

Combining the result of Eq. (3.53) with Eq. (3.63) we can reconstruct the large-b_T behavior of the unsubtracted soft thrust factor:

$$\widetilde{\Sigma}_{+}^{[1],\text{ASY}}\left(\varepsilon;\tau,b_T,y_1\right) = \widetilde{\Sigma}_{+;\text{pure soft}}^{[1],\text{ASY}}\left(\varepsilon;\tau,b_T\right) + \widetilde{\Upsilon}_{+}^{[1],\text{ASY}}\left(\varepsilon;\tau,b_T,y_1\right) =$$

$$= -\frac{\alpha_S}{4\pi}4C_F\left(\frac{1}{\varepsilon}y_1 + 2y_1\log\left(\frac{b_T\mu}{c_1}\right)\right)\delta(\tau) = \delta(\tau)\widetilde{\mathbb{S}}_{2\text{-h},+}^{[1],(0)}\left(\varepsilon;b_T,y_1\right), \quad (3.64)$$

where $\widetilde{\mathbb{S}}_{2\text{-h},+}^{(0)}$ is the contribution of the S_A-hemisphere to the *bare* 2-h soft factor, as defined in Eq. (1.6). From now on, it will be indicated as the[5] (bare) **forward soft factor**. After adding the proper counterterm Z_S^+, the result of Eq. (3.64) can be directly compared with the 1-loop order of $\widetilde{\mathbb{S}}_{2\text{-h}}$ presented in Eq. (A.11). This result will be crucial in devising a factorization theorem suitable for Region 1. Moreover, thanks to the factorization theorems of Eqs. (3.50) and (3.61), Eq. (3.64) can be generalized to all orders as:

$$\widetilde{\Sigma}_{+}\left(\varepsilon;\tau,b_T,y_1\right) \underset{\sim}{^{2\text{-jet limit}}} \widetilde{\Sigma}_{+}^{\text{ASY}}\left(\varepsilon;\tau,b_T,y_1\right) = \delta(\tau)\widetilde{\mathbb{S}}_{2\text{-h},+}^{(0)}\left(\varepsilon;b_T,y_1\right); \quad (3.65\text{a})$$

$$\widetilde{\Sigma}_{-}\left(\varepsilon;\tau,b_T,y_2\right) \underset{\sim}{^{2\text{-jet limit}}} \widetilde{\Sigma}_{-}^{\text{ASY}}\left(\varepsilon;\tau,b_T,y_2\right) = \delta(\tau)\widetilde{\mathbb{S}}_{2\text{-h},-}^{(0)}\left(\varepsilon;b_T,y_2\right), \quad (3.65\text{b})$$

where, by analogy, $\widetilde{\mathbb{S}}_{2\text{-h},-}$ defines the **backward soft factor**. Furthermore, combining the theorems above:

$$\widetilde{\Sigma}\left(\varepsilon;\tau,b_T,y_1-y_2\right) \underset{\sim}{^{2\text{-jet limit}}} \delta(\tau)\widetilde{\mathbb{S}}_{2\text{-h}}^{(0)}\left(\varepsilon;b_T,y_1-y_2\right), \quad (3.66)$$

where $\widetilde{\mathbb{S}}_{2\text{-h}}$ is the *same* soft factor appearing in 2-h cross sections, as showed in Section 1.4.1. In fact, it is straightforward to show that $\widetilde{\mathbb{S}}_{2\text{-h}}$ is given by the product of the forward and the backward soft factors, as shows the following factorization theorem:

$$\widetilde{\mathbb{S}}_{2\text{-h}}(b_T,\mu,y_1-y_2) = \widetilde{\mathbb{S}}_{2\text{-h},+}\left(\varepsilon;b_T,\mu,y_1\right)\widetilde{\mathbb{S}}_{2\text{-h},-}\left(\varepsilon;b_T,\mu,y_2\right). \quad (3.67)$$

---

[5]By writing explicitly "forward" or "backward" in the name of $\widetilde{\mathbb{S}}_{2\text{-h},+}$ the label "2-h" is redundant, as two hemispheres can only be identified by two hadrons.

Collinear approximation

The last contribution to the partonic tensor is associated to the radiation collinear to the frag-menting quark, obtained through the action of T_A. This is a TMD-relevant quantity by default. The approximation gives:

$$T_A \left[\widehat{W}_f^{\mu\nu,[1]}(\varepsilon; z, \tau, k_T) \right] = \int \frac{d\rho}{\rho} \star \widehat{W}_f^{\mu\nu,[0]}(z/\rho, Q) \, \Gamma_{q/q}^{[1]}(\varepsilon; \rho, k_T, \tau), \tag{3.68}$$

where $\Gamma_{q/q}$ is the quark-from-quark GFJF, which is diagonal in quark's flavors. Analogously to the gluon-from-quark GFJF presented in Section 3.3, $\Gamma_{q/q}$ is defined in momentum space as the unsubtracted collinear parts shown in Eq. (1.15), but in addition the explicit dependence on thrust is implemented as in Eq. (D.17). At 1-loop order it is defined[6] as:

$$\Gamma_{q/q}^{[1]}(\varepsilon; z, k_T, \tau) =$$

$$= \int \frac{dl^-}{(2\pi)^D} \delta\left(\tau - \frac{z}{1-z}\frac{k_T^2}{Q^2}\right) \frac{\mathrm{Tr}_C}{N_C} \frac{\mathrm{Tr}_D}{4} \gamma^+ \left(\begin{array}{c} \\ \\ \end{array} + h.c. + \begin{array}{c} \\ \\ \end{array} \right) =$$

$$= \frac{\alpha_S}{4\pi} 2 C_F S_\varepsilon \frac{\Gamma(1-\varepsilon)}{\pi^{1-\varepsilon}} \mu^{2\varepsilon} \frac{1}{k_T^2} \left(\frac{2}{1-z} + (1-\varepsilon)\frac{1-z}{z} \right) \theta(1-z) \, \delta\left(\tau - \frac{z}{1-z}\frac{k_T^2}{Q^2}\right). \tag{3.69}$$

Notice that without the delta that fixes the thrust, the previous expression would have coincided with the unsubtracted quark-from-quark TMD FF in momentum space, see Eq. (A.51). Its Fourier transform gives:

$$\widetilde{\Gamma}_{q/q}^{[1]}(\varepsilon; z, b_T, \tau) =$$
$$= \int d^{2-2\varepsilon}\vec{k}_T \, e^{i\vec{k}_T \cdot \vec{b}_T} \Gamma_{q/q}^{[1]}(\varepsilon; z, k_T, \tau) =$$
$$= \frac{\alpha_S}{4\pi} 2 C_F S_\varepsilon \left(\frac{\mu}{Q}\right)^{2\varepsilon} z^\varepsilon \left(2(1-z)^{-1-\varepsilon} + (1-\varepsilon)\frac{(1-z)^{1-\varepsilon}}{z} \right) \times$$
$$\times \tau^{-1-\varepsilon} \, {}_0F_1\left(1-\varepsilon; -\tau\frac{1-z}{z}\frac{b^2}{4}\right). \tag{3.70}$$

The combination of $\tau^{-1-\varepsilon}$ with the hypergeometric function ${}_0F_1$ has already been computed in Eq. (3.18). However, we derived this result for a function that was regular in $z \sim 1$. Therefore, we can use that solution only for computing the term proportional to $(1-z)^{1-\varepsilon}$, but not for the term proportional to $(1-z)^{-1-\varepsilon}$. The combination $(1-z)^{-1-\varepsilon}\tau^{-1-\varepsilon}{}_0F_1$ can be treated by using a generalized version of the trick expressed in Eq. (3.8). However, the easiest way to obtain an expansion in distributions of τ and z is to apply the usual trick of Eq. (3.8) to $(1-z)^{-1-\varepsilon}$ and $\tau^{-1-\varepsilon}$

---

[6]The definition is obtained by neglecting all the mass corrections, as in Eq. (3.37).

separately:

$$z^{\varepsilon} (1-z)^{-1-\varepsilon} \tau^{-1-\varepsilon} {}_0F_1 \left(1 - \varepsilon; -\tau \frac{1-z}{z} \frac{b^2}{4} \right) =$$

$$= \frac{1}{\varepsilon^2} \delta(\tau) \delta(1-z) - \frac{1}{\varepsilon} \left[\delta(\tau) \left(\frac{1}{1-z} \right)_+ + \delta(1-z) \left(\frac{1}{\tau} \right)_+ \right] +$$

$$+ \delta(\tau) \left(\frac{\log(1-z)}{1-z} \right)_+ - \delta(\tau) \frac{\log z}{1-z} + \delta(1-z) \left(\frac{\log \tau}{\tau} \right)_+ +$$

$$+ \left(\frac{1}{1-z} \right)_+ \left(\frac{1}{\tau} \right)_+ J_0 \left(\sqrt{\tau \frac{1-z}{z}} b \right) + \mathcal{O}(\varepsilon). \tag{3.71}$$

All the terms containing either $\delta(1-z)$ or $\delta(\tau)$ are trivial, since the hypergeometric function evaluated in $\tau = 0$ and/or in $z = 1$ gives just one. The only non-trivial term is the last line of the previous equation:

$$\left(\frac{1}{1-z} \right)_+ \left(\frac{1}{\tau} \right)_+ J_0 \left(\sqrt{\tau \frac{1-z}{z}} b \right). \tag{3.72}$$

Next, we will make use of the following trick, valid for functions of a variable x that varies in the range $0 \le x \le 1$, at most divergent as a simple pole at small values of x:

$$\left(\frac{1}{x} \right)_+ f(x) = \delta(x) \int_0^1 d\alpha \, [f(\alpha) - f(0)] + \left(\frac{1}{x} f(x) \right)_+. \tag{3.73}$$

Proceeding in this way, we find:

$$\left(\frac{1}{1-z} \right)_+ \left(\frac{1}{\tau} \right)_+ J_0 \left(\sqrt{\tau \frac{1-z}{z}} b \right) =$$

$$= \left(\frac{1}{1-z} \right)_+ \left\{ \delta(\tau) \left[-\frac{1-z}{z} \frac{b^2}{4} {}_2F_3 \left(1, 1; 2, 2, 2; -\frac{1-z}{z} \frac{b^2}{4} \right) \right] + \left(\frac{1}{\tau} J_0 \left(\sqrt{\tau \frac{1-z}{z}} b \right) \right)_+ \right\}. \tag{3.74}$$

The contribution multiplying $\delta(\tau)$ can be treated similarly:

$$\left(\frac{1}{1-z} \right)_+ \left[-\frac{1-z}{z} \frac{b^2}{4} {}_2F_3 \left(1, 1; 2, 2, 2; -\frac{1-z}{z} \frac{b^2}{4} \right) \right] =$$

$$= \delta(1-z) \left[G_{1,3}^{3,0} \left(\frac{b^2}{4} \middle| \begin{matrix} 1 \\ 0,0,0 \end{matrix} \right) - \frac{\pi^2}{6} - 2\log^2 \left(\frac{b}{c_1} \right) \right] + \left(-\frac{1}{z} \frac{b^2}{4} {}_2F_3 \left(1, 1; 2, 2, 2; -\frac{1-z}{z} \frac{b^2}{4} \right) \right)_+ \tag{3.75}$$

where $G_{1,3}^{3,0}$ is a Meijer G-function. Since in Region 1 the hypothesis **H.1** holds true (see Eq. (3.41)), we have to determine the large-b asymptotic of $\widetilde{\Gamma}_{q/q}$. At large b_T, the two terms in Eq. (3.75) behaves

as:

$$G_{1,3}^{3,0}\left(\frac{b^2}{4}\,\middle|\,\begin{matrix}1\\0,0,0\end{matrix}\right)-\frac{\pi^2}{6}-2\log^2\left(\frac{b}{c_1}\right)=-\frac{\pi^2}{6}-2\log^2\left(\frac{b}{c_1}\right)+\begin{matrix}\text{terms suppressed}\\\text{in the limit }_{b\to\infty}\end{matrix};\qquad(3.76a)$$

$$\left(-\frac{1}{z}\frac{b^2}{4}\,_2F_3\left(1,1;2,2,2;-\frac{1-z}{z}\frac{b^2}{4}\right)\right)_+=$$

$$=-2\log\left(\frac{b}{c_1}\right)\left(\frac{1}{1-z}\right)_+-\left(\frac{\log(1-z)}{1-z}\right)_++\frac{\log z}{1-z}+\frac{\pi^2}{6}\delta(1-z)+\begin{matrix}\text{terms suppressed}\\\text{in the limit }_{b\to\infty}\end{matrix}.$$

$$(3.76b)$$

On the other hand, the contribution in the last line of Eq. (3.74) has to be computed carefully, as it shows also a non-trivial dependence on τ besides that on z. A rather simple way to study such contribution is to investigate its action on two test functions $T(\tau)$ and $R(z)$. We have:

$$\int_0^1 dz\, R(z)\left(\frac{1}{1-z}\right)_+\int_0^1 d\tau\, T(\tau)\left(\frac{1}{\tau}J_0\left(\sqrt{\tau\frac{1-z}{z}}b\right)\right)_+=$$

$$=\int_0^1 d\tau\frac{T(\tau)-T(0)}{\tau}\left\{R(1)\int_0^1\frac{dz}{1-z}\left[J_0\left(\sqrt{\tau\frac{1-z}{z}}b\right)\right]+\right.$$

$$\left.+\int_0^1 dz\frac{R(z)-R(1)}{1-z}J_0\left(\sqrt{\tau\frac{1-z}{z}}b\right)\right\}=$$

$$=R(1)\int_0^1 d\tau\frac{T(\tau)-T(0)}{\tau}\left[-2\log\left(\frac{b}{c_1}\right)-\log\tau\right]+\begin{matrix}\text{terms suppressed}\\\text{in the limit }_{b\to\infty}\end{matrix}.\qquad(3.77)$$

Therefore, the difficult term in Eq. (3.74) can be approximated as:

$$\left(\frac{1}{1-z}\right)_+\left(\frac{1}{\tau}J_0\left(\sqrt{\tau\frac{1-z}{z}}b\right)\right)_+=$$

$$=-\delta(1-z)\left[2\log\left(\frac{b}{c_1}\right)\left(\frac{1}{\tau}\right)_++\left(\frac{\log\tau}{\tau}\right)_+\right]+\begin{matrix}\text{terms suppressed}\\\text{in the limit }_{b\to\infty}\end{matrix}.\qquad(3.78)$$

Combining together this result with Eqs. (3.76), we can finally write the large-b behavior of the combination of distributions in Eq. (3.72):

$$\left(\frac{1}{1-z}\right)_+\left(\frac{1}{\tau}\right)_+J_0\left(\sqrt{\tau\frac{1-z}{z}}b\right)=$$

$$=-2\log^2\left(\frac{b}{c_1}\right)\delta(\tau)\delta(1-z)-2\log\left(\frac{b}{c_1}\right)\left[\delta(\tau)\left(\frac{1}{1-z}\right)_++\delta(1-z)\left(\frac{1}{\tau}\right)_+\right]-$$

$$-\left[\delta(\tau)\left(\frac{\log(1-z)}{1-z}\right)_+-\delta(\tau)\frac{\log z}{1-z}+\delta(1-z)\left(\frac{\log\tau}{\tau}\right)_+\right]+\begin{matrix}\text{terms suppressed}\\\text{in the limit }_{b\to\infty}\end{matrix}.\qquad(3.79)$$

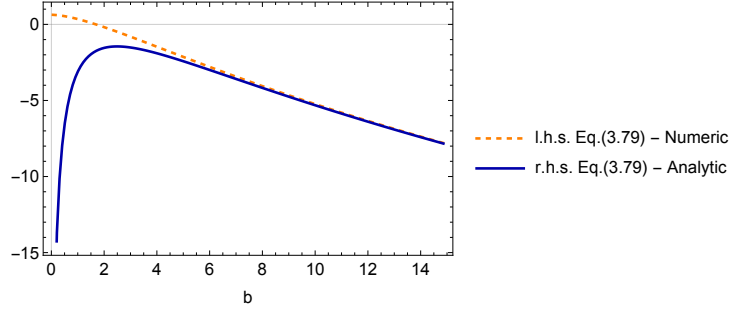Notice how the last line of the previous equation cancels exactly the terms in the third line of

Fig. 3.9 The large-b behaviour of the term $\left(\frac{1}{1-z}\right)_+ \left(\frac{1}{\tau}\right)_+ J_0\left(\sqrt{\tau \frac{1-z}{z}}\, b\right)$ in Eq. (3.79) (solid, blue line), is compared to its numerical counterpart (orange, dashed line). These lines are obtained by integrating with two test functions, $T_\tau(\tau) = e^{-\tau}$ and $T_z(z) = e^{-(1-z)}$.

Eq. (3.71). In fact:

$$
z^\varepsilon (1-z)^{-1-\varepsilon} \tau^{-1-\varepsilon}\, {}_0F_1\left(1-\varepsilon;\, -\tau\,\frac{1-z}{z}\frac{b^2}{4}\right) =
$$

$$
= \frac{1}{\varepsilon^2}\delta(\tau)\delta(1-z) - \frac{1}{\varepsilon}\left[\delta(\tau)\left(\frac{1}{1-z}\right)_+ + \delta(1-z)\left(\frac{1}{\tau}\right)_+\right] -
$$

$$
- 2\log^2\left(\frac{b}{c_1}\right)\delta(\tau)\delta(1-z) - 2\log\left(\frac{b}{c_1}\right)\left[\delta(\tau)\left(\frac{1}{1-z}\right)_+ + \delta(1-z)\left(\frac{1}{\tau}\right)_+\right] +
$$

$$
+ \begin{array}{c}\text{terms suppressed}\\\text{in the limit } {}_{b\to\infty}\end{array} + \mathcal{O}(\varepsilon). \tag{3.80}
$$

This result, together with Eq. (3.18), allows to determine the large-b asymptotic of $\widetilde{\Gamma}_{q/q}$:

$$
\widetilde{\Gamma}_{q/q}^{[1],\,\mathrm{ASY}}(\varepsilon; z, b_T, \tau) =
$$

$$
= \frac{1}{z} Z_{q/q,\,\mathrm{coll.}}^{[1]}(\varepsilon; z)\,\delta(\tau) +
$$

$$
+ \frac{\alpha_S}{4\pi} 2 C_F\, S_\varepsilon\, \delta(1-z)\left\{\delta(\tau)\left[\frac{2}{\varepsilon^2} + \frac{1}{\varepsilon}\left(\frac{3}{2} + 4\log\left(\frac{\mu}{Q}\right)\right)\right] + \frac{2}{\varepsilon}\left(\frac{1}{\tau}\right)_+\right\} +
$$

$$
+ \frac{\alpha_S}{4\pi} 2 C_F\, S_\varepsilon\left\{\delta(\tau)\left[2\log\left(\frac{b_T\,\mu}{c_1}\right)\left(2\left(\frac{1}{1-z}\right)_+ + 1 - \frac{1}{z}\right) - 1 + \frac{1}{z} - \right.\right.
$$

$$
\left.\left. - 4\delta(1-z)\log\left(\frac{b_T\,\mu}{c_1}\right)\left(\log\left(\frac{b_T\,\mu}{c_1}\right) - 2\log\left(\frac{\mu}{Q}\right)\right)\right] - 4\delta(1-z)\left(\frac{1}{\tau}\right)_+\log\left(\frac{b_T\,\mu}{c_1}\right)\right\}. \tag{3.81}
$$

Notice that all the non-trivial z-dependence associated with the poles is encoded into the function $Z_{q/q,\,\mathrm{coll.}}$, which is the UV counterterm of the quark-from-quark collinear FF. This is not a coincidence, but rather the 1-loop expression of a crucial factorization theorem.

In fact, in analogy to what was done with the soft momentum region, the "pure collinear" radiation contribution is obtained after the subtraction of the overlapping terms in the soft-collinear momentum region. Therefore, combining the result of Eqs. (3.81) and (3.63), we can write the following expression for the subtracted collinear part:

$$\widetilde{\Gamma}^{[1],\,\mathrm{ASY}}_{q/q}(\varepsilon;\tau,z,b_T) - \delta(1-z)\,\widetilde{\Upsilon}^{[1],\,\mathrm{ASY}}_{+}(\varepsilon;\tau,b_T,y_1) = \delta(\tau)\,z\,\widetilde{D}^{[1],\,(0)}_{q/q}(\varepsilon;z,b_T,y_1)\,, \qquad (3.82)$$

where $\widetilde{D}^{(0)}_{q/q}$ is the *bare* quark-from-quark TMD FF in b_T-space, presented in Eq. (A.56). It has both its characteristic collinear divergence, encoded into $Z_{q/q,\,\mathrm{coll.}}$, and also the divergences that have to UV-renormalized by adding the counterterm $Z_{q/q,\,\mathrm{TMD}}$. By defining the **subtracted quark-from-quark GFJF** as:

$$\widetilde{\Gamma}^{\mathrm{sub.}}_{q/q}(\varepsilon;z,k_T,\tau,y_1) = \frac{\widetilde{\Gamma}_{q/q}(\varepsilon;z,k_T,\tau)}{\widetilde{\Upsilon}_{+}(\varepsilon;\tau,b_T,y_1)} \qquad (3.83)$$

which is totally analogous to the factorization definition of the TMDs introduced in Eq. (1.21), the result of Eq. (3.82) can be generalized to all orders, leading to:

$$\widetilde{\Gamma}^{\mathrm{sub.}}_{q/q}(\varepsilon;z,k_T,\tau,y_1) \underset{\sim}{\overset{\text{2-jet limit}}{=}} \delta(\tau)\,z\,\widetilde{D}^{(0)}_{q/q}(\varepsilon;z,b_T,y_1) \qquad (3.84)$$

This result, together with Eq. (3.66), will be crucial in developing a suitable factorization theorem for Region 1.

Final result for forward radiation   Combining all the results of this section and inserting them into Eq. (3.40), we obtain the final expression for the contribution of the radiation emitted in the S_A-hemisphere to the partonic tensor. In b_T-space we have:

$$\widetilde{\widehat{W}}^{\mu\nu,[1]}_{f,\mathrm{forward}}(\varepsilon;z,\tau,b_T) =$$

$$= \int \frac{d\rho}{\rho} \star \widehat{W}^{\mu\nu,[0]}_{f}(z/\rho,Q)\left[\delta(1-\rho)\left(\Sigma^{[1]}_{+}(\varepsilon;\tau,k_T) - \widetilde{\Upsilon}^{[1]}_{+}(\varepsilon;\tau,b_T,y_1)\right) + \widetilde{\Gamma}^{[1]}_{q/q}(\varepsilon;\tau,\rho,b_T)\right]$$

$$\underset{\sim}{\overset{\text{2-jet limit}}{}} \int \frac{d\rho}{\rho} \star \widehat{W}^{\mu\nu,[0]}_{f}(z/\rho,Q)\,\delta(\tau)\left[\delta(1-\rho)\widetilde{\mathbb{S}}^{[1],\,(0)}_{2\text{-h},+}(\varepsilon;b_T,y_1) + \rho\,\widetilde{D}^{[1],\,(0)}_{q/q}(\varepsilon;\rho,b_T,y_1)\right]$$

$$(3.85)$$

Notice that the whole dependence on the rapidity cut-off y_1 is washed out in the combination of $\widetilde{\mathbb{S}}_{2\text{-h},+}$ and the TMD FF. Moreover, we could have obtain easily the same result by neglecting from the very beginnin *any* relation between the thrust and the transverse momentum, in all the leading momentum regions associated to the forward radiation. In fact, in Region 1 the detected hadron is so close to the thrust axis that it cannot affect the final state topology by any means.

3.5.1 Factorization theorem for Region 1

Now we have all the necessary ingredients to write the whole partonic tensor at 1-loop order. It is the sum of the backward and the forward radiation expressed in Eqs. (3.38) and (3.85), respectively. Furthermore, it must also include the contribution of the virtual gluon emission, which is given by the 1-loop vertex function in Eq. (C.15). In terms of kinematics approximators, this is the hard momentum region, where the gluon is far off-shell. Therefore, it is well approximated by the action of T_H:

$$\widetilde{\widetilde{W}}_{f,\text{virtual}}^{\mu\nu,[1]}(\varepsilon;z,\tau,b_T) = \int \frac{d\rho}{\rho} \star \widehat{W}_f^{\mu\nu,[0]}(z/\rho,Q)\delta(1-\rho)\delta(\tau)V^{[1]}(\varepsilon), \tag{3.86}$$

where I used the fact that for virtual emissions, both the dependence on $\vec{k}_T$ and on the collinear momentum fraction are trivial. Finally, the partonic tensor at 1-loop for Region 1 in b_T-space is given by:

$$\widetilde{\widetilde{W}}_f^{\mu\nu,[1]}(\varepsilon;z,\tau,b_T) = \widetilde{\widetilde{W}}_{f,\text{virtual}}^{\mu\nu,[1]}(\varepsilon;z,\tau,b_T) + \widetilde{\widetilde{W}}_{f,\text{backward}}^{\mu\nu,[1]}(\varepsilon;z,\tau,b_T) + \widetilde{\widetilde{W}}_{f,\text{forward}}^{\mu\nu,[1]}(\varepsilon;z,\tau,b_T) =$$

$$= H_T^{\mu\nu} N_C e_f^2 \int \frac{d\rho}{\rho} \delta(1-z/\rho) \left[\delta(1-\rho)\delta(\tau)V(\varepsilon) + \delta(1-\rho)\left[J^{[1]}(\varepsilon;\tau) + S_-^{[1]}(\varepsilon;\tau) \right] + \right.$$

$$\left. + \delta(\tau)\left[\delta(1-\rho)\widetilde{\mathbb{S}}_{2\text{-h},+}^{[1],(0)}(\varepsilon;b_T,y_1) + \rho \widetilde{D}_{q/q}^{[1],(0)}(\varepsilon;\rho,b_T,y_1) \right] \right] =$$

$$= H_T^{\mu\nu} N_C e_f^2 \left[\delta(1-z)\left(\delta(\tau)V(\varepsilon) + J^{[1]}(\varepsilon;\tau) + S_-^{[1]}(\varepsilon;\tau) + \delta(\tau)\widetilde{\mathbb{S}}_{2\text{-h},+}^{[1],(0)}(\varepsilon;b_T,y_1) \right) + \right.$$

$$\left. + \delta(\tau)z\widetilde{D}_{q/q}^{[1],(0)}(\varepsilon;z,b_T,y_1) \right], \tag{3.87}$$

where we used the expression for the LO partonic tensor of Eq. (C.6). Notice that *all* the divergences cancel each other, except for the characteristic collinear divergence of the TMD FF, which cannot be dealt by pQCD. In fact, the explicit expression for the sum of all the contribution is:

$$\widetilde{\widetilde{W}}_f^{\mu\nu,[1]}(\varepsilon;z,\tau,b_T)) = H_T^{\mu\nu} N_C e_f^2 \left[\frac{1}{z} Z_{q/q,\text{coll.}}^{[1]}(\varepsilon;z)\delta(\tau) + \right.$$

$$+ \frac{\alpha_S}{4\pi} C_F \left\{ \delta(\tau)\left[\delta(1-z)\left(-9 + \frac{4\pi^2}{3} - 4\log^2\left(\frac{b_T\mu}{c_1}\right) - 6\log\left(\frac{\mu}{Q}\right) + \right. \right. \right.$$

$$+ 8\log\left(\frac{b_T\mu}{c_1}\right)\log\left(\frac{\mu}{Q}\right) - 4\log^2\left(\frac{\mu}{Q}\right) \right) - 8\left(\frac{1}{1-z}\right)_+ \log\left(\frac{b_T\mu}{c_1}\right) +$$

$$\left. + 2\frac{1-z}{z}\left(1 - 2\log\left(\frac{b_T\mu}{c_1}\right) \right) \right] - \delta(1-z)\left(3\left(\frac{1}{\tau}\right)_+ + 4\left(\frac{\log\tau}{\tau}\right)_+ \right) \right\} \right] \tag{3.88}$$

Notice also that the previous expression is RG-invariant. Finally, it is important to stress that the whole dependence on the collinear momentum fraction is encoded into the TMD FF. This result can be easily generalized to all orders by reverting the prescriptions used to switch from the hadronic tensor to the partonic tensor, illustrated in Section 2.4.1. Moreover, because of the divergence cancellation showed in Eq. (3.88), we can drop the ε dependence from the various contributions appearing in the final result and also the label "(0)" from the TMD and the forward soft factor. Therefore, the cross section for $e^+ e^- \to hX$ in Region 1 factorizes as:

$$
\frac{d\sigma_{R_1}}{dz_h \, dP_T^2 \, dT} = \sigma_B \, \pi N_C \, V \int d\tau_S \, d\tau_B \, J(\tau_B) \, S_-(\tau_S) \delta(\tau - \tau_S - \tau_B) \times
$$

$$
\times \int \frac{d^2\vec{b}_T}{(2\pi)^2} \, e^{i \frac{\vec{P}_T}{z_h} \cdot \vec{b}_T} \, \widetilde{\mathbb{S}}_{2\text{-h},+}(b_T, \zeta) \sum_f e_f^2 \, \widetilde{D}_{h/f}(z_h, b_T, \zeta). \tag{3.89}
$$

The rapidity cut-off has been recast into the variable ζ, defined as in Eq. (1.23). This factorized cross section has been obtained by generalizing the 1-loop result. This is a potentially dangerous operation, as new effects may rise at higher orders in perturbation theory. Region 1 is one of the cases where this generalization has to be performed with special care. The reason is that the contribution of the soft radiation is intrinsically asymmetric in this region, as the soft gluons emitted backward contribute only to the thrust (but not to the transverse momentum of the detected hadron), while for the soft gluons emitted forwardly the situation is exactly the opposite. If there are more than two gluons, they can be emitted either in one hemispher or in the other. The asymmetry between these two configuration produces new logarithmic terms due to the correlation between the emissions in different hemispheres. Such terms are usually called Non-Global Logarithms (NGLs). The problem with NGLs is related to their resummation, which involves non-perturbative effects. Their contribution can be included into Eq. (3.89) as an extra factor, see for instance Refs. [49–52]. A correct treatment of NGLs is beyond the purpose of this thesis and they will not be included in the final factorization theorems. In any case, provided that a phenomenological analyses is performed at NLO-NLL accuracy, the formula given in Eq. (3.89) can be considered sufficiently precise, as NGLs arise from NNLO corrections (and beyond).

The same factorized cross section has been obtained within the framework of SCET in Ref. [17], adopting a completely different approach. A similar factorization theorem has been addressed also in Ref. [16].

The factorization theorem of Eq. (3.89) is profoundly different from that devised in Chapter 2. The factorization theorem of Eq. (3.89) is profoundly different from that devised in Chapter 2. First of all, the TMD FFs are not the only factors that encode non-perturbative effects. In fact, the forward soft factor $\widetilde{\mathbb{S}}_{2\text{-h},+}$ has a non-trivial long-distance behavior as well. It can be written explicitly in terms of its perturbative and non-perturbative contributions in analogy to the procedure adopted for the 2-h

soft factor in Section 1.2.1. In fact, a CS-evolution equation for $\widetilde{\mathbb{S}}_{2\text{-h},+}$ can readily be written as:

$$\frac{\partial}{\partial \log \sqrt{\zeta}}\widetilde{\mathbb{S}}_{2\text{-h},+}(b_T, \mu, \zeta) = -\frac{1}{2}\widetilde{K}(b_T, \mu). \qquad (3.90)$$

This is nothing else that the evolution equation with respect to y_1 of the 2-h soft factor, Eq. (1.7a). Notice that $\widetilde{K}$ is the same Collins-Soper kernel appearing in the CS-evolution of the TMDs. Therefore, by making use of the $b^\star$ prescription introduced in Chapter 1, the forward soft factor can be written as a solution of Eq. (3.90):

$$\widetilde{\mathbb{S}}_{2\text{-h},+}(b_T, \mu, \zeta) = e^{\frac{1}{4}\log\left(\frac{\zeta}{Q^2}\right)\left[\int_{\mu_0}^{\mu}\frac{d\mu'}{\mu'}\gamma_K(\alpha_S(\mu')) - \widetilde{K}(b_T^\star;\mu_0)\right]}\sqrt{M_S}(b_T)\, e^{\frac{1}{4}\log\left(\frac{\zeta}{Q^2}\right)g_K(b_T)}, \qquad (3.91)$$

which must be compared to the corresponding expression obtained for $\widetilde{\mathbb{S}}_{2\text{-h}}$ in Eq. (1.14). In the previous equation, the soft model of $\widetilde{\mathbb{S}}_{2\text{-h},+}$ is assumed to be insensitive to the hemisphere into which the soft radiation is emitted. In fact, it depends only on b_T, i.e. (simplifying) only on the transverse momentum of the soft radiation. Therefore it is completely unaware of the plus and minus components, which encode the selection of the emission direction. For this reason, in Eq. (3.91) we have simply $M_{S_+} \equiv \sqrt{M_S}$.

There is another crucial difference between the factorization theorems presented in Chapter 2 and those presented here, concerning the dependence on the rapidity cut-off. The cross section for Region 1 is CS-invariant, and this has already been verified at partonic level, as pointed out at the end of the previous Section. Indeed, the whole dependence on ζ disappear in the combination $\widetilde{\mathbb{S}}_{2\text{-h},+}\widetilde{D}_{h/f}(z_h, b_T, \zeta)$ of Eq. (3.89), even after generalizing to all orders,. This can be directly checked by considering the solutions to the evolution equations for the forward soft factor and the TMD FF, i.e. Eq. (3.91) and (1.26), respectively. We have:

$$\widetilde{\mathbb{S}}_{2\text{-h},+}(b_T, \mu, \zeta)\widetilde{D}_{h/f}(z_h, b_T, \mu, \zeta) = \left(\mathscr{C}_{j/f}(b_T^\star;\mu_b, \zeta_b)\otimes d_{j/h}(\mu_b)\right)(z_h)\times$$
$$\times \exp\left\{\frac{1}{4}\widetilde{K}(b_T^\star;\mu_b)\log\frac{Q^2}{\zeta_b} + \int_{\mu_b}^{\mu}\frac{d\mu'}{\mu'}\left[\gamma_C(\alpha_S(\mu'), 1) - \frac{1}{4}\gamma_K(\alpha_S(\mu'))\log\frac{Q^2}{\mu'^2}\right]\right\}\times$$
$$\times (M_C)_{j,h}(z_h, b_T)\sqrt{M_S(b_T)}\exp\left\{-\frac{1}{4}g_K(b_T)\log z_h^2\frac{Q^2}{M_h^2}.\right\} \qquad (3.92)$$

Despite this equation has been written for an unpolarized TMD FF, it is totally general and can be applied to any TMD. Notice that the neat effect induced by $\widetilde{\mathbb{S}}_{2\text{-h},+}$ is a modification of the TMD model, which is multiplied by a square root of M_S. This is the same modification as that introduced in 2-h cross section in order to absorb the 2-h soft factor into the definition of the TMDs, see Eq. (1.37). Such operation leads to the square root definition of the TMDs, reported in Eq. (1.33). However, in this case the same trick cannot be applied, despite the final results look the same. In fact, naively, one might expect that the square root definition of Eq. (1.33a) would correspond to the combination appearing in the cross section corresponding to Region 1. This clearly cannot be possible, as the

combination of Eq. (3.92) is CS-invariant, while the square root definitions obey to the CS-evolution equations that regulate the behavior with respect to the rapidity cut-off y_n. A direct comparison shows that:

$$\widetilde{D}_{h/f}^{sqrt}(z_h, b_T, \mu, y_n) = \widetilde{\mathbb{S}}_{2\text{-h},+}(b_T, \mu, y_1) \widetilde{D}_{h/f}(z_h, b_T, \mu, y_1) \exp\left(-\frac{y_n}{2}\widetilde{K}(b_T, \mu)\right). \quad (3.93)$$

Therefore, the square root definition and the combination of Eq. (3.92) coincide only if $y_n = 0$.

In conclusion, Region 1 presents two main features which makes it profoundly different from the factorization theorems of Chapter 2. From the point of view of the phenomenological analyses, the TMD model $M_D^{\text{sqrt}} = M_D \times \sqrt{M_S}$ as defined in the square root definition can easily be experimentally accessed as a whole, but its two inner components cannot be disentangled. As for the 2-h cross sections, there are in total three unknown non-perturbative functions, g_K, M_D and M_S. The square root definition is useful in that it effectively decreases the number of unknowns reducing them to M_D^{sqrt} and g_K, as usually done in the standard TMD factorization theorems. Due to these analogies, I will refer to the cross section for Region 1, presented in Eq. (3.89), as a **TMD factorization theorem**.

TMD and collinear-TMD factorizations do not differ only in their phenomenological applications. They are different in the spirit. In fact, the rapidity cut-off is totally irrelevant in TMD factorization, even when the thrust is measured. In this regard, notice that the kinematics argument of Eq. (2.37) widely used to discuss the role of the rapidity cut-off in collinear-TMD factorization brakes down when P_T becomes too small, which is the main feature of Region 1. Therefore, TMD factorization can play a leading role in the investigation of the role of soft physics, as all the interesting dependence on the long-distances effects induced by soft radiations is encoded in the TMD factorized cross section. However, it is totally blind to the effects associated to the rapidity cut-off. As widely discussed in Sections 2.5 and 2.6, it should be assigned a proper physical meaning, given its relation to the measured value of thrust in the collinear-TMD factorization theorems devised in Chapter 2.

3.6 Region 2: collinear-TMD factorization

In the previous section, all the contributions associated to the radiation emitted in the S_A-hemisphere have been considered TMD-relevant. Of course, this is not the only possibility. The main assumption that leads to the TMD factorization theorem of Eq. (3.89) was due to relaxing the hypothesis **H.2**. As stressed at the beginning of Section 3.5, if **H.2** is false, automatically **H.1** must be true. However, if **H.2** is true, then **H.1** can be either true or false. In this section, I will consider the same starting point of Chapter 2, i.e. that both hypotheses are valid (**H.2** true, **H.1** true). Following the same nomenclature of Ref. [17], the kinematic region corresponding to this choice will be indicated as **Region 2**. Since the two approaches to factorization (top-down in the previous Chapter, bottom-up in this one) have to produce the same result, in the following I will show how to recover the collinear-TMD factorization theorem widely discussed in Chapter 2.
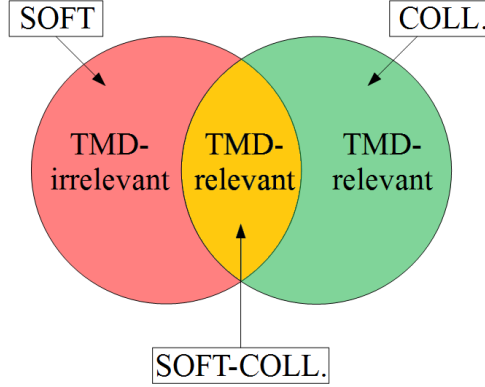
Fig. 3.10 Pictorial representation of leading momentum regions associated to the radiation in the S_A hemisphere in Region 2, where both assumptions **H.1** and **H.2** are true. The soft gluons are TMD-irrelevant while soft-collinear and collinear guons participate actively in the production of TMD effects.

In the kinematic Region 2, the soft radiation is not TMD-relevant. This means that P_T must be larger than in Region 1, although not large enough to significantly affect the topology of the final state, otherwise **H.1** would not be valid. Therefore, the two leading momentum regions, soft and collinear, and the overlapping soft-collinear contributions have to be classified as in Fig. 3.10. In this case, the soft radiation does not produce any significant TMD effect, hence it does not affect the experimentally measured value of P_T. On the other hand, soft-collinear and collinear emissions play an active role in generating the transverse momentum of the detected hadron.

The 1-loop computation of the partonic tensor in Region 2 can be readily performed at this stage, as all the necessary ingredients have been already introduced and worked out in the previous Sections. In fact, all the contributions are anaogous to those of Region 1, except for the term associated to the action of T_S^+, as in this case the soft radiation is TMD-irrelevant. However, this easily follows from the analogous result obtained in Section 3.4 for its opposite hemisphere counterpart, see Eq. (3.22). In fact, we have:

$$T_S^+ \left[\widehat{W}_f^{\mu\nu,\,[1]} (\varepsilon; z, \tau, k_T) \right] = \int \frac{d\rho}{\rho} \star \widehat{W}_f^{\mu\nu,\,[0]} (z/\rho, Q) \, \delta(1-\rho) S_+^{[1]} (\varepsilon; \tau) \, \delta \left(\vec{k}_T \right), \qquad (3.94)$$

where S_+ is the contribution of the S_A hemisphere to the generalized soft thrust function at 1-loop. Thanks to Eq. (3.26), we can use the solution found for S_- in Eq. (3.25). Therefore, we can
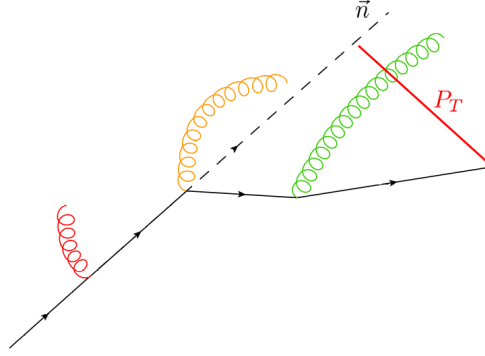
Fig. 3.11 Pictorial representation of the effect of the three kinds of radiation in Region 2. The final P_T, measured with respect to the thrust axis $\vec{n}$, is not affected by the emission/absorption of soft radiation, as the soft gluons (red) are TMD-irrelevant. Instead, soft-collinear (orange) and collinear (green) radiations produce the deflections that lead to the observed transverse momentum.

immediately write the b_T-space expression for the partonic tensor at 1-loop in Region 2:

$$\widetilde{\widetilde{W}}_f^{\mu\nu,[1]}(\varepsilon;z,\tau,b_T) =$$

$$= H_T^{\mu\nu} N_C e_f^2 \int \frac{d\rho}{\rho} \delta(1-z/\rho) \left[\delta(1-\rho)\delta(\tau)V(\varepsilon) + \delta(1-\rho)\left[J^{[1]}(\varepsilon;\tau) + S_-^{[1]}(\varepsilon;\tau) \right] + \right.$$

$$\left. + \delta(1-\rho)\mathcal{S}_+^{[1]}(\varepsilon;\tau,y_1) + \delta(\tau)\rho \widetilde{D}_{q/q}^{[1],(0)}(\varepsilon;\rho,b_T,y_1) \right] =$$

$$= H_T^{\mu\nu} N_C e_f^2 \left[\delta(1-z)\left(\delta(\tau)V(\varepsilon) + J^{[1]}(\varepsilon;\tau) + S_-^{[1]}(\varepsilon;\tau) + \mathcal{S}_+^{[1]}(\varepsilon;\tau,y_1) \right) + \right.$$

$$\left. + \delta(\tau)z\widetilde{D}_{q/q}^{[1],(0)}(\varepsilon;z,b_T,y_1) \right], \tag{3.95}$$

where, as in Region 1, I used Eq. (3.82) to rearrange into the bare quark-from-quark TMD FF the combination of the large-b_T asymptotic behavior of the quark-from-quark GFJF and that of the soft-collinear thrust factor. Notice that we could have obtained this result much more easily if we had removed, from the very beginning, the connection between thrust and transverse momentum in the two TMD-relevant contributions. This is a consequence of the validity of the assumption **H.1**. In fact, if collinear radiations do not contribute to the measured value of thrust, then also the soft-collinear emissions, that have a lower transverse momentum, cannot affect the topology of the final state. Translated into the language of Chapter 2, Eq. (3.95) defines the 1-loop order of the subtracted

partonic tensor. In fact, applying the subtraction procedure described in Section 2.4.1, we obtain:

$$\widehat{W}_f^{\mu\nu,[1],\text{sub.}}(z,\tau) = H_T^{\mu\nu} N_C e_f^2 \left[\delta(1-z)\delta(\tau)V(\varepsilon) + \delta(1-z)\left[S_-^{[1]}(\varepsilon;\tau) + J^{[1]}(\varepsilon;\tau) \right] + \right.$$

$$\left. + \delta(1-z)\mathcal{S}_+^{[1]}(\varepsilon;\tau,y_1) - \delta(\tau)\delta(1-z)Z_{q/q,\text{TMD}}(\varepsilon;y_1) \right] =$$

$$= H_T^{\mu\nu} N_C e_f^2 \frac{\alpha_S}{4\pi} C_F \,\delta(1-z) \left[\delta(\tau)\left(-9 + \frac{2\pi^2}{3} + \log^2\left(\frac{\zeta}{Q^2}\right) - 6\log\left(\frac{\mu}{Q}\right) + \right. \right.$$

$$\left. \left. + 4\log\left(\frac{\zeta}{Q^2}\right)\log\left(\frac{\mu}{Q}\right) - 4\log^2\left(\frac{\mu}{Q}\right) \right) - \left(\frac{1}{\tau}\right)_+ \left(3 + 4\log\left(\frac{\zeta}{Q^2}\right) \right) - 4\left(\frac{\log\tau}{\tau}\right)_+ \right]. \quad (3.96)$$

As anticipated in Chapter 2, the subtracted partonic tensor, properly renormalized, is a *finite* quantity. All the UV and rapidity divergences have been canceled. Moreover, we can readily verify the RG-invariance of the cross section by deriving the previous expression with respect to $\log\mu$: the result is exactly *minus* the anomalous dimension of the TMD at 1-loop. However, the dependence on the rapidity cut-off of $\widehat{W}_f^{\mu\nu,\text{sub.}}$ is regulated differently than the CS-evolution of the TMDs as, clearly, it does not depend on b_T.

3.6.1 Factorization theorem for Region 2

The final factorized cross section valid in Region 2 is easily obtained by generalizing to all orders the 1-loop result of Eq. (3.95). As all divergences cancel among each other, I will drop the ε-dependence in all terms involved in the final result.

$$\frac{d\sigma_{R_2}}{dz_h \, dP_T^2 \, dT} = \sigma_B \,\pi N_C V \int d\tau_{S_+} \, d\tau_{S_-} \, d\tau_B \, J(\tau_B) S_-(\tau_{S_-}) \mathcal{S}_+(\tau_{S_+},\zeta)\, \delta(\tau - \tau_{S_+} - \tau_{S_-} - \tau_B) \times$$

$$\times \int \frac{d^2\vec{b}_T}{(2\pi)^2} \, e^{i\frac{\vec{P}_T}{z_h}\cdot\vec{b}_T} \sum_f e_f^2 \, \widetilde{D}_{h/f}(z_h, b_T, \zeta). \quad (3.97)$$

In this case, the generalization of the 1-loop computation gives the correct final result. In fact, in Region 2 there is no asymmetry in the soft radiation, as it is considered TMD-irrelevant regardless of whether it is emitted backward or forward with respect to the hemispheres identified by the thrust axis. Therefore, Region 2 corresponds to the **collinear-TMD factorization theorem** obtained in Chapter 2, by using a "top-down" approach.

In particular, the partonic cross section for a 2-jet topology of the final state can easily be determined by comparing Eq. (3.97) with Eq. (2.30):

$$\frac{d\widehat{\sigma}_f}{dz \, d\tau} = \sigma_B N_C V \,\delta(1-z)\, e_f^2 \int d\tau_{S_+} \, d\tau_{S_-} \, d\tau_B \, J(\tau_B) S_-(\tau_{S_-}) \mathcal{S}_+(\tau_{S_+},\zeta)\, \delta(\tau - \tau_{S_+} - \tau_{S_-} - \tau_B).$$

$$(3.98)$$

Notice that this is the expected decomposition for the fully perturbative content of the cross section in the 2-jet limit, as shown in Fig. 2.2b.

All the issues discussed in the previous Chapter are therefore valid in Region 2. In particular, there are two main features associated to the collinear-TMD factorization theorem of Eq. (3.97). The first concerns the definition of the TMD FFs, which is the factorization definition of Eq. (1.21). Therefore, a phenomenological analysis performed in Region 2 allows to access directly the TMD model M_D, which is not contaminated by any soft contribution. Secondly, the rapidity cut-off in Eq. (1.21) must play a physical role, well beyond that of a mere computational tool, given its intimate connection with the measured value of thrust. This feature has been widely discussed in Sections 2.5 and 2.6.

The most important consequence is that the thrust-resummation of the cross section in Eq. (3.97) must somehow be influenced by this relation between ζ and T. However, in the Collins factorization formalism this is never made explicit. Consequently, a formula like Eq. (3.97) can only be used for values of thrust not too close to $T = 1$, where the resummation effects are significant. A simple way to obtain a formula valid far enough from the pencil-like configuration is the procedure adopted in the modified formalism described in Section 2.6, which consists in dropping the $\tau = 0$ terms from the fixed order computation of Eq. (3.96). This time, this procedure leaves an explicit rapidity cut-off, i.e. the logarithmic term multiplying the τ-plus distribution in the last line of Eq. (3.96). Without a further constraint (like, for example, the topology cut-off introduced in Section 2.6) ζ can only be related to T through the naive kinematics argument of Eq. (2.37) and set as $\zeta = \tau Q^2$. Of course, this identification can only be done after removing the $\tau = 0$ terms, otherwise it would produce ill-defined contributions like $\delta(\tau) \log \tau$. Following this approach, the expression in Eq. (3.96) leads to the same formula found in the modified formalism and shown in Eq. (2.77).

3.7   Region 3: generalized collinear factorization

The last configuration to be considered corresponds to the case in which the hypothesis **H.1** is false. As already pointed out, this situation implies that the other assumption, **H.2**, holds true. The kinematic region associated to this choice (**H.2** true, **H.1** false) will be named **Region 3**, according to the nomenclature of Ref. [17].

In Region 3, the transverse momentum of the detected hadron is large enough to affect significantly the topology of the final state. This is the physical situation already described in Section 3.3 and represented in Fig. 3.4. In this case, not only the transverse motion of the detected hadron is not affected by soft radiation, but it is large enough to be insensitive also to soft-collinear emissions. Therefore, as in Region 2 the soft contribution is TMD-irrelevant,as well as the overlapping region, associated to soft-collinear radiation. This is represented pictorially in Fig. 3.12. As a consequence, only collinear radiation produces significant TMD effects.
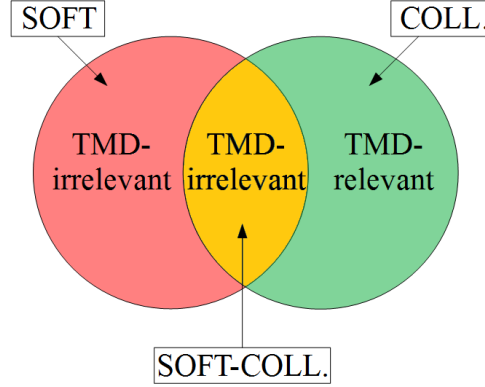
Fig. 3.12 Pictorial representation of leading momentum regions associated to the radiation in the S_A hemisphere in Region 3, where the assumption **H.1** is false and **H.2** is true. Both the soft and soft-collinear gluons are TMD-irrelevant while only collinear guons participate actively in the production of TMD effects.

This kinematic configuration will inevitably produce a different factorization theorem with respect to the cross sections obtained in Chapter 2. Most importantly, this is the only kinematic region where the TMD effects are not described by TMD FFs, but rather by GFJFs, which are as universal as the TMDs but have a further dependence on the invariant mass of the jet to which they are associated. In this case, the invariant mass of the jet is related to thrust as in Eq. (D.1).

The explicit computation at 1-loop order is straightforward, as all the necessary ingredients have already be determined in the previous Sections. Since soft-collinear gluons are TMD-irrelevant,the result of the action of $T_S T_A$ is totally analogous to its opposite hemisphere counterpart, shown in Eq. (3.30). In fact, the approximation gives:

$$T_S T_A \left[\widehat{W}_f^{\mu\nu,[1]} (\varepsilon; z, \tau, k_T) \right] = \int \frac{d\rho}{\rho} \star \widehat{W}_f^{\mu\nu,[0]}(z/\rho, Q) \, \delta(1-\rho) \mathcal{Y}_+^{[1]} (\varepsilon; \tau) \, \delta \left(\vec{k}_T \right). \qquad (3.99)$$

where $\mathcal{Y}_+$ is the soft-collinear thrust function associated to the hemisphere S_A. This can easily be related to the analogous contribution for the opposite hemisphere thanks to Eq. (3.33). Furthermore, differently from the other kinematic regions, the only b_T-dependent quantity, i.e. the quark-from-quark GFJF defined in Eq. (3.69), should not be considered only at large b_T, since in this case the thrust cannot reach the ideal limit $\tau = 0$ because of the size of k_T (the same argument was already discussed
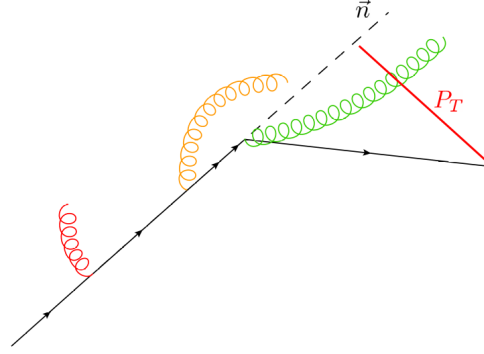
Fig. 3.13 Pictorial representation of the effect of the three kinds of radiation in Region 3. The final P_T, measured with respect to the thrust axis $\vec{n}$, is non affected by the emission/absorption of soft and soft-collinear radiation as the soft gluons (red) and the soft-collinear gluons (orange) are TMD-irrelevant. The transverse motion of the detected hadron is only produced by collinear radiation (green).

in Section 3.3). Therefore, the 1-loop order of the partonic tensor in Region 3 is given by:

$$
\widehat{W}_f^{\mu\nu,[1]}(\varepsilon; z, \tau, k_T) =
$$

$$
= H_T^{\mu\nu} N_C e_f^2 \int \frac{d\rho}{\rho} \delta(1 - z/\rho) \left[\delta(1-\rho)\delta(\tau)V(\varepsilon) + \delta(1-\rho)\left[J^{[1]}(\varepsilon; \tau) + S_-^{[1]}(\varepsilon; \tau) \right] + \right.
$$

$$
\left. + \delta(1-\rho) S_+^{[1]}(\varepsilon; \tau) + \widetilde{\Gamma}_{q/q}^{[1]}(\varepsilon; \rho, b_T, \tau) \right] =
$$

$$
= H_T^{\mu\nu} N_C e_f^2 \left[\delta(1-z)\left(\delta(\tau)V(\varepsilon) + J^{[1]}(\varepsilon; \tau) + S^{[1]}(\varepsilon; \tau) \right) + \Gamma_{q/q}^{[1]}(\varepsilon; z, k_T, \tau) \right], \qquad (3.100)
$$

where I used the S_A-hemisphere counterpart of Eq. (3.34) to reorganize the soft and the soft-collinear terms into the forward radiation contribution to the usual thrust function, which is then combined with its counterpart in the opposite hemisphere. Therefore, the usual soft thrust function appears as a fundamental ingredient of the partonic tensor in Eq. (3.100). Furthermore, notice that in this region there is no trace of rapidity cut-offs, as all the soft and soft-collinear terms are integrated over the transverse momentum.

Since GFJF are defined in k_T-space, the previous expression is not Fourier transformed. The Fourier transform allows to ε-expand $\Gamma_{q/q}$ as shown in Eq. (3.71). Then, it is straightforward to show that all the divergences (except the collinear pole characterizing the GFJF) cancel among themselves also in Region 3.

3.7.1 Factorization theorem for Region 3

The cross section for Region 3 is obtained by generalizing the 1-loop order result for the partonic tensor of Eq. (3.100) to all orders. Since divergences cancel, the ε-dependence is dropped in all terms involved in the factorization theorem. Then the final cross section is:

$$\frac{d\sigma_{R_3}}{dz_h \, dP_T^2 \, dT} =$$

$$= \sigma_B \, \pi N_C \, V \, z_h \int d\tau_S \, d\tau_A \, d\tau_B \, J(\tau_B) \, S(\tau_S) \sum_f e_f^2 \, \Gamma_{h/f}\left(z_h, \frac{P_T}{z_h}, \tau_A\right) \delta(\tau - \tau_S - \tau_A - \tau_B), \quad (3.101)$$

where the factor z_h is the effect of the unconventional normalization used here for GFJFs. Notice that the same factorized cross section has been obtained within the framework of SCET in Ref. [17], adopting a completely different approach.

This cross section has a similar structure to the factorization theorem devised for Region 2. In fact, naively Eq. (3.101) can be obtained from Eq. (3.100) by removing the rapidity cut-off and replacing the TMD FFs with the corresponding GFJFs. We can even define the analogue of the partonic cross section introduced in Chapter 2 by properly modifying the subtraction mechanism of Section 2.4.1. The result would be the same of Eq. (2.31) but with the replacement:

$$\rho \, D_{i/j}(\rho, k_T, \zeta) \longmapsto \Gamma^{[1]}_{i/j}(\rho, k_T, \tau). \quad (3.102)$$

Moreover, the hybrid nature of the collinear-TMD factorization theorem is "transferred" from the structure of the cross section to its TMD part. In fact, GFJFs have all the features of the TMD FFs (they depend on the transverse momentum of the fragmenting parton) and also some typical characteristics of the usual FFs (their evolution is DGLAP-like). However, differently from the TMDs, GFJF are defined without rapidity cut-off, since all the rapidity divergences are regulated by the additional dependence on the invariant mass of the jet, a role played by thrust in this case. Therefore, they should be considered more like a "generalized" version of usual FFs, and not as an extension of the TMD FFs. For this reasons, I will refer to the cross section presented in Eq. (3.101) as **generalized collinear factorization theorem**.

Despite the similarities, the factorization theorems of Region 2 and of Region 3 are remarkably different. In fact, the factorized cross section of Eq. (3.101) is not of any use for the investigation of the physical meaning of the rapidity cut-off, as all its contributions are defined without any explicit rapidity regulator. Further considerations on GFJFs are beyond the purpose of this thesis. For more details we refer to Ref. [45].

	H.1	**H.2**
R_1	true	false
R_2	true	true
R_3	false	true

Table 3.1 Kinematic regions and initial assumptions.

3.8   Algorithm for Region selection

So far, three different factorization theorems corresponding to as many different kinematics regions have been developed: TMD factorization for Region 1 in Eq. (3.89), collinear-TMD factorization for Region 2 in Eq. (3.97) and generalized collinear factorization for Region 3 in Eq. (3.101). Each region corresponds to a different physical configuration and, in particular, the transverse momentum of the detected hadron increases as we move from region 1 to region 3. In fact, in region 1 the soft radiation contributes actively to the transverse deviation of the hadron with respect to the thrust axis, which must then have a low transverse momentum, otherwise it would not be sensitive to these tiny corrections. On the other hand, in Region 3, the detected hadron has a transverse momentum large enough to be among the causes of the spread of the jet in which it is detected, inevitably decreasing the value of thrust. However, lacking a proper criterion to discriminate among the regions, these three factorization theorems are hardly useful for phenomenological analyses. Moreover, the boundaries of the three regions are not sharply defined, making the description of data difficult, especially in the overlapping regions.

In order to define a suitable algorithm for selecting each individual region, it is useful to review the approximations that lead to the three factorization theorems presented in this Chapter. Depending on the initial assumptions **H.1** and **H.2**, organized[7] as in Tab. 3.1, the leading momentum regions associated to the forward radiation contribute differently to the observed TMD effects and hence the soft, soft-collinear and collinear terms can be classified on the basis of their TMD-relevance, as in Tab. 3.2. In other words, Tab. 3.1 implies Tab. 3.2. Moreover, I have shown how the final results

	T_S^+	$T_S T_A$	T_A
R_1	TMD-relevant	TMD-relevant	TMD-relevant
R_2	TMD-irrelevant	TMD-relevant	TMD-relevant
R_3	TMD-irrelevant	TMD-irrelevant	TMD-relevant

Table 3.2 Kinematic regions and TMD-relevance. The symbol * reminds that the soft approximation in this case only refers to gluons radiated in the same portion of space occupied by the jet in which is detected the hadron h.

---

[7]Notice that the combination where both the initial assumptions are false does not correspond to any kinematic regions as it is kinematically forbidden, see Eqs. (3.41) and (3.42).

could have been found by neglecting the correlation between thrust and transverse momentum from the very beginning, at the level of definition of the various factors contributing to the forward radiation. Such approximations make the perturbative computations much easier, as all the issues related to the 2-jet limit in b_T-space clearly disappear when τ and k_T are independent variables.

This is equivalent to implementing the following approximations in the definitions of the various factors in transverse momentum space, Eqs. (3.44), (3.55) and (3.69):

$$\delta\left(\tau - \frac{l^-}{q^-}\right) = \delta\left(\tau - \frac{k_T}{Q}e^{-y}\right) \sim \delta(\tau) \quad \text{both in } \Sigma_+ \text{ and in } \Upsilon_+; \tag{3.103a}$$

$$\delta\left(\tau - \frac{z}{1-z}\frac{k_T^2}{Q^2}\right) = \delta\left(\tau - (1-z)ze^{-2y}\right) \sim \delta(\tau) \quad \text{in } \Gamma_{q/q}, \tag{3.103b}$$

where y is the rapidity of the emitted gluon. Analogously, the result of Region 2 could have been obtained by leaving Σ^+ unchanged and setting:

$$\delta\left(\tau - \frac{l^-}{q^-}\right) = \delta\left(\tau - \frac{k_T}{Q}e^{-y}\right) \sim \delta(\tau) \quad \text{in } \Upsilon_+; \tag{3.104a}$$

$$\delta\left(\tau - \frac{z}{1-z}\frac{k_T^2}{Q^2}\right) = \delta\left(\tau - (1-z)ze^{-2y}\right) \sim \delta(\tau) \quad \text{in } \Gamma_{q/q}. \tag{3.104b}$$

Finally, in Region 3 all the relations between thrust and transverse momentum have to be kept into the definitions of the factors:

$$\delta\left(\tau - \frac{z}{1-z}\frac{k_T^2}{Q^2}\right) = \delta\left(\tau - (1-z)ze^{-2y}\right) \quad \text{not approximated in } \Gamma_{q/q}. \tag{3.105}$$

Eqs. (3.103), (3.104) and (3.105) follow directly from the classification of Tab. 3.2. The simplest criterion consists in comparing the size of k_T with respect to the typical scale induced by thrust. In particular, in Region 1 Eq. (3.103a) can be interpreted as $\tau Q \ll k_T$, while, since in Region 3 the only TMD-relevant quantity is left unapproximated, Eq. (3.105) can be interpreted as $k_T \sim \sqrt{\tau}Q$, which is also the maximum value kinematically allowed for P_T. As a consequence, Region 2 covers the whole intermediate configuration $\tau Q \lesssim k_T \lesssim \sqrt{\tau}Q$. Notice that this interpretation is in agreement with the size of the topology cut-off introduced in the modified formalism presented in Section 2.6. Since k_T is directly related to the transverse momentum P_T of the detected hadron through Eq. (B.11), these interpretations can be transferred to hadronic quantities. In particular:

$$R_1 \longrightarrow \frac{P_T}{z_h} \ll \tau Q; \tag{3.106a}$$

$$R_2 \longrightarrow \tau Q \lesssim \frac{P_T}{z_h} \lesssim \sqrt{\tau}Q; \tag{3.106b}$$

$$R_3 \longrightarrow \frac{P_T}{z_h} \sim \sqrt{\tau}Q. \tag{3.106c}$$

This criteria use only the typical scales associated to the value of thrust, i.e. τQ as a soft scale and $\sqrt{\tau} Q$ as a collinear scales. These are the values commonly used as reference scales in thrust-resummed quantities, see for instance Ref. [53]. Moreover, this has been proposed as a selection criterion for BELLE data in Ref. [17]. In addition, since the factorized cross sections of Regions 1 and 2 involve TMD FFs, we should also add a cut in P_T, because the Fourier transform acts as an analytic continuation that extends unnaturally the TMDs beyond the (physical) small transverse momentum region. In this case, the requirement comes directly from power counting:

$$P_T \ll P^+ = z_h \frac{Q}{\sqrt{2}}. \tag{3.107}$$

The application of this algorithm to the BELLE data [8] in the 2-jet region, assumed to correspond to $0.7 \leq T \leq 1$, produces the results shown in Fig. 3.14, where Regions 1, 2 and 3 have been color coded to red, orange and green, respectively. The cut in P_T for constraining the range of applicability of TMDs is indicated by the red dashed vertical line. From the phenomenological point of view this kind of data selection inevitably raises the issue of matching different regions, since Fig. 3.14 shows that there are at least two different overlapping regions in each panel. The problem of matching different kinematic regions, each corresponding to a different factorization theorem, is not new in the context of TMD physics. This, in fact, has recently been one of the most debated issues when dealing with phenomenological applications of 2-h cross sections, that have two distinct regimes associated to as many factorization theorems: collinear factorization at large-q_T and TMD factorization at small-q_T, see Section 1.4.1. In the case of $e^+e^- \to hX$ there are three different regions, making the matching even more problematic. A suitable matching procedure has been proposed in Ref. [17].

The set of rules devised above is not the only possible choice to obtain a valid criterion to make a selection on data. In particular, it oversimplifies the complex structure of the three kinematic regions, as it only considers the typical thrust scale associated to the two leading momentum regions, soft and collinear. Most importantly, the approximations of Eq. (3.106) do not take into account the rapidity of the detected hadron, which, remarkably, is the crucial information to discriminate between a configuration where the transverse deflection is due to soft and soft-collinear radiation and one in which only soft-collinear emissions play an active role in generating TMD effects. This is of course strictly connected to the boundary between Region 1 and Region 2. Therefore, in the following I will present a different criterion which takes into account also the information encoded in the hadron rapidity. It is devised on the basis of the 1-loop order computation, as the argument of the deltas constraining thrust and transverse momentum are different at higher order in pQCD.

The approximations of Eqs. (3.103), (3.104) and (3.105) are considered the fundamental tool to implement the selection algorithms. The partonic quantities in the deltas are promoted to their hadronic equivalent, i.e $z \mapsto z_h$ and $k_T \mapsto P_T/z_h$ (see Section 2.4.1). Then, denominating y_P the rapidity of the detected hadron, Eq. (2.37), I introduce the following quantities:
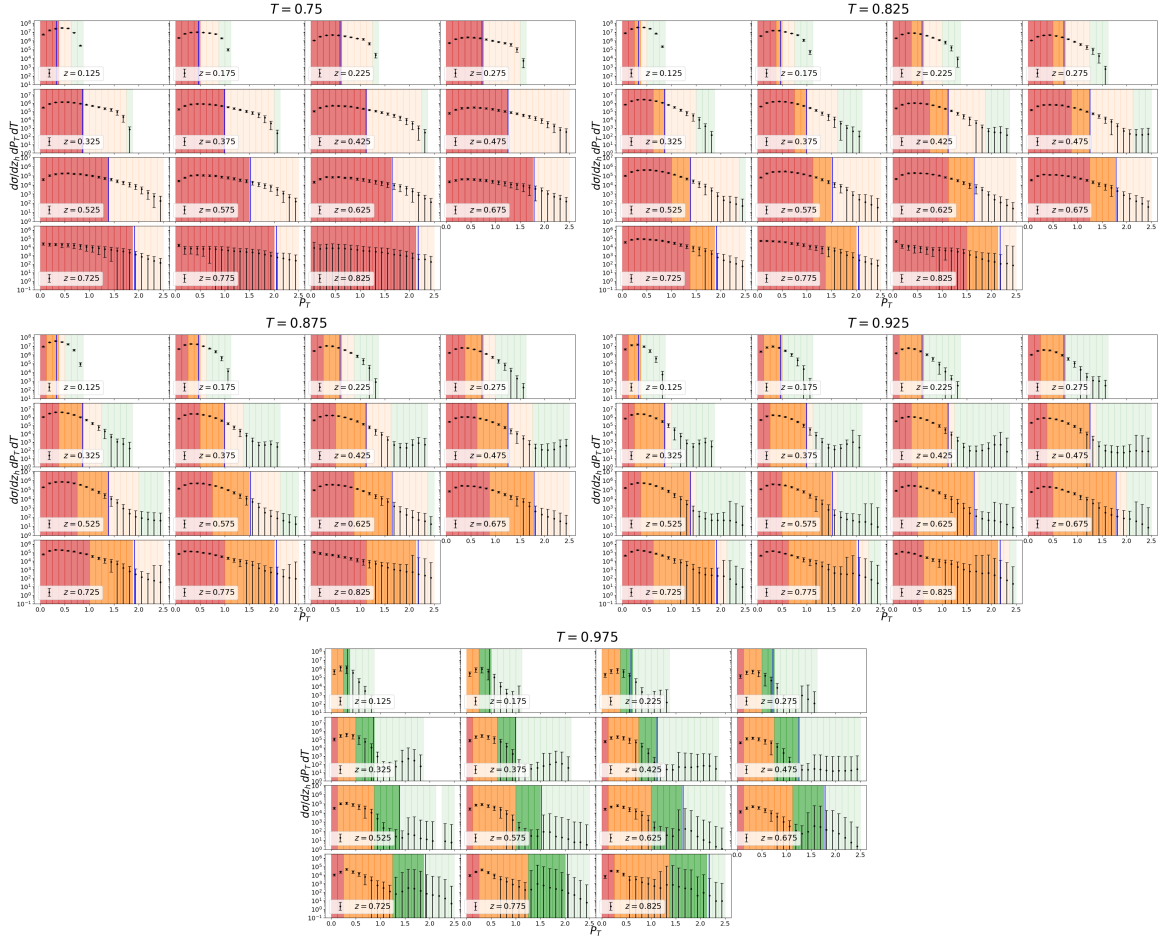
Fig. 3.14 BELLE data [8] selected according to the criteria of Eqs. (3.106). Red bins correspond to Region 1, orange bins to Region 2 and green bins to Region 3. The shaded areas correspond to bins outside the TMD-regime, where Eq. (3.107) is not satisfied. The purpose of this representation is to capture at a glance how the three kinematic regions are distributed through the whole thrust spectrum, for a 2-jet topology. Here we do not focus on the details of each thrust bin. A different and more detailed representation can be found in Appendix F.

- **Soft Ratio** r_S, defined as:

$$r_S = \frac{P_T}{z_h Q} e^{-y_P}.$$ (3.108)

- **Collinear Ratio** r_C, defined as:

$$r_C = z_h (1 - z_h) e^{-2y_P}.$$ (3.109)

Then, by comparing these ratios to thrust, it is possible to obtain an algorithm that takes into account also the role of soft-collinear radiation. In fact, we can write the analogue of Eqs (3.103), (3.104) and (3.105), to the hadronic level, as follows.

Region 1 is characterized by:

$$r_S(z_h, P_T) \ll \tau \quad \text{both for soft and soft-collinear radiation;}$$ (3.110a)

$$r_C(z_h, P_T) \ll \tau \quad \text{for collinear radiation.}$$ (3.110b)

On the other hand, Region 2 is associated to:

$$r_S(z_h, P_T) \sim \tau \quad \text{for soft radiation;}$$ (3.111a)

$$r_S(z_h, P_T) \ll \tau \quad \text{for soft-collinear radiation;}$$ (3.111b)

$$r_C(z_h, P_T) \ll \tau \quad \text{for collinear radiation.}$$ (3.111c)

Finally, in Region 3 we have:

$$r_S(z_h, P_T) \sim \tau \quad \text{both for soft and soft-collinear radiation;}$$ (3.112)

$$r_C(z_h, P_T) \sim \tau \quad \text{for collinear radiation.}$$ (3.113)

Therefore, Region 3 is the only kinematic region where r_S is never neglected. This constitutes the first rule:

1. If $r_S \ll \tau$ we can only be either in Region 1 or in Region 2, but not in Region 3.

Next, a small soft ratio characterizes both Region1 and Region 2, which can be discriminated according to the rapidity of the detected hadron. In particular, if the soft ratio is small because of the size of P_T/z_h, regardless of the rapidity y_P, then r_S will be denoted as **momentum dominated**. In this case we are in Region 1, because the soft ratio is neglected even if the rapidity is large, i.e. both for soft and soft-collinear radiation. If instead the smallness of the soft is due to the largeness of the rapidity y_P, then r_S will be denoted as **rapidity dominated**. In this case we are in Region 2, as r_S can be neglected only when the rapidity is large, i.e. only for soft collinear radiation.

In order to discriminate between these two configurations, we can compare the contributions of the transverse momentum and the rapidity to the soft ratio and write the second rule:
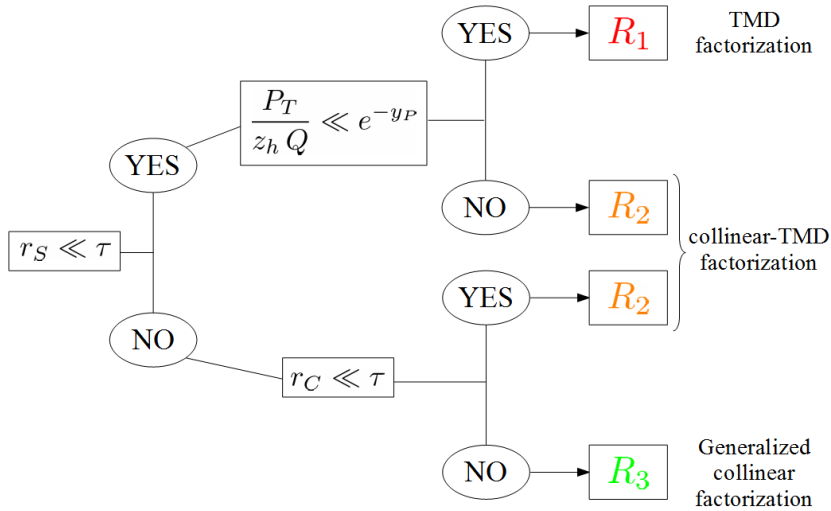
Fig. 3.15 Flow-chart representation of the algorithm based on soft and collinear ratios.

2. If $\frac{P_T}{z_h Q} \ll e^{-y_P}$ the soft ratio is momentum dominated and we are in Region 1. Otherwise the soft ratio is rapidity dominated and we are in Region 2.

This exhausts all the possibilities implied by the first rule. When $r_S \sim \tau$ the first rule is violated. In this case Region 1 is automatically excluded as it is the only kinematic region where the soft ratio is always considered small, both for soft and soft-collinar radiation. Therefore, we have the third rule:

4. If $r_S \sim \tau$ we can only be either in Region 2 or in Region 3, but not in Region 1.

Next, the size of the collinear ratio discriminates between Region 2 and Region 3. In fact, if also the collinear ratio cannot be neglected, i.e. $r_C \sim \tau$, then we are in Region 3. Otherwise we are in Region 2. This generates the last rule:

5. If $r_C \ll \tau$ we are in Region 2, otherwise we are in Region 3.

A similar set of criteria based on kinematic ratios was proposed for SIDIS in Refs. [54, 55].

This algorithm is represented graphically in Fig. 3.15. Notice how, within this criterion, Region 2 can be reached following two different routes, while Region 1 and Region 3 can only be reached through one path. This is in agreement with the naive expectation that Region 2 corresponds to the dominant kinematic configuration, as it describes the "intermediate" situation where P_T is neither too small (as in Region 1) nor too large (as in Region 3). This automatically influences the data selection, showed in Fig. 3.16. Differently from the rough algorithm of Fig. 3.14, here there is a neat prevalence of orange bins, corresponding to Region 2. Most importantly, there are *monocromatic panels* where only one kinematic configuration is realized. This is an incredibly big advantage for phenomenological analyses, as it overcomes the issue of matching, which concerns only the panels where more than one Region (i.e. color) appears.
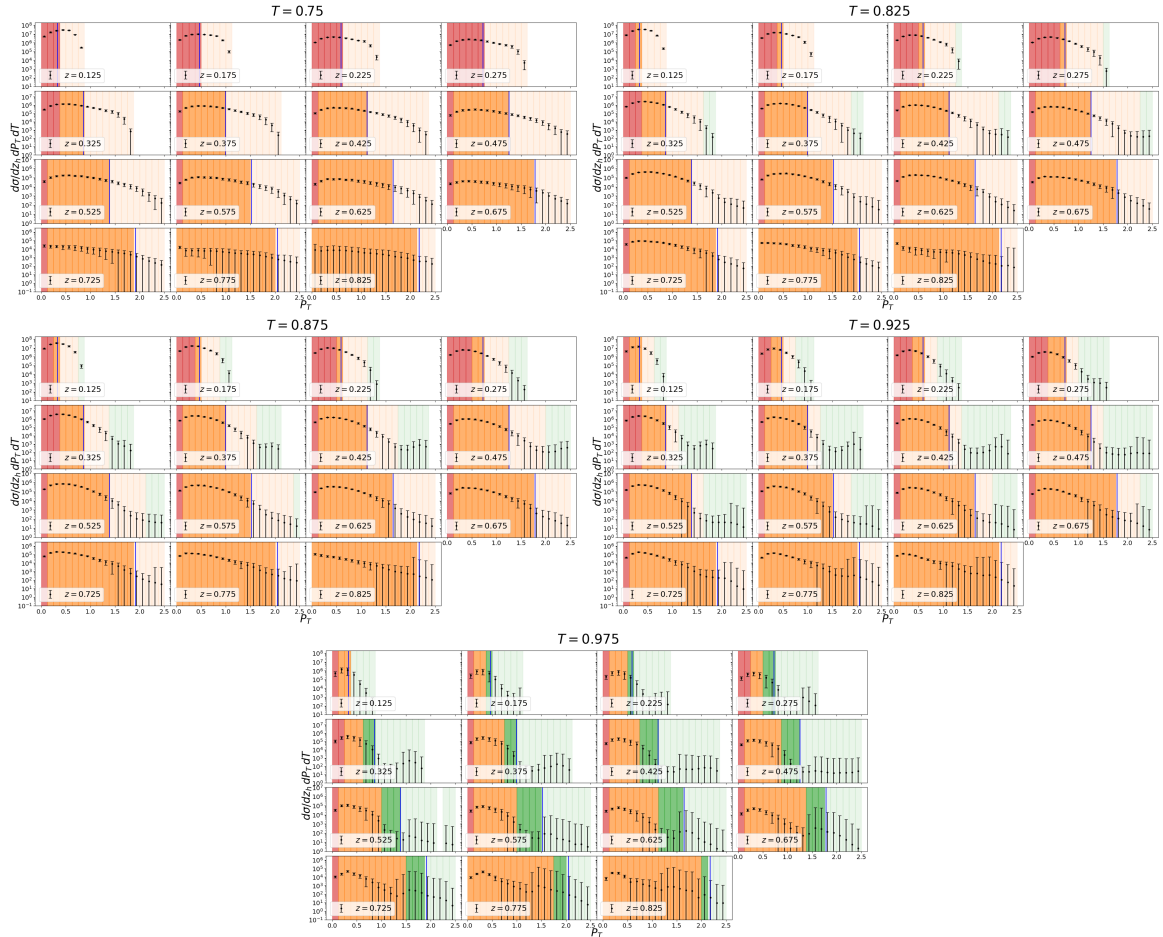
Fig. 3.16 BELLE data [8] selected according represented in Fig. 3.15. Red bins correspond to Region 1, orange bins to Region 2 and green bins to Region 3. The shaded areas correspond to bins outside the TMD-regime, where Eq. (3.107) is not satisfied. The purpose of this representation is to capture at a glance how the three kinematic regions are distributed through the whole thrust spectrum, for a 2-jet topology. Here we do not focus on the details of each thrust bin. A different and more detailed representation can be found in Appendix F.

Leaving aside Region 3 (green bins) which is not described by factorization theorems involving TMD FFs, the great opportunity offered by the algorithm presented above is in its application for the comparison between Region 1 and Region 2, corresponding to red and orange bins, respectively. In fact, as discussed at the end of Section 3.5.1, the TMD factorization theorem devised for Region 1 allows to access the square root model M_D^{sqrt}, while the collinear-TMD factorization theorem obtained for Region 2 gives the chance to extract directly the TMD model M_D. A direct comparison can shed light on the (still unknown) soft model M_S, which deforms the TMDs defined by the square root definition. Since the algorithm presented in this Section allows to bypass the matching issues in a rather large number of bins, this comparison can safely be carried out.

Finally, it is important to stress again that the soft model is the same unknown function which appears in the 2-h cross sections. Its independent extraction from a process which belongs to another hadron class is promisingly one of the most powerful phenomenological tools for future studies.

3.9 Conclusions

The "bottom-up" approach to factorization is extremely powerful, as it allows us to construct the factorization theorems, piece by piece, starting from the full QCD Feynman diagrams. The structure of the final factorized cross section becomes transparent even at relatively low orders in the perturbative expansion. In this Chapter, I have applied this procedure to $e^+e^- \to hX$, for a 2-jet final state configuration, with a twofold purpose.

First of all, explicit perturbative computations require to extend the definitions given for the soft factors and for the TMDs in Chapter 1, in order to take into account also the dependence on thrust. This operation produces a large variety of integrated and unintegrated objects that not only generalize the definitions of soft factors and TMDs, but also include and extend the usual thrust-dependent functions, usually encountered in the study of e^+e^- annihilation processes. All these new thrust-dependent operators have been defined and computed at 1-loop in Section 3.5.

Secondly, the "bottom-up" approach has been adopted to recover the results of Chapter 2, where instead a "top-down" procedure was applied. Not only the same collinear-TMD factorization theorem comes out in a natural way from explicit perturbative computations, but it is framed in a much more general context where other kinematic configurations are generated and lead to different factorization theorems. In fact, the whole proof of factorization devised in Chapter 2 was founded on two assumptions: the transverse momentum of the detected hadron is neither too large to affect significantly the topology of the final state (**H.1**), nor too small to be considered affected by the emission/absorption of soft radiation (**H.2**). Modifying this initial hypothesis inevitably leads to a different factorization theorem, which corresponds to a different kinematic region. Since these two assumptions cannot be false at the same time, there are in total three different kinematic regions, defined as:

- Region 1, corresponding to set **H.1** true and **H.2** false, treated in Section 3.5. In this region the soft radiation participates actively to TMD effects. In fact, the resulting factorization theorem is very similar to the standard TMD factorized cross section known to hold in the 2-h class, than to the case studied in Chapter 2. In fact, the TMD FFs describing the non-perturbative hadronization process that generates the detected hadron appears in the cross section as if they were defined through the square root definition used in $e^+e^- \to h_1 h_2$, SIDIS and Drell-Yan scattering. Their TMD model, which describes their characteristic long-distance behavior, is contaminated by the non-perturbative content of the soft radiation by a square root of the soft model, confirming that in Region 1 soft emissions play a leading role in generating TMD effects. Thanks to all these similarities, we can identify the factorized cross section obtained for Region 1 as a TMD factorization theorem.

- Region2, corresponding to the case in which both the hypotheses hold true, treated in Section 3.6. This is the same initial set-up of Chapter 2 and in fact the same collinear-TMD factorization theorem is recovered.

- Region 3, corresponding to set **H.1** false and **H.2** true, treated in Section 3.7. Here all the effects of soft and even soft-collinear radiation are irrelevant for TMD effects, as their contribution can be neglected, given the (large) size of the transverse momentum of the detected hadron. Since in this case the measured value of thrust takes part in the collinear radiation contribution, the final factorization theorem cannot involve TMD FFs. In fact, they are replaced by the corresponding GFJFs, defined similarly to the (unsubtracted) TMDs but with a further dependence on the invariant mass of the jet to which they are associated. The hybrid nature of the collinear-TMD factorization theorems is totally encoded in these functions, which share both characteristics of the TMD FFs, and also of the usual FFs. However, they are very different from TMDs, as in their definition there is no trace of any rapidity cut-off, as all the rapidity divergences are naturally regulated by the further dependence on the invariant jet mass. For this reason, GFJFs should be considered more as a generalized version of the usual FFs than an extended counterpart of the TMDs. Therefore, the factorized cross section devised for Region 3 has been denoted as a generalized collinear factorization theorem.

As all these kinematic regions contain different kind of information on TMD physics, it is extremely important to devise a solid methodology to identify them unequivocally among the large set of data provided by BELLE Collaboration [8]. In Section 3.8 I show how a standard algorithm based only on the typical soft and collinear energy scales associated to the value of thrust does not catch all the features encoded into the rich structure behind a process like $e^+e^- \to hX$. Therefore, I propose a finer algorithm that allows to select the data taking into account not only soft and collinear radiation, but also the role of soft-collinear emissions. With this criteria, there is a rather large amount of data which is described by a single factorization theorem, bypassing all the issues related to the matching procedure to describe data at the boundaries of the corresponding kinematic regions. This is a very

promising phenomenological tool, as the direct comparison between an extraction made in Region 1 and another made in Region 2 would shed light on the effects of the soft radiation in the standard TMD factorization.

Conclusions

The factorization of hadronic processes is one of the most important tools in the study of strong interactions. In fact, any modern approach to QCD must wisely balance what can be predicted exclusively by perturbation theory and what has to determined with different, non-perturbative techniques. Incredible efforts are currently undertaken to push perturbative computations to higher and higher perturbative orders, and to improve phenomenological analyses to obtain an ever increasing accuracy in the extractions of non-perturbative, universal functions. These twofolded endeavor has its point of contact in the factorization theorems, where a cross section is carefully cast in such a way that all the universal non-perturbative content is singled out from whatever can be predicted by making use of perturbative QCD.

One of the most interesting cases to which the factorization procedure can be applied regards the study of the effects of the transverse motion of the partons confined inside the hadrons. In fact, such transverse momentum dependent effects offer an incredibly rich source of physical information, as they disclose the entire 3-dimensional structure of hadrons. In the past years, proper TMD factorization theorems have been devised, within different approaches, mainly for three reference hadronic processes: e^+e^- annihilation into two back-to-back hadrons, Semi-Inclusive DIS at small values of momentum transfer and Drell-Yan scattering for a back-to-back lepton pair. The universal, non-perturbative content involved in the cross sections of these three processes has been organized into TMD parton densities, which generalize the commonly used collinear PDFs and FFs, accounting for the dependence on the transverse momentum of partons inside the hadron. These results have been a breakthrough both from the theoretical and from the phenomenological point of view, as they have extended and generalized the original factorization theorems sensitive only to collinear momentum fractions.

With the increment of the experimental potentialities, the variety of accessible hadronic processes is quickly increasing, making it necessary to develop suitable factorization theorems based on rigorous proofs, which are progressively becoming more and more complex from the computational point of view. Nowadays, in addition to the above mentioned reference processes, there are other interesting processes that encode valuable TMD information. In particular, the cross section measured by the BELLE Collaboration [8] has triggered a great interest among the experts of TMD phenomena. This process is a e^+e^- annihilation into a single hadron h, where the transverse momentum of h is

117

measured with respect to the thrust axis. Despite this might look as a rather simple hadronic process, it is actually very hard to give a rigorous proof of the factorization of its cross section in terms of known universal functions. The lack of any publication on this subject until the summer of 2020 [12, 16] testifies the level of difficulty of this task.

This thesis has the ambitious purpose to exploit the Collins factorization formalism [7] to devise a rigorous factorization theorem for the cross section of $e^+e^- \to hX$. This goal can be achieved only after a careful review of the building blocks appearing in a factorized cross section. In Chapter 1 I present the most general definitions of soft and collinear factors in terms of light-cone momentum fraction and transverse momentum. In particular, a consequence of these definitions is that only TMDs can be considered truly universal objects, provided they are defined by the factorization definition presented in Eq. (1.21). In fact, soft factors depend inevitably on the total number N of collinear contributions involved in the process, each one associated to a reference hadron experimentally accessible: the target for TMD PDFs, the detected hadrons for TMD FFs. This property, indicated as N-h universality, induces a classification on hadronic processes, which can then be organized in N-h classes, according to their soft content. Processes belonging to different N-h classes must show a different contribution of the soft radiation; hence, ultimately, they lead to different factorization theorems. In particular, the three benchmark processes for TMD factorization belong to the 2-h class, while the process considered by BELLE belongs to the 1-h class. Therefore, its factorized cross sections should show different structures. Moreover, TMDs have been historically defined in a way suitable for the three reference processes, by absorbing part of the soft radiation contribution inside their definition, which consequently does not coincide with the factorization definition presented in Section 1.3. This commonly used definition has been referred to as "square root" definition all along this thesis. Being specifically devised for the 2-h class, it cannot be extended straightforwardly to $e^+e^- \to hX$.

This totally general considerations are the background on which any factorization theorem should necessarily be founded. In Chapter 2 I have shown how these ideas can successfully be applied through a "top-down" factorization approach to $e^+e^- \to hX$. As long as the transverse momentum of the detected hadron is neither too large to affects significantly the topology of the final state, nor too small to be sensitive to the deflections due to the emission/absorption of soft radiation, the factorization procedure leads to a new, and somehow unexpected, structure of the final cross section. It is a sort of hybrid of collinear and TMD factorization. It encodes the same structure of a collinear factorized cross sections, but the partonic cross section is convoluted with a TMD FF instead of a collinear FF. I denoted this as "collinear-TMD factorization" theorem. This is perhaps the most important result presented in this thesis; hence, an entire Chapter is devoted to investigation of the features and properties of this new kind of factorization theorem. First of all, according to expectations, the TMD FFs appearing in the final cross section must be defined by the factorization definition. Therefore, from the phenomenology point of view, the TMD FFs extracted from SIDIS and $e^+e^- \to h_1 h_2$ cannot be used straightforwardly within the factorization theorem presented in Eq. (2.26). Furthermore, the

final cross section is not CS-invariant, as both the partonic cross section and the TMD FFs depend on the rapidity cut-off introduced by the factorization procedure to regularize the rapidity divergences. I do not interpret this as a failure or an inconsistency of the factorization theorem, but rather as an opportunity to study new aspects of TMD physics, that standard TMD factorization theorems cannot describe. In fact, there is a strong connection between the rapidity cut-off and the measured value of thrust, as it can easily be deduced by a simple kinematic argument: the rapidity of the detected hadron (provided the two initial assumptions on the size of its transverse momentum hold true) has a natural lower limit fixed by thrust. Therefore, if the rapidity cut-off can be somehow linked to a measurable quantity, it cannot be considered as a mere computational tool, but instead it should be assigned a specific physical meaning. Detailed investigation of this physical meaning may shed light on totally new aspects of the hadronization mechanism and on the confinement of partons. The collinear-TMD factorized cross section devised for $e^+e^- \to hX$ is then the first physical observable that can disclose the deeply hidden features of strong interactions.

In Chapter 3 I apply a "bottom-up" approach to the factorization of the $e^+e^- \to hX$ cross section, by constructing the factorization theorem piece by piece, starting from the full QCD Feynman diagrams and proceeding order by order in perturbation theory. This alternative road to factorization is extremely powerful, as the structure of the factorized cross section becomes transparent even at low orders in the perturbative expansion. Of course, given the same initial assumptions on the size of the transverse momentum of the detected hadron, this approach has to lead to the same results of the "top-down" approach. This has been explicitly verified by generalizing to all orders the 1-loop result for the partonic version of the process.

Furthermore, I have also considered the possibilities related to different choices of initial hypotheses. Therefore, the collinear-TMD factorization theorem was framed in a general context where other kinematic configurations lead to different factorization theorems. There are in total three kinematic regions. In Region 1, the transverse momentum of the detected hadron is low enough to be sensitive to soft radiation. As a result, soft gluons play an active role in generating TMD effects and the final cross section is more similar to the usual 2-h class factorization theorems. In fact, the TMD model is modified by the same non-perturbative soft contribution that appears in the commonly used square root definition. Therefore, the factorized cross section valid for Region 1 can be considered a TMD factorization theorem. Region 2 is the intermediate configuration that produces the collinear-TMD factorization theorem discussed above. Finally, in Region 3 the transverse momentum of the detected hadron is large enough to produce significant effects to the topology of the final state. Therefore, the fragmentation process shows a thrust-dependence that is absent is the definition of the TMD. As a consequence, the corresponding factorized cross section involves generalized Fragmentation Jet Functions (GFJFs) instead of TMD FFs. As GFJFs are more similar to a generalized version of the usual collinear FFs than to an extended definition of TMDs, I have denoted the Region 3 cross section as "generalized collinear factorization theorem".

Conclusions

Finally, I have proposed an algorithm to select data according to the corresponding kinematic regions. This can be an extremely powerful tool for phenomenological analyses, as it allows to bypass the long-standing problem of matching different kinematic regions. In particular, comparing the results of the extraction of the TMD FFs from Region 1 and Region 2, it will be possible to shed light on the role of soft radiations in generating TMD effects, as such a combined phenomenological analysis can in principle allow to access and extract the soft model, M_S. Moreover, after the non-perturbative building blocks of the standard TMD factorization will have been determined, the general scheme proposed in this thesis could be extended to many other hadronic processes, possibly involving more than two TMDs.

In conclusion, the work presented in this thesis looks incredibly promising. Not only because it presents new kinds of observables, like the collinear-TMD factorized cross section of $e^+ e^- \to hX$, which may describe some interesting and still unknown features of non-perturbative QCD, but also because the general approach devised in this thesis gives top priority to the universality properties of the non-perturbative objects involved in the factorization procedure. Hopefully, in the future, these new perspectives may disclose the inner, unrevealed secrets of strong interactions.

Appendix A

Review of the Collins formalism

This Appendix is a short review of the kinematics approximators defined in [7] that have been widely used all along this paper. Their definition is based on the power counting rules:

1. Given the typical (large) energy scale Q of a process, the hard, collinear and soft momenta are weighted as:

$$
\begin{aligned}
P_{\text{hard}} &\sim (Q, Q, Q); \\
P_{\text{coll.}} &\sim (Q, \lambda_S, \lambda); \\
P_{\text{soft}} &\sim (\lambda_S, \lambda_S, \lambda_S);
\end{aligned}
\tag{A.1}
$$

where $\lambda << Q$ is some IR energy scale and $\lambda_S = \lambda^2/Q$. Such scaling allow to classify sets of subgraphs inside a generic Feynman diagram. According to this classification, the hard subgraph will contain particles carrying hard momenta and so on.

2. Any extra collinear line attached to the hard subgraph gives a suppression. Extra means any line besides the minimal number of fermions required by the kinematics of the process and any number of scalar polarized gluons.

3. Any soft line attached to the hard subgraph gives a suppression.

4. Any fermionic line connecting collinear and soft subgraphs gives a suppression.

All the gluons connecting soft and collinear subgraphs and hard and collinear subgraphs are collected into Wilson lines (or gauge links). They are path-ordered exponential operators defined as:

$$
W_\gamma = P \left\{ \exp \left[-i g_0 \int_0^1 ds \, \dot{\gamma}^\mu(s) A^a_{(0)\mu}(\gamma(s)) t_a \right] \right\},
\tag{A.2}
$$

where γ is a generic path and P denotes the path ordering (i.e. when the exponential is expanded the fields corresponding to higher values of s are to be placed to the left). The coupling constant and

the gluon field are bare quantities, as indicated by the label "0". In the previous formula, t_a are the generating matrices of the gauge group, in the appropriate representation. The Wilson lines guarantee that PDFs and FFs (in both collinear and TMD cases) are gauge invariant, by linking the quark to the anti-quark fields. If this direction γ^μ is a straight line the Wilson line depends only on the endpoints of the path and can be written in a compact way as:

$$W_n(x_2, x_1, n) = P\left\{\exp\left[-ig_0 \int_{x_1}^{x_2} d\lambda\, n^\mu A_{(0)\,\mu}^a(\lambda n) t_a\right]\right\}, \tag{A.3}$$

If the strongly boosted particle is a quark, the associated Feynman rules are:

$$\underrightarrow{\quad\quad} = \frac{i}{k \cdot n + i0}; \tag{A.4}$$

$$\underset{a}{\overrightarrow{\quad\quad}} = -ig_0\, n^\mu t_a. \tag{A.5}$$

In the Collins factorization formalism, the Wilson lines associated to soft contributions are tilted off the light-cone. In the following, $w_1 = (1, 0, \vec{0}_T)$ and $w_2 = (0, 1, \vec{0}_T)$ will represent the plus- and minus-directions respectively, while the tilted directions will be defined as:

$$n_1 = (1, -e^{-2y_1}, \vec{0}_T), \qquad\qquad n_2 = (-e^{2y_2}, 1, \vec{0}_T). \tag{A.6}$$

The auxiliary parameters y_1 and y_2 will acts as rapidity cut-offs and will regulate the rapidity divergences due to the Wilson lines associated to the collinear contributions, which are straight along the light-cone.

Since we are interested in 2-jet topologies, we will label the hemisphere associated with the plus-direction as "A" and the opposite hemisphere as "B" (backward emission, along minus-direction). Therefore, in each Feynman diagram we will identify an hard subgraph, labeled as "H", a soft subgraph, labeled as "S" and two collinear subgraphs, labeled either "A" or "B" depending on the leading direction of the collinear particles that flow inside them. The classification is not unique, but depends on the kinematic configuration (or region R) associated to the particles involved. The operation of choosing a certain kinamtic region "R" is defined to be the action of the kinematic approximator T_R. In practice, any generic T_R is based on the following recipe:

1. In the collinear subgraphs approximate the circulating soft momenta as:

$$k \sim w_2 \frac{k \cdot n_1}{w_2 \cdot n_1} \quad \text{for A}, \qquad\qquad k \sim w_1 \frac{k \cdot n_2}{w_1 \cdot n_2} \quad \text{for B}. \tag{A.7}$$

2. In the hard subgraph neglect all the masses and approximate the circulating collinear momenta as:

$$k \sim w_1 \frac{k \cdot w_2}{w_1 \cdot w_2} \quad \text{for A,} \qquad\qquad k \sim w_2 \frac{k \cdot w_1}{w_1 \cdot w_2} \quad \text{for B.} \qquad (A.8)$$

Notice that the circulating soft momenta are totally neglected in the hard subgraph.

3. The attachment of a soft gluon to a collinear subgraph is approximated as (Grammer-Yennie approximation):

$$A(\ldots,k,\ldots)^\mu S(\ldots,k,\ldots)_\mu \sim A(\ldots,\widehat{k},\ldots)^\mu \frac{\widehat{k}_\mu\, n_{1,\nu}}{k \cdot n_1 + i0} S(\ldots,k,\ldots)_\nu,$$

$$B(\ldots,k,\ldots)^\mu S(\ldots,k,\ldots)_\mu \sim B(\ldots,\widehat{k},\ldots)^\mu \frac{\widehat{k}_\mu\, n_{2,\nu}}{k \cdot n_2 + i0} S(\ldots,k,\ldots)_\nu. \qquad (A.9)$$

where $\widehat{k}$ are the approximated momenta defined in Eq. (A.7) and the $i0$-prescription is correct when the momentum k flows out of the collinear subgraph.

4. The attachment of a collinear gluon to the hard subgraph is approximated as (Grammer-Yennie approximation):

$$H(\ldots,k,\ldots)^\mu A(\ldots,k,\ldots)_\mu \sim H(\ldots,\widehat{k},\ldots)^\mu \frac{\widehat{k}_\mu\, w_{2,\nu}}{k \cdot w_2 + i0} A(\ldots,k,\ldots)_\nu,$$

$$H(\ldots,k,\ldots)^\mu B(\ldots,k,\ldots)_\mu \sim H(\ldots,\widehat{k},\ldots)^\mu \frac{\widehat{k}_\mu\, w_{1,\nu}}{k \cdot w_1 + i0} B(\ldots,k,\ldots)_\nu. \qquad (A.10)$$

where $\widehat{k}$ are the approximated momenta defined in Eq. (A.8) and the $i0$-prescription is correct when the momentum k flows out of the hard subgraph.

5. For a Dirac line leaving the hard subgraph and entering in the collinear-A subgraph, insert the projector $\mathrm{P} = \frac{1}{2}\gamma^+\gamma^-$. The same rule applies for a Dirac line leaving the collinear-B subgraph and entering in the hard subgraph. For a quark line in the reverse direction, insert $\overline{\mathrm{P}} = \frac{1}{2}\gamma^-\gamma^+$.

Soft factors and collinear parts are functions initially defined only over a rather small region in the transverse momentum space, according to power counting rules. The Fourier transform to the impact parameter space can be regarded as a kind of analytic continuation, because at fixed b_T we can roughly access all transverse momenta with $k_T \leq \frac{1}{b_T}$, even trespassing the original momentum region. In particular, the small b_T region is associated with large transverse momenta, where perturbative QCD can be applied and a power expansion in α_s allows us to perform explicit calculations. This can be proved by a direct application of the factorization procedure to the small b_T approximation of the Fourier transformed function. For the soft factor this can be found in Section 1.2, while for collinear parts see for instance Refs. [7, 56].
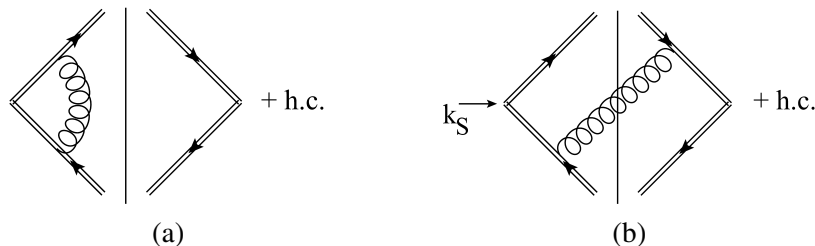
Fig. A.1 Feynman graphs contributing to the small b_T behavior of the 1 loop soft factor $\widetilde{\mathbb{S}}_{\text{2-h}}$. (a): Virtual diagrams (zero in dimensional regularization). (b) Real diagrams.

Despite the undeniable advantage provided by the possibility to perform explicit calculations in the small b_T region, perturbative QCD is not enough to reproduce integrated quantities, which correspond to the Fourier transformed functions evaluated in $b_T = 0$. These can be recovered from the operator definitions, that obviously give a non-perturbative, all-order point of view. Therefore in $b_T = 0$, Eqs. (1.2) and (1.6) simply confirm that the integrated soft factor is the identity matrix, while Eq. (1.17) reproduces the integrated PDFs and FFs. The failure of perturbative QCD in $b_T = 0$ is due to the fact that the integral over $\vec{k}_T$ is intrinsically ill defined, since it extends well beyond the physical momentum region where the TMDs and the soft factor are defined. As a consequence, new UV divergences arise and the counterterms Z_S and Z_C in Eqs. (1.2) and (1.17) are not sufficient to cancel them. Therefore, the perturbative approach lead to definition of integrated functions as *bare* quantities and they need a renormalization in order to acquire physical meaning and reproduce the correct results. In the following, such renormalization procedure will be investigated for both the 2-h soft factor, in Section A.1 and the TMDs, in Section A.2. All the quantities computed in this section will be function of b_T, however when used into Eqs. (1.14), (1.26), such dependence must be replaced by the $b^\star$ prescription.

In the last section A.3, I will review the explicit formulas for 1-loop FFs.

A.1   Small b_T behaviour of 2-h Soft Factor

The Feynman graphs in Fig. A.1 show that in the small b_T region the (renormalized) 2-h soft factor is given by:

$$\widetilde{\mathbb{S}}_{\text{2-h}}(b_T, \mu, y_1 - y_2) = 1 - \frac{\alpha_S(\mu)}{4\pi} 8C_F (y_1 - y_2) \log\left(\frac{b_T \mu}{c_1}\right) + \mathcal{O}\left(\alpha_S^2, e^{-2(y_1 - y_2)}\right), \qquad \text{(A.11)}$$

where $c_1 = 2e^{-\gamma_E}$. The perturbative expansion of the previous equation should be valid at small b_T; however in this region $\log(b_T \mu / c_1)$ becomes large and sufficiently near to $b_T = 0$ it completely oversizes α_S so that the expansion becomes meaningless. Resummation in principle solves this

problem. The soft kernel can be directly obtained from Eq. (A.11) by using Eqs. (1.7):

$$\widetilde{K}(b_T, \mu) = -\frac{\alpha_S(\mu)}{4\pi} 16 C_F \log\left(\frac{b_T \mu}{c_1}\right) + \mathcal{O}\left(\alpha_S^2\right). \tag{A.12}$$

This expressions implies that $\widetilde{K}(b_T, \mu)$ is large and positive as b_T decreases. Therefore, the resummed soft factor of Eq. (1.10) explodes in $b_T = 0$, as in its exponent the soft kernel multiplies the rapidity cut-off combination $(y_1 - y_2)$, which has to be intended as a large and positive number. An improvement can be reached by providing a resummed version[1] for $\widetilde{K}$ by using its evolution equation solution, Eq. (1.9). Given that the α_S-expansion of the soft kernel has the following structure:

$$\widetilde{K}(b_T; \mu) = \sum_{n=1} \left(\frac{\alpha_S(\mu)}{4\pi}\right)^n \sum_{l=0}^{n} \widetilde{K}^{[n,l]} \log^l\left(\frac{\mu}{\mu_b}\right), \tag{A.13}$$

where μ_b has been defined in Eq. (1.27)(a). On the other hand, the anomalous dimension γ_K is expanded as:

$$\gamma_K(\alpha_S(\mu)) = \sum_{n=1} \left(\frac{\alpha_S(\mu)}{4\pi}\right)^n \gamma_K^{[n]}, \tag{A.14}$$

Therefore, Eq. (1.9) can be recast as follows:

$$\begin{aligned}
\widetilde{K}(b_T; \mu) &= \widetilde{K}(b_T; \mu_b) - \int_{\mu_b}^{\mu} \frac{d\mu'}{\mu'} \gamma_K(\alpha_s(\mu')) = \\
&= \sum_{n=1} \left\{ \left(\frac{\alpha_S(\mu)}{4\pi}\right)^n \widetilde{K}^{[n,0]} - \gamma_K^{[n]} \int_{\mu_b}^{\mu} \frac{d\mu'}{\mu'} \left(\frac{\alpha_S(\mu')}{4\pi}\right)^n \right\} = \\
&= \sum_{l\geq 0} \log^{-l}\left(\frac{\mu}{\mu_b}\right) g_{l+2}^K(x) = \underbrace{g_2^K(x)}_{\text{LL}} + \underbrace{\frac{1}{\log\left(\frac{\mu}{\mu_b}\right)} g_3^K(x) + \ldots}_{\text{NLL}}
\end{aligned} \tag{A.15}$$

where:

$$x = \frac{\alpha_S(\mu)}{4\pi} \log\left(\frac{\mu}{\mu_b}\right), \tag{A.16}$$

The recipe to reach the NLL accuracy is the following [57]:

- The anomalous dimension γ_K of the soft kernel is expanded up to 2-loops. The 1-loop coefficient can be found directly obtained from Eq. (A.12). For 2-loops coefficient see for instance

---

[1]Actually, it is inappropriate to count the logs of a quantity, like the soft kernel, which is already the result of a resummation procedure.

Refs. [58, 56]:

$$\gamma_K^{[1]} = 16 C_F; \tag{A.17a}$$

$$\gamma_K^{[2]} = 2 C_A C_F \left(\frac{536}{9} - \frac{8\pi^2}{3} \right) - \frac{160}{9} C_F n_f. \tag{A.17b}$$

where n_f is the total number of fermion fields considered.

- All the other quantities are expanded up to 1-loop. In this case the only other term is the part of the soft kernel without logs, i.e. computed at reference scale $\mu = \mu_b$. At 1-loop it is just zero, as follows from Eq. (A.12):

$$\widetilde{K}^{[1,0]} = 0; \tag{A.18}$$

This recipe results in:

$$g_2^K(x) = \frac{\gamma_K^{[1]}}{2\beta_0} \log\left(1 - 2\beta_0 x\right); \tag{A.19a}$$

$$g_3^K(x) = \frac{x^2}{1 - 2\beta_0 x} \left[\gamma_K^{[1]} \frac{\beta_1}{\beta_0} - \gamma_K^{[2]} + \frac{1}{x} \widetilde{K}^{[1]} \right]. \tag{A.19b}$$

where β_0 and β_1 are the coefficients of the beta functions up to 2 loop:

$$\beta_0 = \frac{11}{3} C_A - \frac{2}{3} n_f, \tag{A.20a}$$

$$\beta_1 = \frac{34}{3} C_A^2 - \frac{10}{3} C_A n_f - 2 C_F n_f. \tag{A.20b}$$

Notice that the NLL expression of $\widetilde{K}$ coincides with Eq. (A.12) in the limit $\alpha_S \to 0$. With this estimate, the divergence of $\widetilde{K}$ is much less severe but it is still there. An easy way to solve the problem and ensure that the perturbative QCD computation agrees with the operator definition prediction is to introduce a cut-off that prevents the soft transverse momentum to reach the UV region when it is integrated out. This can be implemented in b_T-space by introducing a new parameter $b_{\text{MIN}} \neq 0$ that provides a minimum value for b_T. A modification of the $b^\star$ prescription, Eq. (1.4), is a simple way to insert this cut-off directly in the definition of the soft factor. For example, we can use the modified $b^\star$ prescription of Ref. [59]:

$$\vec{b}_T^\star (b_c(b_T)) = \vec{b}_T^\star \left(\sqrt{b_T^2 + b_{\text{MIN}}^2} \right). \tag{A.21}$$

Then, the integrated soft factor is given by the unintegrated $\widetilde{\mathbb{S}}_{2\text{-h}}$ evaluated in $b_T^\star (b_c(0)) = b_{\text{MIN}}$. If μ can be considered a large energy scale (e.g. if it can be set equal to the hard energy scale Q of the process) then we can set $b_{\text{MIN}} = c_1/\mu$. Consequently, all logs in Eqs. (A.11) and (A.12) as well as the soft kernel are zero in $b_T = 0$, while the soft factor is unity Despite this kind of regularization has

been devised for the 2-h soft factor, it applies equally well to the general soft factor $\mathbb{S}_{\text{N-h}}$, where N can be any integer greater than 2.

A.2 Small b_T behaviour of TMDs

Formally, the integrated TMD is the Fourier transformed TMD computed at $b_T = 0$. In order to recover this result from Eq. (1.26) by applying perturbative QCD, the Fourier transformed TMD has to be renormalized, otherwise it would vanish in $b_T = 0$. This can be guessed from the structure of the perturbative Sudakov factor in Eq. (1.26). Differently from the soft case, in the exponent $\widetilde{K}$ multiplies $\sim \log \zeta \propto -y_1$. Therefore, in the large rapidity limit we have a suppression as $b_T \to 0$. A more rigorous proof can be found for instance in Ref. [59]. Alternatively, it also follows from the resummed expression of the TMD. By using also the results of the previous section, we can compute the general resummed structure of the (perturbative) Sudakov factor. This operation is easily done by separating out the part that depends on the rapidity cut-off ζ from the rest of the exponent appearing in the perturbative Sudakov factor:

$$
\begin{aligned}
\exp&\left\{ \frac{1}{4} \widetilde{K}(b_T; \mu_b) \log \frac{\zeta}{\mu_b^2} + \int_{\mu_b}^{\mu} \frac{d\mu'}{\mu'} \left[\gamma_D(\alpha_S(\mu'), 1) - \frac{1}{4} \gamma_K(\alpha_S(\mu')) \log \frac{\zeta}{\mu'^2} \right] \right\} = \\
&= \exp\left\{ \frac{1}{2} \widetilde{K}(b_T; \mu_b) \log \left(\frac{\mu}{\mu_b} \right) + \int_{\mu_b}^{\mu} \frac{d\mu'}{\mu'} \left[\gamma_D(\alpha_S(\mu'), 1) - \frac{1}{2} \gamma_K(\alpha_S(\mu')) \log \left(\frac{\mu}{\mu'} \right) \right] \right\} \times \\
&\times \exp\left\{ \frac{1}{4} \log \frac{\zeta}{\mu^2} \left[\widetilde{K}(b_T; \mu_b) - \int_{\mu_b}^{\mu} \frac{d\mu'}{\mu'} \gamma_K(\alpha_S(\mu')) \right] \right\}.
\end{aligned}
\tag{A.22}
$$

Notice that the general structure for the resummed version of the last exponent has already been given in Eq. (A.15). Therefore, we only have to focus on the second line of Eq. (A.22). The rapidity-independent part of the TMD anomalous dimension (obtained setting $\zeta = \mu^2$) has a small coupling series totally analogous to that of the anomalous dimension of the soft kernel:

$$
\gamma_C(\alpha_S(\mu), 1) = \sum_{n=1} \left(\frac{\alpha_S(\mu)}{4\pi} \right)^n \gamma_C^{[n]},
\tag{A.23}
$$

127

Therefore, the exponent in the second line of Eq. (A.22) can be recasted as:

$$
\frac{1}{2}\widetilde{K}(b_T;\mu_b)\log\left(\frac{\mu}{\mu_b}\right) + \int_{\mu_b}^{\mu}\frac{d\mu'}{\mu'}\left[\gamma_D(\alpha_S(\mu'),1) - \frac{1}{2}\gamma_K(\alpha_S(\mu'))\log\left(\frac{\mu}{\mu'}\right)\right] =
$$

$$
= \sum_{n=1}\left\{\frac{1}{2}\left(\frac{\alpha_S(\mu)}{4\pi}\right)^n\widetilde{K}^{[n,0]}\log\left(\frac{\mu}{\mu_b}\right) + \right.
$$

$$
\left. + \gamma_C^{[n]}\int_{\mu_b}^{\mu}\frac{d\mu'}{\mu'}\left(\frac{\alpha_S(\mu')}{4\pi}\right)^n - \frac{1}{2}\gamma_K^{[n]}\int_{\mu_b}^{\mu}\frac{d\mu'}{\mu'}\left(\frac{\alpha_S(\mu')}{4\pi}\right)^n\log\left(\frac{\mu}{\mu'}\right)\right\} =
$$

$$
= \sum_{l\geq 0}\log^{1-l}\left(\frac{\mu}{\mu_b}\right)g_{l+1}(x) = \underbrace{\underbrace{\log\left(\frac{\mu}{\mu_b}\right)g_1(x)}_{\text{LL}} + g_2(x) + \dots}_{\text{NLL}} \tag{A.24}
$$

where x has been defined in Eq. (A.16). Following the usual recipe to get the NLL accuracy, with:

$$
\gamma_C^{[1]} = 6C_F, \tag{A.25}
$$

both for TMD PDFs and TMD FFs, the functions g_1 and g_2 are given by:

$$
g_1(x) = \frac{\gamma_K^{[1]}}{4\beta_0}\left[1 + \frac{\log(1-2\beta_0 x)}{2\beta_0 x}\right], \tag{A.26a}
$$

$$
g_2(x) = \frac{\gamma_K^{[1]}}{4\beta_0}\frac{\beta_1}{\beta_0}\left[\frac{x}{1-2\beta_0 x} + \frac{1}{2\beta_0}\left(\log(1-2\beta_0 x) + \frac{1}{2}\log(1-2\beta_0 x)^2\right)\right] -
$$

$$
- \frac{\gamma_K^{[2]}}{8\beta_0^2}\left[\frac{2\beta_0 x}{1-2\beta_0 x} + \log(1-2\beta_0 x)\right] - \frac{\gamma_D^{[1]}}{2\beta_0}\log(1-2\beta_0 x). \tag{A.26b}
$$

Finally, up to NLL the perturbative Sudakov factor is:

$$
\begin{array}{c}\text{pert. Sudakov}\\ \text{factor}\end{array} \overset{\text{low } b_T}{\sim} \left(\frac{b_T\,\mu}{c_1}\right)^{\frac{\gamma_K^{[1]}}{4\beta_0}} \times \begin{array}{c}\text{log}\\ \text{corrections}\end{array}. \tag{A.27}
$$

Therefore, the perturbative Sudakov factor produces a suppression as $b_T \to 0$. Notice that this holds true independently from the rapidity cut-off.

The Wilson coefficients cannot modify this behavior. Their α_S expansion has the following structure:

$$
\widetilde{\mathscr{C}}_f^j(\rho,b_T;\mu,\zeta) = \sum_{n=0}^{\infty}\left(\frac{\alpha_S(\mu)}{4\pi}\right)^n\sum_{k=0}^{2n}\sum_{l=0}^{[k/2]}\widetilde{\mathscr{C}}_f^{j\,[n,k-l,l]}(\rho)\log^{k-l}\left(\frac{\mu}{\mu_b}\right)\log^l\left(\frac{\zeta}{\mu_b^2}\right), \tag{A.28}
$$

where $[k/2]$ denotes the integer part of k. If the scales are fixed according to the standard choices of Eqs. (1.27), all the logs disappear and the only b_T dependence in the Wilson coefficients is given by

$\alpha_S(\mu_b)$. Hence, the TMD at reference scale (see Eq. (1.26)) can be written as:

$$\left(\widetilde{\mathscr{C}}_j^k(b_T; \mu_b, \zeta_b) \otimes c_{k,h}(\mu_b) \right)(\xi) =$$

$$= \sum_{n=0} \left(\frac{\alpha_S(\mu_b)}{4\pi} \right)^n \left(\widetilde{\mathscr{C}}_f^{j\,[n,0,0]} \otimes c_{k,h}(\mu_b) \right)(\xi). \tag{A.29}$$

Recalling that the convolution $\otimes$ of two generic functions f and g is defined as

$$(f \otimes g)(\xi) = \int_x^1 \frac{d\rho}{\rho} f(\xi/\rho) g(\rho), \tag{A.30}$$

and that the Wilson Coefficients of the final state have a normalization factor $\rho^{2-2\varepsilon}$ when the convolution is made explicit (see for instance Ref. [58]) we have:

$$\text{TMD at} \atop \text{reference scale} \overset{\text{low } b_T}{\sim} \begin{cases} f_{j/h}(x, \mu_b) + \mathcal{O}(\alpha_S(\mu_b)) & \text{initial state} \\[2mm] z^{-2+2\varepsilon} d_{h/j}(z, \mu_b) + \mathcal{O}(\alpha_S(\mu_b)) & \text{final state,} \end{cases} \tag{A.31}$$

where we used that the Wilson coefficients at lowest order are just delta functions, both in flavor and in the collinear momentum fraction. Furthermore, since $\mu_b \propto 1/b_T$, when $b_T \to 0$ the energy scale becomes very large and α_S can be really considered a small parameter and we are allowed to neglect $\mathcal{O}(\alpha_S)$. Eq. (A.31), together with Eq. (A.27), implies the vanishing of the TMDs evaluated in $b_T = 0$, preventing finding the usual PDFs and FFs in contrast with the operator definition of Eq. (1.17). Analogously to the soft factor case, this problem can be solved by introducing a new parameter $b_{\text{MIN}} \neq 0$ that provides a minimum value for b_T. This will act as a cut-off preventing the collinear transverse momentum to reach the UV region in the integration. Then, the integrated TMD is given by the unintegrated TMD evaluated in $b_T^\star(b_c(0)) = b_{\text{MIN}} \equiv c_1/\mu$:

$$\int d^{2-2\varepsilon} \vec{k}_T \, C_{f,h}(\xi, k_T; \mu, \zeta) = \widetilde{C}_{f,h}(\xi, b_{\text{MIN}}; \mu, \zeta) = \begin{cases} f_{j/h}(x, \mu) \times \begin{smallmatrix} \text{suppressed} \\ \text{terms} \end{smallmatrix} & \text{initial state,} \\[3mm] z^{-2+2\varepsilon} d_{h/j}(z, \mu) \times \begin{smallmatrix} \text{suppressed} \\ \text{terms} \end{smallmatrix} & \text{final state.} \end{cases} \tag{A.32}$$

The b_{MIN} renormalization is not the only way to make sense of the integral over $\vec{k}_T$. If TMDs are not at the core of the factorization theorem under examination, a common renormalization procedure is to define the integrated TMDs as the *bare version* of the usual PDFs or FFs. Formally:

$$\int d^{2-2\varepsilon} \vec{k}_T \, C_{j,h}(\xi, k_T; \mu, \zeta) = \begin{cases} f_{j/h}^{\overline{(0)}}(x, \mu) & \text{initial state,} \\[3mm] z^{-2+2\varepsilon} d_{h/j}^{\overline{(0)}}(z, \mu) & \text{final state.} \end{cases} \tag{A.33}$$

Here, the label "$\overline{(0)}$" stands for bare functions of renormalized fields (that's where the μ-dependence on the r.h.s of the previous equations come from). In this form, it appears as the integration makes the soft-collinear subtractions trivial, because the $\mathbb{S}_{2\text{-h}}$ appearing in the factorization definition (Eq. (1.21)) is unity when integrated over all soft transverse momentum. To get renormalized quantities, we have to cancel order by order the UV divergences introduced by the integration through an UV counterterm, in the following indicated as $Z_{\text{coll.}}$. This will necessarily depend on the plus component of the momentum of the reference parton, i.e. on the collinear momentum fraction ξ. Hence, the renormalized quantities are not simple products of the bare quantities with the UV counterterm, like in Eq. (1.21), but rather convolutions:

$$c_{j,h}(\xi, \mu) = \left((Z_{\text{coll.}})_j^k \left(\alpha_S(\mu) \right) \otimes c_{k,h}^{(0)} \right)(\xi),\tag{A.34}$$

where, as in Eq. (1.21), the label "(0)" denotes a bare quantity computed with bare fields. With this definition, we can interpret the renormalized integrated TMDs as the usual PDFs and FFs used in collinear factorized cross sections. Notice that the OPE of the TMDs at reference scale involves renormalized PDFs and FFs, as the bare version of the Wilson coefficients can be trivially defined as the "unsubtracted hard part" in the collinear factorization theorem that fixes the structure of TMDs at small b_T. In fact, straightforwardly:

$$\widetilde{C}_{j,h}(b_T; \mu, \zeta) \overset{\text{low } b_T}{\sim} \widetilde{\mathscr{C}}_j^{k\,(0)}(b_T; \mu, \zeta) \otimes c_{k,h}^{(0)} =$$
$$= \left(\widetilde{\mathscr{C}}_j^{l\,(0)}(b_T; \mu, \zeta) \otimes \left(Z_{\text{coll.}}^{-1} \right)_l^m (\alpha_S(\mu)) \right) \otimes \left((Z_{\text{coll.}})_m^k (\alpha_S(\mu)) \otimes c_{k,h}^{(0)} \right) =$$
$$= \widetilde{\mathscr{C}}_j^m(b_T; \mu, \zeta) \otimes c_{m,h}(\mu),\tag{A.35}$$

where the dependence on the collinear momentum fraction has been neglected for simplicity.

A.3   Unpolarized Fragmentation Functions in pQCD

This section is a review of the main formulas for Unpolarized Fragmentation Functions. I will focus on the gluon-from-quark and the quark-from-quark case, as they are the only relevant configurations for 1-loop analyses of e^+e^- annihilation. The cases quark-from-gluon and gluon-from-gluon can be found in the related literature.

In the following, labeling k the total moment momentum entering in the collinear subgraph, the momentum of the outgoing parton is $P = \left(zk^+, 0, \vec{0}_T \right)$, where z is the light-cone momentum fraction. All the quantities will be computed in the Collins renormalization scheme, which differs from $\overline{\text{MS}}$ because the common factor:

$$S_\varepsilon = \frac{(4\pi)^\varepsilon}{\Gamma(1-\varepsilon)}\tag{A.36}$$

is not ε-expanded.

Often, we have to compute UV-counterterms. This will be achieved by constraining the integrations on k_T from μ to infinity. It is useful to recall:

$$\int_\mu^\infty dk_T^2 \left(k_T^2\right)^{-1-\varepsilon} = \frac{\mu^{-2\varepsilon}}{\varepsilon}, \quad \mathrm{Re}(\varepsilon) > 0; \tag{A.37a}$$

$$\int_\mu^\infty dk_T^2 \left(k_T^2\right)^{-1-\varepsilon} \log\left(\frac{\zeta}{k_T^2}\right) = \mu^{-2\varepsilon} \left(-\frac{1}{\varepsilon^2} + \frac{1}{\varepsilon} \log\left(\frac{\zeta}{\mu^2}\right)\right), \quad \mathrm{Re}(\varepsilon) > 0. \tag{A.37b}$$

Since TMDs are properly defined in b_T-space, we also have to perform Fourier transforms. Useful formulas are:

$$\int d^{2-2\varepsilon}\vec{k}_T \, e^{i\vec{k}_T \cdot \vec{b}_T} \frac{1}{k_T^2} = Q^{-2\varepsilon} \frac{\pi^{1-\varepsilon}}{\Gamma(1-\varepsilon)} \left(\frac{b}{c_1}\right)^{2\varepsilon} e^{-2\varepsilon\gamma_E} \Gamma(-\varepsilon)\Gamma(1-\varepsilon), \quad \mathrm{Re}(\varepsilon) < 0; \tag{A.38a}$$

$$\int d^{2-2\varepsilon}\vec{k}_T \, e^{i\vec{k}_T \cdot \vec{b}_T} \frac{1}{k_T^2} \log\left(\frac{\zeta}{k_T^2}\right) =$$

$$= Q^{-2\varepsilon} \frac{\pi^{1-\varepsilon}}{\Gamma(1-\varepsilon)} \left(\frac{b}{c_1}\right)^{2\varepsilon} e^{-2\varepsilon\gamma_E} \Gamma(-\varepsilon)\Gamma(1-\varepsilon) \left(-H_{-1-\varepsilon} + 2\log\left(\frac{b}{c_1}\right) + \log\left(\frac{\zeta}{Q^2}\right)\right),$$

$$\mathrm{Re}(\varepsilon) < 0; \tag{A.38b}$$

where $c_1 = 2e^{-\gamma_E}$, $b = b_T Q$, γ_E is the Euler-Mascheroni constant and $H_{-1-\varepsilon}$ is the harmonic number evaluated at $-1-\varepsilon$.

A.3.1 Gluon-from-quark

The gluon-from-quark configuration starts from $\mathcal{O}(\alpha_S)$. Then, from the definition of Eq. (1.15), the lowest order of the gluon-from-quark TMD FF in momentum space is:

$$\frac{\alpha_S}{4\pi} D_{g/q}^{[1]}(\varepsilon; z, \vec{k}_T) = \frac{1}{z} \int \frac{dk^+ dk^-}{(2\pi)^D} \frac{\mathrm{Tr}_C}{N_C} \frac{\mathrm{Tr}_D}{4} \left(\gamma^+ \; {}_{k} \vcenter{\hbox{}} \right) =$$

$$= \frac{\alpha_S}{4\pi} 2 C_F S_\varepsilon \frac{\Gamma(1-\varepsilon)}{\pi^{1-\varepsilon}} \mu^{2\varepsilon} \frac{1}{k_T^2} \frac{1+(1-z)^2 - \varepsilon z^2}{z^3} \theta(1-z). \tag{A.39}$$

Notice that there are no soft-collinear subtractions for the 1-loop gluon-from-quark TMD FF, as the configuration in which the emitting fermion turns soft or is reflected backward is suppressed by power counting. Furthermore, since there are no contributions from virtual emissions, this function is already renormalized, i.e. there is no need for a TMD UV counterterm Z_{TMD}.

According to the discussion in the end of the previous section, the integration of $D_{g/q}$ over transverse momentum gives the bare gluon-from-quark collinear FF, as in Eq. (A.33). Being a scaleless integral, in full dimensional regularization the result is zero. However, the renormalized gluon-from-quark collinear FF does not vanish, as it equals its UV counterterm. From Eq. (A.33):

$$\frac{\alpha_S}{4\pi} d_{g/q}^{(0),[1]}(\varepsilon; z) = z^{2-2\varepsilon} \int d^{2-2\varepsilon}\vec{k}_T \frac{\alpha_S}{4\pi} D_{g/q}^{[1]}(z, \vec{k}_T) = 0 =$$
$$= \frac{\alpha_S}{4\pi} \left[d_{g/q}^{[1]}(\varepsilon; z) - Z_{g/q,\text{coll}}^{[1]}(\varepsilon; z) \right] \tag{A.40}$$

Therefore, by using Eq. (A.37a):

$$\frac{\alpha_S}{4\pi} d_{g/q}^{[1]}(\varepsilon; z) \equiv \frac{\alpha_S}{4\pi} Z_{g/q,\text{coll}}^{[1]}(\varepsilon; z) = -\frac{\alpha_S}{4\pi} 2C_F \frac{S_\varepsilon}{\varepsilon} \frac{1+(1-z)^2}{z} \theta(1-z). \tag{A.41}$$

On the other hand, the Fourier transform of Eq. (A.39) gives the gluon-from-quark TMD FF:

$$\frac{\alpha_S}{4\pi} \widetilde{D}_{g/q}^{[1]}(\varepsilon; z, b_T) = \int d^{2-2\varepsilon}\vec{k}_T \, e^{i\vec{k}_T \cdot \vec{b}_T} \frac{\alpha_S}{4\pi} D_{g/q}^{[1]}(z, \vec{k}_T) =$$
$$= \frac{\alpha_S}{4\pi} S_\varepsilon \left(\frac{\mu}{Q}\right)^{2\varepsilon} \left(\frac{b}{c_1}\right)^{2\varepsilon} e^{-2\varepsilon\gamma_E} \Gamma(-\varepsilon)\Gamma(1-\varepsilon) \frac{1+(1-z)^2 - \varepsilon z^2}{z^3} \theta(1-z) =$$
$$= \frac{\alpha_S}{4\pi} \frac{1}{z^2} Z_{g/q,\text{coll}}^{[1]}(\varepsilon; z) + \frac{\alpha_S}{4\pi} 2C_F \left(\frac{1}{z} - 2\log\left(\frac{b_T \mu}{c_1}\right) \frac{1+(1-z)^2}{z^3}\right). \tag{A.42}$$

Notice that in the final result survives a pole in ε. This is the collinear divergence associated with the FF, the cause of the the failure of pQCD in predicting such observables. The perturbative, finite, quantities associated with TMDs are the Wilson coefficients. Once collinear and TMD parton densities have been computed, the Wilson coefficient are determined through Eq. (A.35). For FFs, at 1-loop:

$$\widetilde{\mathscr{C}}_{j/f}^{[1]}(z, b_T; \mu, \zeta) = \widetilde{C}_{j/f}^{[1]}(\varepsilon; z, b_T; \mu, \zeta) - \frac{d_{j/f}^{[1]}(\varepsilon; z)}{z^{2-2\varepsilon}} \tag{A.43}$$

For the gluon-from-quark configuration we have:

$$\frac{\alpha_S}{4\pi} \widetilde{\mathscr{C}}_{g/q}^{[1]}(z, b_T) = \frac{\alpha_S}{4\pi} 2C_F \left[\frac{1}{z} - 2\left(\log\left(\frac{b_T \mu}{c_1}\right) - \log z\right) \frac{1+(1-z)^2}{z^3} \right]. \tag{A.44}$$

A.3.2 Quark-from-quark

For the quark-from-quark configuration, the computations are more difficult. The lowest order is just a delta function, but for the $\mathscr{O}(\alpha_S)$ we have to consider both virtual and real gluon emission, besides the non-trivial subtraction mechanism. For virtual gluon emissions, the bare unsubtracted collinear

contribution is:

$$\frac{\alpha_S}{4\pi} D^{\overline{(0)},[1];\,\text{unsub.}}_{q/q,\,\text{virtual}}(\varepsilon; z) = \frac{1}{z}\,\delta\left(P^+ - zP^+\right)\int \frac{d^D k}{(2\pi)^D}\frac{\text{Tr}_C}{N_C}\frac{\text{Tr}_D}{4}\left(\gamma^+ \left\langle\!\!\!\!\!\! \right\rangle\right) + h.c. =$$

$$= -\frac{\alpha_S}{4\pi}4C_F S_\varepsilon \mu^{2\varepsilon}\int_0^\infty dk_T^2\,\left(k_T^2\right)^{-1-\varepsilon}\delta(1-z)\int_0^1 d\alpha\,\frac{\alpha}{1-\alpha}. \tag{A.45}$$

As in Eq. (A.33) the label "$\overline{(0)}$" stands for bare functions of renormalized fields. To get the true bare quantity, function of bare fields (labeled by "(0)"), we have to subtract the 1-loop wave function renormalization factor:

$$\frac{\alpha_S}{4\pi}Z_2^{[1]}(\varepsilon) = -\frac{\alpha_S}{4\pi}C_F\frac{S_\varepsilon}{\varepsilon}. \tag{A.46}$$

Since in Eq. (A.45) there is a scaleless integral, the previous equation is zero in full dimensional regularization. However, there is also an *unregulated* rapidity divergence, which must be canceled in the subtraction mechanism. The subtraction term is given by the following soft-collinear contribution:

$$\frac{\alpha_S}{4\pi}S^{[1]}_{2\text{-h, virtual}}(\varepsilon) = \int\frac{d^D k}{(2\pi)^D}\frac{\text{Tr}_C}{N_C}\left(\left\langle\!\!\!\!\!\! \right\rangle\right) + h.c. =$$

$$= \frac{\alpha_S}{4\pi}4C_F S_\varepsilon \mu^{2\varepsilon}\int_0^\infty dk_T^2\,\left(k_T^2\right)^{-1-\varepsilon}\delta(1-z)\left[\frac{1}{2}\log\left(\frac{\zeta}{k_T^2}\right) - \int_0^1 d\alpha\,\frac{1}{1-\alpha}\right], \tag{A.47}$$

where ζ is the rapidity cut-off, fixed as in Eq. (1.23). Notice that this term also presents an unregulated rapidity divergence, that cancels exactly that in Eq. (A.45). Finally, the 1-loop subtracted bare virtual contribution to the quark-from-quark TMD FF is:

$$\frac{\alpha_S}{4\pi}D^{\overline{(0)},[1]}_{q/q,\,\text{virtual}}(\varepsilon; z) = \frac{\alpha_S}{4\pi}\left[D^{\overline{(0)},[1];\,\text{unsub.}}_{q/q,\,\text{virtual}}(\varepsilon; z) - \delta(1-z)S^{[1]}_{2\text{-h, virtual}}(\varepsilon)\right] =$$

$$= \frac{\alpha_S}{4\pi}4C_F S_\varepsilon \mu^{2\varepsilon}\int_0^\infty dk_T^2\,\left(k_T^2\right)^{-1-\varepsilon}\delta(1-z)\left[1 - \frac{1}{2}\log\left(\frac{\zeta}{k_T^2}\right)\right] = 0 =$$

$$= \frac{\alpha_S}{4\pi}\left[D^{[1]}_{q/q,\,\text{virtual}}(\varepsilon; z) - Z^{[1]}_{q/q,\,\text{TMD}}(\varepsilon)\delta(1-z)\right] = 0, \tag{A.48}$$

where $Z^{[1]}_{q/q,\,\text{TMD}}$ is related to the UV counterterm of $D^{\overline{(0)},[1]}_{q/q,\,\text{virtual}}$ as:

$$Z^{[1]}_{q/q,\,\text{TMD}} = \left[\text{UV c.t. of } D^{\overline{(0)},[1]}_{q/q,\,\text{virtual}} \right] - Z^{[1]}_2 \tag{A.49}$$

Then finally:

$$\frac{\alpha_S}{4\pi} D^{[1]}_{q/q,\,\text{virtual}}(\varepsilon; z) = \frac{\alpha_S}{4\pi} Z^{[1]}_{q/q,\,\text{TMD}}(\varepsilon, \zeta) \delta(1-z) = \frac{\alpha_S}{4\pi} 2 C_F S_\varepsilon \left\{ -\frac{1}{\varepsilon^2} + \frac{1}{\varepsilon} \left[\log\left(\frac{\zeta}{\mu^2}\right) - \frac{3}{2} \right] \right\}. \tag{A.50}$$

Notice that $D_{q/q,\,\text{virtual}}$ is also the virtual emission cotribution to the collinear quark-from-quark FF.

For real gluon emission, the bare unsubtracted collinear contribution is:

$$\frac{\alpha_S}{4\pi} D^{\overline{(0)},[1];\text{unsub.}}_{q/q,\,\text{real}}(\varepsilon; z, k_T) =$$

$$= \frac{1}{z} \int \frac{dk^+ dk^-}{(2\pi)^D} \frac{\text{Tr}_C}{N_C} \frac{\text{Tr}_D}{4} \gamma^+ \left(\left[\begin{array}{c} \end{array} + h.c. \right] + \begin{array}{c} \end{array} \right) =$$

$$= \frac{\alpha_S}{4\pi} 2 C_F S_\varepsilon \frac{\Gamma(1-\varepsilon)}{\pi^{1-\varepsilon}} \mu^{2\varepsilon} \frac{1}{k_T^2} \left(\frac{2}{z(1-z)} + (1-\varepsilon) \frac{1-z}{z^2} \right) \theta(1-z). \tag{A.51}$$

As for the virtual case, there is an unregulated rapidity divergence in $z = 1$. The subtraction mechanism solves the problem, as the soft-collinear contribution cancels exactly such divergence.

$$\frac{\alpha_S}{4\pi} S^{[1]}_{\text{2-h, real}}(\varepsilon, k_T) = \int \frac{dk^+ dk^-}{(2\pi)^D} \frac{\text{Tr}_C}{N_C} \left(\begin{array}{c} \end{array} \right) + h.c. =$$

$$= \frac{\alpha_S}{4\pi} 2 C_F S_\varepsilon \frac{\Gamma(1-\varepsilon)}{\pi^{1-\varepsilon}} \mu^{2\varepsilon} \frac{1}{k_T^2} \left(2 \int_0^1 d\alpha \frac{1}{1-\alpha} - \log\left(\frac{\zeta}{k_T^2}\right) \right). \tag{A.52}$$

Therefore, the bare subtracted quark-from-quark TMD FF in momentum space is:

$$\frac{\alpha_S}{4\pi} D^{\overline{(0)},[1]}_{q/q,\,\text{real}}(\varepsilon; z, k_T, \zeta) = \frac{\alpha_S}{4\pi} \left[D^{\overline{(0)},[1];\text{unsub.}}_{q/q,\,\text{real}}(\varepsilon; z, k_T) - \delta(1-z) S^{[1]}_{\text{2-h, real}}(\varepsilon, k_T) \right] =$$

$$= \frac{\alpha_S}{4\pi} 2 C_F S_\varepsilon \frac{\Gamma(1-\varepsilon)}{\pi^{1-\varepsilon}} \mu^{2\varepsilon} \frac{1}{k_T^2} \left(\frac{2}{z(1-z)_+} + \delta(1-z) \log\left(\frac{\zeta}{k_T^2}\right) + (1-\varepsilon) \frac{1-z}{z^2} \right). \tag{A.53}$$

From Eq. (A.33), the integration over transverse momentum gives zero in full dimensional regularization. Nevertheless, it gives the contribution of the real gluon emission to the bare colliner quark-from-quark FF:

$$
\frac{\alpha_S}{4\pi} d_{q/q,\mathrm{real}}^{\overline{(0)},[1]}(\varepsilon;z) = z^{2-2\varepsilon} \int d^{2-2\varepsilon}\vec{k}_T \frac{\alpha_S}{4\pi} D_{q/q,\mathrm{real}}^{\overline{(0)},[1]}(\varepsilon;z,k_T,\zeta) = 0 =
$$
$$
= \frac{\alpha_S}{4\pi} \left\{ d_{q/q,\mathrm{real}}^{[1]}(\varepsilon;z) - \left[\mathrm{UV\ c.t.\ of\ } d_{q/q,\mathrm{real}}^{\overline{(0)},[1]} \right] \right\}. \tag{A.54}
$$

This result, together with the virtual emission contribution of Eq. (A.50), gives the renormalized quark-from-quark collinear FF. Notice that we do not have to consider the quark self-energy contribution, as it has been already included into the virtual emission term. Therefore:

$$
\frac{\alpha_S}{4\pi} d_{q/q}^{[1]}(\varepsilon;z) = \left[\mathrm{UV\ c.t.\ of\ } d_{q/q,\mathrm{real}}^{\overline{(0)},[1]} \right] + D_{q/q,\mathrm{virtual}}^{[1]}(\varepsilon;z) =
$$
$$
= \frac{\alpha_S}{4\pi} Z_{q/q,\mathrm{coll}}^{[1]}(\varepsilon;z) = -\frac{\alpha_S}{4\pi} 2 C_F \frac{S_\varepsilon}{\varepsilon} \left(\frac{2}{(1-z)_+} - 1 - z + \frac{3}{2}\delta(1-z) \right) \tag{A.55}
$$

Notice that the virtual and the real contributions for the integrated subtraction term are exactly equal and opposite. Hence they cancel in the sum, Eq. (A.54). This explicit computation, shows that the subtraction mechanism is trivial for integrated TMDs, as the soft factor appearing in the factorization definition, Eq. (1.21), is unity.

The Fourier transform of Eq. (A.54) gives the bare quark-from-quark TMD FF in b_T-space. By using Eqs. (A.38) we have:

$$
\frac{\alpha_S}{4\pi} \widetilde{D}_{q/q,\mathrm{real}}^{\overline{(0)},[1]}(\varepsilon;z,b_T,\zeta) = \int d^{2-2\varepsilon}\vec{k}_T\, e^{i\vec{k}_T \cdot \vec{b}_T} \frac{\alpha_S}{4\pi} D_{q/q,\mathrm{real}}^{\overline{(0)},[1]}(\varepsilon;z,k_T,\zeta) =
$$
$$
= \frac{\alpha_S}{4\pi} S_\varepsilon \left(\frac{\mu}{Q} \right)^{2\varepsilon} \left(\frac{b}{c_1} \right)^{2\varepsilon} e^{-2\varepsilon\gamma_E} \Gamma(-\varepsilon)\Gamma(1-\varepsilon) \times
$$
$$
\times \left[\frac{2}{z(1.-z)_+} + (1-\varepsilon)\frac{1-z}{z^2} + \delta(1-z)\left(-H_{-1-\varepsilon} + 2\log\left(\frac{b}{c_1} \right) + \log\left(\frac{\zeta}{Q^2} \right) \right) \right] =
$$
$$
= \frac{\alpha_S}{4\pi} \left[-Z_{q/q,\mathrm{TMD}}^{[1]}(\varepsilon,\zeta)\delta(1-z) + \frac{1}{z^2} Z_{q/q,\mathrm{coll}}^{[1]}(\varepsilon;z) \right] +
$$
$$
+ \frac{\alpha_S}{4\pi} 2 C_F \left[\frac{1}{z^2} - \frac{1}{z} - 2\log\left(\frac{b_T\mu}{c_1} \right) \left(\frac{2}{(1-z)_+} + \frac{1}{z^2} + \frac{1}{z} \right) -
$$
$$
- 2\delta(1-z)\left(\log\left(\frac{b_T\mu}{c_1} \right) \log\left(\frac{\zeta}{\mu^2} \right) + \log^2\left(\frac{b_T\mu}{c_1} \right) \right) \right] \tag{A.56}
$$

The renormalized quark-from-quark TMD FF is obtained by summing the virtual emission contribution from Eq. (A.50). As for the case of integrated quantities, the wave function renormalization factor has already been included into the virtual term. Notice how the combination of real and virtual emission

leaves only the collinear pole of the TMD, associated with $Z_{q/q,\text{coll}}$:

$$\frac{\alpha_S}{4\pi}\,\widetilde{D}^{\overline{(0)},[1]}_{q/q,\text{real}}(\varepsilon;z,b_T,\zeta) = \frac{\alpha_S}{4\pi}\left[\widetilde{D}^{\overline{(0)},[1]}_{q/q,\text{real}}(\varepsilon;z,b_T,\zeta) + D^{[1]}_{q/q,\text{virtual}}(\varepsilon;z)\right] =$$

$$= \frac{\alpha_S}{4\pi}\frac{1}{z^2}Z^{[1]}_{q/q,\text{coll}}(\varepsilon;z) +$$

$$+ \frac{\alpha_S}{4\pi}2C_F\left[\frac{1}{z^2} - \frac{1}{z} - 2\log\left(\frac{b_T\,\mu}{c_1}\right)\left(\frac{2}{(1-z)_+} + \frac{1}{z^2} + \frac{1}{z}\right) - \right.$$

$$\left. - 2\delta(1-z)\left(\log\left(\frac{b_T\,\mu}{c_1}\right)\log\left(\frac{\zeta}{\mu^2}\right) + \log^2\left(\frac{b_T\,\mu}{c_1}\right)\right)\right] \tag{A.57}$$

Finally, the quark-from-quark Wilson coefficient can be obtained by inserting Eq. (A.57) and Eq. (A.54) into Eq. (A.43):

$$\frac{\alpha_S}{4\pi}\,\widetilde{\mathscr{C}}^{[1]}_{q/q}(z,b_T,\zeta) = \frac{\alpha_S}{4\pi}2C_F\left[\frac{1}{z^2} - \frac{1}{z} - 2\left(\log\left(\frac{b_T\,\mu}{c_1}\right) - \log z\right)\left(\frac{2}{(1-z)_+} + \frac{1}{z^2} + \frac{1}{z}\right) - \right.$$

$$\left. - 2\delta(1-z)\left(\log\left(\frac{b_T\,\mu}{c_1}\right)\log\left(\frac{\zeta}{\mu^2}\right) + \log^2\left(\frac{b_T\,\mu}{c_1}\right)\right)\right] \tag{A.58}$$

A.4 Unpolarized Fragmentation Functions at LL and NLL accuracy

The TMDs expressed as solution of RG and CS evolution equations, Eq. (1.26), have the same structure of resummed quantities and, indeed, they can be actually obtained through a resummation of the soft gluons emissions in 2-h class cross sections. In fact, they have a reference scale piece, encoded into the OPE, multiplying the exponential associated to the evolution-dependent part, encoded into the Sudakov factor. Therefore, they should be computed by properly counting the large logarithms in the exponent of the Sudakov factor. In the following, I will focus on the Unpolarized TMD FFs. With the help of Eqs. (A.16) (A.26) and (A.19), besides the explicit expressions for the NLO Wilson coefficients of Eqs. (A.44) and (A.58), we can easily build:

- The LL-accuracy by setting the Wilson coefficient to LO and the perturbative Sudakov factor at LL:

$$\widetilde{D}^{LL}_{1,f/h}(z,b_T;\mu,\zeta) = \frac{1}{z^2}d_{h/f}(z,\mu_b)\,\exp\left\{\log\left(\frac{\mu}{\mu_b}\right)g_1(x) + \frac{1}{4}\log\left(\frac{\zeta}{Q^2}\right)g_2^K(x)\right\} \times$$

$$\times M_{D_{1,f/h}}(z,b_T)\,\exp\left\{-\frac{1}{4}g_K(b_T)\log\left(z^2\frac{\zeta}{M_h^2}\right)\right\}. \tag{A.59}$$

- The NLL-accuracy, by setting the Wilson coefficient to NLO and the perturbative Sudakov factor at NLL:

$$
\widetilde{D}_{1,\,f/h}^{NLL}(z, b_T; \mu, \zeta) = \frac{1}{z^2} \Big(d_{h/f}(z, \mu_b) +
$$

$$
+ \frac{\alpha_S(\mu_b)}{4\pi} \int_z^1 \frac{d\rho}{\rho} \left\{ d_{h/f}(z/\rho, \mu_b) \left[\rho^2 \mathscr{C}_{q/q}^{[1]}(\rho) \right] + d_{h/g}(z/\rho, \mu_b) \left[\rho^2 \mathscr{C}_{g/q}^{[1]}(\rho) \right] \right\} \Big) \times
$$

$$
\times \exp \left\{ \log\left(\frac{\mu}{\mu_b}\right) g_1(x) + g_2(x) \frac{1}{4} \log\left(\frac{\zeta}{Q^2}\right) \left(g_2^K(x) + \frac{1}{\log\left(\frac{\mu}{\mu_b}\right)} g_3^K(x) \right) \right\} \times
$$

$$
\times M_{D_{1,\,f/h}}(z, b_T) \exp \left\{ -\frac{1}{4} g_K(b_T) \log\left(z^2 \frac{\zeta}{M_h^2} \right) \right\} \tag{A.60}
$$

Appendix B

Kinematics of $e^+e^- \rightarrow hX$

The initial state of the hadronic process is an e^+e^- pair, where the electron has momentum l_1 and the positron l_2. The two leptons annihilate in a virtual photon[1] with momentum q, associated to a total energy $Q = \sqrt{q^2}$ available in the c.m. . The observed hadron, of momentum P, belongs to a jet initiated by a parton produced in the e^+e^- annihilation of momentum k. The study of kinematics is strictly connected to the choice of the frame. Clearly, this is completely arbitrary since the cross section will be Lorentz invariant. Three main frames are useful in deriving the final form of the factorized cross section.

1. **Hadron frame**, labeled by (h). This is the frame where the outgoing hadron h has no transverse components and it moves very fast along the (positive) $Z_{(h)}$-direction:

$$\vec{P}_{T,(h)} = \vec{0}_T. \tag{B.1}$$

Furthermore, since h is strongly boosted in the plus direction its plus component is very large, of order $\sim Q$. As a consequence, its minus component has to be very small in order to satisfy the on-shell condition $P^2 = 2P_{(h)}^+ P_{(h)}^- = M_h^2$. Therefore, in this frame, the full four-momentum P can be written as:

$$P = \left(P_{(h)}^+, \frac{M^2}{2P_{(h)}^+}, \vec{0}_T \right) \sim Q\left(1, \frac{M^2}{Q^2}, 0 \right). \tag{B.2}$$

The fragmenting parton belongs by definition to the same collinear group of the outgoing hadron, hence it has a very large plus component, a low transverse momentum and an even lower minus component. It is almost on-shell, with a very low virtuality. Neglecting all the suppressed components, k and P become exactly collinear, i.e. $k \propto P$. This can be made explicit by setting:

$$k_{(h)}^+ = \frac{1}{z} P_{(h)}^+, \tag{B.3}$$

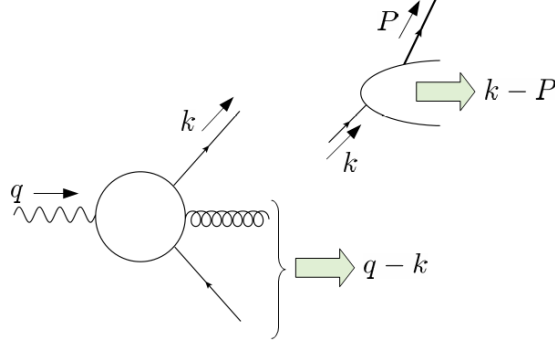[1]since the c.m. energy is around 10 GeV, heavy EW bosons are exluded.

139

Fig. B.1 Momentum flow that determines the kinematics boundaries on $\widehat{z}$.

Therefore $P \sim \widehat{z}\, k$, and

$$k = \left(\frac{P^+_{(h)}}{\widehat{z}}, k^-_{(h)}, \vec{k}_{T,(h)} \right) \sim Q \left(1, \frac{\lambda^2}{Q^2}, \frac{\lambda}{Q} \right), \tag{B.4}$$

where $\lambda \ll Q$ is the infrared scale introduced by power counting (see Appendix A). Since power counting rules are defined in the hadron frame, this is the most appropriate frame where to implement factorization. We can interpret $\widehat{z}$ as the collinear momentum fraction that the outgoing hadron takes off the fragmenting parton. Clearly $\widehat{z}$ has kinematics boundaries, due to the requirement that all the particles crossing the final state cut are physical, i.e. they have positive energy. With the help of Fig. B.1 and by applying the power counting rules, we obtain the following constraints:

- Positive energy for the final state of the jet

$$(k-P)^0_{(h)} \sim k^+_{(h)} - P^+_{(h)} = P^+_{(h)} \left(\frac{1}{\widehat{z}} - 1 \right) \geq 0, \tag{B.5}$$

which gives $\widehat{z} \leq 1$.

- Positive energy in the hard part of the process (given that $q^-_{(h)} > 0$)

$$(q-k)^0_{(h)} \geq 0 \rightarrow q^+_{(h)} - k^+_{(h)} = \frac{Q}{\sqrt{2}} \left(1 - \frac{P^+_{(h)}}{q^+} \frac{1}{\widehat{z}} \right) \geq 0. \tag{B.6}$$

The fractional energy z_h is defined as:

$$z_h = 2 \frac{P \cdot q}{q^2} = \frac{P^+_{(h)}}{q^+} = 2 \frac{E_{\text{c.m.}}}{Q} \tag{B.7}$$

where $E_{\text{c.m.}}$ is the energy of the detected hadron in the center of mass frame. Then Eq. (B.6) gives the kinematics boundary: $\widehat{z} \geq z_h$, with $z_h \leq 1$.
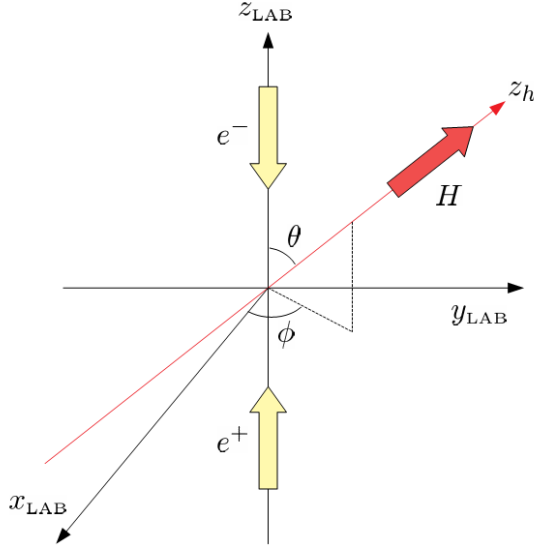
Fig. B.2 The LAB frame and the (h)-frame are both c.m. frames, but differ by a spatial rotation.

2. **c.m. frame**, labeled by (c.m.). In this frame the spatial momentum of q is zero

$$\vec{q}_{(\text{c.m.})} = \vec{0}. \tag{B.8}$$

Since rotations send null spatial vectors into null spatial vectors, the condition in Eq. (B.8) is defined modulo a rotation in space. Therefore, if we set the Z-axis of this frame to be the direction of the outgoing hadron, we can identify the hadron frame with the c.m. frame and apply power counting and the whole factorization procedure directly in this frame. This is a big advantage, since usually the calculation of the hard part of the cross section is much easier in the c.m. frame but in general it does not coincide with the hadron frame, which on the other hand makes simpler the application of the factorization procedure[2]. Hence, from now on, we will set c.m $\equiv (h)$.

Notice that the LAB frame, in which the Z-axis coincide with the beam axis, is a valid c.m. frame but it is not the hadron frame, as they differ by a spatial rotation, as shown in Fig. (B.2). The lepton pair is back-to-back in both the frames, but the direction of their spatial momenta is different.

---

[2]For example, this is the case of $e^+e^- \to h_A h_B X$, with the two hadrons almost back-to-back. In this case, the hadron frame is defined as the frame in which both hadrons have zero transverse momentum, i.e. where they are *exactly* back-to-back. However, a spatial rotation can fix only one hadron and the c.m. frame cannot be identified with the (h)-frame. The two frames are actually connected by a light boost in the transverse direction, where the boost parameter is (proportional to) $q_{T,(h)}$. As a consequence, we need boost-dependent projectors connecting the collinear and the hard parts of the cross section. In principle, we can use a boost also in the case of the production of a single hadron, however the boost will depend on $q_{T,(h)}$ which, in this case, is not observed.

3. **Parton frame**, labeled by (p). As explained in Ref. [7], in order to properly define a fragmentation function we need a frame in which the fragmenting parton has zero transverse momentum. This is the parton frame, defined by requiring

$$\vec{k}_{T,(p)} = \vec{0}_T. \tag{B.9}$$

In principle we have two Lorentz transformations available that we can use to reach the parton frame from the hadron frame: a rotation of the (small) angle between the fragmenting parton and the outgoing hadron and a (light) transverse boost in the $\vec{k}_{T,(h)}$ direction. By defining $\vec{k} = \vec{k}_{T,(h)}/k_{(h)}^+$, the angle of the rotation is $\alpha = -\sqrt{2}k$, while the parameter of the boost is $\vec{\beta} = \sqrt{2}\vec{k}$. The two choices give the same result:

$$k = \left(k_{(h)}^+, k_{(h)}^- - \frac{k_{T,(h)}^2}{2k_{(h)}^+}, \vec{0}_T \right)_p + \mathcal{O}\left(\frac{\lambda^2}{Q^2} \right) \left(1, \frac{\lambda^2}{Q^2}, 1 \right); \tag{B.10}$$

$$P = \left(\widehat{z}k_{(h)}^+, \frac{M^2 + \widehat{z}^2 k_{T,(h)}^2}{2\widehat{z}k_{(h)}^+}, -\widehat{z}\vec{k}_{T,(h)} \right)_p + \mathcal{O}\left(\frac{M^2, \lambda^2}{Q^2} \right) \left(1, \frac{M^2, \lambda^2}{Q^2}, 1 \right). \tag{B.11}$$

Notice that the plus components remain the same in the two frames (apart from power suppressed corrections). In this frame we can identify the $Z_{(p)}$-axis as the axis of the experimental jet of hadrons in which h is detected. In fact, all the (almost) collinear particles in the jet have been generated by the same fragmenting parton and hence the sum of their spatial momenta has to be equal to $\vec{k}_{(p)} = |\vec{k}|\widehat{Z}_{(p)}$, that lies on the (positive) Z direction in this frame.

Since, $P_{T,(p)}$ gives the transverse momentum of the outgoing hadron with respect the jet axis, its measurement probes the transverse motion of the partons inside the detected hadron. However, the determination of the jet axis is not easy. The direction of the fragmenting parton (positive $Z_{(p)}$-axis) coincides with the partonic thrust axis $\widehat{n}_{\text{part.}}$, which is the direction that maximizes the partonic thrust $\widehat{T}$ defined as

$$\widehat{T} = \frac{\sum_i |\vec{k}_{(\text{c.m.}),i} \cdot \widehat{n}_{\text{part.}}|}{\sum_i |\vec{k}_{(\text{c.m.}),i}|}, \tag{B.12}$$

where the sum runs over all the partons produced in the hard scattering, and $\vec{k}_{(\text{c.m.}),i} \equiv \vec{k}_{(h),i}$ is the spatial momentum of the i-th outgoing in the c.m. frame. For example, in the case of two (back-to-back) partons $\widehat{T} = 1$ and $\widehat{n}_{\text{part.}}$ is the axis of the parton pair, while for three partons $\widehat{T} = \max\{x_1, x_2, x_3\} \geq 2/3$, with $x_i = 2|\vec{k}_{(h),i}|/Q$, and $\widehat{n}_{\text{part.}}$ is the direction of the i-th parton. However, the partonic thrust axis cannot be accessed experimentally. The thrust axis provided by the measurement is the *hadronic* thrust axis $\widehat{n}_{\text{had.}}$, which is the direction that maximizes the hadronic thrust T defined as

$$T = \frac{\sum_i |\vec{P}_{(\text{c.m.}),i} \cdot \widehat{n}_{\text{had.}}|}{\sum_i |\vec{P}_{(\text{c.m.}),i}|}, \tag{B.13}$$

where now the sum runs over all the detected particles in the c.m. frame (e.g. the LAB frame). The variable T describes the topology of the final state and it ranges from 0.5 to 1, where the lower limit corresponds to a spherical distribution of final state particles, while the upper limit realizes a pencil-like event. Its value is close to its partonic counterpart, but they are not the same. As shown in Ref. [46], the observed distribution of hadronic thrust is related to the distribution with respect to the partonic thrust (which can be computed in perturbation theory) by a correlation function $C(T, \widehat{T})$ that is sharply peaked around $T \sim \widehat{T}$. Therefore, the direction which maximizes the hadronic thrust is approximately the same axis that maximizes the partonic thrust, i.e. $\widehat{n}_{\text{part.}} \sim \widehat{n}_{\text{had.}} \equiv \widehat{n}$. The estimate of how much they differ can be made more quantitative in the simple case of a 2-jet configuration. In fact, in this case we have $\widehat{T} = 1$ and $T \sim 1 - (M_1^2 + M_2^2)/Q^2$ (see Ref. [46], where $M_{1,2}$ is the invariant mass of the hadronic jets. Hence $\widehat{T} - T \sim \mathcal{O}(M^2/Q^2)$. This approximation is crucial for the interpretation of the transverse momentum measured in the BELLE experiment. In fact, the transverse momentum of the detected hadron with respect to the (hadronic) thrust axis can be really considered as the transverse momentum with respect to the jet axis, the direction of the fragmenting parton.
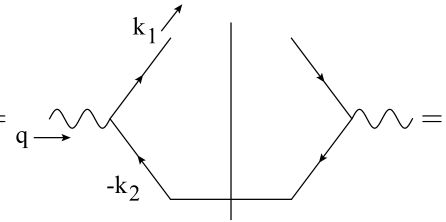
Appendix C

Virtual gluon emission up to NLO

In this section I will review the results for the contribution of the virtual vertex corrections in e^+e^- annihilations up to NLO. Such contributions enter as fundamental functions appearing in the factorization theorems. For instance, they are the vertex functions V and $V^\star$ in the factorization of the partonic tensor of $e^+e^- \to hX$ for a 2-jet configuration, as depicted in Fig. 2.2b.

At lowest order (LO) the virtual emission contribution coincides with the LO partonic tensor in the 2-jet topology case., as shown in Fig C.1. In fact, at LO the subtraction mechanism described in the Section 2.4.1 is trivial. From Eq. (2.33) we have:

$$\widehat{W}_j^{\mu\nu;\,[0]}(z, T) = \widetilde{\widehat{W}}_j^{\mu\nu;\,\text{uns.};\,[0]}(z, T). \tag{C.1}$$

Notice that at LO the total transverse momentum of the radiation collinear to the fragmenting quark is trivially zero, as there is no radiation at all. Therefore, in transverse momentum space the unsubtracted partonic tensor multiplies a $\delta(\vec{k}_T)$ which gives just 1 after the Fourier transform. This is the reason of the lack of any b_T dependence in the previous equation. Moreover, the LO is finite and hence also any ε-dependence has been removed. The r.h.s of the Eq. (C.1) is given by the lowest order Feynman diagrams for the topology considered. The squared matrix element, summed over all spins and colors of the fragmenting quark, is given by:

$$= e_f^2 \sum_{s_1, c} \bar{u}_{c,f}(k_1, s_1)\, \gamma^\mu \, \slashed{k}_2 \, \gamma^\nu \, u_{c,f}(k_1, s_1) = e_f^2 N_C \,\text{Tr}\{\slashed{k}_1 \, \gamma^\mu \, \slashed{k}_2 \, \gamma^\nu\}, \tag{C.2}$$
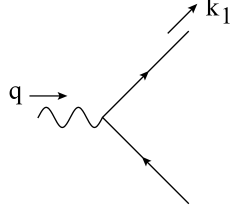
Fig. C.1 The lowest order Feynman graph contributing to the (unsubtracted) partonic tensor for a 2-jet topology.

The projections onto the relevant Lorentz structures, as in Eqs. (2.7), are:

$$-g_{\mu\nu}M_f^{\mu\nu;\,[0]} = 8\,e_f^2 N_C(1-\varepsilon)\,k_1\cdot k_2 = 4\,e_f^2 N_C(1-\varepsilon)Q^2; \tag{C.3}$$

$$\frac{k_{1,\mu}\,k_{1,\nu}}{Q^2}M_f^{\mu\,\nu\,[0]} = 0, \tag{C.4}$$

where we used momentum conservation $k_1 + k_2 = q$. Since the projection of Eq. (C.4) is zero, the final state tensor will be written as in Eq. (2.12) and the partonic cross section will only have the transverse projection. Moreover, the configuration described by Eq. (C.2) is an exact, pencil-like, final state. Therefore the dependence on the thrust is trivially $\delta(1-T)$. The phase space integral only involves k_2:

$$-g_{\mu\nu}\widehat{W}_f^{\mu\nu\,[0]}(\widehat{z},T) =$$
$$= \frac{1}{4\pi}\int\frac{d^D k_2}{(2\pi)^D}\left(-g_{\mu\nu}M_f^{\mu\,\nu\,[0]}\right)(2\pi)^D\,\delta^{(D)}\left(q-k_1-k_2\right)(2\pi)\,\delta\left(k_2^2\right)\theta(k_2^+)\,\theta(k_2^-)\,\delta(1-T) =$$
$$= 2\,e_f^2 N_C(1-\varepsilon)\,\delta\left(1-z\right)\delta\left(1-T\right) = 2\widehat{F}_{1,f}^{[0]}, \tag{C.5}$$

where the factor $1/(4\pi)$ is the normalization of the hadronic tensor fixed according to Eq. (2.5). Finally:

$$\widehat{W}_f^{\mu\,\nu\,[0]}(z,\tau) = H_T^{\mu\nu}\,\widehat{F}_{1,f}^{[0]}(z,\tau), \tag{C.6}$$

where the transverse tensor $H_T^{\mu\nu}$ has been defined in Eq. (2.13). The resulting partonic cross section follows from Eq. (2.10a) and is given by:

$$\frac{d\widehat{\sigma}_f^{[0]}}{dz\,dT} = \sigma_B z\widehat{F}_{1,f}^{[0]}(z,\tau) = \frac{4\pi\alpha^2}{3Q^2}\,e_f^2 N_C\,\delta\left(1-z\right)\delta\left(1-T\right) \tag{C.7}$$

where the Born cross section σ_B has been defined in Eq. (2.11). Hence the LO is in practice just a constant. Then, it is useful to define the following quantities:

$$H_{0,f} = e_f^2 2N_C (1 - \varepsilon); \tag{C.8a}$$

$$H_0 = \sum_f H_{0,f}, \tag{C.8b}$$

At Next-Lowest Order (NLO), the emitted gluon is virtual and the final state still hosts two particles: the outgoing quark, of flavor f and momentum k_1, and the antiquark crossing the final state cut, of momentum k_2. Momentum conservation sets $q = k_1 + k_2$. The 1-loop squared amplitude is given by:

$$M_{f,V}^{\mu\nu\,[1]}(\varepsilon; \mu, Q) = \quad \quad + h.c. =$$

$$= e_f^2 \int \frac{d^{4-2\varepsilon} l}{(2\pi)^{4-2\varepsilon}} \, \bar{u}(k_1) \left(-ig_0 \gamma^\alpha t^a\right) \frac{i(\not{k}_1 - \not{l})}{(k_1 - l)^2 + i0} \gamma^\mu \frac{i(-\not{k}_2 - \not{l})}{(k_2 + l)^2 + i0} \times$$

$$\times (-ig_0 \gamma^\beta t^b) \not{k}_2 \gamma^\nu u(k_1) \frac{-ig_{\alpha\beta}\delta_{ab}}{l^2 + i0} + h.c. =$$

$$= i e_f^2 g^2 \mu^{2\varepsilon} C_F N_C \int \frac{d^{4-2\varepsilon} l}{(2\pi)^{4-2\varepsilon}} \frac{\text{Tr}\left\{\not{k}_1 \gamma^\alpha (\not{k}_1 - \not{l}) \gamma^\mu (\not{k}_2 + \not{l}) \gamma_\alpha \not{k}_2 \gamma^\nu\right\}}{[(k_1 - l)^2 + i0] \, [(k_2 + l)^2 + i0] \, [l^2 + i0]} + h.c. \tag{C.9}$$

This expression can be properly simplified by decomposing the Dirac structure in its scalar, vector and tensor parts, by using momentum conservation and the Passarino-Veltman reduction formula [60]. This leads to:

$$M_{f,V}^{\mu\nu\,[1]}(\varepsilon; \mu, Q) = M_f^{\mu\nu\,[0]} V^{[1]}(\varepsilon; \mu, Q), \tag{C.10}$$

which simply asserts that the 1-loop squared matrix element for the virtual emission of a gluon is the lowest order $M_f^{[0]}$, computed in Eq. (C.2), "dressed" with the vertex factor V. As a consequence, the corresponding contribution to the final state tensor will be simply proportional to the lowest order, computed in Eq. (C.5). Hence:

$$W_{f,V}^{\mu\nu,[1]}(\varepsilon; z, \tau, \mu, Q) = H_T^{\mu\nu} \widehat{F}_{1,f}^{[0]}(z, \tau) V^{[1]}(\varepsilon; \mu, Q). \tag{C.11}$$

Virtual gluon emission up to NLO

The 1-loop vertex factor is given by:

$$\frac{\alpha_S}{4\pi} V^{[1]}(\varepsilon; \mu, Q) = ig^2 \mu^{2\varepsilon} C_F \left\{ -4(1-\varepsilon)^2 \frac{I_0^{(3)}}{2(1-\varepsilon)} + \right.$$

$$\left. + 2Q^2 \left[I_0 + \frac{2}{Q^2} I_0^{(3)} - (1-\varepsilon) \left(-\frac{1}{Q^2} \frac{I_0^{(3)}}{2(1-\varepsilon)} \right) \right] \right\} + h.c., \tag{C.12}$$

where I introduced the integrals I_0 and $I_0^{(3)}$ defined as:

$$I_0 = \int \frac{d^{4-2\varepsilon} l}{(2\pi)^{4-2\varepsilon}} \frac{1}{[(k_1-l)^2 + i0][(k_2+l)^2 + i0][l^2 + i0]} =$$

$$= \frac{i}{\varepsilon} \frac{\Gamma(1+\varepsilon)}{(4\pi)^{2-\varepsilon}} (-Q^2)^{-1-\varepsilon} B(-\varepsilon, 1-\varepsilon); \tag{C.13}$$

$$I_0^{(3)} = \int \frac{d^{4-2\varepsilon} l}{(2\pi)^{4-2\varepsilon}} \frac{1}{[(k_1-l)^2 + i0][(k_2+l)^2 + i0]} =$$

$$= i \frac{\Gamma(\varepsilon)}{(4\pi)^{2-\varepsilon}} (Q^2)^{-\varepsilon} B(1-\varepsilon, 1-\varepsilon). \tag{C.14}$$

Therefore:

$$\frac{\alpha_S}{4\pi} V^{[1]}(\varepsilon; \mu, Q) = -\frac{\alpha_S}{4\pi} C_F S_\varepsilon \left(\frac{\mu}{Q} \right)^{2\varepsilon} (-1)^{-\varepsilon} \frac{\Gamma(1-\varepsilon)^3 \Gamma(1+\varepsilon)}{\Gamma(1-2\varepsilon)} \times$$

$$\times \left(-\frac{2\Gamma(-\varepsilon)}{\varepsilon \Gamma(1-\varepsilon)} + \frac{(-1)^{-\varepsilon}(3+2\varepsilon)\Gamma(\varepsilon)}{(1-2\varepsilon)\Gamma(1+\varepsilon)} \right) + h.c. =$$

$$= -\frac{\alpha_S}{4\pi} 2 C_F S_\varepsilon \left[\frac{2}{\varepsilon^2} + \frac{2}{\varepsilon} \left(\frac{3}{2} + \log \frac{\mu^2}{Q^2} \right) + 8 - \pi^2 + 3\log \frac{\mu^2}{Q^2} + \left(\log \frac{\mu^2}{Q^2} \right)^2 \right] \tag{C.15}$$

Finally, the contribution of the virtual gluon emission up to NLO is given by:

$$W_{f,V}^{\mu\nu}(\varepsilon; z, \tau, \mu, Q) = H_T^{\mu\nu} e_f^2 N_C \delta(1-z) \delta(1-T) \left(1 + \frac{\alpha_S}{4\pi} V^{[1]}(\varepsilon; \mu, Q) \right). \tag{C.16}$$

Appendix D

Thrust and 2-jet topology

In e^+e^- annihilation, the 2-jet case is the most probable configuration, as any further jet is associated to an extra power of α_S at partonic level. Therefore, often it is useful to define the variable $\tau = 1 - T$ and study the behavior of the cross section in the small-τ limit, which corresponds to a 2-jet topology of the final state. In this case, the thrust axis $\vec{n}$ defines two opposite hemispheres: S_A, which points along the direction of the thrust axis, and S_B, which points backwards, along the direction $\vec{\bar{n}}$ opposite to $\vec{n}$. Then, from Eq. (B.13) the value of τ is well approximated by the sum of the invariant masses of the two jets produced in the final state (see Ref. [46, 47]):

$$\tau = \frac{M_A^2}{Q^2} + \frac{M_B^2}{Q^2}. \tag{D.1}$$

This relation is extremely important in perturbative calculations, since the invariant masses M_A and M_B can be computed explicitly at partonic level by considering the full momentum flowing into each hemisphere. Clearly, the r.h.s. of Eq. (D.1) is trivially zero only when all partons emitted into each hemisphere are virtual. All other cases require at least one real emission. Therefore, at 1-loop level the non-trivial configurations have three real particles in the final state. A 2-jet topology can be achieved either when one of them is soft or when two of them move collinearly.

Despite its importance, the study of thrust is not covered by Collins factorization formalism, as the soft and collinear factors defined in Sections 1.2 and 1.3 do not take it into account. However, thrust can be introduced in the formalism thanks to Eq. (D.1), which relates it to the total momentum flowing into soft and collinear contributions, with the further constraint of the hemisphere selection. Actually, this further information is relevant only for soft radiation, which can really be emitted in each hemisphere with the same probability. The collinear cases are simpler, as the property of being collinear already constrain the particles to be emitted only into one hemisphere. Moreover, thrust acts *naturally* as a rapidity cut-off and rapidity divergences are regulated by the topology of the final state instead that by tilting the soft Wilson lines, see Appendix A. Therefore, usually rapidity cut-offs are not included into a standard presentation of the thrust-dependent functions. The implementation

of the thrust-dependency into the "full" Collins factorization formalism, i.e. keeping all the rapidity cut-offs, is investigated in Chapter 3. Notice that, again, this issue is relevant only for soft factors, as the collinear contributions are already defined without rapidity cut-offs in the Collins factorization formalism. In this section I will follow the standard methods by removing any track of the rapidity regulators from the kinematics approximators T_R reviewed in Appendix A, leaving to the thrust the task to regulate the rapidity divergences. I will add a label "∘" to the approximators defined without the rapidity cut-offs. Since only the approximators of soft momentum regions are affected by this modification, at 1-loop we have trivially $^\circ T_A \equiv T_A$ and $^\circ T_B \equiv T_B$.

In the following I will use the same conventions used through this thesis, labeling with k_1, k_2 and k_3 the momenta of the quark, the antiquark and the gluon. The quark is assumed to generate the collinear factor in the S_A-hemisphere, while the antiquark generates the collinear factor in the opposite direction. All the TMD effects are not considered in this section. Therefore, all the quantities are integrated over $\vec{k}_T$, the total transverse momentum entering into the relevant collinear subgraph.

D.1   Soft Thrust Function

The 1-loop soft thrust function $S(\varepsilon, \tau)$ is obtained as a result of the application of the soft approximator $^\circ T_S$, i.e. by eikonal-approximating the propagators of the quark and the antiquark along the plus- and the minus-direction respectively. The soft approximation applied to the r.h.s of Eq. (D.1) gives:

$$k_1^{(S)} = \left(q^+, 0, \vec{0}_T \right), \tag{D.2}$$

$$k_2^{(S)} = \left(0, q^-, \vec{0}_T \right), \tag{D.3}$$

$$k_3^{(S)} = \left(l^+, l^-, \vec{l}_T \right), \tag{D.4}$$

where $q^+ = q^- = Q/\sqrt{2}$. Notice that the soft approximation leaves k_3 unchanged in its functional form, but the size of all its components are now of order λ^2/Q, where λ is a very low energy scale according to power counting. Depending on the hemisphere in which the soft gluon has been emitted, we have two different, equally probable, configurations:

$$\tau = y_2^{(S)} = \frac{l^-}{q^-}, \text{ if } S_A \text{ emission, i.e. } l^+ > l^-; \tag{D.5a}$$

$$\tau = y_1^{(S)} = \frac{l^+}{q^+}, \text{ if } S_B \text{ emission, i.e. } l^- > l^+. \tag{D.5b}$$

Therefore, by defining the usual light-like directions $w_1 = (1, 0, \vec{0}_T)$ and $w_2 = (0, 1, \vec{0}_T)$, the 1-loop soft thrust function is obtained as:

$$\frac{\alpha_S}{4\pi} S^{[1]}(\varepsilon, \tau) = \int \frac{d^D l}{(2\pi)^D} \frac{\mathrm{Tr}_C}{N_C} \left(\begin{array}{c} {}_{1\bullet w_1} \\ {}^l \\ {}_{1\bullet w_2} \end{array} + h.c. \right) (2\pi)\delta_+\left(l^2\right) \times$$

$$\times \left[\delta\left(\tau - \frac{l^-}{q^-}\right)\theta\left(l^+ - l^-\right) + \delta\left(\tau - \frac{l^+}{q^+}\right)\theta\left(l^- - l^+\right) \right] =$$

$$= \frac{\alpha_S}{4\pi} 8 C_F S_\varepsilon \left(\frac{\mu}{Q}\right)^{2\varepsilon} \tau^{-1-2\varepsilon} \frac{1}{\varepsilon}. \tag{D.6}$$

Notice that all the divergences of $S(\varepsilon, \tau)$ are regulated by dimensional regularization, and we did not encounter any unregulated rapidity divergence. As anticipated, this is due to the explicit presence of τ, that acts as a regulator. In fact, the expression in Eq. (D.6) is divergent if either ε or τ vanish. The ε-expansion of Eq. (D.6) follows from its integrability property. In fact, $S^{[1]}(\varepsilon, \tau)$ is integrable with respect to τ, but its trivial expansion in powers of ε does not. This problem is solved by considering an expansion in terms of τ *distributions* instead of functions. Then, one can easily prove that:

$$\tau^{-1-\varepsilon} = -\frac{1}{\varepsilon}\delta(\tau) + \left(\frac{1}{\tau}\right)_+ - \varepsilon\left(\frac{\log \tau}{\tau}\right)_+ + \mathcal{O}\left(\varepsilon^2\right), \quad \mathrm{Re}\,\varepsilon < 0, \tag{D.7}$$

which is a easy application of the trick of Eq. (3.8).

D.2   Jet Thrust Function (backward emission)

The 1-loop jet thrust function $J(\varepsilon, \tau)$ is obtained by applying the collinear approximator either T_A or T_B, i.e. eikonal-approximating the propagator of the parton that goes into the opposite (light-like) direction. The jet thrust function is integrated over the associated collinear momentum fraction. In the factorization of $e^+ e^- \to hX$ this is realized by the contribution of the radiation emitted backward with respect to the detected hadron. Therefore, in the following I will consider the gluon collinear to the antiquark, which is directed into the S_B-hemisphere. The case of a gluon collinear to the quark is totally analogous. The T_B approximator applied to the momenta gives:

$$k_1^{(B)} = \left(q^+, 0, \vec{0}_T\right), \tag{D.8}$$

$$k_2^{(B)} = \left(\frac{l_T^2}{2(q^- - l^-)}, q^- - l^-, -\vec{l}_T\right), \tag{D.9}$$

$$k_3^{(B)} = \left(\frac{l_T^2}{2l^-}, l^-, \vec{l}_T\right), \tag{D.10}$$

As in the previous case, the backward approximation leaves k_3 unchanged in its functional form, but resizes its components as $l^+ \sim \lambda^2/Q$, $l^- \sim Q$ and $l_T \sim \lambda$, where λ is a very low energy scale according to power counting. The emission of the collinear gluon into the S_A-hemisphere is suppressed by the action of T_B, therefore we only have to consider the emission in the S_B-hemisphere:

$$\tau = y_1^{(B)} = \frac{l_T^2}{Q^2} \frac{q^-}{l^-} \frac{1}{1 - \frac{l^-}{q^-}}, \text{ if } S_B \text{ emission, i.e. } l^- > l^+. \tag{D.11}$$

By defining $k = k_2^{(B)} + k_3^{(B)}$ as the total momentum entering into the antiquark hemisphere, the 1-loop jet thrust function is:

$$\frac{\alpha_S}{4\pi} J^{[1]}(\varepsilon, \tau) = 2 (2\pi)^{D-1} \int \frac{dk^+ d^{D-2}\vec{k}_T}{(2\pi)^D} \int \frac{d^D k_2}{(2\pi)^D} \times$$

$$\times \frac{\mathrm{Tr}_C}{N_C} \frac{\mathrm{Tr}_D}{4} \gamma^- \left[\left(\begin{array}{c} \text{(k-k}_2\text{)}\cdot w_1 \\ k \nearrow \; {}_{-k} \\ k - k_2 \\ -k_2 \end{array} + h.c. \right) + k \nearrow \; \begin{array}{c} {}_{-k} \; k - k_2 \; {}_{-k} \\ -k_2 \end{array} \right] \times$$

$$\times (2\pi)\delta_+ \left(k_2^2 \right) (2\pi)\delta_+ \left((k - k_2)^2 \right) \delta^{(D-2)}(\vec{k}_T) \delta \left(\tau - \frac{k^+}{q^+} \right) \theta \left(k^- - k_2^- \right) =$$

$$= \frac{\alpha_S}{4\pi} 4 C_F S_\varepsilon \left(\frac{\mu}{Q} \right)^{2\varepsilon} \tau^{-1-\varepsilon} \left[B(2 - \varepsilon, -\varepsilon) + \frac{1-\varepsilon}{2} B(1 - \varepsilon, 2 - \varepsilon) \right]. \tag{D.12}$$

Notice that in $J(\varepsilon, \tau)$ the thrust acts as a regulator for the rapidity divergences, as in Eq. (D.6). As a consequence, there is no overlapping with the soft momentum region and, contrary to the Collins factorization scheme, no subtraction is required.

D.3 Fragmenting Jet Function

The fragmenting jet function (FJF) $J_{j/h}$ describes the fragmentation of the parton j to the hadron h and, iin addition to the light-cone momentum fraction, the invariant mass of the jet is measured [61]. In the following, I will review the 1-loop computation of their partonic version, focusing on the gluon-from-quark and quark-from-quark case. Also, I assume that the gluon is emitted collinearly to the quark, i.e. into the S_A-hemisphere. Therefore, such functions are obtained through the action of the approximator T_A. From Eq. (D.1), the invariant mass of the the the jet is $M_A^2 = \tau Q^2$ and hence the

thrust-dependence will replace the dependence on M_A. The action of T_A gives the momenta:

$$k_1^{(A)} = \left(zq^+, 0, \vec{0}_T \right),$$ (D.13)

$$k_2^{(A)} = \left(0, q^-, \vec{0}_T \right),$$ (D.14)

$$k_3^{(A)} = \left((1-z)q^+, \frac{l_T^2}{2(1-z)q^+}, \vec{l}_T \right),$$ (D.15)

where z represents the fractional energy associated to the partonic process:

$$z = \frac{2k_1 \cdot q}{q^2} = \frac{k_1^+}{q^+}.$$ (D.16)

The emission of the collinear gluon into the S_B-hemisphere is suppressed by the action of T_A, hence the only relevant configuration is given by:

$$\tau = y_2^{(A)} = \frac{z}{1-z} \frac{l_T^2}{Q^2}, \text{ if } S_A \text{ emission, i.e. } l^+ > l^-.$$ (D.17)

In the following, $k = k_1^{(A)} + k_3^{(A)}$ identifies the total momentum entering the considered S_A-hemisphere.

D.3.1 Gluon-from-quark

The 1-loop gluon-from-quark fragmentation jet function is given by:

$$\frac{\alpha_S}{4\pi} J_{g/q}^{[1]}(\varepsilon; \tau, z) = \int \frac{dk^-}{(2\pi)^D} d^{2-2\varepsilon}\vec{k}_T \frac{\mathrm{Tr}_C}{N_C} \frac{\mathrm{Tr}_D}{4} \gamma^+ \left(\includegraphics \right) \times$$

$$\times (2\pi) \delta\left((k-k_1)^2 \right) \delta\left(\tau - \frac{z}{1-z} \frac{k_T^2}{Q^2} \right) \theta(1-z) =$$

$$= \frac{\alpha_S}{4\pi} 2 C_F S_\varepsilon \left(\frac{\mu}{Q} \right)^{2\varepsilon} \theta(1-z) \left(\frac{z}{1-z} \right)^\varepsilon \frac{1+(1-z)^2 - \varepsilon z^2}{z^2} \tau^{-1-\varepsilon}.$$ (D.18)

D.3.2 Quark-from-quark

The case of a fragmenting fermion involves more Feynman graphs. The 1-loop quark-from-quark fragmentation jet function is given by:

$$
\frac{\alpha_S}{4\pi} J^{[1]}_{q/q}(\varepsilon; \tau, z) = \int \frac{dk^-}{(2\pi)^D} d^{2-2\varepsilon}\vec{k}_T \times
$$

$$
\times \frac{\mathrm{Tr}_C}{N_C} \frac{\mathrm{Tr}_D}{4} \gamma^+ \left[\left(\vphantom{\Big|} \qquad \qquad \right)_{(k-k_1)\cdot w_2} + h.c. \right] + \left(\vphantom{\Big|} \qquad \qquad \right) \Bigg] \times
$$

$$
\times \theta(1-z)\, \delta\left(\tau - \frac{z}{1-z} \frac{k_T^2}{Q^2} \right) =
$$

$$
= \frac{\alpha_S}{4\pi} 4 C_F\, S_\varepsilon \left(\frac{\mu}{Q} \right)^{2\varepsilon} \theta(1-z)\, z^\varepsilon \left[(1-z)^{-1-\varepsilon} + \frac{1-\varepsilon}{2} \frac{(1-z)^{1-\varepsilon}}{z} \right] \tau^{-1-\varepsilon}. \tag{D.19}
$$

Appendix E

Solution of Integrals through Mellin transforms

In this section, I present the solution of the non-trivial integral appearing in the Fourier transform of the soft thrust factor in Section 3.5. The Mellin transform trick is taken from Ref. [62].

Consider the integral of Eq. (3.46). Its solution can be obtained by exploiting the convolution property of the Mellin transforms:

$$\int_0^\infty dy\, h(y)\, g(ay) = \int_{\delta-i\infty}^{\delta+i\infty} \frac{du}{2\pi i} a^{-u} \widehat{h}(1-u)\widehat{g}(u) \tag{E.1}$$

where $\widehat{f}$ denotes the Mellin transform of the function f. The off-set δ in Eq. (E.1) is a real number that lies in the intersection of the convergence region of $\widehat{h}$ and $\widehat{g}$.

This property can be applied to $I_\varepsilon a, r$ if we first change variable $x \mapsto y^{-2}$. Then:

$$I_\varepsilon(a, r) = 2 \int_0^\infty dy\, \underbrace{\frac{y^{-1-\varepsilon}}{1 - ry^2}\theta(1-y)}_{h_{\varepsilon,r}(y)} \underbrace{J_{-\varepsilon}(ay)}_{g_\varepsilon(ay)} \tag{E.2}$$

The Mellin transforms are:

$$\widehat{h}_{\varepsilon,r}(u) = -\frac{1}{r}\frac{1}{3+\varepsilon-u}{}_2F_1\left(1, \frac{3+\varepsilon-u}{2}; \frac{5+\varepsilon-u}{2}; \frac{1}{r}\right), \quad \text{for } \mathrm{Re}(u) < 3 + \mathrm{Re}(\varepsilon); \tag{E.3}$$

$$\widehat{g}_\varepsilon(u) = 2^{-1+u}\frac{\Gamma\left(-\frac{\varepsilon}{2}+\frac{u}{2}\right)}{\Gamma\left(1-\frac{\varepsilon}{2}-\frac{u}{2}\right)}, \quad \text{for } \mathrm{Re}(\varepsilon) < \mathrm{Re}(u) < \frac{3}{2}. \tag{E.4}$$
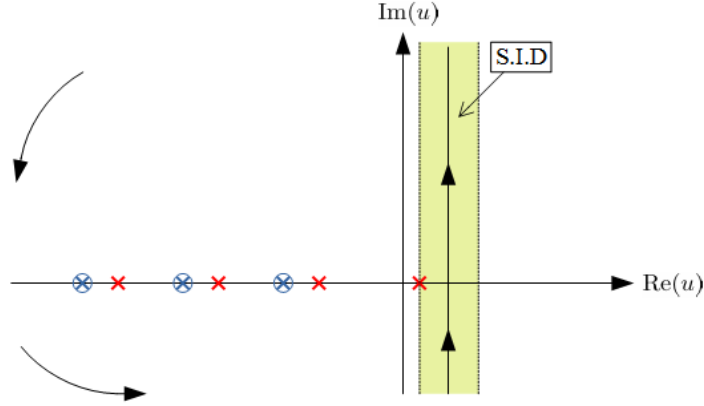
Fig. E.1 Graphical representation of the Mellin conjugate space. The integrand function in Eq. (E.8) has two sets of poles in $u = -2k + \varepsilon$, for $k \geq 0$ and in $u = -2k - \varepsilon$, for $k \geq 1$. The first set is due associated with the Gamma function $\Gamma\left(-\frac{\varepsilon}{2} + \frac{u}{2}\right)$, the second to the hypergeometric function. The green strip between ε and $3/2$ is the "strip of initial definition" (SID) and coincides with the intersection of the convergence regions of the two functions g_ε and $h_{\varepsilon,r}$. The integration path must lie into the SID. Finally, since the hypergeometric function produces an essential singularity in $u \to +\infty$, we must close the contour to the left.

Therefore, we can choose $\mathrm{Re}(\varepsilon) < \delta < 3/2$. Finally:

$$
\begin{aligned}
I_\varepsilon(a, r) &= \\
&= -\frac{1}{r} \int_{\delta - i\infty}^{\delta + i\infty} \frac{du}{2\pi i} \left(\frac{a}{2}\right)^{-u} \frac{\Gamma\left(-\frac{\varepsilon}{2} + \frac{u}{2}\right)}{\Gamma\left(1 - \frac{\varepsilon}{2} - \frac{u}{2}\right)} \frac{1}{2 + \varepsilon + u} {}_2F_1\left(1, 1 + \frac{\varepsilon}{2} + \frac{u}{2}; 2 + \frac{\varepsilon}{2} + \frac{u}{2}; \frac{1}{r}\right) = \\
&= S_1(\varepsilon, a, r) + S_2(\varepsilon, a, r)
\end{aligned}
\tag{E.5}
$$

where we have defined the two series:

$$
S_1(\varepsilon, a, r) = -\frac{1}{r} \sum_{k=0}^{\infty} \underset{u=-2k+\varepsilon}{\mathrm{Res}} f_\varepsilon(u, r),
\tag{E.6}
$$

$$
S_2(\varepsilon, a, r) = -\frac{1}{r} \sum_{k=1}^{\infty} \underset{u=-2k-\varepsilon}{\mathrm{Res}} f_\varepsilon(u, r)
\tag{E.7}
$$

with:

$$
f_\varepsilon(u, r) = \left(\frac{a}{2}\right)^{-u} \frac{\Gamma\left(-\frac{\varepsilon}{2} + \frac{u}{2}\right)}{\Gamma\left(1 - \frac{\varepsilon}{2} - \frac{u}{2}\right)} \frac{1}{2 + \varepsilon + u} {}_2F_1\left(1, 1 + \frac{\varepsilon}{2} + \frac{u}{2}; 2 + \frac{\varepsilon}{2} + \frac{u}{2}; \frac{1}{r}\right).
\tag{E.8}
$$

Consider first S_1. We have:

$$
S_1(\varepsilon, a, r) = -\left(\frac{a}{2}\right)^{-\varepsilon} r^\varepsilon \sum_{k=0}^{\infty} \frac{(-1)^k}{k!} \left(\frac{a}{2}\right)^{2k} r^{-k} \frac{1}{\Gamma(1 + k - \varepsilon)} B_{1/r}(1 + \varepsilon - k, 0)
\tag{E.9}
$$

156

If $r = r_1 \equiv e^{-2y_1}$, as in the first term of Eq. (3.45), we are interested in the limit $r_1 \to 0$. Since:

$$
\begin{aligned}
B_{1/r_1}(1+\varepsilon-k,0) = \\
= -(-1)^{-\varepsilon+k}\frac{\Gamma(2+\varepsilon-k)\Gamma(-\varepsilon+k)}{1+\varepsilon-k} - r_1^{-1-\varepsilon+k}\left(\frac{\Gamma(\varepsilon-k)\Gamma(2+\varepsilon-k)}{(1+\varepsilon-k)\Gamma(1+\varepsilon-k)^2}r + \mathcal{O}\left(r_1^2\right)\right),
\end{aligned}
\tag{E.10}
$$

we have:

$$
\begin{aligned}
S_1(\varepsilon,a,r_1) = -(-1)^{-\varepsilon}\frac{\pi}{\sin(\varepsilon\pi)}r_1^{\varepsilon/2}J_{-\varepsilon}\left(\frac{a}{\sqrt{r_1}}\right) - \\
- \left(\frac{a}{2}\right)^{-\varepsilon}\frac{1}{\varepsilon^2\Gamma(-\varepsilon)}{}_1F_2\left(-\varepsilon;1-\varepsilon,1-\varepsilon;-\frac{a^2}{4}\right) + \mathcal{O}\left(r_1^2\right)
\end{aligned}
\tag{E.11}
$$

On the other hand, if $r = 1/r_2 \equiv e^{-2y_2}$, as in the second term of Eq. (3.45) we are interested in the limit $r_2 \to 0$. Since:

$$
B_{r_2}(1+\varepsilon-k,0) = r_2^{1+\varepsilon-k}\left(\frac{1}{1+\varepsilon-k} + \mathcal{O}\left(r_2\right)\right),
\tag{E.12}
$$

Therefore:

$$
\begin{aligned}
S_1\left(\varepsilon,a,\frac{1}{r_2}\right) = \\
= -\left(\frac{a}{2}\right)^{-\varepsilon}\frac{1}{(1+\varepsilon)\Gamma(1-\varepsilon)}{}_1F_2\left(-1-\varepsilon;1-\varepsilon,-\varepsilon;-\frac{a^2}{4}\right)r_2 + \mathcal{O}\left(r_2^2\right) = \mathcal{O}\left(r_2\right).
\end{aligned}
\tag{E.13}
$$

Consider now S_2. We have:

$$
\begin{aligned}
S_2(\varepsilon,a,r) = -\frac{a}{4r}\left(\frac{a}{2}\right)^{\varepsilon}\Gamma(-1-\varepsilon) - \left(\frac{a}{2}\right)^{\varepsilon}\sum_{k=2}^{\infty}\frac{1}{k!}\left(\frac{a}{2}\right)^{2k}r^{-k}\Gamma(-\varepsilon-k) = \\
= \left(\frac{a}{2}\right)^{\varepsilon}\Gamma(-\varepsilon) + \frac{\pi}{\sin(\varepsilon\pi)}r^{\varepsilon/2}J_{\varepsilon}\left(\frac{a}{\sqrt{r}}\right).
\end{aligned}
\tag{E.14}
$$

If $r = r_1$, we cannot expand anymore the previous result around $r_1 \sim 0$. However, if $r = 1/r_2$, then $S_2(\varepsilon,a,1/r_2) = \mathcal{O}(r_2)$ and it can be neglected. Notice that all the contributions involving y_2 are suppressed. Hence, only y_1, the leading rapidity cut-off in the S_A-hemisphere, will survive in the final result. In fact, using Eqs. (E.11) (E.14), we have:

$$
\begin{aligned}
I_{\varepsilon}(a,r_1) = \frac{\pi}{\sin(\varepsilon\pi)}r_1^{\varepsilon/2}\left[J_{\varepsilon}\left(\frac{a}{\sqrt{r_1}}\right) - (-1)^{-\varepsilon}J_{-\varepsilon}\left(\frac{a}{\sqrt{r_1}}\right)\right] + \left(\frac{a}{2}\right)^{\varepsilon}\Gamma(-\varepsilon) - \\
- \left(\frac{a}{2}\right)^{-\varepsilon}\frac{1}{\varepsilon^2\Gamma(-\varepsilon)}{}_1F_2\left(-\varepsilon;1-\varepsilon,1-\varepsilon;-\frac{a^2}{4}\right) + \mathcal{O}(r_1)
\end{aligned}
\tag{E.15}
$$

where the combination of the Bessel-J functions can be rearranged as:

$$\frac{\pi}{\sin(\varepsilon\pi)} r_1^{\varepsilon/2} \left[J_\varepsilon\left(\frac{a}{\sqrt{r_1}}\right) - (-1)^{-\varepsilon} J_{-\varepsilon}\left(\frac{a}{\sqrt{r_1}}\right) \right] = -2(-r_1)^{\varepsilon/2} K_{-\varepsilon}\left(\frac{a}{\sqrt{-r_1}}\right). \tag{E.16}$$

The other integral instead is suppressed as $r_2 \to 0$:

$$I_\varepsilon\left(a, \frac{1}{r_2}\right) = \mathcal{O}(r_2). \tag{E.17}$$

The solution of the integral of Eq. (3.56) can be obtained through the same procedure used to solve the integration in Eq. (3.46). The result is:

$$\int_0^\infty \frac{x^{\varepsilon/2}}{x - r_1} J_{-\varepsilon}\left(\frac{a}{\sqrt{x}}\right) = -2(-r_1)^{\varepsilon/2} K_{-\varepsilon}\left(\frac{a}{\sqrt{-r_1}}\right) + \left(\frac{a}{2}\right)^\varepsilon \Gamma(-\varepsilon), \tag{E.18}$$

Notice that, differently from Eqs. (E.15) and (E.17), this is an exact result.

Appendix F

Color-coded representation of the kinematic regions

In this Appendix I will present the same plots shown in Figs. 3.14 and 3.16, but from a different perspective. Each panel corresponding to the set of criteria proposed in Ref. [17], see Eq. (3.106), will be directly compared to the analogue panel obtained by applying the more refined algorithm proposed in this thesis, shown in Fig. 3.15. As the size of these figures is augmented, all labels should result more visible and easier to read. In the following plots, BELLE data [8] are presented according to the color-coding associated to the three kinematic regions of $e^+e^- \to hX$. Red bins correspond to Region 1, orange bins to Region 2 and green bins to Region 3. Clearly, only thrust values corresponding to 2-jet topologies are considered, namely all bins with $0.75 \le T \le 1.0$. As far as z_h is concerned, all available bins are included. The shaded areas correspond to bins for which the value of P_T falls outside of the TMD-regime. The cut-off in P_T of Eq. (3.107) is represented by a vertical blue line in each panel. In the implementation of this cut, the symbol $\ll$ "much smaller than" is rendered as "less than 25%". Instead, for the algorithm of Fig. 3.15, the symbol $\ll$ "much smaller than" is evaluated as "less than 30%".

Some general features of the two different set of criteria for the data selections become evident from the direct comparison. First of all, the criteria of Ref. [17] suggest a strong dominance of Region 1. Instead, with the more refined algorithm presented in this thesis, most of the BELLE data turn out to belong to Region 2, as expected, while only the lower z_h bins correspond to Region 1. This fits perfectly with the physical expection that in Region 1 it is much easier for soft radiation to transversely deflect a low-energetic hadron than in Region 2. On the other hand, the distribution of the green bins, associated to Region 3, seem not to be affected by the two different kinds of data selection. In both cases, Region 3 starts becoming relevant for TMD studies only at very large values of thrust. In fact, green bins appear on the left of the cut in P_T only in the very last bin, for $T = 0.975$. This fits perfectly with the physical epectation that in Region 3 a hadron detected near the jet boundary can hardly be associated to the "pure" TMD-regime, unless the jet is extremely narrow, i.e. at very large values of thrust.
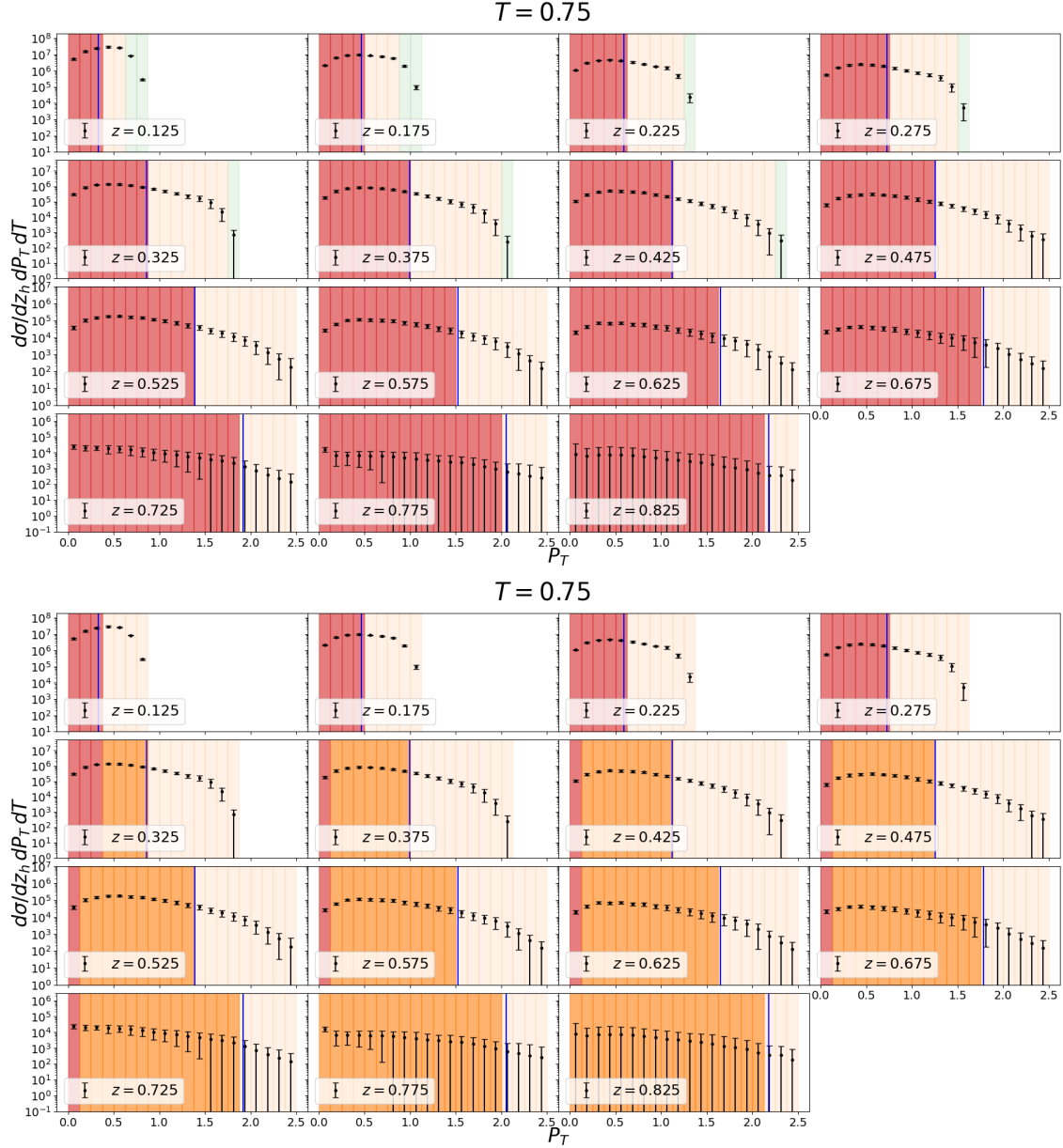
159

Fig. F.1 BELLE data for thrust $T = 0.750$ selected according to the criteria of Eq. (3.106) (upper panel) and to the algorithm of Fig. 3.15 (lower panel). Here Region 3 (green bins) is not realized. The criteria of Ref. [17] suggest a total dominance of Region 1. Instead, with the more refined algorithm presented in this thesis, we find that only the lower z_h bins correspond to Region 1, while most of the BELLE data belong to Region 2.
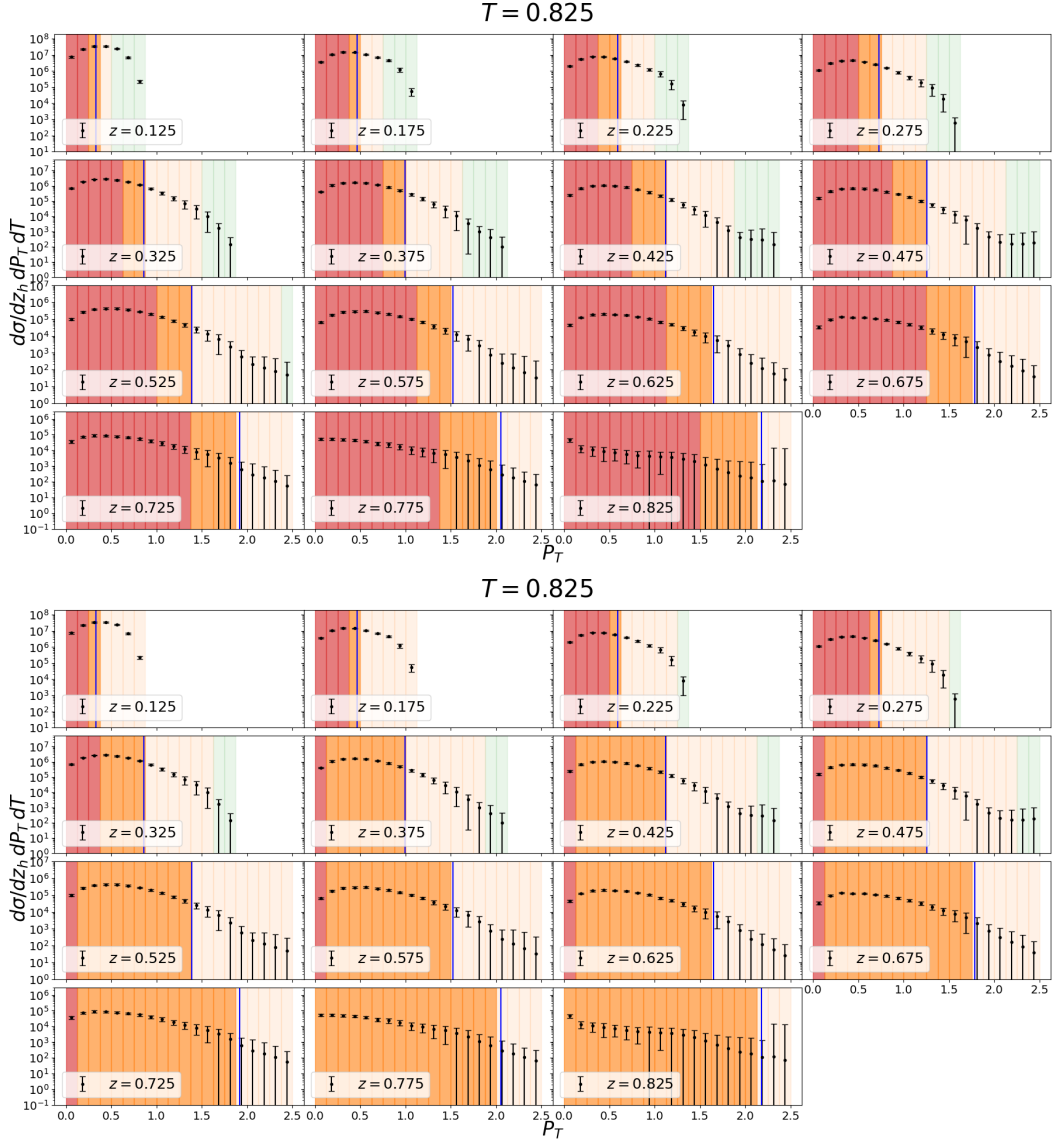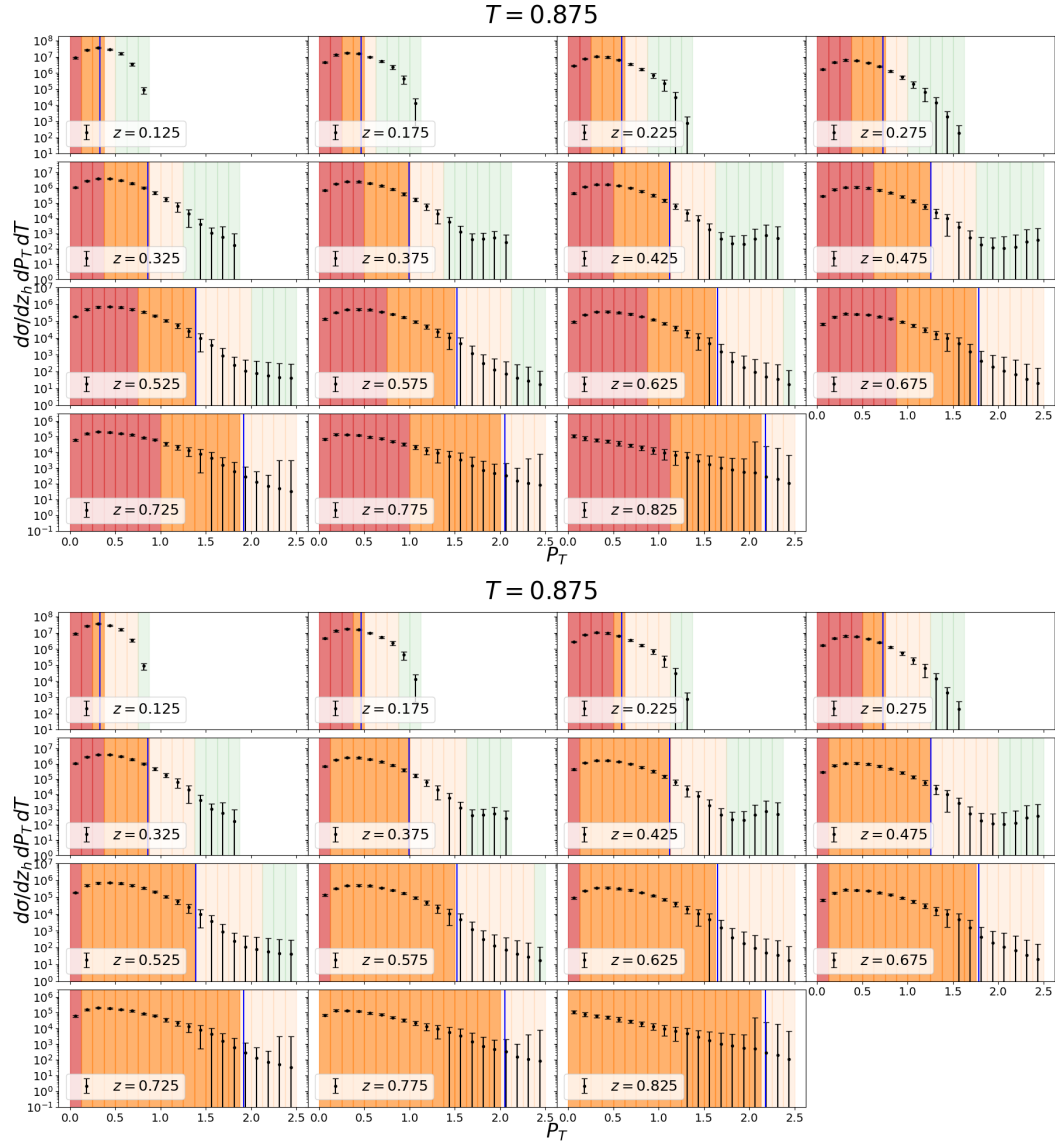
Fig. F.2 BELLE data for thrust $T = 0.825$ selected according to the criteria of Eq. (3.106) (upper panel) and to the algorithm of Fig. 3.15 (lower panel). Here Region 3 (green bins) is not realized. The criteria of Ref. [17] suggest a total dominance of Region 1. Instead, with the more refined algorithm presented in this thesis, we find that only the lower z_h bins correspond to Region 1, while most of the BELLE data belong to Region 2.

Fig. F.3 BELLE data for thrust $T = 0.875$ selected according to the criteria of Eq. (3.106) (upper panel) and to the algorithm of Fig. 3.15 (lower panel). Here Region 3 (green bins) is not realized. The criteria of Ref. [17] suggest that Region 1 and Region 2 are equally distributed on the left of the cut in P_T. Therefore, a phenomenological analysis performed according to this criteria necessarily requires a matching procedure in order to properly describe the bins at the boundaries between Region 1 and Region 2. Instead, with the more refined algorithm presented in this thesis, we find that only the lower z_h bins correspond to Region 1, while most of the BELLE data belong to Region 2. With this selection, the issues related to the matching problem are less severe.
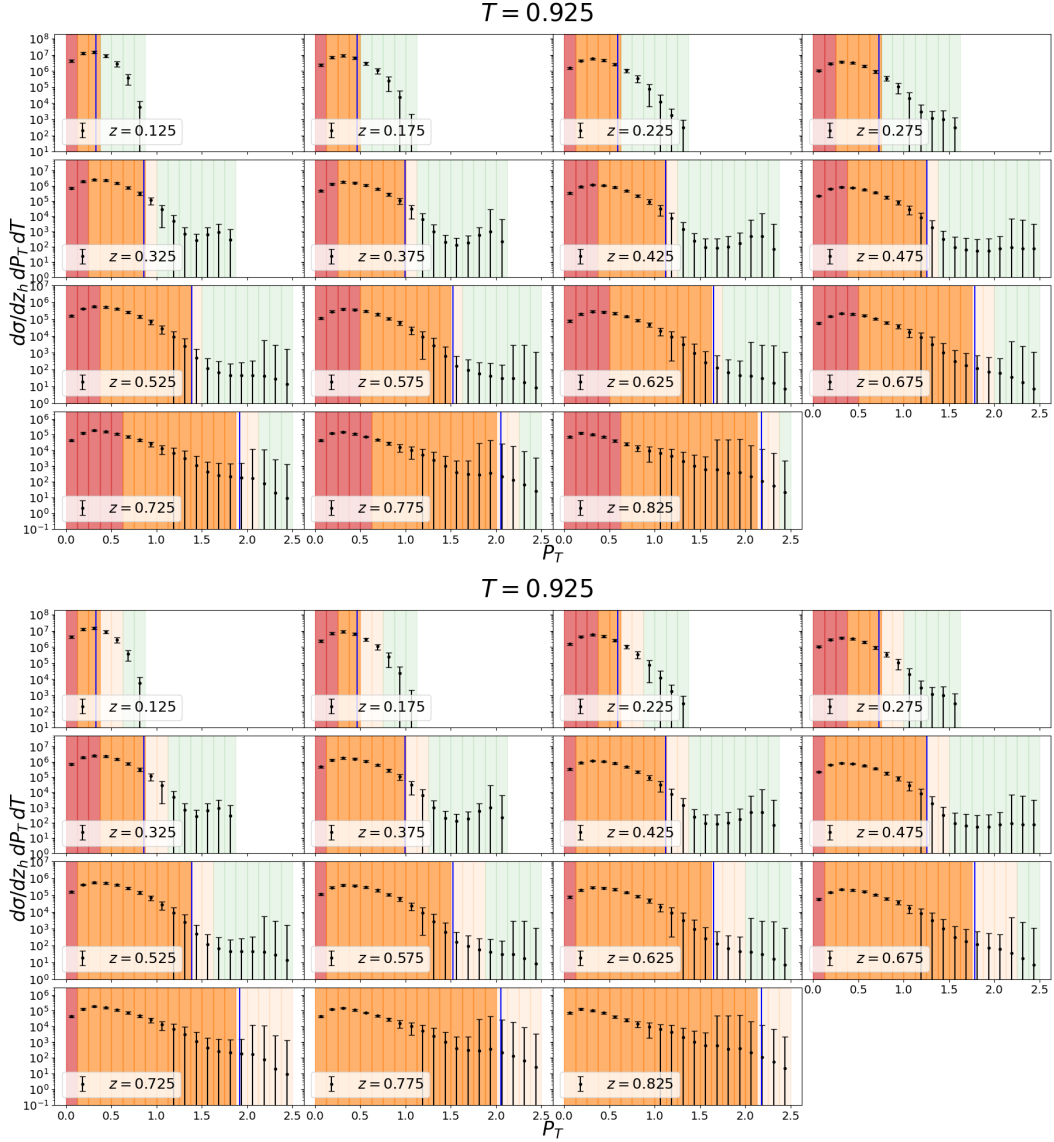
Fig. F.4 BELLE data for thrust $T = 0.925$ selected according to the criteria of Eq. (3.106) (upper panel) and to the algorithm of Fig. 3.15 (lower panel). Here Region 3 (green bins) is not realized. The criteria of Ref. [17] suggest that Region 1 and Region 2 are both present on the left of the cut in P_T. Therefore, a phenomenological analysis performed according to this criteria necessarily requires a matching procedure in order to properly describe the bins at the boundaries of Region 1 and Region 2. Instead, with the more refined algorithm presented in this thesis, we find that only the lower z_h bins correspond to Region 1, while most of the BELLE data belong to Region 2. With this selection, the issues related to the matching problem are less severe.
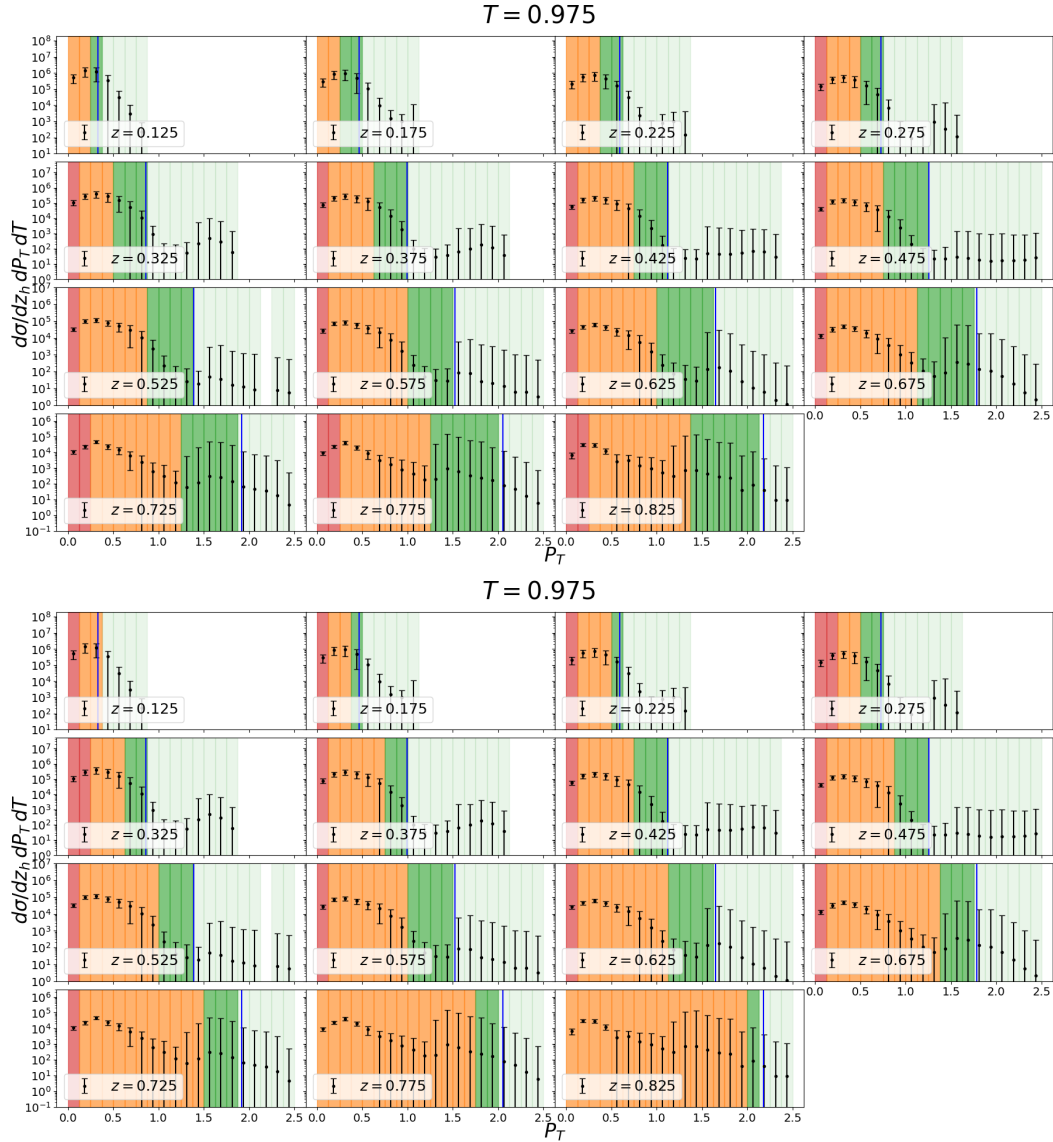
Fig. F.5 BELLE data for thrust $T = 0.925$ selected according to the criteria of Eq. (3.106) (upper panel) and to the algorithm of Fig. 3.15 (lower panel). Here Region 3 (green bins) appears together with the other two kinematic regions. Both the criteria of Ref. [17] and the more refined algorithm presented in this thesis suggest that all three regions are relevant in all the z_h-bins. Therefore, in this case, a proper matching procedure would be necessary to appropriately describe the transitions from one region to the following one. Notice that there are two boundaries: one between Region 1 and Region 2, and one between Region 2 and Region 3.

Bibliography

[1] J. D. Bjorken. Asymptotic Sum Rules at Infinite Momentum. *Phys. Rev.*, 179:1547–1553, 1969.

[2] J. D. Bjorken and Emmanuel A. Paschos. Inelastic Electron Proton and gamma Proton Scattering, and the Structure of the Nucleon. *Phys. Rev.*, 185:1975–1982, 1969.

[3] Richard P. Feynman. Very high-energy collisions of hadrons. *Phys. Rev. Lett.*, 23:1415–1417, 1969.

[4] S. D. Drell, Donald J. Levy, and Tung-Mow Yan. A Theory of Deep Inelastic Lepton-Nucleon Scattering and Lepton Pair Annihilation Processes. 1. *Phys. Rev.*, 187:2159–2171, 1969.

[5] S. D. Drell, Donald J. Levy, and Tung-Mow Yan. A Theory of Deep Inelastic Lepton Nucleon Scattering and Lepton Pair Annihilation Processes. 2. Deep Inelastic electron Scattering. *Phys. Rev. D*, 1:1035–1068, 1970.

[6] S. D. Drell, Donald J. Levy, and Tung-Mow Yan. A Theory of Deep Inelastic Lepton-Nucleon Scattering and Lepton Pair Annihilation Processes. 3. Deep Inelastic electron-Positron Annihilation. *Phys. Rev. D*, 1:1617–1639, 1970.

[7] John Collins. *Foundations of perturbative QCD*. Cambridge University Press, 2011.

[8] R. Seidl et al. Transverse momentum dependent production cross sections of charged pions, kaons and protons produced in inclusive e^+e^- annihilation at $\sqrt{s} = 10.58$ GeV. *Phys. Rev.*, D99(11):112006, 2019.

[9] Umberto D'Alesio, Francesco Murgia, and Marco Zaccheddu. First extraction of the Λ polarizing fragmentation function from Belle e^+e^- data. *Phys. Rev. D*, 102(5):054001, 2020.

[10] Umberto D'Alesio, Francesco Murgia, and Marco Zaccheddu. Λ polarizing fragmentation function from Belle e^+e^- data. In *28th International Workshop on Deep Inelastic Scattering and Related Subjects*, 7 2021.

[11] Umberto D'Alesio, Francesco Murgia, and Marco Zaccheddu. General helicity formalism for two-hadron production in e^+e^- annihilation within a TMD approach. arXiv:2108.05632 [hep-ph].

[12] M. Boglione and A. Simonelli. Universality-breaking effects in e^+e^- hadronic production processes. *Eur. Phys. J. C*, 81(1):96, 2021.

[13] M. Boglione and A. Simonelli. Factorization of $e^+e^- \to HX$ cross section, differential in z_h, P_T and thrust, in the 2-jet limit. *JHEP*, 02:076, 2021.

[14] M. Boglione, J. O. Gonzalez-Hernandez, and A. Simonelli. Phenomenological extraction of a universal TMD fragmentation function from single hadron production in e^+e^- annihilations. In *28th International Workshop on Deep Inelastic Scattering and Related Subjects*, 8 2021.

Bibliography

[15] M. Boglione and A. Simonelli. Kinematic regions in the $e^+e^- \to hX$ factorized cross section in a 2-jet topology with thrust. arXiv:2109.11497 [hep-ph].

[16] Zhong-Bo Kang, Ding Yu Shao, and Fanyi Zhao. QCD resummation on single hadron transverse momentum distribution with the thrust axis. *JHEP*, 12:127, 2020.

[17] Yiannis Makris, Felix Ringer, and Wouter J. Waalewijn. Joint thrust and TMD resummation in electron-positron and electron-proton collisions. *JHEP*, 02:070, 2021.

[18] Leonard Gamberg, Zhong-Bo Kang, Ding Yu Shao, John Terry, and Fanyi Zhao. Transverse Λ polarization in e^+e^- collisions. *Phys. Lett. B*, 818:136371, 2021.

[19] John C. Collins, Davison E. Soper, and George F. Sterman. Transverse Momentum Distribution in Drell-Yan Pair and W and Z Boson Production. *Nucl.Phys.*, B250:199, 1985.

[20] John C. Collins. Sudakov form-factors. *Adv. Ser. Direct. High Energy Phys.*, 5:573–614, 1989.

[21] John C. Collins, Davison E. Soper, and George F. Sterman. Factorization of Hard Processes in QCD. *Adv. Ser. Direct. High Energy Phys.*, 5:1–91, 1989.

[22] John Collins and Jian-Wei Qiu. k_T factorization is violated in production of high-transverse-momentum particles in hadron-hadron collisions. *Phys. Rev. D*, 75:114014, 2007.

[23] Rafael F. del Castillo, Miguel G. Echevarria, Yiannis Makris, and Ignazio Scimemi. TMD factorization for dijet and heavy-meson pair in DIS. *JHEP*, 01:088, 2021.

[24] C. D. White. An Introduction to Webs. *J. Phys.*, G43(3):033002, 2016.

[25] Chris D. White. Wilson Lines and Webs in Higher-Order QCD. *Few Body Syst.*, 59(2):8, 2018.

[26] Alexey A. Vladimirov. Exponentiation for products of Wilson lines within the generating function approach. *JHEP*, 06:120, 2015.

[27] Giulio Falcioni, Einan Gardi, Mark Harley, Lorenzo Magnea, and Chris D. White. Multiple Gluon Exchange Webs. *JHEP*, 10:010, 2014.

[28] Alessandro Bacchetta, Sabrina Cotogno, and Barbara Pasquini. The transverse structure of the pion in momentum space inspired by the AdS/QCD correspondence. *Phys. Lett. B*, 771:546–552, 2017.

[29] Vincenzo Barone, Alessandro Drago, and Philip G. Ratcliffe. Transverse polarisation of quarks in hadrons. *Phys. Rept.*, 359:1–168, 2002.

[30] Daniel Boer, P. J. Mulders, and F. Pijlman. Universality of T odd effects in single spin and azimuthal asymmetries. *Nucl. Phys. B*, 667:201–241, 2003.

[31] Dennis W. Sivers. Single spin production asymmetries from the hard scattering of point - like constituents. *Phys. Rev.*, D41:83, 1990.

[32] Stanley J. Brodsky, Dae Sung Hwang, and Ivan Schmidt. Single hadronic spin asymmetries in weak interaction processes. *Phys. Lett. B*, 553:223–228, 2003.

[33] John C. Collins. Leading twist single transverse-spin asymmetries: Drell-Yan and deep inelastic scattering. *Phys. Lett. B*, 536:43–48, 2002.

[34] Andrei V. Belitsky, X. Ji, and F. Yuan. Final state interactions and gauge invariant parton distributions. *Nucl. Phys. B*, 656:165–198, 2003.

[35] John C. Collins. Fragmentation of transversely polarized quarks probed in transverse momentum distributions. *Nucl. Phys.*, B396:161–182, 1993.

[36] S. Mert Aybat, John C. Collins, Jian-Wei Qiu, and Ted C. Rogers. The QCD Evolution of the Sivers Function. *Phys.Rev.*, D85:034043, 2012.

[37] S. Mert Aybat and Ted C. Rogers. TMD Parton Distribution and Fragmentation Functions with QCD Evolution. *Phys.Rev.*, D83:114042, 2011.

[38] Y. Guan et al. Observation of Transverse $\Lambda/\bar{\Lambda}$ Hyperon Polarization in e^+e^- Annihilation at Belle. *Phys. Rev. Lett.*, 122(4):042001, 2019.

[39] A. Accardi et al. Electron Ion Collider: The Next QCD Frontier: Understanding the glue that binds us all. *Eur. Phys. J. A*, 52(9):268, 2016.

[40] E.C. Aschenauer, S. Fazio, J.H. Lee, H. Mantysaari, B.S. Page, B. Schenke, T. Ullrich, R. Venugopalan, and P. Zurita. The electron–ion collider: assessing the energy dependence of key measurements. *Rept. Prog. Phys.*, 82(2):024301, 2019.

[41] Jui-yu Chiu, Ambar Jain, Duff Neill, and Ira Z. Rothstein. The Rapidity Renormalization Group. *Phys. Rev. Lett.*, 108:151601, 2012.

[42] Jui-Yu Chiu, Ambar Jain, Duff Neill, and Ira Z. Rothstein. A Formalism for the Systematic Treatment of Rapidity Logarithms in Quantum Field Theory. *JHEP*, 05:084, 2012.

[43] John C. Collins and Ted C. Rogers. Equality of Two Definitions for Transverse Momentum Dependent Parton Distribution Functions. *Phys. Rev. D*, 87(3):034018, 2013.

[44] Miguel G. Echevarría, Ahmad Idilbi, and Ignazio Scimemi. Soft and Collinear Factorization and Transverse Momentum Dependent Parton Distribution Functions. *Phys. Lett. B*, 726:795–801, 2013.

[45] Ambar Jain, Massimiliano Procura, and Wouter J. Waalewijn. Fully-Unintegrated Parton Distribution and Fragmentation Functions at Perturbative k_T. *JHEP*, 04:132, 2012.

[46] S. Catani, G. Turnock, B. R. Webber, and L. Trentadue. Thrust distribution in e^+e^- annihilation. *Phys. Lett.*, B263:491–497, 1991.

[47] S. Catani, L. Trentadue, G. Turnock, and B.R. Webber. Resummation of large logarithms in e+ e- event shape distributions. *Nucl. Phys. B*, 407:3–42, 1993.

[48] Thomas Becher and Matthew D. Schwartz. A precise determination of α_s from LEP thrust data using effective field theory. *JHEP*, 07:034, 2008.

[49] M. Dasgupta and G.P. Salam. Resummation of nonglobal QCD observables. *Phys. Lett. B*, 512:323–330, 2001.

[50] A. Banfi, G. Marchesini, and G. Smye. Away from jet energy flow. *JHEP*, 08:006, 2002.

[51] Andrew J. Larkoski, Ian Moult, and Duff Neill. Non-Global Logarithms, Factorization, and the Soft Substructure of Jets. *JHEP*, 09:143, 2015.

[52] Thomas Becher, Rudi Rahn, and Ding Yu Shao. Non-global and rapidity logarithms in narrow jet broadening. *JHEP*, 10:030, 2017.

[53] Matthew D. Schwartz. *Quantum Field Theory and the Standard Model*. Cambridge University Press, 2014.

Bibliography

[54] M. Boglione, J. Collins, L. Gamberg, J.O. Gonzalez-Hernandez, T.C. Rogers, and N. Sato. Kinematics of Current Region Fragmentation in Semi-Inclusive Deeply Inelastic Scattering. *Phys. Lett. B*, 766:245–253, 2017.

[55] M. Boglione, A. Dotson, L. Gamberg, S. Gordon, J.O. Gonzalez-Hernandez, A. Prokudin, T.C. Rogers, and N. Sato. Mapping the Kinematical Regimes of Semi-Inclusive Deep Inelastic Scattering. *JHEP*, 10:122, 2019.

[56] John Collins and Ted C. Rogers. Connecting Different TMD Factorization Formalisms in QCD. *Phys. Rev. D*, 96(5):054011, 2017.

[57] Alessandro Bacchetta, Valerio Bertone, Chiara Bissolotti, Giuseppe Bozzi, Filippo Delcarro, Fulvio Piacenza, and Marco Radici. Transverse-momentum-dependent parton distributions up to N^3LL from Drell-Yan data. *JHEP*, 07:117, 2020.

[58] Miguel G. Echevarria, Ignazio Scimemi, and Alexey Vladimirov. Unpolarized Transverse Momentum Dependent Parton Distribution and Fragmentation Functions at next-to-next-to-leading order. *JHEP*, 09:004, 2016.

[59] J. Collins, L. Gamberg, A. Prokudin, T. C. Rogers, N. Sato, and B. Wang. Relating Transverse Momentum Dependent and Collinear Factorization Theorems in a Generalized Formalism. *Phys. Rev.*, D94(3):034014, 2016.

[60] G. Passarino and M.J.G. Veltman. One Loop Corrections for e^+e^- Annihilation Into $\mu^+\mu^-$ in the Weinberg Model. *Nucl. Phys. B*, 160:151–207, 1979.

[61] Massimiliano Procura and Iain W. Stewart. Quark Fragmentation within an Identified Jet. *Phys. Rev. D*, 81:074009, 2010. [Erratum: Phys.Rev.D 83, 039902 (2011)].

[62] George Fikioris. Integral Evaluation Using the Mellin Transform and Generalized Hypergeometric Functions: Tutorial and Applications to Antenna Problems. *IEEE Transactions on Antennas and Propagation*, 54(12):3895, 2006.